e-ISSN 2598-9596

FaST

Jurnal Sains dan Teknologi

Vol.10, No.1, Mei 2026

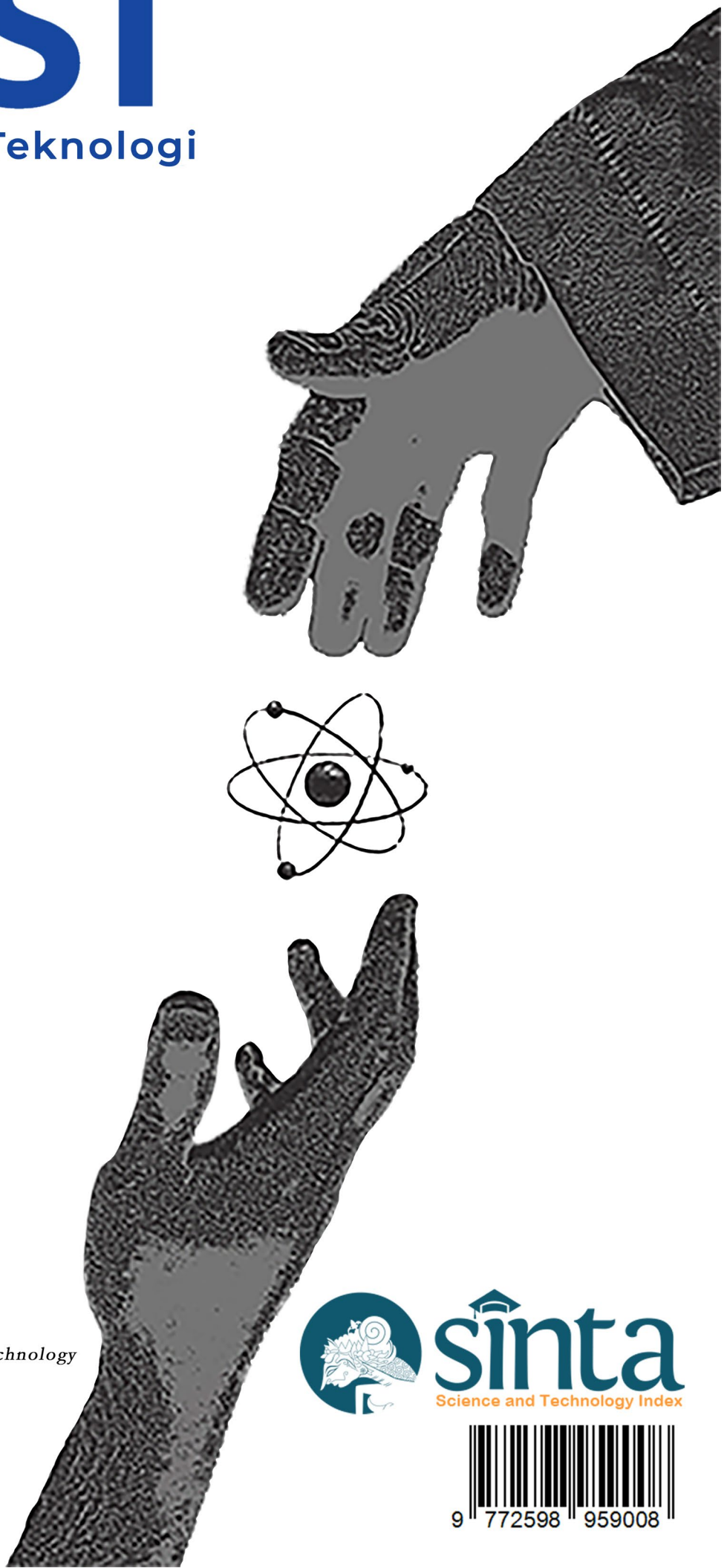

Published by the Faculty of Science and Technology
Universitas Pelita Harapan

UPH

sinta
Science and Technology Index

9 772598 959008

FaST - Jurnal Sains dan Teknologi, Vol. 10, No.1, May 2026
e-ISSN 2598-9596
Available online at: https://ojs.uph.edu/index.php/FaSTJST/issue/view/662

EDITORIAL TEAM

FaST - Jurnal Sains dan Teknologi, Vol. 10, No.1, May 2026
e-ISSN 2598-9596
Available online at: https://ojs.uph.edu/index.php/FaSTJST/issue/view/662

CONTENTS

FaST - Jurnal Sains dan Teknologi, Vol. 10, No.1, Mei 2026
e-ISSN 2598-9596
DOI: https://doi.org/10.19166/fastjst.v10i1.10486
Available online at: https://ojs.uph.edu/index.php/FaSTJST/article/view/10486

3D-Printed Porous Tantalum Scaffolds for Bone Regeneration: A Narrative Review of Structural Design, Biological Performance, and Clinical Applications

Michael Lizar[1*)], Xingshuang Ma[1)]
[1]The Key Laboratory of Biorheological Science and Technology, Ministry of Education, College of Bioengineering, Chongqing University, Chongqing 400044, China

ABSTRACT

Bone fractures remain a major clinical challenge in orthopedic surgery, requiring biomaterials that closely mimic the structural and mechanical properties of native bone. Although titanium and its alloys are widely used, their limited porosity and elastic modulus mismatch may compromise osseointegration and long-term implant stability. Three-dimensional (3D)-printed porous tantalum (Ta) scaffolds have emerged as promising alternatives due to their high biocompatibility, corrosion resistance, and osteoconductive potential. This narrative review comprehensively evaluates the structural design, additive manufacturing strategies, mechanical performance, biological interactions, and clinical applications of 3D-printed porous Ta scaffolds for bone regeneration. Particular attention is given to scaffold architecture, pore geometry optimization, and scaffold–cell interactions, including the incorporation of bone marrow–derived mesenchymal stem cells (BMSCs). Advances in additive manufacturing techniques, such as Selective Laser Melting and Laser Engineered Net Shaping, enable the fabrication of highly interconnected porous structures with bone-mimetic mechanical properties. Evidence from in vitro and in vivo studies indicates that pore sizes of 400–600 μm and porosity around 80% provide a favorable microenvironment for cell adhesion, proliferation, and osteogenic differentiation. Functionalization strategies and activation of osteogenic signaling pathways further enhance mineralization and interfacial integration. Overall, the integration of 3D-printed porous Ta scaffolds with regenerative cellular strategies represents a promising approach for bone defect repair, spinal fusion, and joint reconstruction. Continued optimization of scaffold design and validation through long-term clinical studies are essential to facilitate translational application.

ARTICLE INFO

Keywords: additive manufacturing; bone regeneration; mesenchymal stem cells; porous tantalum; tissue engineering

***Corresponding author**:
michaelizar@gmail.com

Article history:
Submitted 07 Jan 2026
Revised 18 Feb 2026
Accepted 23 Feb 2026
Online Available 17 Apr 2026
Published 20 May 2026

1. Introduction

Bone fractures in orthopedics represent a complex clinical challenge, particularly in significant segmental defects, delayed union, or compromised bone quality. Effectively managing these conditions requires bone implants that provide mechanical support, biological integration, and enhanced bone regeneration. Traditionally, metallic biomaterials such as titanium (Ti) and its alloys have been widely used due to their mechanical strength and corrosion resistance. However, Ti exhibits several limitations, including low volumetric porosity, a relatively high elastic modulus, and limited osseointegration, leading to stress shielding and implant failure. Tantalum (Ta) has emerged as a promising alternative biomaterial in recent years due to its excellent biocompatibility, high volumetric porosity, and mechanical properties that closely mimic cancellous bone. These characteristics support its use in various orthopedic applications. Clinical success has been demonstrated particularly in procedures such as tibial tubercle advancement, where porous tantalum has shown outcomes comparable to autologous bone grafts, with reduced complications and improved patient satisfaction [1]. Broader applications, including hip and knee arthroplasty, osteonecrosis treatment, and spinal fusion, have also shown promising results, as reported in other studies [2]. The development of additive manufacturing (AM) technologies, or 3D printing, has further enabled the precise fabrication of porous Ta scaffolds with controlled geometry and tailored mechanical properties [3]. Bone remodelling is regulated by a dynamic balance between bone formation and resorption, involving osteoblasts, osteocytes, and osteoclasts. Osteoblasts synthesize the bone matrix, osteocytes in the matrix serve as mechanosensors, and osteoclasts resorb bone to maintain skeletal homeostasis [4,5,6]. Disruption in this balance leads to impaired healing, particularly in challenging fracture environments (**Fig. 1**). Advances in regenerative medicine have introduced mesenchymal stem cells (MSCs), particularly those derived from bone

FaST - Jurnal Sains dan Teknologi, Vol. 10, No.1, Mei 2026
e-ISSN 2598-9596
DOI: https://doi.org/10.19166/fastjst.v10i1.10486
Available online at: https://ojs.uph.edu/index.php/FaSTJST/article/view/10486

marrow (BMSCs), as a powerful tool for enhancing osteogenesis. When combined with porous Ta scaffolds, MSCs contribute to both structural support and biological functionality. This review evaluates the potential of 3D-printed porous Ta scaffolds integrated with MSCs, focusing on fabrication methods, biological performance, and clinical relevance in bone regeneration.

2. Review Methodology

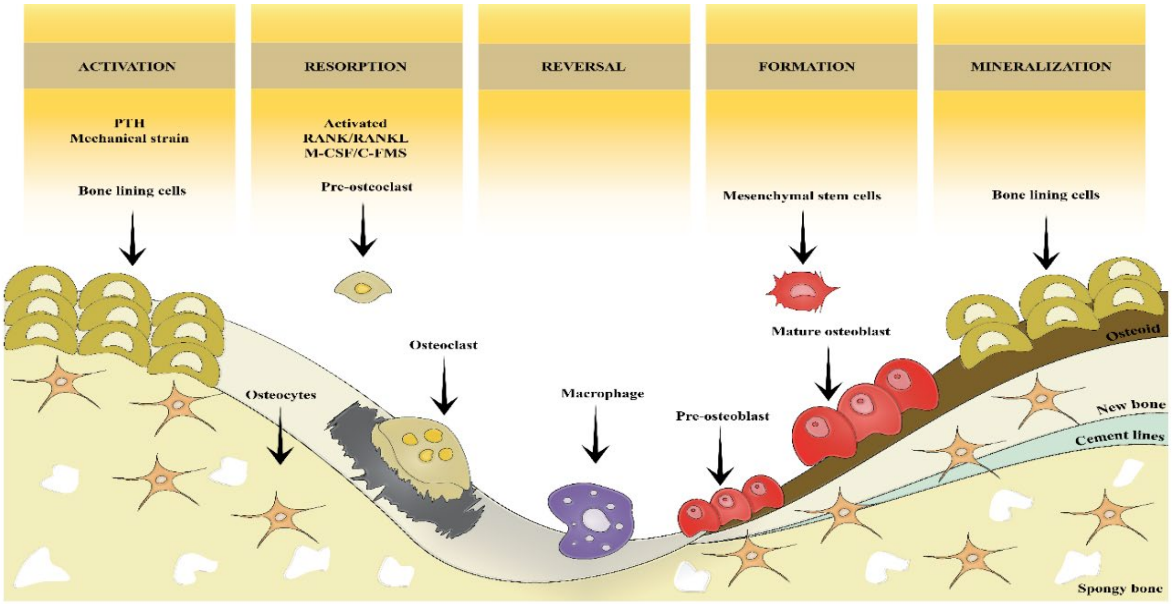

Figure 1. Bone remodeling process consists of five phases: activation, resorption, reversal, formation, and mineralization.

The research was carried out as a narrative review. The terms "porous tantalum," "3D printing," "additive manufacturing," "bone regeneration," "osseointegration," and "mesenchymal stem cells" were combined to search PubMed, Scopus, and Web of Science databases for pertinent peer-reviewed publications published between January 2010 and December 2025. Translational research, clinical studies including orthopedic and dental applications, in vitro studies, and in vivo animal models were prioritized. Articles that just discussed titanium and made no analogy to tantalum were not included. Methodological rigor, relevance to scaffold construction, mechanical performance, biological results, and clinical translation were all prioritized throughout the selection process. After screening titles and abstracts for relevance, studies were selected based on thematic relevance and methodological quality. Duplicate records were excluded

2.1 3D Printing Techniques for Bone Implants

Earlier scaffold fabrication methods, including metal-fiber and powder metallurgy-based loose sintering and plasma spraying, often result in inconsistent pore geometry, non-uniform porosity, and poor interconnectivity. For example, Torres et al. (2014) highlighted irregular pore structures using conventional PM, and Wauthle et al. (2015) pointed out that these older techniques cannot produce the fully connected porous architectures achievable with additive manufacturing [7,8]. These shortcomings often compromise scaffold functionality, mechanical strength, and biological performance. Additionally, conventional approaches lack the precision and adaptability to fabricate patient-specific implants with complex geometries. To address these challenges, additive manufacturing (AM), also known as 3D printing, has emerged as a transformative technology in orthopedic biomaterials. AM enables the direct fabrication of complex, customized structures based on computer-aided design (CAD) models. Its advantages include tunable pore size, high structural accuracy, shortened production time, and potential scalability for clinical use [9,10,11]. These features make AM highly suitable for producing implants replicating natural bone's mechanical and architectural properties. Metal-based AM technologies for scaffold fabrication fall into two primary categories: powder bed fusion (PBF) and directed energy deposition (DED) (**Fig. 2**).

FaST - Jurnal Sains dan Teknologi, Vol. 10, No.1, Mei 2026
e-ISSN 2598-9596
DOI: https://doi.org/10.19166/fastjst.v10i1.10486
Available online at: https://ojs.uph.edu/index.php/FaSTJST/article/view/10486

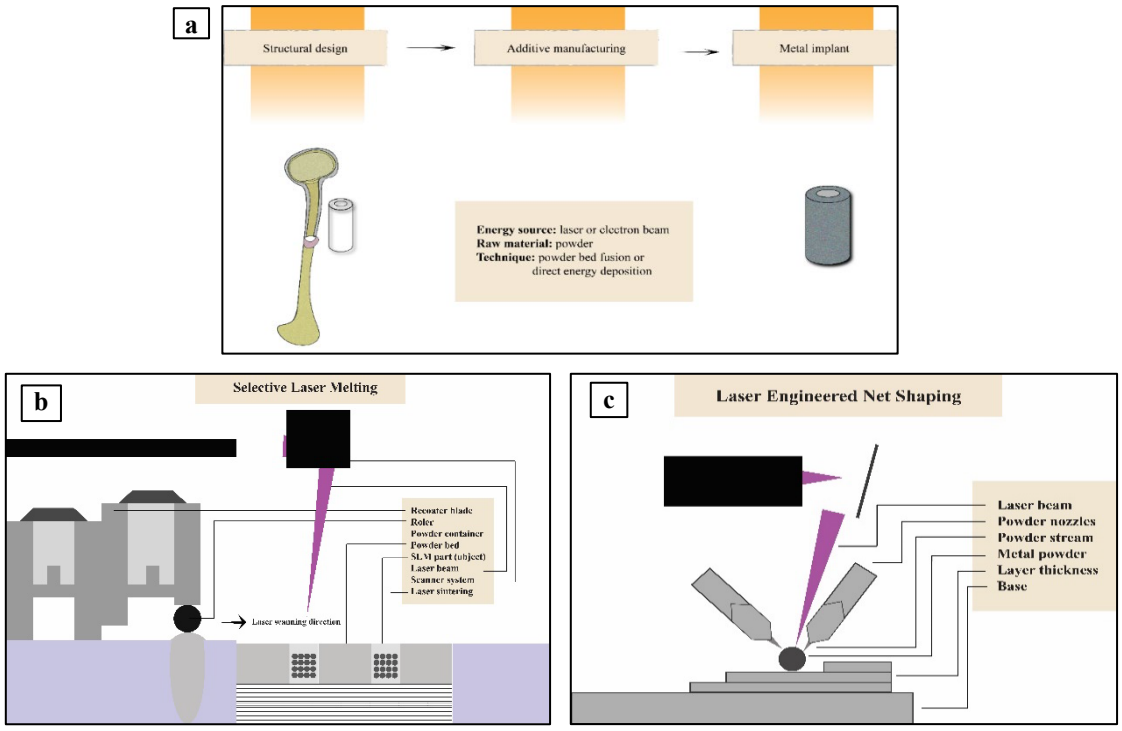

Figure 2 Additive manufacturing process. (a) The steps of the manufacturing process of metal materials; (b) Selective Laser Melting (SLM); (c) Laser Engineered Net Shaping (LENS)

In PBF systems, such as selective laser sintering (SLS), selective laser melting (SLM), electron beam melting (EBM), and direct metal laser sintering (DMLS), a high-energy beam selectively fuses layers of metal powder to build the scaffold layer by layer. These techniques offer high resolution and excellent control over porosity and interconnectivity. In contrast, DED methods, including laser engineered net shaping (LENS), direct metal deposition (DMD), and 3D fiber deposition, simultaneously deposit and melt metal powders onto a substrate [12,13]. LENS, for instance, uses a laser to create a melt pool into which metal powder is injected, enabling precise control over deposition and layer bonding. SLM is particularly effective in creating fully dense metal structures with well-defined pore networks, while LENS excels at producing functionally graded or hybrid structures with tailored mechanical properties. SLM [14,15] and LENS [16,17] have been successfully applied to fabricate porous tantalum scaffolds, offering reproducibility and versatility for orthopedic applications (**Table 1**) [18,19]. Their ability to produce scaffolds with optimal pore sizes (typically 300–600 µm) and high porosity (70–90%) allows for improved cell infiltration, vascularization, and load-bearing capacity. These technologies lay the groundwork for next-generation scaffolds that integrate mechanical strength with biological function, especially when combined with mesenchymal stem cells (MSCs) for enhanced osteogenesis.

Table 1 Additive Manufacturing Techniques

Methods	Process Characteristics	Type Materials	Category	Advantages	Limitations
SLM [14,15]	Preparing the powder bed Layer-by-layer addition of the powder A laser beam is used to melt the thin layer of metal powder	Metal powder	Powder bed fusion	High density, High processing with controlled pore interconnectivity and porosity	Costly Relatively slow process
LENS [16,17]	Metal substrate deposition The high-power laser beams are used to melt metal powder	Metal powder	Directed energy deposition	Ability to tailor the deposition parameter with a high degree of control	Higher residual stress

FaST - Jurnal Sains dan Teknologi, Vol. 10, No.1, Mei 2026
e-ISSN 2598-9596
DOI: https://doi.org/10.19166/fastjst.v10i1.10486
Available online at: https://ojs.uph.edu/index.php/FaSTJST/article/view/10486

Inert shroud gas is used to shield the melt pool	Fully dense shapes and excellent material properties

Several critical factors must be considered in developing 3D-printed porous metal scaffolds, including material selection, pore size, porosity, pore structure, surface modification, and mechanical strength. These parameters can be precisely designed and evaluated using AM technologies before mass production. As a bio-inert metal, tantalum exhibits excellent biocompatibility, favorable mechanical properties, and safety for biomedical applications [20]. AM-produced porous Ta scaffolds offer controlled pore architecture, a key determinant in bone ingrowth. The CAD-based design enables predefinition of interparticle pore geometry, directly influencing the scaffold's mechanical behavior and osteoconductive properties [21]. Optimal scaffold designs should incorporate interconnected pores that facilitate vascularization and nutrient transport while maintaining mechanical integrity. Studies suggest effective pore sizes for bone in-growth range from 100 µm to over 400 µm [20,21]. Cheng et al. found that larger pores (653 µm) enhance osteogenic differentiation [22], while Biemond et al. observed improved bone formation in scaffolds with pore sizes of 1200 µm compared to 900 µm [23]. Pore throat size, the narrowest passage linking adjacent pores, critically influences cellular infiltration and nutrient transport. Narrow throats impede oxygen and cell penetration, while huge ones can hinder uniform bone coverage and integration [24,25]. Porosity, defined as the volume percentage of void space in the scaffold, is closely linked to pore size, strut thickness, and lattice geometry. Human trabecular bone typically exhibits porosity between 70% and 90%. Scaffolds mimicking this porosity range (e.g., 80% in porous Ta) balance bone ingrowth potential and mechanical performance, maintaining elastic moduli in the 2.5–4 GPa [26,27]. The pore structure is also vital in determining compressive strength and biological performance. AM enables consistent pore geometry, such as wave, diamond, or cubic structures, through CAD modeling, overcoming the limitations of traditional fabrication methods [28, 29]. Biemond et al. reported that wave structures enhance mechanical interlocking via increased friction, whereas cubic geometries improve in vivo bone ingrowth [23]. Diamond lattice structures favor cell attachment and proliferation due to their interconnected architecture and uniform stress distribution [30]. In addition to geometry, surface modification techniques are critical in enhancing scaffold bioactivity and long-term integration. Methods such as anodization, calcium phosphate coatings, and hydrothermal treatments can improve osteoinductivity and reduce the risk of implant rejection by promoting stronger interactions with host tissue [31,32]. Mechanical properties, including load-bearing capacity, fatigue resistance, and mitigation of stress shielding, are also vital for ensuring the long-term functionality of orthopedic implants. Additively manufactured (AM) scaffolds designed with open, non-stochastic lattice architectures, such as diamond or gyroid topologies, have demonstrated superior mechanical stability and enhanced biological integration, making them promising candidates for load-bearing bone applications [33].

2.2 Biocompatibility & Comparative Scaffold Studies

The structural architecture and mechanical performance of porous tantalum scaffolds play a central role in their biological functionality and clinical reliability. Parameters such as pore size, porosity, interconnectivity, surface modification, and fabrication technique directly influence compressive strength, elastic modulus, and osteoconductive behavior. A synthesis of reported design configurations and mechanical benchmarks for 3D-printed porous tantalum scaffolds is summarized in (**Table 2**).

Table 2 Comparative Study of Recent Studies of 3D-Printed Porous Tantalum

Study	Fabrication	MSC Integration	Scaffold Modification	Model	Results
Zhang et al. (2023) [96]	SLM-printed PTa with hydrothermal nano-topography	Rat BMSCs (in vitro)	Nano-structured surface via alkali–heat–hydrothermal treatment	Rabbit mandibular defect (in vivo)	Nano-topography significantly enhanced BMSC adhesion, osteogenic differentiation (↑ALP, mineralization), and early bone formation.

FaST - Jurnal Sains dan Teknologi, Vol. 10, No.1, Mei 2026
e-ISSN 2598-9596
DOI: https://doi.org/10.19166/fastjst.v10i1.10486
Available online at: https://ojs.uph.edu/index.php/FaSTJST/article/view/10486

Liu et al. (2025) [97]	3D-printed PTa with polydopamine; MZIF-8 drug delivery	BMSC regulation via macrophage polarization	Polydopamine + MZIF-8 + melatonin for immunoregulatory release	Osteoporotic rat femur (in vivo)	Promoted M2 macrophage shift, inhibited inflammation, enhanced BMSC osteogenesis via P38-MAPK
Jiao et al. (2023) [98]	SLM-printed PTa scaffolds (60%, 70%, 80% porosity)	Rat BMSCs (in vitro)	Varying porosity only	Rat femoral defect (in vivo)	70–80% porosity provided maximal BMSC proliferation, osteogenic gene expression, and bone ingrowth; 70% porosity was optimal
Yu et al. (2024) [99]	SLM-printed PTa with corrosion-resistant surface	Human BMSCs (in vitro)	Review of customized PTa (no specific coating)	-	Confirmed high BMSC proliferation, osteogenesis, corrosion resistance, and overall biocompatibility
Zhao et al. (2025) [100]	Porous Ta integrated with gelatin nanoparticle (GNP) hydrogel	BMSC + endothelial co-culture	GNP hydrogel for growth factor delivery and angiogenesis	In vivo vascularized bone model	Promoted both osteogenesis and angiogenesis, indicating vascularized bone regeneration

The selection of biologically compatible and mechanically reliable materials is essential to support bone remodeling. An ideal implant material should mimic the elastic modulus of bone, offer sufficient mechanical strength, induce osteogenesis, and remain inert within the physiological environment [34]. Tantalum (Ta), a rare transition metal with atomic number 73, has been utilized in biomedical applications since the 1940s due to its unique properties, including high corrosion resistance, a relatively high modulus of elasticity, and an exceptionally high melting point (~3000°C) [35]. Its chemical stability prevents adverse reactions with body fluids, making it suitable for long-term orthopedic implantation. Despite its favorable characteristics, the high melting point of Ta presents challenges in traditional fabrication. Early generations of synthetic implants relied on cobalt-chromium (Co–Cr) sintered beads or plasma-sprayed titanium (Ti) alloys, which suffered from poor porosity, high stiffness, and low frictional coefficients, limiting their integration with native bone [36,37]. To overcome these limitations, porous tantalum trabecular metal (PTTM) scaffolds were developed using Zimmer Biomet's Trabecular Metal™ Technology. PTTM mimics cancellous bone structurally and functionally, featuring a high-friction, low-modulus porous surface with interconnected pores and high porosity [38, 39]. Porous tantalum trabecular metal (PTTM) scaffolds exhibit a highly regular, open-cell architecture composed of repeating dodecahedral units, facilitating efficient cellular infiltration and vascularization. Fabrication typically involves pyrolysis of thermosetting polymer foams to generate a vitreous carbon template with approximately 98% porosity. Pure tantalum is then deposited onto this carbon framework via chemical vapor deposition/infiltration (CVD/CVI), resulting in a conformal tantalum coating with a typical thickness of 40–60 µm. The depth and uniformity of the coating are influenced by pore size and interconnectivity, and these structural parameters critically affect mechanical stability, load transfer capability, and cellular adhesion behavior [40, 41].

Chemical Vapor Deposition (CVD) is a key technique for fabricating high-precision porous tantalum (Ta) scaffolds. This method introduces precursor gases into a vacuum reaction chamber, which thermally decomposes or reacts with a heated substrate to deposit a solid Ta layer. By precisely controlling chamber pressure and temperature, a uniform and adherent coating forms on the scaffold template while excess gases are evacuated from the system [42]. The biological performance of CVD-fabricated porous tantalum has been validated through in vitro and in vivo studies. For instance, Hacking et al. evaluated these scaffolds in a canine spine model and observed organized fibrous tissue, enhanced bone density, and neovascularization within 4–16 weeks, demonstrating the scaffold's rapid osseointegration and mechanical stability [43]. Lu et al. explored porous cubic Ta scaffolds for lumbar interbody fusion (LIF) in rabbits, using designs with ~500 µm pores and 86.8% porosity. Energy dispersive spectroscopy confirmed material purity. BMSCs cultured on the scaffold for seven days showed excellent adhesion and proliferation, and in vivo evaluation at 12 months revealed complete

FaST - Jurnal Sains dan Teknologi, Vol. 10, No.1, Mei 2026
e-ISSN 2598-9596
DOI: https://doi.org/10.19166/fastjst.v10i1.10486
Available online at: https://ojs.uph.edu/index.php/FaSTJST/article/view/10486

histologic fusion, confirming the implant's osteoconductive potential [44]. Tanzer et al. enhanced bone formation in another study by applying low-intensity ultrasound to cylindrical porous Ta implants in canine long bones. After six weeks, stimulated implants demonstrated significantly increased bone ingrowth (8–18%) compared to controls (2.7–8.5%), highlighting the synergistic benefits of combining mechanical stimulation with porous scaffolds [45].

Bobyn et al. studied porous cylindrical Ta implants fabricated by CVD and implanted into canine bone. They utilized two pore sizes, approximately 430 µm (small) and 650 µm (large), with volume porosity between 75% and 80% and observed bone ingrowth over 52 weeks. Histologically, small-pore scaffolds achieved greater bone ingrowth at 52 weeks (95% CI 76.9–82.5%) compared to large-pore designs (95% CI 68.3–73.0%) [27]. In an earlier canine acetabular cup study, Bobyn et al. demonstrated that porous Ta (75–80%) supported higher ultimate strength relative to Co-Cr sintered-bead (~30–35%) and Ti fiber metal (~40–50%) porous coatings [46]. Higher porosity thus not only fosters cell adhesion, proliferation, and osteoblastic differentiation, but also enhances interface mechanical strength (**Fig. 3**).

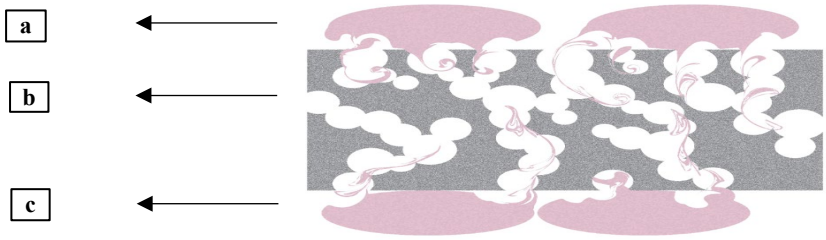

Figure 3. Process of bone in-growth into porous Ta scaffold. (a) The attachment of bone cells on the scaffold; (b) Pore size and porosity become a vital parameter to enhance bone in-growth; (c) The deep formation of bone

Kim et al. investigated the performance of porous tantalum trabecular metal (PTTM) implants compared to titanium tapered screw-vent (TSV) dental implants in a canine mandible model. Implant stability was assessed using resonance frequency analysis (RFA), yielding Implant Stability Quotient (ISQ) values ranging from 43.4 to 79.1 between 2 and 12 weeks, falling within comparable ranges for humans (50–62) and canines (59.7–89.7), with an average clinical stability threshold around 60. Histological evaluation demonstrated progressive osseointegration, evidenced by increasing bone-to-implant contact and bone ingrowth within the porous structure over the 12-week healing period. These results highlight the potential of PTTM implants to support enhanced osseointegration through bone ingrowth mechanisms during early healing [47].

Battula et al. evaluated porous tantalum trabecular metal (PTTM) and titanium tapered screw-vent (TSV) implants in a canine model, introducing ligatures after 12 weeks to induce peri-implantitis, and retrieved implants between 24 and 38 weeks [48]. Despite peri-implant inflammation, both implant designs supported tissue formation and bone healing, and there was no significant difference in tissue response between PTTM and TSV under diseased conditions. These findings suggest that implant macrodesign (porous versus threaded) does not markedly influence biological outcomes once peri-implantitis is established.

Lee et al. evaluated new bone formation in porous tantalum trabecular metal (PTTM) implants compared to titanium tapered screw-vent (TSV) dental implants in a canine mandible model [49]. Histological analysis revealed that both implant types exhibited progressive bone formation at 2 weeks and organized fibrous tissue at 12 weeks; however, PTTM demonstrated faster and more abundant bone deposition, alongside indications of ongoing remodeling, relative to TSV. These findings suggest that PTTM implants may promote enhanced osseointegration and hold promise for translation into human clinical studies.

A growing body of research supports the biocompatibility and therapeutic potential of 3D-printed porous tantalum (Ta), particularly when combined with bone marrow mesenchymal stem cells (BMMSCs). BMMSCs are a prime choice for bone tissue engineering due to their availability, ease of isolation/culture, and low immunogenicity [50]. Fu et al. demonstrated that rabbit-derived BMMSCs seeded onto porous cylindrical Ta scaffolds adhered and proliferated over seven days in vitro, and in osteonecrotic femoral models, scaffolds with BMMSCs achieved significantly superior bone formation at weeks 3 and 6 compared to scaffolds without BMMSCs [51]. Wu et al. evaluated the biocompatibility

FaST - Jurnal Sains dan Teknologi, Vol. 10, No.1, Mei 2026
e-ISSN 2598-9596
DOI: https://doi.org/10.19166/fastjst.v10i1.10486
Available online at: https://ojs.uph.edu/index.php/FaSTJST/article/view/10486

and osteoconductivity of 3D-printed porous tantalum (Ta) scaffolds implanted into the lateral epicondyle of rabbit femora. The implants featured a multiscale pore architecture, including macro-pores of 400–600 µm, interconnected micro-pores of 200–400 µm, particle sizes of 20–50 µm, and inter-particle interstices of 50–200 µm, with an overall porosity ranging from 65% to 80%. In vitro, the scaffolds supported robust cell adhesion and proliferation over eight days. Histological evaluation after 12 weeks of implantation revealed completely new bone coverage within the pores and no signs of host tissue toxicity, confirming their excellent biocompatibility and osteointegration potential [52].

Luo et al. characterized 3D-printed porous Ta implants in a rabbit femur epicondyle model, detailing a multi-scale pore structure: macro-pores of 400–600 µm, interconnected micro-pores of 200–400 µm, particle sizes of 20–50 µm, and inter-particle interstices of 50–200 µm, achieving overall porosity between 65–80%. In vitro, these scaffolds supported robust cell adhesion and proliferation over eight days, and histology at 12 weeks showed completely new bone coverage within pores, indicating no host toxicity [53]. Similarly, Wauthle et al. examined porous cylindrical Ta fabricated via selective laser melting (SLM), reporting a strut size of ~150 µm, a pore size of ~500 µm, and ≈80% porosity. Their rat femur model confirmed non-toxicity in vitro and substantial bone growth around and within the implants after 12 weeks under load-bearing conditions, demonstrating that SLM-processed Ta scaffolds support biomechanical functionality [8].

Wang et al. further demonstrated that porous Ta and Ti scaffolds with identical structures fabricated via SLM exhibited comparable osteointegration and osteogenesis. Notably, Ta scaffolds achieved mechanical properties, ultimate strength of ~394 MPa and Young's modulus of ~3.1 GPa, closely mimicking cancellous bone, alongside favorable cell performance, reinforcing the suitability of Ta for load-bearing applications [54].

In a complementary study, Balla et al. evaluated the biocompatibility of porous Ta coatings on Ti substrates fabricated using Laser Engineered Net Shaping (LENS). Human fetal osteoblasts (hFOBs) were seeded onto samples with 27% and 55% porosity. The porous Ta scaffolds, particularly those with 45% porosity and mean pore sizes exceeding 500 µm, supported robust cell adhesion and proliferation with no cytotoxic effects. In contrast, the Ti group with lower porosity (27%) showed reduced cell density. These findings suggest that porous Ta coatings significantly enhance osteoconductivity and promote superior osseointegration when processed via LENS technology [18]. Bandyopadhyay et al. observed the effects of porous Ta rods fabricated by LENS in the early osseointegration stage. The experimental design consists of three groups (Ti, Ta, Titania nanotube (TNT) with porosity of 30%) compared to dense Ti as the control, implanted in the rat distal femur model for 5 to 12 weeks. In vivo study also explained that osteoid formation was comparatively higher at 12 weeks in Ta and TNT groups, and a reduced gap width at the bone-implant interface was seen in the Ti group. A clear gap was seen in the control group, indicating Ti's poor biocompatibility. However, at five weeks, the TNT group showed comparable results to the Ta group in the early osseointegration stage. Porous Ta fabricated by LENS shows a well-ingrown bone into the implant's pores [55].

In a porcine anterior lumbar interbody fusion (ALIF) model, Zou et al. demonstrated that porous tantalum rings, filled with autograft and implanted at L2-3, L4-5, and L6-7, supported complete trabecular bone ingrowth into central holes and porous structures at 3 months, especially when combined with alendronate; carbon-fiber cages did not exhibit the same enhancement [56]. A follow-up study in the same ALIF model Zou et al. reported that bone volume and histologic fusion of Ta rings were comparable to vertebral bone and superior to carbon-fiber cages, affirming Ta's osteoconductive stability in load-bearing spinal applications [57].

Fraser et al. used a rabbit tibial gap–healing model to assess titanium implants' integration and biomechanical performance modified with a porous tantalum (Ta) midsection, compared to solid titanium controls. Implants were retrieved at 4, 8, and 12 weeks. Histomorphometric analysis showed significantly greater bone–implant contact (BIC) surrounding Ta-modified implants at all time points, and removal torque testing confirmed increased mechanical stability. Interestingly, the group's early gene expression of osteogenic markers was elevated at 4 weeks, indicating accelerated healing. In a subsequent biomechanical evaluation reported by Fraser et al., nanoindentation and resonance-frequency analyses revealed no significant differences in stiffness or hardness of the peri-implant bone–Ta interface between 4 and 12 weeks, suggesting that Ta modification enhances osteogenic response without altering the mechanical properties of the bone–implant interface [58,59].

FaST - Jurnal Sains dan Teknologi, Vol. 10, No.1, Mei 2026
e-ISSN 2598-9596
DOI: https://doi.org/10.19166/fastjst.v10i1.10486
Available online at: https://ojs.uph.edu/index.php/FaSTJST/article/view/10486

Mrosek et al. evaluated osteochondral defect repair in mature sheep using porous tantalum (PTTM) implants, both with and without an autologous periosteal graft (TMPG), compared to untreated controls. After 16 weeks, TMPG and PTTM scaffolds supported secure fixation and subchondral bone integration, exhibiting healthier neo-cartilage layers than the empty defects. Although the TMPG group demonstrated early implant stability within three months, the periosteal graft did not enhance neo-cartilage formation. In contrast, the Ta-only PTTM scaffold promoted effective bone healing in significant animal defects, highlighting its potential utility in orthopedic applications [60].

Ren et al. examined the ability of porous tantalum rods to repair tibial defects caused by firearm injuries in rabbits. Animals were divided into three groups: firearm injury with Ta implant (Group A), non-firearm injury with Ta implant (Group B), and firearm injury control (Group C). Implants were evaluated at intervals from 4 to 16 weeks. At 4 weeks, rods were covered in fibrous tissue; by 16 weeks, dense tissue fully encapsulated the implants, and radiographic scoring revealed significantly greater bone filling in Group A compared to controls, demonstrating porous Ta's effectiveness in enhancing bone healing [61].

2.3 Porous Tantalum Mechanical Properties

The mechanical performance of bone implants is strongly influenced by size, structure, architecture, and material properties, all of which modulate osseointegration. An osteoconductive surface enables bone to adhere and grow into pores, facilitating direct bone–implant contact [62]. In early healing, fibrous tissue often envelops implant surfaces, potentially infiltrating porous coatings. Studies show viable cells colonize porous Ta, consistent with osteoconductive behavior [63]. The mechanical properties of porous Ta are also critical: while bulk Ta has an elastic modulus of ~185 GPa, porosity reduces this to approximately 3 GPa, closer to human cancellous bone (cortical bone is ~20 GPa), minimizing stress shielding [64]. With advanced manufacturing and CAD design, 3D-printed porous Ta scaffolds can achieve tailored pore architecture and mechanical functionality for long-term load-bearing applications.

Zardiackas et al. found that porous tantalum foam (Hedrocel™) exhibited significantly higher cantilever bending strength (110 ± 14 MPa), compressive strength (~60 MPa), and tensile strength (~63 MPa) compared to cancellous bone. Its fatigue endurance limits (23 MPa in compression and 35 MPa in bending at 5×10^6 cycles) also surpassed those of both cancellous and cortical bone. These robust mechanical properties, alongside its known biocompatibility, underscore the suitability of porous Ta foam for load-bearing orthopedic implants [38]. Hacking et al. investigated the biomechanical strength and histological progression of soft tissue ingrowth into porous tantalum implants in a canine model. Peel tests at 4, 8, and 16 weeks revealed mean soft tissue attachment strengths of 61 ± 37 g/mm, 71 ± 38 g/mm, and 89 ± 43 g/mm, respectively, indicating statistically normal distributions and rapid integration. Histological analyses demonstrated mature, vascularized fibrous tissue formation within the porous structure, which increased in density over time, signifying progressive healing and improved interface bonding [43].

Porous tantalum scaffolds are designed to replicate the mechanical properties of cancellous bone, offering a tangent elastic modulus in the range of 2–3 GPa, comparable to human cancellous bone, while maintaining an optimal balance between stiffness and biological function [65,66]. This reduced modulus helps mitigate stress shielding risks while providing sufficient load-bearing capacity for bone ingrowth and graft stability. That balance is critical: an implant that is too compliant may risk structural failure, whereas an overly stiff device can lead to bone resorption and implant loosening due to stress shielding [67] and the general physical properties of pure tantalum showed in (**Table 3**) [68,69]

Table 3 General physical properties of pure tantalum [70,71]

Indicators	Value
Elastic modulus	185 GPa
Yield strength	165 MPa
Elongation to failure	40%
Tensile strength	205 MPa
Density	16.9 g/cm^3
Melting points	3000 ^{o}C
Hardness (HV)	110

FaST - Jurnal Sains dan Teknologi, Vol. 10, No.1, Mei 2026
e-ISSN 2598-9596
DOI: https://doi.org/10.19166/fastjst.v10i1.10486
Available online at: https://ojs.uph.edu/index.php/FaSTJST/article/view/10486

Wauthle et al. investigated the mechanical testing of static and dynamic porous Ta fabricated by SLM. Based on the experiment, the actual static mechanical properties of porous Ta with a yield strength of 12.7 ± 0.6 MPa and elastic modulus of 1.22 ± 0.07 GPa are close to the range of human cancellous bone. However, these results have a lower modulus value and could lower the stress-shielding effects. In ex vivo testing (torsion), two out of five explants have a robust bone interface to repair the bone defect with maximum torque (450 Nmm) applied. The maximum torque (331.3 Nmm) and average rotation of 59.1 ° were applied to three failed explants. The results did not significantly indicate that the bone-implant interface was as strong as the host bone. The porous Ta has good fatigue behavior, as shown by its high ductility properties and fatigue limit of 7.45 MPa, which is relatively high resistance. Thus, porous Ta's fabrication by the SLM technology performs excellent osteoconductive properties and is considered for serial manufacturing implants in comprehensive orthopedic research [8].

Guo et al. compared 3D-printed porous tantalum (Ta) scaffolds fabricated via selective laser melting (SLM) with Ti6Al4V controls. Both had a 300–400 μm pore size and 80% porosity and were implanted into rabbit femoral defects. In vitro, human bone marrow mesenchymal stem cells (hBMSCs) exhibited superior adhesion and full spread on Ta scaffolds after seven days. In vivo, at 12 weeks, Ta scaffolds showed significantly greater new bone area and thickness than Ti6Al4V implants, confirming Ta's effective osteogenesis and osseointegration [70]. SLM-fabricated porous tantalum scaffolds have a compressive strength of 78.54 MPa compared to 71.04 MPa for porous Ti6Al4V, and elastic moduli of 2.34 GPa versus 2.27 GPa, respectively. These values closely mimic human cancellous bone and help reduce stress shielding by matching physiological stiffness [70].

Blanco et al. investigated the in vitro proliferation of bone marrow-derived mesenchymal stem cells (BMSCs) co-cultured on porous titanium (Ti) and tantalum (Ta) scaffolds for inter-somatic spinal fusion. Over 14 days, BMSCs adhered and proliferated on both scaffold types, with a slightly higher proliferation rate observed in the Ti group. Nevertheless, the porous Ta scaffold exhibited comparable biocompatibility, demonstrating its ability to support cell attachment and growth. Although the study could not quantify the exact number of cells adhering to each scaffold, both materials showed promise for spinal fusion or reconstructive applications, highlighting Ta's potential in clinical settings [71].

Han Wang et al. compared the static mechanical properties of additively manufactured porous tantalum (Ta) and titanium (Ti) scaffolds fabricated via selective laser melting (SLM). They found that porous Ti exhibited a significantly higher equivalent stress (393.6 ± 1.4 MPa) compared to porous Ta (139.8 ± 14.5 MPa; $p < .05$). Additionally, the Young's modulus of the Ta group (3.10 ± 0.03 GPa) was significantly lower than that of Ti (5.42 ± 0.07 GPa; $p < .05$), aligning Ta's stiffness more closely with that of cancellous bone. Push-out tests conducted at 2-, 4-, and 8-weeks post-implantation revealed similar peak bone–implant bonding strength in both groups. However, the Ta implants showed lower displacement under load, suggesting better damping and cushioning, while Ti displayed higher microhardness. Overall, porous Ta scaffolds exhibit a favorable combination of mechanical compatibility and bone integration for long-term use [72].

Balla et al. evaluated the mechanical properties of porous Ta fabricated by LENS technology. The porous Ta has an open pore volume, with the microstructure appearing to vary in pore size and interconnectivity. Then, the 0.2% proof strength and Young modulus elasticity show a function of relative density. 0.2% proof strength ranges from 100 to 746 MPa, while Young's modulus is 1.5 to 20 GPa. These mechanical properties are similar to human cortical bone [18]. Bandyopadhyay et al. performed push-out testing in porous Ta fabricated by LENS to evaluate the bone-material interlocking interface. Field emission scanning electron microscopy (FESEM) analysis assessed the bone-implant interface's morphological characteristics. The FESEM micrograph at five and twelve weeks shows that volume fraction porosity plays a crucial role in the early stage of osteointegration. The porous Ta with a porosity of 30 % shows a well-ingrown bone at five weeks of implantation that demonstrates bone-material interlocking. However, when the push-out was performed, the broken bone material indicates that the mechanical properties were similar, if not more substantial, than the bone's strength [58].

Wei et al. developed a biphasic construct combining porous tantalum (pTa) fabricated via chemical vapor deposition (CVD) and a 3D collagen membrane (3D CM), each seeded with BMSCs or chondrocytes, for repairing large goat femoral osteochondral defects. Mechanical evaluation revealed a compressive strength of 43.04 MPa for pTa and 3.40 MPa for 3D CM, with tensile and shear strengths also measured at the pTa–CM interface using porcine fibrin sealant. The study further confirmed that

FaST - Jurnal Sains dan Teknologi, Vol. 10, No.1, Mei 2026
e-ISSN 2598-9596
DOI: https://doi.org/10.19166/fastjst.v10i1.10486
Available online at: https://ojs.uph.edu/index.php/FaSTJST/article/view/10486

porous Ta's elastic modulus sits between the cortical and cancellous bone range, conducive to bone remodeling, without impeding mechanical performance or cell viability [73].

2.4 Molecular Mechanisms (MAPK/ERK, Macrophage polarization, BMP signaling)

Additive manufacturing (AM), fabricated porous tantalum (pTa) scaffolds are engineered to harmonize mechanical strength with biological activity, supporting cell attachment, proliferation, and osseointegration. These scaffolds, designed with precise pore architecture, have consistently demonstrated excellent biocompatibility and non-toxicity in both in vitro and in vivo settings [74]. The surface properties, including micro- and nano-scale topography and hydrophilicity, play a critical role in initial cell adhesion; scaffold modifications with bioactive coatings, such as peptides or extracellular matrix molecules, further facilitate this attachment and subsequent cell growth. Incorporating osteoconductive agents such as bone morphogenetic proteins (BMPs) or growth factors into the scaffold matrix has been shown to stimulate osteogenesis and vascularization, enhancing graft integration and bone regeneration in both laboratory and animal models [75].

Zhou et al. reported that mesenchymal stem cell (MSC)-seeded porous tantalum scaffolds demonstrate considerable potential for bone regeneration due to their favorable mechanical properties, biocompatibility, and capacity to support MSC adhesion, proliferation, and osteogenic differentiation. The synergistic interaction between scaffold architecture and cellular activity suggests translational relevance for bone tissue engineering and orthopedic reconstruction, particularly in the management of complex defects and degenerative bone conditions. Quantitative assessments, including MTT assays, alkaline phosphatase (ALP) activity, calcium deposition analysis, bone volume fraction (BV/TV), and push-out mechanical testing, consistently indicate enhanced osteogenesis and improved interfacial integration when porous tantalum is combined with MSCs.[76].

An inflammatory microenvironment orchestrated by macrophages is pivotal to bone repair. Sun et al. demonstrated that tantalum nanoparticles (TaNPs) are non-cytotoxic to RAW 264.7 macrophages, which can effectively phagocytose these particles without compromising viability. Moreover, TaNPs (5 μg/mL) suppressed the expression of pro-inflammatory genes (IL-1β, IL-18, TNF-α, iNOS) and induced anti-inflammatory markers (IL-10, TGF-β1, VEGFA) under LPS and IFN-γ stimulation. The study also observed increased M2-like polarization and reduced intracellular ROS, suggesting that TaNPs promote a reparative macrophage phenotype and regulate immune responses, beneficial for bone regeneration [77].

Porous tantalum (Ta) scaffolds functionalized with bone morphogenetic protein-7 (BMP-7) have shown enhanced osteochondral repair in preclinical models. Wang et al. developed a porous Ta rod loaded with BMP-7 and implanted it into rabbit medial femoral condyle osteochondral defects. Histological analysis at 16 weeks post-operation revealed significantly greater regeneration of both subchondral bone and cartilage, fibrocartilage and fibrous tissue, compared to unmodified Ta implants and empty controls. Micro-CT and biomechanical testing confirmed increased bone volume fraction and superior interface strength in the BMP-7-modified group. These results support combining osteo-inductive factors like BMP-7 with porous Ta scaffolds to stimulate MSC differentiation and improve graft integration in bone repair [78].

In a porcine ALIF model, Huang et al. evaluated porous tantalum (Ta) pedicle-screw implants and carbon-fiber cages, both with and without concurrent alendronate (ALN) administration. Histological analysis at 3 months revealed that Ta implants, particularly those with pedicle screw fixation, achieved improved bone ingrowth and fusion strength. Animals treated with ALN showed notably greater bone volume in the Ta implant's central hole and porous structure than untreated counterparts, while fibrous tissue presence remained comparable. Importantly, long-term ALN withdrawal did not sustain enhanced bone ingrowth, indicating that its benefits are limited to the early post-operative phase [79].

Dou et al. investigated the molecular mechanism by which porous tantalum (pTa) scaffolds promote osteogenic differentiation of bone marrow mesenchymal stem cells (BMMSCs). They demonstrated that BMMSCs cultured on pTa exhibited significantly higher mRNA expression of osteogenic markers, osterix (OSX), collagen I (COL-I), osteonectin (OSN), and osteocalcin (OCN), compared to titanium controls. This upregulation was accompanied by increased phosphorylation of ERK, indicating activation of the MAPK/ERK signaling cascade. Notably, inhibition of ERK using

FaST - Jurnal Sains dan Teknologi, Vol. 10, No.1, Mei 2026
e-ISSN 2598-9596
DOI: https://doi.org/10.19166/fastjst.v10i1.10486
Available online at: https://ojs.uph.edu/index.php/FaSTJST/article/view/10486

U0126 attenuated both ERK phosphorylation and the elevated expression of osteogenic genes, confirming that pTa induces osteogenesis through the MAPK/ERK pathway in vitro [80].

Guo et al. investigated the osteogenic potential of 3D-printed porous tantalum scaffolds versus porous Ti6Al4V scaffolds using human bone marrow–derived mesenchymal stem cells (hBMSCs). They found significantly enhanced expression of early osteogenic markers, RUNX2, ALP, and COL1, in the Ta group compared to Ti and controls. Late markers OCN and OPN were similar on day 7 but showed elevated levels in the Ta group on day 14, indicating sustained osteogenic differentiation promoted by porous tantalum scaffolds [54].

2.5 Clinical Evidence of Porous Tantalum Application in Medical

Beyond experimental and preclinical investigations, porous tantalum has demonstrated substantial clinical applicability across multiple orthopedic and dental indications. Its high porosity, interconnected architecture, and favorable elastic modulus enable enhanced mechanical interlocking, bone in-growth, and long-term implant stability in load-bearing environments. Accumulating clinical evidence from dental implants, hip arthroplasty, osteonecrosis management, and knee revision procedures underscores the translational potential of porous tantalum-based devices. The following sections summarize representative clinical outcomes across major application domains, highlighting functional recovery, implant survivorship, and radiographic evidence of osseointegration.

2.5.1 Dental Surgery Application

The clinical application of porous tantalum trabecular metal (PTTM) in dental implants has expanded significantly. PTTM-enhanced titanium implants offer superior osseointegration and are increasingly preferred for immediate placement procedures over conventional dental implants. In a rabbit femoral condyle model, Al Deeb et al. reported that PTTM-enhanced implants achieved significantly higher bone-to-implant contact (BIC: $57.9 \pm 6.5\%$ vs. $47.6 \pm 8.0\%$) and increased peri-implant bone volume compared to traditional titanium screws ($p < 0.05$) [81]. Additionally, Cui et al., study using vacuum plasma-sprayed micro-nano porous Ta–coated Ti implants found that the Ta coating enhanced hydrophilicity, protein adsorption, and mesenchymal stem cell activity, while canine mandible implants showed increased bone mineral density and new bone formation [82]. These recent findings confirm that PTTM modifications improve implant osseointegration and mechanical stability. Such advances support the use of PTTM implants, especially for immediate dental applications and in patients with high clinical risks or compromised sites.

Edelmann et al. conducted a retrospective analysis comparing porous tantalum trabecular metal (PTTM) implants to Tapered Screw-Vent (TSV) titanium implants, both used with and without demineralized bone matrix (DBM), for immediate post-extraction dental placement. The study found that PTTM implants combined with DBM had a significantly lower risk of peri-implant bone loss and a higher probability of bone gain after one year, compared to their TSV counterparts. This suggests incorporating DBM with PTTM implants provides a bone-preserving strategy equivalent to autografts for immediate placement protocols [83].

Bencharit et al. compared porous tantalum trabecular metal (PTTM) implants to titanium alloy implants during early wound healing in the human oral cavity. In a split-mouth design involving 12 patients, one PTTM and one Ti implant were placed in the mandible. Biopsies taken in two weeks showed significantly higher expression of neovascularization, wound healing, and osteogenesis genes, including BMPs, collagens, and growth factors in the PTTM group compared to the Ti controls. Histological analysis for four weeks revealed greater bone infiltration and vascularization around PTTM surfaces. These findings suggest that PTTM implants enhance early bone ingrowth and vascularization, leading to faster and more robust bone healing than standard titanium implants [84].

2.5.2 Hip-Joint Implant Application

Unger et al. evaluated the performance of a trabecular metal (TM) monoblock acetabular cup in revision total hip arthroplasty (THA). In a cohort of 60 patients with prior acetabular component failure, followed by an average of 42 months, radiographs showed full graft incorporation and no postoperative infection or aseptic loosening cases. Harris Hip Scores improved significantly from a preoperative average of 74.8 to 94.4 at final follow-up, indicating excellent implant stability and bone ingrowth facilitated by

FaST - Jurnal Sains dan Teknologi, Vol. 10, No.1, Mei 2026
e-ISSN 2598-9596
DOI: https://doi.org/10.19166/fastjst.v10i1.10486
Available online at: https://ojs.uph.edu/index.php/FaSTJST/article/view/10486

TM implants' high friction coefficient and porous architecture [85]. Haidemenopoulos et al. conducted a histological analysis of a retrieved porous tantalum (Ta) monoblock acetabular cup removed four years post-implantation in a female THA patient. Using optical and scanning electron microscopy, they observed gradual human bone ingrowth into the first two rows of porous cells, reaching a depth of approximately 1.5–2 mm, with bone deposition directly on Ta struts and progressive densification into hydroxyapatite as evidenced by matching Ca:P ratios [86]. Moen et al. performed a radiographic evaluation of 51 THA patients with implanted porous Ta monoblock cups. At an average follow-up of 10.3 years, helical CT scans with metal suppression protocols revealed no signs of periprosthetic osteolysis in the pelvis or proximal femur. This suggests that the monoblock porous architecture may reduce osteolytic risk compared to conventional designs [87]. Tsao et al. do not apply to femoral head implants. Instead, current evidence shows that modern porous Ta rods, such as Runze- or AM-fabricated TaBw01 devices, offer excellent mechanical stability in ONFH. Clinical implants demonstrate no radiographic signs of loosening or radiolucency, and their elastic modulus is well-matched to native bone, providing initial fixation and long-term integration [88].

In early-stage osteonecrosis of the femoral head (ARCO I–II), implantation of porous tantalum rods has shown promising results. Huang et al. compared a newly developed Runze porous Ta rod to a standard Zimmer Ta implant in a cohort study with at least three years of follow-up, reporting comparable improvements in Harris Hip Scores and demonstrating substantial bone ingrowth into the rod's porous architecture [89]. Similarly, Zhang et al. analyzed outcomes in 86 ARCO II patients. They concluded that mechanical stability depends heavily on precise implant alignment and rod length, noting that optimized placement enhances long-term graft support [90].

In a clinical study by Zhao et al., the authors evaluated a novel technique that combined autologous bone marrow mesenchymal stem cells (BMMSCs) with porous tantalum rod implantation and vascularized iliac bone grafting to treat end-stage osteonecrosis of the femoral head (ARCO IIIc–IV). Over a mean follow-up of 64 months, the joint-preserving surgery resulted in a success rate of 89.5% for stage IIIc hips and 75% for stage IV hips, significantly reducing the need for total hip arthroplasty. Harris Hip Scores improved markedly from 38.7 preoperatively to 77.2 postoperatively, demonstrating both safety and effective restoration of hip function in end-stage ONFH patients [91].

2.5.3 Knee Implant Application

A multicenter retrospective cohort study by Kayani et al. (2024) followed 152 patients who underwent revision TKA using porous Ta metaphyseal cones (mean follow-up: 5.6 years). This study, including cases of aseptic loosening and infection, reported 100% cone survival (no revisions of cones themselves) and 83.8% overall implant survival, with consistent radiographic evidence of osseointegration and satisfactory functional scores [92].

Hadley et al. conducted a single-center study involving 228 revision TKAs with tibial Ta cones, reporting 97% survivorship free of aseptic cone removal and 88% overall cone survival at a mean follow-up of 6.3 years (range 5–10 years). Only minor radiolucencies appeared in <5% of cases, suggesting durable fixation and bone ingrowth [93].

A 2024 finite-element analysis by Piovan et al. alongside preliminary clinical data showed that 3D-printed patient-specific metaphyseal Ta cones achieved favorable load distribution and stress stability, suggesting superior biomechanical performance compared to traditional stems [94].

Mao et al. researched a patient-specific 3D-printed porous tantalum (Ta) prosthesis for knee joint revision surgery in an 84-year-old man, using experimental mechanical testing and finite element analysis (FEA) derived from patient CT data, a novel methodology in clinical practice. By conducting mechanical tests on several pore and wire combinations produced using selective laser melting (SLM), the researchers determined the ideal design (600 μm pore, 900 μm wire), which resulted in a Young's modulus of 5.72 GPa and a yield strength of 172 MPa. This design satisfied all mechanical and biomechanical safety standards, with prosthesis strength surpassing load stress, tibial strain within the optimal range of 400–3,000 με, and tibial stress remaining below 60 MPa. Following implantation in 2017, a five-year follow-up demonstrated exceptional bone-prosthesis integration and complete patient recovery. This research creates a clinically proven framework for biomechanical matching using CT-based design optimization and finite element analysis, establishing new benchmarks for individualized orthopedic implants. It underscores the need for future models to combine anisotropic bone

FaST - Jurnal Sains dan Teknologi, Vol. 10, No.1, Mei 2026
e-ISSN 2598-9596
DOI: https://doi.org/10.19166/fastjst.v10i1.10486
Available online at: https://ojs.uph.edu/index.php/FaSTJST/article/view/10486

characteristics and localized bone density to improve mechanical precision, thereby promoting individualized, load-bearing, and physiologically integrated approaches in revision arthroplasty [95].

3. MSC-driven bone generation using 3D printed Tantalum Scaffolds

Integrating mesenchymal stem cells (MSCs) with 3D-printed porous tantalum (PTa) scaffolds has become a practical approach for promoting bone regeneration. Recent studies have concentrated on augmenting these scaffolds using bioactive surface changes, nano-topography, and biological agents to enhance MSC adhesion, differentiation, and in vivo bone formation. The following table juxtaposes five recent experiments, emphasizing critical manufacturing techniques, MSC integration, scaffold improvements, assessment models, and results. The comparative study showed in **Table 4** that nano-topography of PTa significantly enhanced BMSC adhesion, as reported by Zhang et al. (2023) [96]. Liu et al also reported that porous pTa promoted M2 macrophage shift, inhibited inflammation, and enhanced BMSC osteogenesis via P38-MAPK [97]. Jiao et al. also state that 70–80% porosity of PTa provided maximal BMSC proliferation, osteogenic gene expression, and bone ingrowth; 70% porosity was optimal [98]. Yu et al.confirmed a review of customized PTa high BMSC proliferation, osteogenesis, corrosion resistance, and overall biocompatibility [99]. Zhao et al. reported that porous Ta promoted osteogenesis and angiogenesis, indicating vascularized bone regeneration [100].

Table 4 Comparative Study of Recent Studies of 3D-Printed Porous Tantalum

Study	Fabrication	MSC Integration	Scaffold Modification	Model	Results
Zhang et al. (2023) [96]	SLM-printed PTa with hydrothermal nano-topography	Rat BMSCs (in vitro)	Nano-structured surface via alkali–heat–hydrothermal treatment	Rabbit mandibular defect (in vivo)	Nano-topography significantly enhanced BMSC adhesion, osteogenic differentiation (↑ALP, mineralization), and early bone formation.
Liu et al. (2025) [97]	3D-printed PTa with polydopamine; MZIF-8 drug delivery	BMSC regulation via macrophage polarization	Polydopamine + MZIF-8 + melatonin for immunoregulatory release	Osteoporotic rat femur (in vivo)	Promoted M2 macrophage shift, inhibited inflammation, enhanced BMSC osteogenesis via P38-MAPK
Jiao et al. (2023) [98]	SLM-printed PTa scaffolds (60%, 70%, 80% porosity)	Rat BMSCs (in vitro)	Varying porosity only	Rat femoral defect (in vivo)	70–80% porosity provided maximal BMSC proliferation, osteogenic gene expression, and bone ingrowth; 70% porosity was optimal
Yu et al. (2024) [99]	SLM-printed PTa with corrosion-resistant surface	Human BMSCs (in vitro)	Review of customized PTa (no specific coating)	-	Confirmed high BMSC proliferation, osteogenesis, corrosion resistance, and overall biocompatibility
Zhao et al. (2025) [100]	Porous Ta integrated with gelatin nanoparticle (GNP) hydrogel	BMSC + endothelial co-culture	GNP hydrogel for growth factor delivery and angiogenesis	In vivo vascularized bone model	Promoted both osteogenesis and angiogenesis, indicating vascularized bone regeneration

4. Conclusions and Future Directions

Three-dimensional (3D)-printed porous tantalum (Ta) scaffolds represent a significant advancement in musculoskeletal tissue engineering. Their favorable mechanical compatibility, corrosion resistance, and high biocompatibility provide an effective platform for supporting bone ingrowth and long-term osseointegration. Additive manufacturing technologies, including selective laser melting and laser-

engineered net shaping, enable precise control of pore size, porosity, and internal architecture, allowing the fabrication of scaffolds that closely mimic native bone structure and mechanical behavior.

The incorporation of bone marrow–derived mesenchymal stem cells (BMSCs) further enhances the regenerative capacity of porous Ta constructs by promoting osteogenic differentiation, extracellular matrix deposition, and mineralization. Emerging translational studies indicate that patient-specific porous Ta implants designed using biomechanical modeling and finite element analysis demonstrate promising mid-term clinical outcomes, reinforcing the clinical feasibility of personalized scaffold strategies.

Future research should prioritize optimization of graded pore architectures to better replicate cortical–cancellous transitions, alongside long-term in vivo evaluation of remodeling, vascularization, and fatigue resistance under physiological loading conditions. Standardization of scaffold design parameters, manufacturing reproducibility, and regulatory pathways will be critical for accelerating broader clinical adoption. Additionally, integrating immunomodulatory strategies and coupled osteogenic–angiogenic approaches may further enhance therapeutic outcomes for complex bone defects.

Despite continued challenges, including manufacturing scalability and limited long-term randomized clinical data, the convergence of advanced additive manufacturing, regenerative cell therapy, and biomechanical optimization positions porous tantalum scaffolds as a promising strategy for next-generation orthopedic reconstruction.

5. Policy on the Use of Generative Artificial Intelligence (AI)

Generative artificial intelligence (ChatGPT, OpenAI) was used solely for language editing and clarity improvement. The authors take full responsibility for the originality, accuracy, and integrity of the content of this manuscript.

Acknowledgement

M.L. conducted the comprehensive literature review, prepared all graphical illustrations using Adobe Illustrator®, interpreted the data, and drafted the manuscript. All co-authors contributed to critical revision of the intellectual content and approved the final version prior to submission. M.X.S. provided overall supervision and guidance throughout the study.

Strength of the Study

This review provides a comprehensive and integrative synthesis of 3D-printed porous tantalum (Ta) scaffolds by systematically linking scaffold design parameters, additive manufacturing techniques, mechanical performance, biological mechanisms, and clinical outcomes. Unlike prior reviews that primarily focus on titanium-based biomaterials or broadly discuss metallic scaffolds, this study specifically centers on porous Ta and consolidates interdisciplinary evidence spanning material science, mechanobiology, molecular signaling pathways, and long-term clinical follow-up data.

A key strength lies in the integration of mechanical benchmarks with cellular, osteogenic, and immunomodulatory pathways, thereby bridging fundamental laboratory research with translational orthopedic applications. By contextualizing scaffold architecture within both biomechanical requirements and biological responses, this review offers a clinically oriented framework that supports patient-specific implant design and future precision-based bone repair strategies.

Limitation of the Study

Several limitations should be acknowledged. First, as a narrative review, the study does not employ a formal systematic review protocol or meta-analytic approach; therefore, selection bias cannot be entirely excluded. Although efforts were made to prioritize methodological rigor and thematic relevance, the absence of quantitative synthesis limits direct statistical comparability across studies.

Second, substantial heterogeneity exists among the included studies with respect to scaffold architecture, pore geometry, additive manufacturing platforms, animal models, mesenchymal stem cell sources, and outcome assessment methods. This variability restricts direct quantitative comparison of mechanical and biological outcomes.

Third, although preclinical evidence is extensive, long-term human clinical studies, particularly

large-scale randomized controlled trials, remain limited. In addition, manufacturing variability across additive platforms may influence reported mechanical properties and biological performance, potentially affecting reproducibility and translational standardization.

Future systematic analyses and standardized reporting frameworks are warranted to strengthen evidence comparability and accelerate clinical translation.

Figure Preparation and Copyright Statement

All schematic illustrations (Figures 1–3) were independently developed by the authors using Adobe Illustrator® based on synthesized concepts derived from the reviewed literature. No previously published copyrighted images were reproduced. Where conceptual elements were adapted from existing studies, appropriate citations have been provided in the corresponding figure legends.

References

[1] Fernandez-Fairen, M., Querales, V., Jakowlew, A., Torres, A., Murcia, A., & Gil-Garay, E. (2010). Tantalum is a good bone graft substitute in tibial tubercle advancement. *Clinical Orthopaedics and Related Research*, *468*(5), 1284–1295. https://doi.org/10.1007/s11999-009-1115-0

[2] Huang, G., Pan, S.-T., & Qiu, J.-X. (2021). The clinical application of porous tantalum and its new development for bone tissue engineering. *Materials*, *14*(10), 2647. https://doi.org/10.3390/ma14102647

[3] Ni, J., Ling, H., Zhang, S., Wang, Z., Peng, Z., Benyshek, C., Zan, R., Miri, A. K., Li, Z., Zhang, X., Lee, J., Lee, K. J., Kim, H. J., Tebon, P., Hoffman, T., Dokmeci, M. R., Ashammakhi, N., Li, X., & Khademhosseini, A. (2019). Three-dimensional printing of metals for biomedical applications. *Materials today. Bio*, *3*, 100024. https://doi.org/10.1016/j.mtbio.2019.100024

[4] Hadjidakis, D. J., & Androulakis, I. I. (2006). Bone remodeling. *Annals of the New York Academy of Sciences*, *1092*, 385–396. https://doi.org/10.1196/annals.1365.035

[5] Arias, C. F., Herrero, M. A., Echeverri, L. F., Oleaga, G. E., & López, J. M. (2018). Bone remodeling: A tissue-level process emerging from cell-level molecular algorithms. *PloS one*, *13*(9), e0204171. https://doi.org/10.1371/journal.pone.0204171

[6] Florencio-Silva, R., Sasso, G. R., Sasso-Cerri, E., Simões, M. J., & Cerri, P. S. (2015). Biology of Bone Tissue: Structure, Function, and Factors That Influence Bone Cells. *BioMed research international*, *2015*, 421746. https://doi.org/10.1155/2015/421746

[7] Torres, Y., Lascano, S., Bris, J., Pavón, J., & Rodriguez, J. A. (2014). Development of porous titanium for biomedical applications: A comparison between loose sintering and space-holder techniques. *Materials Science and Engineering: C*, *44*, 330–334. https://doi.org/10.1016/j.msec.2013.11.036

[8] Wauthle, R., van der Stok, J., Amin Yavari, S., Van Humbeeck, J., Kruth, J. P., Zadpoor, A. A., Weinans, H., Mulier, M., & Schrooten, J. (2015). Additively manufactured porous tantalum implants. *Acta biomaterialia*, *14*, 217–225. https://doi.org/10.1016/j.actbio.2014.12.003

[9] Kruth, J. P., Levy, G., Klocke, F., & Childs, T. H. C. (2007). Consolidation phenomena in laser and powder-bed based layered manufacturing. *CIRP Annals - Manufacturing Technology*, *56*(2), 730–759. https://doi.org/10.1016/j.cirp.2007.10.004

[10] Izadi, M., Farzaneh, A., Mohammed, M., Gibson, I., & Rolfe, B. (2020). A review of laser engineered net shaping (LENS) build and process parameters of metallic parts. *Rapid prototyping journal*, *26*(6), 1059-1078. https://doi.org/10.1108/RPJ-04-2018-0088

[11] Kapat, K., Srivas, P. K., Rameshbabu, A. P., Maity, P. P., Jana, S., Dutta, J., Majumdar, P., Chakrabarti, D., & Dhara, S. (2017). Influence of Porosity and Pore-Size Distribution in Ti6Al4 V Foam on Physicomechanical Properties, Osteogenesis, and Quantitative Validation of Bone Ingrowth by Micro-Computed Tomography. *ACS applied materials & interfaces*, *9*(45), 39235–39248. https://doi.org/10.1021/acsami.7b13960

[12] Dejene, N. D., & Lemu, H. G. (2023). Current status and challenges of powder bed fusion-based metal additive manufacturing: Literature review. *Metals, 13*(2), 424. https://doi.org/10.3390/met13020424

[13] Wu, Y., Lu, Y., Zhao, M., Bosiakov, S., & Li, L. (2022). A critical review of additive manufacturing techniques and associated biomaterials used in bone tissue engineering. *Polymers*, *14*(10), 2117. https://doi.org/10.3390/polym14102117

[14] Hu, D., & Kovacevic, R. (2003). Sensing, modeling and control for laser based additive manufacturing. *International Journal of Machine Tools and Manufacture*, *43*(1), 51–60. https://doi.org/10.1016/S0890-6955(02)00163-3

[15] Yap, C. Y., Chua, C. K., Dong, Z. L., Liu, Z. H., Zhang, D. Q., Loh, L. E., & Sing, S. L. (2015). Review of selective laser melting: Materials and applications. *Applied Physics Reviews*, *2*(4), 041101. https://doi.org/10.1063/1.4935926
[16] Balla, V. K., Banerjee, S., Bose, S., & Bandyopadhyay, A. (2010). Direct laser processing of a tantalum coating on titanium for bone replacement structures. *Acta Biomaterialia, 6*(6), 2329–2334. https://doi.org/10.1016/j.actbio.2009.11.021
[17] Hussein, K. H., Park, K. M., Kang, K. S., & Woo, H. M. (2016). Biocompatibility evaluation of tissue-engineered decellularized scaffolds for biomedical application. *Materials Science and Engineering: C, 67*, 766–778. https://doi.org/10.1016/j.msec.2016.05.068
[18] Gibson, I., Rosen, D. W., & Stucker, B. (2020). *Additive manufacturing technologies* (3rd ed.). Springer. https://doi.org/10.1007/978-3-030-56127-7
[19] Wang, Z., Wang, C., Li, C., Qin, Y., Zhong, L., Chen, B., Li, Z., Liu, H., Chang, F., & Wang, J. (2017). Analysis of factors influencing bone ingrowth into three-dimensional printed porous metal scaffolds: A review. *Journal of Alloys and Compounds*, *717*, 271–285. https://doi.org/10.1016/j.jallcom.2017.05.079
[20] Matena, J., Petersen, S., Gieseke, M., Kampmann, A., Teske, M., Beyerbach, M., Murua Escobar, H., Haferkamp, H., Gellrich, N.-C., & Nolte, I. (2015). SLM produced porous titanium implant improvements for enhanced vascularization and osteoblast seeding. *International Journal of Molecular Sciences, 16*(4), 7478–7492. https://doi.org/10.3390/ijms16047478
[21] Hulbert, S. F., Young, F. A., Mathews, R. S., Klawitter, J. J., Talbert, C. D., & Stelling, F. H. (1970). Potential of ceramic materials as permanently implantable skeletal prostheses. *Journal of Biomedical Materials Research*, *4*(3), 433–456. https://doi.org/10.1002/jbm.820040309
[22] Cheng, A., Humayun, A., Cohen, D. J., Boyan, B. D., & Schwartz, Z. (2014). Additively manufactured 3D porous Ti-6Al-4V constructs mimic trabecular bone structure and regulate osteoblast proliferation, differentiation and local factor production in a porosity and surface roughness dependent manner. *Biofabrication*, *6*(4), 045007. https://doi.org/10.1088/1758-5082/6/4/045007
[23] Biemond, J. E., Aquarius, R., Verdonschot, N., & Buma, P. (2011). Frictional and bone ingrowth properties of engineered surface topographies produced by electron beam technology. *Archives of Orthopaedic and Trauma Surgery*, *131*(5), 711–718. https://doi.org/10.1007/s00402-010-1218-9
[24] Vaiani, L., Boccaccio, A., Uva, A. E., Palumbo, G., Piccininni, A., Guglielmi, P., Cantore, S., Santacroce, L., Charitos, I. A., & Ballini, A. (2023). Ceramic Materials for Biomedical Applications: An Overview on Properties and Fabrication Processes. *Journal of functional biomaterials*, *14*(3), 146. https://doi.org/10.3390/jfb14030146
[25] Otsuki, B., Takemoto, M., Fujibayashi, S., Neo, M., Kokubo, T., & Nakamura, T. (2006). Pore throat size and connectivity determine bone and tissue ingrowth into porous implants: Three-dimensional micro-CT based structural analyses of porous bioactive titanium implants. *Biomaterials*, *27*(35), 5892–5900. https://doi.org/10.1016/j.biomaterials.2006.08.013
[26] Prananingrum, W., Naito, Y., Galli, S., Bae, J., Sekine, K., Hamada, K., Tomotake, Y., Wennerberg, A., Jimbo, R., & Ichikawa, T. (2016). Bone ingrowth of various porous titanium scaffolds produced by a moldless and space holder technique: An in vivo study in rabbits. *Biomedical Materials*, *11*(1), 015012. https://doi.org/10.1088/1748-6041/11/1/015012
[27] Bobyn, J. D., Stackpool, G. J., Hacking, S. A., Tanzer, M., & Krygier, J. J. (1999). Characteristics of bone ingrowth and interface mechanics of a new porous tantalum biomaterial. *Journal of Bone and Joint Surgery - British Volume*, *81*(5), 907–914. https://doi.org/10.1302/0301-620x.81b5.9283
[28] Li, J. P., Habibovic, P., van den Doel, M., Wilson, C. E., de Wijn, J. R., van Blitterswijk, C. A., & de Groot, K. (2007). Bone ingrowth in porous titanium implants produced by 3D fiber deposition. *Biomaterials*, *28*(18), 2810–2820. https://doi.org/10.1016/j.biomaterials.2007.02.020
[29] Navarro, M., Michiardi, A., Castaño, O., & Planell, J. A. (2008). Biomaterials in orthopaedics. *Journal of the Royal Society Interface*, *5*(27), 1137–1158. https://doi.org/10.1098/rsif.2008.0151
[30] Rezvani Sichani, H., Atapour, M., Ashrafizadeh, F., Galati, M., & Saboori, A. (2024). Mechanical, electrochemical and permeability behaviour of Ti6Al–4V scaffolds fabricated by electron beam powder bed fusion for orthopedic implant applications: The role of cell type and cell size. *Journal of Materials Research and Technology*, *28*, 3240–3257. https://doi.org/10.1016/j.jmrt.2023.12.260
[31] Yang, W., Yu, H., Liang, H., Li, D., & Zhang, Y. (2022). Properties of additive-manufactured open porous titanium structures for patient-specific load-bearing implants. *Frontiers in Mechanical Engineering*, *7*, Article 830126. https://doi.org/10.3389/fmech.2021.830126
[32] Liang, Y., Li, H., Xu, J., Li, X., Qi, M., & Hu, M. (2014). Biological properties of titanium cages modified with hydroxyapatite: A cellular and molecular analysis. *International Journal of Molecular Sciences*, *15*(6), 9952–9964. https://doi.org/10.3390/ijms15069952

[33] Krishna, B. V., Bose, S., & Bandyopadhyay, A. (2007). Fabrication of porous hydroxyapatite scaffolds by selective laser sintering and their interaction with osteoblast cells. *Acta Biomaterialia*, *3*(6), 997–1006. https://doi.org/10.1016/j.actbio.2007.04.007
[34] Alvarez, K., & Nakajima, H. (2009). Design of porous metallic materials for biomedical applications. *Materials*, *2*(2), 790–832. https://doi.org/10.3390/ma2020790
[35] Karageorgiou, V., & Kaplan, D. (2005). Porosity of 3D biomaterial scaffolds and osteogenesis. *Biomaterials*, *26*(27), 5474–5491. https://doi.org/10.1016/j.biomaterials.2005.02.002
[36] Matassi, F., Botti, A., Sirleo, L., Carulli, C., & Innocenti, M. (2013). Case series: Mineral bone metabolism in orthopedic care. *Clinical Cases in Mineral and Bone Metabolism*, *10*(2), 111–115.
[37] Bobyn, J. D., Pillar, R. M., Cameron, H. U., & Weatherly, G. C. (1980). The interface mechanics of porous-coated implants. *Clinical Orthopaedics and Related Research*, (*150*), 263–278.
[38] Zardiackas, L. D., Parsell, D. E., Dillon, L. D., Mitchell, D. W., Nunnery, L. A., & Poggie, R. (2001). Porous tantalum structures for orthopedic implants: Bone adaptation and mechanical properties. *Journal of Biomedical Materials Research*, *58*(2), 180–187. https://doi.org/10.1002/1097-4636(2001)58:2<180::AID-JBM1005>3.0.CO;2-5
[39] Levine, B. R., Sporer, S., Poggie, R. A., Della Valle, C. J., & Jacobs, J. J. (2006). Experimental and clinical performance of porous tantalum in orthopedic implants. *Biomaterials*, *27*(20), 4671–4678. https://doi.org/10.1016/j.biomaterials.2006.04.041
[40] Cohen, R. (2002). A porous tantalum trabecular metal: basic science. *American Journal of Orthopedics* (*Belle Mead, N.J.*), *31*(4), 216–217. PMID: 12008853
[41] Cohen, R. (2006). Experimental and clinical performance of porous tantalum in orthopedic surgery. *Biomaterials*, *27*(27), 4671–4678. https://doi.org/10.1016/j.biomaterials.2006.04.041
[42] Martin, P. M. (2010). Overview of film and coating deposition methods. In P. M. Martin (Ed.), *Handbook of deposition technologies for films and coatings* (3rd ed., pp. 1–18). William Andrew Publishing
[43] Hacking, S. A., Bobyn, J. D., Toh, K., Tanzer, M., & Krygier, J. J. (2000). The influence of porous tantalum structure on bone ingrowth and implant fixation. *Journal of Biomedical Materials Research*, *52*(4), 631–638.
[44] Lu, M., Xu, S., Lei, Z. X., Lu, D., Cao, W., Huttula, M., Hou, C. H., Du, S. H., Chen, W., Dai, S. W., Li, H. M., & Jin, D. D. (2019). Application of a novel porous tantalum implant in a rabbit anterior lumbar spine fusion model: in vitro and in vivo experiments. *Chinese Medical Journal* (*English*), *132*(1), 51–59. https://doi.org/10.1097/CM9.0000000000000030
[45] Tanzer, M., Kantor, S., & Bobyn, J. D. (2001). Enhancement of bone growth into porous-coated implants using non-invasive low intensity ultrasound. *Journal of Orthopaedic Research*, *19*(2), 195–199. https://doi.org/10.1016/S0736-0266(00)00034-6
[46] Bobyn, J. D., Toh, K. K., Hacking, S. A., Tanzer, M., & Krygier, J. J. (1999). Characterization of porous tantalum implants in animal models. *Journal of Biomedical Materials Research*, *4*, 347–354.
[47] Kim, D. G., Huja, S. S., Tee, B. C., Larsen, P. E., Kennedy, K. S., Chien, H. H., Lee, J. W., & Wen, H. B. (2013). Bone ingrowth and initial stability of titanium and porous tantalum dental implants: A pilot canine study. *Implant Dentistry, 22*(4), 399–405. https://doi.org/10.1097/ID.0b013e31829b17b5
[48] Battula, S., Lee, J. W., Wen, H. B., Papanicolaou, S., Collins, M., & Romanos, G. E. (2015). Evaluation of different implant designs in a ligature-induced peri-implantitis model: A canine study. *The International Journal of Oral & Maxillofacial Implants*, *30*(3), 534–545.doi:10.11607/jomi.3737.
[49] Lee, J. W., Wen, H. B., Gubbi, P., & Romanos, G. E. (2018). New bone formation and trabecular bone microarchitecture of highly porous tantalum compared to titanium implant threads: A pilot canine study. *Clinical Oral Implants Research, 29*(2), 164–174. doi:10.1111/clr.13074.
[50] Wang, Y., Xu, Y., Jiang, Y., Liu, L., & Yang, Y. (2022). Advances in surface modification of tantalum and porous tantalum for rapid osseointegration: A thematic review. *Frontiers in Bioengineering and Biotechnology*, *10*, 983695. https://doi.org/10.3389/fbioe.2022.983695
[51] Fu, W. M., Yang, L., Wang, B. J., Xu, J. K., Wang, J. L., Qin, L., & Zhao, D. W. (2016). Porous tantalum seeded with bone marrow mesenchymal stem cells attenuates steroid-associated osteonecrosis. *European review for medical and pharmacological sciences*, *20*(16), 3490–3499.
[52] Wu, L. C., Hsieh, Y. Y., Hsu, T. S., Liu, P. Y., Tsuang, F. Y., Kuo, Y. J., Chen, C. H., Van Huynh, T., & Chiang, C. J. (2024). 3D-printed porous titanium suture anchor: a rabbit lateral femoral condyle model. *BMC musculoskeletal disorders*, *25*(1), 559. https://doi.org/10.1186/s12891-024-07666-w
[53] Luo, C., Wang, C., Wu, X., Xie, X., Wang, C., Zhao, C., Zou, C., Lv, F., Huang, W., & Liao, J. (2021). Influence of porous tantalum scaffold pore size on osteogenesis and osteointegration: A comprehensive study based on 3D-printing technology. *Materials Science and Engineering: C*, 129, 112382. https://doi.org/10.1016/j.msec.2021.112382
[54] Wang, H., Su, K., Su, L., Liang, P., Ji, P., & Wang, C. (2019). Comparison of 3D-printed porous tantalum and titanium scaffolds on osteointegration and osteogenesis. *Materials Science and Engineering: C*, *104*, 109908. https://doi.org/10.1016/j.msec.2019.109908

[55] Bandyopadhyay, A., Mitra, I., Shivaram, A., Dasgupta, N., & Bose, S. (2019). Direct comparison of additively manufactured porous titanium and tantalum implants toward in vivo osseointegration. *Additive Manufacturing*, *28*, 259–266. https://doi.org/10.1016/j.addma.2019.04.025
[56] Zou, X., Xue, Q., Li, H., Bünger, M., Lind, M., & Bünger, C. (2003). Effect of alendronate on bone ingrowth into porous tantalum and carbon fiber interbody devices: An experimental study on spinal fusion in pigs. *Acta Orthopaedica*, *74*(5), 596–603. https://doi.org/10.1080/00016470310018027
[57] Zou, X., Li, H., Bünger, M., Egund, N., Lind, M., & Bünger, C. (2004). Bone ingrowth characteristics of porous tantalum and carbon fiber interbody devices: An experimental study in pigs. *The Spine Journal*, *4*(1), 99–106. https://doi.org/10.1016/S1529-9430(03)00407-8
[58] Fraser, D., Funkenbusch, P. D., Ercoli, C., & Meirelles, L. (2019). Bone response to porous tantalum implants in a gap-healing model. *Clinical Oral Implants Research*, *30*(2), 156–168. https://doi.org/10.1111/clr.13402
[59] Fraser, D., Funkenbusch, P., Ercoli, C., & Meirelles, L. (2019). Biomechanical analysis of the osseointegration of porous tantalum implants. *Journal of Prosthetic Dentistry, 123*(6), 811–820. https://doi.org/10.1016/j.prosdent.2019.09.014
[60] Mrosek, E. H., Chung, H. W., Fitzsimmons, J. S., O'Driscoll, S. W., Reinholz, G. G., & Schagemann, J. C. (2016). Porous tantalum biocomposites for osteochondral defect repair: A follow-up study in a sheep model. *Bone & Joint Research*, *5*(9), 403–411. https://doi.org/10.1302/2046-3758.59.BJR-2016-0070.R1
[61] Ren, B., Zhai, Z., Guo, K., Liu, Y., Hou, W., Zhu, Q., & Zhu, J. (2015). Porous tantalum-enhanced osteogenesis around implants. *International Journal of Clinical and Experimental Medicine*, *8*(3), 5055–5062. PMID: 26131078. Available at PubMed Central: https://www.ncbi.nlm.nih.gov/pmc/articles/PMC4483870/
[62] Albrektsson, T., & Johansson, C. (2001). Current interpretations of osseointegration. *European Spine Journal*, *10*(*Suppl 2*), S96–S101. https://doi.org/10.1007/s005860000292
[63] Koutsostathis, S. D., Tsakotos, G. A., Papakostas, I., & Macheras, G. A. (2009). Porous tantalum in orthopaedic surgery: Clinical perspectives. *Journal of Orthopaedics*, *6*, e3.
[64] Huang, B., Zou, X., Li, H., Xue, Q., & Bünger, C. (2013). Long-term performance of porous tantalum fusion cages in a goat cervical spine model. *European Spine Journal*, *22*(2), 287–297. https://doi.org/10.1007/s00586-012-2373-2
[65] Fan, H., Wang, G., Xiu, P., Wang, Y., & Yang, Y. (2021). Highly porous 3D-printed tantalum scaffolds have better biomechanical and microstructural properties than titanium scaffolds. *BioMed Research International*, *2021*, 2899043. https://doi.org/10.1155/2021/2899043
[66] Wei, et al. (2023). Fabrication of porous tantalum with low elastic modulus and tunable pore size for bone repair. *ACS Biomaterials Science & Engineering*, *9*, 23–34. https://doi.org/10.1021/acsbiomaterials.2c01239
[67] Bauer, T. W., & Schils, J. (1999). The pathology of total joint arthroplasty. *Skeletal Radiology*, *28*(8), 483–494. https://doi.org/10.1007/s002560050541
[68] Pokrass, C. (1990). *Tantalum in metals handbook*. In C. Pokrass (Ed.), Properties and Selection: Nonferrous Alloys and Special-Purpose Materials (Vol. 2, 10th ed., p. 571). ASM International.
[69] Black, J. (1994). Clinical applications of tantalum biomaterials. *Clinical Materials*, *16*(4), 167–173.
[70] Guo, Y., Xie, K., Jiang, W., Wang, L., Li, G., Zhao, S., Wu, W., & Hao, Y. (2019). In vitro and in vivo study of 3D-printed porous tantalum scaffolds for repairing bone defects. *ACS Biomaterials Science & Engineering*, *5*(2), 1123–1133. https://doi.org/10.1021/acsbiomaterials.8b01094
[71] Blanco, J. F., Sánchez-Guijo, F. M., Carrancio, S., Muntion, S., García-Briñon, J., & del Cañizo, M.-C. (2011). Titanium and tantalum as mesenchymal stem cell scaffolds for spinal fusion: An in vitro comparative study. *European Spine Journal*, *20*(*Suppl 3*), 353–360. https://doi.org/10.1007/s00586-011-1901-8
[72] Wang, H., Su, K., Su, L., Liang, P., Ji, P., & Wang, C. (2019). Comparison of 3D-printed porous tantalum and titanium scaffolds on osteointegration and osteogenesis. *Materials Science and Engineering: C*, *104*, 109908. https://doi.org/10.1016/j.msec.2019.109908
[73] Wei, X., Liu, B., Liu, G., Yang, F., Cao, F., Dou, X., Yu, W., Wang, B., Zheng, G., Cheng, L., Ma, Z., Zhang, Y., Yang, J., Wang, Z., Li, J., Cui, D., Wang, W., Xie, H., Li, L., Zhang, F., Lineaweaver, W. C., & Zhao, D. (2019). Mesenchymal stem cell–tantalum scaffold constructs accelerate bone regeneration. *Stem Cell Research & Therapy*, *10*, 72. https://doi.org/10.1186/s13287-019-1176-273
[74] Liu, A., Wang, C., Zhao, Z., Zhu, R., Deng, S., Zhang, S., ... Li, D. (2025). Progress of porous tantalum surface-modified biomaterial coatings in bone tissue engineering. *Journal of Materials Science: Materials in Medicine*, *36*(26). https://doi.org/10.1007/s10856-025-06871-w
[75] Liu, X., Xie, Y., Yang, F., Huang, Y., Wang, C., Dai, K., & Zhang, X. (2023). Preparation, modification, and clinical application of porous tantalum scaffolds. *Frontiers in Bioengineering and Biotechnology*, *11*, 112793. https://doi.org/10.3389/fbioe.2023.1127939
[76] Zhou, Z., & Liu, D. (2022). Mesenchymal stem cell-seeded porous tantalum-based biomaterial: A promising choice for promoting bone regeneration. *Colloids and Surfaces B: Biointerfaces*, *215*, 112491. https://doi.org/10.1016/j.colsurfb.2022.112491

[77] Sun, Y., Li, Z., Zhao, P., Huang, W., Liu, H., Li, Y., Zhou, J., Wang, K., & Zhang, C. (2022). Differential effects of tantalum nanoparticles versus tantalum microparticles on macrophage polarization in inflammatory microenvironments. *Biomaterials Advances*, *153*, 213345. https://doi.org/10.1016/j.mtbio.2022.100340

[78] Wang, Q., Zhang, H., Gan, H., Wang, H., Li, Q., & Wang, Z. (2018). Application of combined porous tantalum scaffolds loaded with bone morphogenetic protein 7 to repair of osteochondral defect in rabbits. *International Orthopaedics*, *42*(7), 1437–1448. https://doi.org/10.1007/s00264-018-3800-7

[79] Huang, B., Zou, X., Li, H., Xue, Q., & Bünger, C. (2013). Short-term alendronate treatment does not maintain a residual effect on spinal fusion with interbody devices and bone graft after treatment withdrawal: an experimental study on spinal fusion in pigs. *European spine journal : official publication of the European Spine Society, the European Spinal Deformity Society, and the European Section of the Cervical Spine Research Society*, *22*(2), 287–295. https://doi.org/10.1007/s00586-012-2513-7

[80] Dou, X., Wei, X., Liu, G., Wang, S., Lv, Y., Li, J., Ma, Z., Zheng, G., Wang, Y., Hu, M., Yu, W., & Zhao, D. (2019). Effect of porous tantalum on promoting the osteogenic differentiation of bone marrow mesenchymal stem cells in vitro through the MAPK/ERK signaling pathway. *Journal of Orthopaedic Translation*, *19*, 81–93. https://doi.org/10.1016/j.jot.2019.03.006

[81] Al Deeb, M., AlFarraj, A. A., & Anil, S. (2023). Osseointegration of Tantalum Trabecular Metal in Titanium Dental Implants: Histological and Micro-CT Study. *Journal of Functional Biomaterials*, *14*(7), 355. https://doi.org/10.3390/jfb14070355

[82] Cui, J., Zhang, S., Huang, M., Mu, X., Hei, J., Yau, V., & He, H. (2023). Micro-nano porous structured tantalum-coated dental implants promote osteogenic activity in vitro and enhance osseointegration in vivo. *Journal of biomedical materials research. Part A*, *111*(9), 1358–1371. https://doi.org/10.1002/jbm.a.37538

[83] Edelmann, A. R., Patel, D., Allen, R. K., Gibson, C. J., Best, A. M., & Bencharit, S. (2019). Immediate loading protocols using porous tantalum dental implants: A clinical evaluation. *Journal of Prosthetic Dentistry*, *121*(3), 404–412. https://doi.org/10.1016/j.prosdent.2018.04.022

[84] Bencharit, S., Morelli, T., Barros, S., Seagroves, J. T., Kim, S., Yu, N., Byrd, K., Brenes, C., & Offenbacher, S. (2019). Comparing Initial Wound Healing and Osteogenesis of Porous Tantalum Trabecular Metal and Titanium Alloy Materials. *The Journal of oral implantology*, *45*(3), 173–180. https://doi.org/10.1563/aaid-joi-D-17-00258

[85] Unger, A. S., Lewis, R. J., & Gruen, T. (2005). Evaluation of a porous tantalum uncemented acetabular cup in revision total hip arthroplasty—two- to four-year clinical and radiographic results. *Journal of Arthroplasty*, *20*(8), 1002–1010. https://doi.org/10.1016/j.arth.2005.01.023

[86] Haidemenopoulos, G. N., Malizos, K. N., Zervaki, A. D., & Bargiotas, K. (2017). Human bone ingrowth into a porous tantalum acetabular cup. AIMS Materials Science, 4(6), 1220–1230. https://doi.org/10.3934/matersci.2017.6.1220

[87] Moen, T. C., Ghate, R., Salaz, N., Ghodasra, J., & Stulberg, S. D. (2011). A monoblock porous tantalum acetabular cup has no osteolysis on CT at 10 years. Clinical orthopaedics and related research, 469(2), 382–386. https://doi.org/10.1007/s11999-010-1500-8

[88] Tsao, A. K., Roberson, J. R., Christie, M. J., Dore, D. D., Heck, D. A., Robertson, D. D., & Poggie, R. A. (2005). Cementless porous tantalum acetabular components in primary THA: 5-year follow-up. *Journal of Bone and Joint Surgery American*, *87*(1), 22–28.

[89] Huang, W., Gong, X., Sandiford, S., He, X., Li, F., Li, Y., Liu, Z., Qin, L., Yang, J., Zhu, S., Wang, J., Tu, X., Ye, L., & Hu, N. (2019). Outcome after a new porous tantalum rod implantation for treatment of early-stage femoral head osteonecrosis. *Annals of translational medicine*, *7*(18), 441. https://doi.org/10.21037/atm.2019.08.86

[90] Zhang, Y., Wang, Y., Wang, Z., Zhang, H., Liu, S., Lin, Y., Li, H., & Li, L. (2024). Biomechanical evaluation and surgical strategy analysis of a novel porous tantalum acetabular cup using finite element method. *Journal of Orthopaedic Surgery and Research*, *19*(1), 231. https://doi.org/10.1186/s13018-024-05416-1

[91] Zhao, D., Liu, B., Wang, B., Yang, L., Xie, H., Huang, S., Zhang, Y., & Wei, X. (2015). Autologous bone marrow mesenchymal stem cells associated with tantalum rod implantation and vascularized iliac grafting for the treatment of end-stage osteonecrosis of the femoral head. *BioMed Research International*, *2015*, 240506. https://doi.org/10.1155/2015/240506

[92] Kayani, B., Howard, L. C., Neufeld, M. E., Greidanus, N. V., Masri, B. A., & Garbuz, D. S. (2024). Porous tantalum metaphyseal cones for severe femoral and tibial bone defects in revision total knee arthroplasty are reliable for fixation at mean 5-year follow-up. *The Journal of Arthroplasty*, *39*(9), S374–S379. https://doi.org/10.1016/j.arth.2024.03.022

[93] Hadley, M. L., Harmer, J. R., Wright, B. H., Larson, D. R., Abdel, M. P., Berry, D. J., & Lewallen, D. G. (2024). Porous Tantalum Tibial Metaphyseal Cones in Revision Total Knee Arthroplasty: Excellent 10-Year Survivorship. *The Journal of arthroplasty*, *39*(8S1), S263–S269. https://doi.org/10.1016/j.arth.2024.04.059

[94] Piovan, G., Bori, E., Padalino, M., Pianigiani, S., & Innocenti, B. (2024). Biomechanical analysis of patient specific cone vs conventional stem in revision total knee arthroplasty. *Journal of orthopaedic surgery and research*, *19*(1), 439. https://doi.org/10.1186/s13018-024-04936-0

[95] Mao, S., Liu, Y., Wang, F., He, P., Wu, X., Ma, X., & Luo, Y. (2023). Design and biomechanical analysis of patient-specific porous tantalum prostheses for knee joint revision surgery. *International Journal of Bioprinting*, *9*(4), 735. https://doi.org/10.18063/ijb.73

[96] Zhang, C., Zhou, Z., Liu, N., Chen, J., Wu, J., Zhang, Y., Lin, K., & Zhang, S. (2023). Osteogenic differentiation of 3D-printed porous tantalum with nano-topographic modification for repairing craniofacial bone defects. *Frontiers in bioengineering and biotechnology*, *11*, 1258030. https://doi.org/10.3389/fbioe.2023.1258030

[97] Liu, A., Liao, H., Zhang, X., Deng, S., Wang, C., Zhao, Z., Jiang, G., Li, D., Hu, J., & Hu, Z. (2025). A novel tantalum scaffold promoting osteoporotic osseointegration by controlled immune regulation. *International Journal of Bioprinting*, *11*(2), 474–493. https://doi.org/10.36922/ijb.8595

[98] Jiao, J., Hong, Q., Zhang, D., Wang, M., Tang, H., Yang, J., Qu, X., & Yue, B. (2023). Influence of porosity on osteogenesis, bone growth and osteointegration in trabecular tantalum scaffolds fabricated by additive manufacturing. *Frontiers in Bioengineering and Biotechnology*, *11*, 1117954. https://doi.org/10.3389/fbioe.2023.1117954

[99] Yu, H., Xu, M., Duan, Q., Li, Y., Liu, Y., Song, L., Cheng, L., Ying, J., & Zhao, D. (2024). 3D-printed porous tantalum artificial bone scaffolds: fabrication, properties, and applications. *Biomedical materials (Bristol, England), 19*(4), 10.1088/1748-605X/ad46d2. https://doi.org/10.1088/1748-605X/ad46d2

[100] Zhao, Z., Wang, M., Shao, F., Liu, G., Li, J., Wei, X., Zhang, X., Yang, J., Cao, F., Wang, Q., Wang, H., & Zhao, D. (2021). Porous tantalum-composited gelatin nanoparticles hydrogel integrated with mesenchymal stem cell-derived endothelial cells to construct vascularized tissue in vivo. *Regenerative Biomaterials*, *8*(6), rbab051. https://doi.org/10.1093/rb/rbab051

FaST - Jurnal Sains dan Teknologi, Vol.10, No.1, Mei 2026
e-ISSN 2598-9596
DOI: https://doi.org/10.19166/fastjst.v10i1.10884
Available online at: https://ojs.uph.edu/index.php/FaSTJST/article/view/10884

Effect of Steaming Time on The Protein Quality and Functional Properties of Soybean Paste

Natasya Crisly, Lucia Crysanthy Soedirga*
Food Technology Study Program, Faculty of Science and Technology, Universitas Pelita Harapan, Tangerang, Indonesia

ABSTRACT

Thermal processing is essential for enhancing the nutritional quality and protein digestibility of soybeans. Steaming, which uses hot vapor to minimize direct contact between the food and water, as in boiling, thereby better preserves nutrient content. However, excessive heating can decrease the quality and functional properties of the protein; therefore, the selected cooking time, specifically the steaming time, must be determined. This study investigated the effects of varying steaming times (25, 40, and 55 minutes) on the protein quality—specifically protein content and in-vitro protein digestibility—and functional properties, including emulsion stability and water holding capacity, of soybean paste. Results indicated that prolonged steaming significantly reduced both protein quality and functional properties. Extended thermal exposure resulted in excessive protein denaturation and aggregation, thereby disrupting the structural integrity required for effective water binding and emulsion stabilization. The selected steaming time was 25 minutes, yielding a protein content of 29.62 ± 1.10% and an in vitro protein digestibility of 44.40 ± 0.36%. Furthermore, at this selected steaming time, the soybean paste exhibited the highest emulsion stability and water holding capacity values of 92.79±1.76% and 71.25±1.77%, respectively. These findings support SDG 2 (Zero Hunger), SDG 3 (Good Health and Well-being), and SDG 12 (Responsible Consumption and Production) by establishing a resource-efficient method for producing high-quality, sustainable plant-based proteins. This 25-minute steaming duration establishes a standardized approach to enhancing the nutritional and functional profiles of soybean-based ingredients.

ARTICLE INFO

Keywords: food security; legumes; protein quality; sustainable diet.; protein

***Corresponding author:**
lucia.soedirga@uph.edu

Article history:
Submitted 03 Feb 2026
Revised 06 Mar 2026
Accepted 11 Mar 2026
Online Available 17 Apr 2026
Published 20 May 2026

1. Introduction

Soybeans are a type of legume known as a high-quality source of plant-based protein. Soybeans are considered one of the best food sources for fulfilling the body's protein needs compared to other types of nuts or legumes. In addition to their high protein content, which ranges from 35% to 40%, soybeans also contain other essential nutrients, including dietary fiber (9%), fat (20%), and water (8.5%). In general, the utilization of plant-based protein sources, such as soybeans, is highly relevant to efforts to achieve Sustainable Development Goal (SDG) 2: Zero Hunger, particularly the target of preventing malnutrition and ensuring access to nutritious and sustainable food. The amino acid composition of soybeans closely resembles milk and whey protein, especially when compared to other plant-based sources such as peas and barley. In terms of protein quality, the Digestible Indispensable Amino Acid Score (DIAAS) of soy protein is also comparable with animal protein sources such as milk and eggs. Typically, the DIAAS of milk and eggs ranges from 1.00 to 1.31, indicating their very high protein quality, while the digestibility of soybeans ranges from 0.84 to 0.92. This value is considerably higher than that of other plant-based materials and nearly approaches the DIAAS scores of milks and eggs, which are animal protein sources. Therefore, protein from soybeans can serve as an ideal alternative to animal protein [1,2].

The protein quality of soybeans can be further enhanced through various processing techniques, including cooking, soaking, germination (sprouting), extrusion, fermentation, and protein isolation or concentration. Among these thermal treatments, including heating, irradiation, and autoclaving, are commonly applied as standard methods in the processing of plant-based proteins. This is because they are effective at reducing the content of toxic and antinutritional compounds, such as protease inhibitors, which inhibit digestive enzymes, thereby increasing protein digestibility. The heating process also facilitates the decomposition of large protein molecules into smaller peptides and amino acids, thereby making them more readily absorbed by the body. However, prolonged heating can promote protein

FaST - Jurnal Sains dan Teknologi, Vol.10, No.1, Mei 2026
e-ISSN 2598-9596
DOI: https://doi.org/10.19166/fastjst.v10i1.10884
Available online at: https://ojs.uph.edu/index.php/FaSTJST/article/view/10884

aggregation, thereby limiting amino acid release during digestion and reducing both bioavailability and nutritional value of the protein [2,3]

In addition to improving nutritional value, thermal processing of soybeans enhances sensory attributes, such as taste and aroma, thereby increasing consumer acceptability. Cooking can enhance flavor and aroma, inactivate pathogenic microorganisms, prolong shelf life, and improve nutrient bioavailability. Furthermore, cooking can enhance the nutritional value and physiological properties of food. Nevertheless, each cooking technique has a different impact on the physicochemical quality and nutritional content of the food material. This variation is influenced by factors such as temperature, heating time, and treatment intensity [2,4].

The conventional cooking methods commonly used nowadays are steaming, boiling, and frying. Steaming is a cooking technique that uses hot steam to achieve the desired degree of doneness. This method minimizes direct contact between food and water, thereby preserving nutrient content (e.g., protein, vitamin C, glucosinolates, and polyphenols) and complex structures within the food. Vegetables such as white cauliflower, broccoli, and Brussels sprouts exhibit preferable physicochemical, nutritional, and sensory characteristics when steamed rather than boiled [5]. Steaming also preserves the natural color of the food material, as it does not excessively trigger the Maillard reaction, which is common during frying. In addition, the resulting texture of the steamed ingredients is typically softer and moister, with higher moisture content. One factor influencing the steaming method is time. The steaming time requires investigation to ensure that the nutritional content of the cooked products is preserved or enhanced while minimizing energy consumption [6]. However, to date, no studies have investigated the variation of cooking time, specifically steaming time, on the characteristics of cooked soybeans.

The urgency of this study lies not only in food innovation but also in its direct contribution to the Sustainable Development Goals (SDGs), particularly SDG 2: Zero Hunger and SDG 3: Good Health and Well-being by enhancing nutritional utilization, and SDG 12 (Responsible Consumption and Production) by promoting resource-efficient processing. By refining the processing of a sustainable, locally sourced protein (soybean), this research aims to support Target 2.2 (ending malnutrition through high-quality food) and Target 3.4 (reducing premature mortality from non-communicable diseases by promoting healthier plant-based diets, as soybean is inherently cholesterol-free and naturally low in saturated fat—two primary dietary risk factors for cardiovascular diseases).

Soybeans are typically cooked by the boiling method, as demonstrated by Wijayanti et al. [7]. Moreover, cooked soybeans are typically milled into flour, whereas in this study, steamed soybeans of varying durations will be processed into a paste. This approach offers several benefits, including increased efficiency of soybean paste (SP) application in various plant-based products, as it eliminates the need for drying and milling, thereby enhancing process efficiency (SDG 12) and potentially retaining higher levels of soluble protein. The use of a paste form can retain higher levels of soluble protein, thereby enhancing the functionality and nutritional quality of soybean in more applicable formulations. Therefore, this research aims to determine the effect of steaming time on SP production and its impact on the quality and functional properties of soybean protein, thereby supporting the development of nutritious and sustainable food products.

2. Research Methodology

2.1 Materials and Equipment

The tools used in this study included analytical balance (Ohaus), table balance (Sartorius), blender (Phillips), chopper (Phillips), steamer (Phillips), stove, oven (Memmert UNB 500), water bath (Memmert), desiccator (Duran), glassware (Iwaki Pyrex), heater (Barnstead), Kjeldahl digestion dan distillation system (Buchi), centrifuge (Hettich Zentrifugen EBA 200), chromameter (Konica Minolta CR- 400). The materials needed in this research are soybeans, water, selenium (p.a, Smart Lab), K_2SO_4 (Smart Lab, Indonesia), H_2O_2 (Smart Lab, Indonesia), H_2SO_4 (Smart Lab, Indonesia), boric acid (Smart Lab, Indonesia), NaOH (Smart Lab, Indonesia), HCl (Smart Lab, Indonesia), hexane (Smart Lab, Indonesia), ethanol (Smart Lab, Indonesia), phosphate buffer, α-amylase enzyme, protease enzyme (Smart Lab, Indonesia), dan amyloglucosidase enzyme (Sigma Aldrich).

FaST - Jurnal Sains dan Teknologi, Vol.10, No.1, Mei 2026
e-ISSN 2598-9596
DOI: https://doi.org/10.19166/fastjst.v10i1.10884
Available online at: https://ojs.uph.edu/index.php/FaSTJST/article/view/10884

2.2 Processing of SP

The SP production procedure was developed based on Apriliana et al. [8], Nazarena et al.[9] and Pradhananga [10] with modifications. Dehulled yellow soybeans were selected for this study and purchased from the online market in Jakarta. The process started with washing, draining and subsequent soaking the soybeans in 0.5% sodium bicarbonate solution (1:2, w/v ratio) for six hours; this crucial step serves to soften the cell wall, remove off-flavor compounds, and inactivate the lipoxygenase enzyme, although the time must be controlled to prevent the rupture of beans and subsequent leaching of protein reserves. Following soaking and draining, the soybeans are steamed for 25, 40, or 45 minutes [10]. Based on protein content in soybean paste at various steaming times during preliminary trials (20, 25, 30, 40, 50, and 55 minutes), it was observed that protein content increased from 20 to 25 minutes but declined at 30 minutes. Furthermore, a 15-minute steaming interval yielded a greater difference in protein content than 5- or 10-minute intervals. Consequently, the steaming time selected as a factor in this study begins at 25 minutes and proceeds with 15-minute intervals, specifically at 40 and 55 minutes. After steaming, the cooked beans are drained again and blended to yield the final SP. This paste is then analyzed for protein content (Kjeldahl method), In Vitro Protein Digestibility (IVPD) (enzymatic method), Water-Holding Capacity (WHC), and Emulsion Stability (ES), with the selected steaming time determined by protein content and IVPD.

The protein content measurement is conducted using the Kjeldahl method (AOAC 928.08) [11]. This analysis began with sample preparation, followed by digestion. After digestion, the analysis proceeds to the distillation stage. The resulting distillate is titrated with 0.2 N HCl until the solution turns pink. Following the titration step, the protein content of the sample can be calculated using the following formula (**Eq.1**). The production of soybean paste involves steaming, which triggers extensive protein denaturation and the formation of insoluble protein-carbohydrate complexes. Both colorimetric methods (Lowry and Bradford) require proteins to be in a solubilized, accessible state. In contrast, the Kjeldahl method uses high-temperature acid digestion (H_2SO_4) to completely mineralize the organic matrix, converting all organic nitrogen to ammonium sulfate ($[NH4]_2SO_4$). This ensures that protein quantification remains independent of changes in solubility or structural folding induced by steaming time.

$$Protein\ (\%) = \frac{V1-V2\ x\ N\ HCl x 14.008 x 6.25}{W x 100} \quad (1)$$

V1= volume sample (ml)
V2 = volume blank (ml)
W= weight of sample (g)

The protein digestibility analysis is conducted in vitro, a laboratory method that mimics the gastrointestinal tract [12], utilizing the enzyme pepsin to cleave proteins into amino acids. The procedure starts by preparing a 5 g sample and adding 20 mL of pH 2 Whaffole buffer. Afterwards, 2 mL of 1% pepsin solution is added, and the mixture is incubated for 1 hour at 40°C. To halt digestion and precipitate undigested protein, the sample is filtered and centrifuged, followed by the addition of 5 mL of 5% trichloroacetic acid (TCA). After settling for 1 hour, a 5 mL aliquot of the filtrate is taken for subsequent protein content determination, and the final protein digestibility is calculated by comparing the remaining (undigested) protein in the filtrate against the total initial protein, using the formula as stated in **Eq. 2**.

$$IVPD\ (\%) = \frac{protein\ content\ (enzyme\ treated)}{total\ protein\ content} \quad (2)$$

The WHC of the SP is analyzed using the centrifugal method [13], which begins by mixing a 2 g sample with 10mL of deionized water in a centrifugation tube. The tube is then subjected to centrifugation for 20 minutes at a speed of 3,000 rpm, leading to the separation of a supernatant from the solid pellet. The supernatant is carefully decanted, weighed, and its weight is recorded, allowing the WHC value—which represents the percentage of water retained by the sample—to be calculated using the formula (**Eq.3**) [14].

FaST - Jurnal Sains dan Teknologi, Vol.10, No.1, Mei 2026
e-ISSN 2598-9596
DOI: https://doi.org/10.19166/fastjst.v10i1.10884
Available online at: https://ojs.uph.edu/index.php/FaSTJST/article/view/10884

$$WHC\ (\%) = \frac{W1 - W2}{W} x100\% \quad (3)$$

W1= weight of water added (g)
W2 = weight of supernatant (g)
W= weight of sample (g)

The ES analysis began by mixing 0.5 g of the sample with 5 mL of distilled water and 5 mL of soybean oil, then homogenizing for 1 hour using a vortex mixer. The mixture was initially centrifuged at 3000 rpm for 15 min. Subsequently, the sample was incubated in a water bath at 80°C for 30 min. After cooling at room temperature for 15 min, the sample underwent a second centrifugation cycle at 3000 rpm for 15 min until a visible separation layer formed. Phase separation was quantified by measuring the volume of the supernatant oil layer. The incorporation of additional water and oil was performed to evaluate the dough's emulsifying capacity under thermal stress. The lower percentage of ES indicates a stable protein-lipid interface capable of maintaining the fat fraction within the matrix during heat treatment. The percentage of ES is calculated using the following formula, as shown in **Eq. 4** [15].

$$ES\ (\%) = \frac{Ve}{Vt} x100\% \quad (4)$$

Ve: volume of emulsion layer
Vt: total volume of emulsion

2.3 Statistical Analysis

To determine the effect of steaming the soybean to produce SP, a completely randomized design with three levels of one factor, namely 25 minutes, 40 minutes, and 55 minutes. This research involved three replications, each with three repetitions. The data were analyzed using SPSS version 25, One-Way ANOVA, and Duncan post hoc tests.

3. Result and Discussion

3.1 Effect of Soybean Steaming Time on The Protein Quality of SP

Protein quality is assessed in this study using protein content and protein digestibility. Protein content measures the total amount of protein, while protein digestibility measures the extent to which the protein can be digested and absorbed by the body. Steaming is a heat-based processing method that uses hot vapor to cook the material until it reaches the desired level of doneness. Because the food has little to no direct contact with water, this technique helps retain nutrients such as protein, reduces anti-nutritional factors, and maintains physical attributes such as color [5]. The factors influencing the steaming method are temperature and time. Appropriate temperature and steaming time must be used to ensure that the cooked material achieves the optimal flavor profile and maintains or enhances its physicochemical characteristics [6]. However, during the steaming process, the steam temperature is generally relatively stable at 100°C. Therefore, the factor that most significantly affects the steaming process is the steaming time.

Table 1 shows the protein quality of SP in various steaming times and indicates a significant difference in protein content and protein digestibility of the SP across the varied steaming times. The 55-minute steaming time resulted in significantly lower protein content than both the 25-minute and 40-minute treatments. This observation suggests that prolonged steaming induces thermal degradation of soybean protein, reducing total protein content. This finding is consistent with Liao et al. [16], who reported a decrease in the protein content of black soybeans as the steaming cycle duration increased, with the value decreasing from 36.55% to 34.48% over time. Moreover, the results of this study are also supported by Samben and Puspaningrum [17]. The lowest protein content of pigeon pea was observed

FaST - Jurnal Sains dan Teknologi, Vol.10, No.1, Mei 2026
e-ISSN 2598-9596
DOI: https://doi.org/10.19166/fastjst.v10i1.10884
Available online at: https://ojs.uph.edu/index.php/FaSTJST/article/view/10884

at 30 minutes of steaming (12.66%), whereas steaming for 10 minutes resulted in the highest protein content (12.98%).

Table 1 Protein Quality of SP in Various Steaming Time

Steaming time (minutes)	Protein content (%)	IVPD (%)
25	29.62±1.10[a]	44.40±0.36[c]
40	30.21±1.99[a]	33.20±0.09[b]
55	28.54±2.74[b]	27.67±0.52[a]

Notes: Value in the table shown by the average±SD. Value with different superscript in the same column has a significant difference at 5%

Furthermore, prolonged steaming time can lead to excessive Maillard browning, resulting in numerous amino acid amine groups reacting with sugars. This results in lower residual protein in the final product because a significant amount of protein is consumed during the Maillard reaction. The 25-minute and 40-minute steaming times did not differ significantly in protein content. However, both steaming durations yielded the highest protein content, whereas the 55-minute duration yielded the lowest. During the 25-minute and 40-minute time, the increase in protein is a function of mass balance; as heat facilitates the evaporation of water, the relative proportion of the remaining solid matter (including nitrogenous compounds) increases. This represents the optimal point of dehydration where the nutrient density is maximized. However, at 55 minutes, the intense heat causes amino acid amine groups to covalently bond with reducing sugars, forming melanoidins. This chemical transformation leads to a measurable decrease in residual total protein, as the nitrogen is incorporated into complex Maillard products that may alter the recovery during analysis. Thus, the 25–40 minute range serves as the peak equilibrium between physical moisture loss and chemical stability [18].

Table 1 also shows that as steaming time increases, the SP's IVPD decreases. During the steaming process, protein denaturation occurs, initially increasing protein availability. This protein denaturation is beneficial because the protein's structure unfolds, making it more accessible to enzymes and easier to hydrolyze. However, excessive or prolonged heating can trigger the Maillard reaction, in which the free amino groups of proteins (especially lysine) react with the carbonyl groups of carbohydrates. This reaction can form cross-links, thereby reducing protein solubility and increasing resistance to proteolytic enzymes. Consequently, this leads to a reduction in digestibility and the overall availability of amino acids (particularly lysine) [19,20]. Although initial denaturation unfolds the protein structure, prolonged heating can cause denatured protein molecules to aggregate, forming strong bonds (e.g., disulfide bonds) that subsequently lead to coagulation. Coagulation causes the protein matrix to become denser and more compact, thereby limiting the access of digestive enzymes to the matrix and its hydrolysis. As steaming time increases, Maillard reactions and protein aggregation become more pronounced, ultimately reducing protein digestibility [21,22].

According to Ohanenye et al. [23], the IVPD value for soybeans is approximately 56%. Although the IVPD value obtained in this study did not meet the reference value, the 25-minute steaming time showed the highest significant IVPD (44.40±0.36%) compared with the 40-minute (33.20±0.09%) and 55-minute (27.67±0.52%) treatments. The result indicates that a 25-minute steaming is sufficient to inactivate trypsin inhibitors and properly denature the protein without causing heat-related structural damage. This balance yields the highest digestibility. The significant decrease of protein and IVPD at 40- and 55-minutes shows that longer steaming time promotes further cross-linking within the protein matrix, which makes the protein harder for enzymatic hydrolysis, thus resulting in a decrease of IVPD [20,24,25]. This finding is also consistent with Adeleye et al. [26], who reported a decrease in protein digestibility of pigeon pea when cooked at 140°C (27.66%) compared to 100°C (64.95%).

3.2 Effect of Soybean Steaming Time on The Functional Properties of SP's Protein

ES is the ability of a protein to stabilize an emulsion (a mixture of oil and water). At the same time, WHC can bind protein to water. WHC is a functional property of a protein that measures the material's ability to bind and retain water molecules [14]. The WHC value will influence the product characteristics when the raw material, in this case, SP, is processed into a final product. A high WHC value will make the product chewier and less dry and will also increase its yield [13,15,27]. **Table 2** shows the functional properties of SP's protein in various steaming times. Based on **Table 2**, ES and WHC decreased

FaST - Jurnal Sains dan Teknologi, Vol.10, No.1, Mei 2026
e-ISSN 2598-9596
DOI: https://doi.org/10.19166/fastjst.v10i1.10884
Available online at: https://ojs.uph.edu/index.php/FaSTJST/article/view/10884

significantly as steaming time increased, indicating structural damage to the protein caused by excessive heat, thereby reducing the SP's ability to stabilize emulsions and bind water.

Table 2 Functional Properties of SP's in Various Steaming Time

Steaming time (minutes)	ES (%)	WHC (%)
25	92.79±1.76^{c}	71.25±1.77^{c}
40	87.23±1.89^{b}	58.41±1.45^{b}
55	84.13±2.11^{a}	52.29±2.46^{a}

Notes: Value on the table shown by the average±SD. Value with different superscript in the same column has a significant difference at 5%

Before steaming, soybean proteins are mainly globular, with hydrophobic groups trapped inside the molecule and hydrophilic groups exposed on the surface. When heating begins—particularly during the first 25 minutes—the protein unfolds in a controlled manner, initiating denaturation without structural damage. Controlled denaturation creates conditions that allow the protein to function effectively in stabilizing emulsions and binding water. As the protein unfolds, previously buried hydrophobic groups become exposed to the surface, enabling these interactions. This exposed structure creates ideal conditions for coating the emulsion droplets formed within the soybean paste, resulting in a more stable emulsion and yielding the highest significant ES value of 92.79±1.76 %. The open protein structure also facilitates the formation of a more elastic gel matrix or a loose protein network. This elastic network condition creates larger interstitial spaces, allowing water to be bound both physically and chemically through hydrogen bonds, resulting in the highest WHC value of 71.25±1.77 % [28, 29, 30].

However, when the heating time is prolonged to 40 minutes and 55 minutes, the protein undergoes excessive denaturation and aggregation. This excessive aggregation causes proteins to bind permanently to one another via disulfide bonds, which leads to the formation of larger and insoluble aggregates, which in turn diminishes the protein's ability to stabilize emulsions and bind water [24,31, [32]. Once the proteins form these larger and more rigid aggregates, they can no longer effectively coat the emulsion system in the SP. This is demonstrated by the significantly lower ES value of 84.13±2.11% compared with the 25-minute steaming time. Furthermore, the increasingly rigid and dense matrix reduces the volume of the internal spaces, meaning it can no longer physically hold water. This causes water to be expelled from the matrix, and the protein loses its ability to bind or retain water, as evidenced by consistently lower WHC values (52.29±2.46%). The decreasing of WHC is also shown in field bean protein isolate that undergo steaming for 15, 30 and 45 minutes. The 45 minutes steaming resulting in a low WHC value (2.550±0.01%) compared to 15 minutes (2.785±0.01%) and 30 minutes (2.745±0.01%). The decreasing value of ES is also shown in brindle beans during steaming process using autoclaves. The ES of raw brindle bean is the highest (58%) compared to 5 minutes steaming (54%) and 20 minutes steaming (52%) [33,34].

Table 1 and **Table 2** demonstrate a linear relationship between the protein quality and the functional properties of SP. Steaming for 55 minutes resulted in a significant loss of protein quality, with IVPD falling to nearly half (27.67±0.52%) of the 25-minute value (44.40±0.36%). This suggests that prolonged heating induces protein-protein aggregation, making the protein less accessible to enzymes (Table 1) and less effective in stabilizing food systems (**Table 2**). The correlation between lower IVPD and decreased WHC and ES indicates that thermal damage to the protein structure is the primary cause of functional failure. This structural degradation is correlated with the results in Table 2, where (WHC) and ES show a downward trend. Specifically, the decrease in IVPD from 25 to 55 minutes corresponds to decreases in WHC from 71.25±1.77% to 52.29±2.46% and ES from 92.79±1.76% to 84.13±2.11%, as unfolded or aggregated proteins lose the surface-exposed hydrophilic and hydrophobic groups necessary for water binding and oil-water stabilization. These findings indicate that the thermal degradation of the protein primary/secondary structure (**Table 1**) is the underlying driver for the functional failures observed in the final food system (**Table 2**).

4. Conclusion

Steaming time significantly affects the protein quality and the functional properties of SP's protein. As steaming time increased, protein content and digestibility decreased, indicating a loss of protein quality.

Prolonged heating also reduced the ability of SP to stabilize emulsions and bind water, demonstrating a corresponding decline in its functionality. The selected steaming time for producing SP was 25 minutes. At the 25-minute steaming time, the SP exhibited protein content and protein digestibility of 29.62% and 44.40%, respectively. In addition, at this optimal steaming time, the SP showed ES and WHC values of 92.79±1.76% and 71.25±1.77%, respectively.

Acknowledgement

The authors would like to express their sincere gratitude to the Community Research and Centre Development, Universitas Pelita Harapan, for their support in facilitating this research through the internal funding scheme of Universitas Pelita Harapan, number 418/LPPM-UPH/VII/2025.

References

[1] F. D. Palupi, Y. Kristianto, and A. H. Santoso, "Efek perkecambahan kedelai (glycine max) terhadap mutu gizi formula modisco gizi buruk substitusi tepung kecambah kedelai," *Jurnal Dunia Gizi*, vol. 5, no. 2, pp. 60–68, 2022, https://doi.org/10.33085/jdg.v5i2.5484.

[2] P. Qin, T. Wang, and Y. Luo, "A Review on plant-based proteins from soybean: health benefits and soy product development," *J. Agric. Food Res.*, vol. 7, p. 100265, Mar. 2022, https://doi.org/10.1016/j.jafr.2021.100265.

[3] A. Fitriani, D. R. Toni, and S. N. Rahmadhia, "Chemical characteristics of kepok banana bud (musa paradisiaca linn.) flakes with variations of mocaf flour," *Journal of Functional Food and Nutraceutical*, pp. 97–105, Feb. 2024, https://doi.org/10.33555/jffn.v5i2.114.

[4] M. W. Muthee, F. M. Khamis, X. Cheseto, C. M. Tanga, S. Subramanian, and J. P. Egonyu, "Effect of cooking mMethods on nutritional value and microbial safety of edible rhinoceros beetle grubs (oryctes sp.)," *Heliyon*, vol. 10, no. 3, p. e25331, Feb. 2024, https://doi.org/10.1016/j.heliyon.2024.e25331.

[5] K. Nowak, S. Rohn, and M. Halagarda, "Impact of cooking techniques on the dietary fiber profile in selected cruciferous vegetables," *Molecules*, vol. 30, no. 3, p. 590, Jan. 2025, https://doi.org/10.3390/molecules30030590.

[6] Z. Liu *et al.*, "Impact of steam processing on the physicochemical properties and flavor profile of takifugu flavidus: a comprehensive quality evaluation," *Foods*, vol. 14, no. 9, p. 1537, Apr. 2025, https://doi.org/10.3390/foods14091537.

[7] E. D. Wijayanti, N. Harini, and D. Elianarni, "Pengaruh konsentrasi ragi dan proporsi kacang tunggak (Vigna unguiculata L.) dan kacang kedelai (Glycine max (L.) Merrill) terhadap sifat fisikokimia dan organoleptik tempe," *Food Technology and Halal Science Journal*, vol. 8, no. 1, pp. 104–116, Jan. 2025, https://doi.org/10.22219/fths.v8i1.37593.

[8] N. W. Apriliana, S. Susanti, and Y. Pratama, "Pengaruh rasio pasta kacang hijau-beras hitam terhadap karakteristik sensoris flakes sereal," *Jurnal Teknologi Pangan*, vol. 3, no. 1, pp. 91–95, Jun. 2019, https://doi.org/10.14710/jtp.2019.23792.

[9] Y. Nazarena, N. Malahayati, and G. Priyanto, "Pengaruh perendaman kedelai terhadap mutu sari kedelai," *Jurnal Sains dan Teknologi Pangan*, vol. 6, no. 2, Apr. 2021, https://doi.org/10.33772/jstp.v6i2.16123.

[10] M. Pradhananga, "Effect of processing and soybean cultivar on *natto* quality using response surface methodology," *Food Sci. Nutr.*, vol. 7, no. 1, pp. 173–182, Jan. 2019, https://doi.org/10.1002/fsn3.848.

[11] V. Haritha and A. Bukya, "Preparation and quality characterization of herbal nutritional powder," *Int. J. Res. Appl. Sci. Eng. Technol.*, vol. 13, no. 7, pp. 241–249, Jul. 2025, https://doi.org/10.22214/ijraset.2025.72969.

[12] S. Bahri, M. Mukhtar, and K. L. Nibras, "Kecernaan invitro silase pakan komplit menggunakan jerami jagung organik dan anorganik," *Jurnal Ilmu dan Industri Peternakan*, vol. 8, no. 1, pp. 84–95, Jun. 2022, https://doi.org/10.24252/jiip.v8i1.23808.

[13] A. H. Prayitno and G. S. Wibisono, "Physical quality of culled duck meatball substituted with edamame flour filler," *Jurnal Ilmu dan Teknologi Peternakan Tropis*, vol. 2, no. 9, pp. 318–324, 2022, https://doi.org/10.33772/jitro.v9i2.21053.

[14] L. C. Soedirga and E. D. Amadea, "Enhancing nutritional and functional properties of plant-based meatballs: a study on kepok banana flower, brown lentils, and wheat gluten," *Caraka Tani: Journal of Sustainable Agriculture*, vol. 40, no. 4, p. 496, Sep. 2025, https://doi.org/10.20961/carakatani.v40i4.98807.

[15] M. Penchalaraju and S. J. D. Bosco, "Leveraging Indian pulses for plant-based meat: functional properties and development of meatball analogues," *Int. J. Food Sci. Technol.*, vol. 57, no. 9, pp. 5869–5877, Sep. 2022, https://doi.org/10.1111/ijfs.15908.

[16] X. Liao *et al.*, "Effects of 'nine steaming nine sun-drying' on proximate composition, protein structure and volatile compounds of black soybeans," *Food Res. Int.*, vol. 155, p. 111070, May 2022, https://doi.org/10.1016/j.foodres.2022.111070.

[17] R. K. Samben and D. H. D. Puspaningrum, "Kandungan protein, serat, dan daya terima kacang gude pada perbedaan perlakuan suhu dan waktu," *Seminar Ilmiah Nasional Teknologi, Sains, dan Sosial Humaniora (SINTESA)*, vol. 3, Jan. 2021, https://doi.org/10.36002/snts.v0i0.1245.
[18] I. Wainaina *et al.*, "Thermal treatment of common beans (*Phaseolus vulgaris* L.): Factors determining cooking time and its consequences for sensory and nutritional quality," *Compr. Rev. Food Sci. Food Saf.*, vol. 20, no. 4, pp. 3690–3718, Jul. 2021, https://doi.org/10.1111/1541-4337.12770.
[19] P. Masson and S. Lushchekina, "Conformational stability and denaturation processes of proteins investigated by electrophoresis under extreme conditions," *Molecules*, vol. 27, no. 20, p. 6861, Oct. 2022, https://doi.org/10.3390/molecules27206861.
[20] J. Zhang, J. Wang, M. Li, S. Guo, and Y. Lv, "Effects of heat treatment on protein molecular structure and in vitro digestion in whole soybeans with different moisture content," *Food Research International*, vol. 155, p. 111115, May 2022, https://doi.org/10.1016/j.foodres.2022.111115.
[21] J. A. J. Housmans, G. Wu, J. Schymkowitz, and F. Rousseau, "A guide to studying protein aggregation," *FEBS J.*, vol. 290, no. 3, pp. 554–583, Feb. 2023, https://doi.org/10.1111/febs.16312.
[22] X. Qian, Y. Gu, B. Sun, and X. Wang, "Changes of aggregation and structural properties of heat-denatured gluten proteins in fast-frozen steamed bread during frozen storage," *Food Chem.*, vol. 365, p. 130492, Dec. 2021, https://doi.org/10.1016/j.foodchem.2021.130492.
[23] I. Ohanenye *et al.*, "Legume seed protein digestibility as influenced by traditional and emerging physical processing technologies," *Foods*, vol. 11, no. 15, p. 2299, Aug. 2022, https://doi.org/10.3390/foods11152299.
[24] J. Du *et al.*, "Effects of ultrasonic and steam-cooking treatments on the physicochemical properties of bamboo shoots protein and the stability of O/W emulsion," *Heliyon*, vol. 9, no. 9, p. e19825, Sep. 2023, https://doi.org/10.1016/j.heliyon.2023.e19825.
[25] A. G. A. Sá, Y. M. F. Moreno, and B. A. M. Carciofi, "Food processing for the improvement of plant proteins digestibility," *Crit. Rev. Food Sci. Nutr.*, vol. 60, no. 20, pp. 3367–3386, Nov. 2020, https://doi.org/10.1080/10408398.2019.1688249.
[26] O. O. Adeleye, S. T. Awodiran, A. O. Ajayi, and T. F. Ogunmoyela, "Effect of high-temperature, short-time cooking conditions on in vitro protein digestibility, enzyme inhibitor activity and amino acid profile of selected legume grains," *Heliyon*, vol. 6, no. 11, p. e05419, Nov. 2020, https://doi.org/10.1016/j.heliyon.2020.e05419.
[27] I. de l. Angeles Gremasqui, M. A. Giménez, M. O. Lobo, N. C. Sammán, and P. Díaz-Calderón, "Effect of the addition of hydrolyzed broad bean flour (*vicia faba.* l) on the functional, pasting and rheological properties of a wheat-broad bean flour paste," *Journal of Food Measurement and Characterization*, vol. 19, no. 2, pp. 1362–1372, Feb. 2025, https://doi.org/10.1007/s11694-024-03050-3.
[28] K. O. Falade and S. A. Akeem, "Physicochemical properties, protein digestibility and thermal stability of processed african mesquite bean (prosopis africana) flours and protein isolates," *Journal of Food Measurement and Characterization*, vol. 14, no. 3, pp. 1481–1496, Jun. 2020, https://doi.org/10.1007/s11694-020-00398-0.
[29] T. S. Naiker, H. Baijnath, E. O. Amonsou, and J. J. Mellem, "Effect of steaming and dehydration on the nutritional quality and functional properties of protein isolates produced from *lablab purpureus* (L.) sweet (hyacinth bean)," *J. Food Process. Preserv.*, vol. 44, no. 2, Feb. 2020, https://doi.org/10.1111/jfpp.14334.
[30] K. Yang *et al.*, "Structural changes induced by direct current magnetic field improve water holding capacity of pork myofibrillar protein gels," *Food Chem.*, vol. 345, p. 128849, May 2021, https://doi.org/10.1016/j.foodchem.2020.128849.
[31] N. Goyal, R. Thakur, and B. K. Yadav, "Physical approaches for modification of vegan protein sources: a review," *Food Bioproc. Tech.*, vol. 17, no. 12, pp. 4405–4428, Dec. 2024, https://doi.org/10.1007/s11947-024-03368-2.
[32] L. Wang, J. Dong, Y. Zhu, R. Shen, L. Wu, and K. Zhang, "Effects of microwave heating, steaming, boiling and baking on the structure and functional properties of quinoa (*Chenopodium quinoa* Willd.) protein isolates," *IJFST*, vol. 56, no. 2, pp. 709–720, Feb. 2021, https://doi.org/10.1111/ijfs.14706.
[33] E. A. Akande, O. A. Oladipo, and O. S. Kelani, "Effects of steaming on the physicochemical properties and the cooking time of jack beans (*canavalia ensiformis*)," *Journal of Experimental Biology and Agricultural Sciences*, vol. 1, no. 6, p. 6, 2013.
[34] J. A. C. Bento, P. Z. Bassinello, R. N. Carvalho, M. A. de Souza Neto, M. Caliari, and M. S. Soares Júnior, "Functional and pasting properties of colorful bean (*Phaseolus vulgaris* L) flours: Influence of the cooking method," *J. Food Process. Preserv.*, vol. 45, no. 11, Nov. 2021, https://doi.org/10.1111/jfpp.15899.

FaST - Jurnal Sains dan Teknologi, Vol. 10, No. 1, Mei 2026
e-ISSN 2598-9596
DOI: https://doi.org/10.19166/fastjst.v10i1.10886
Available online at: https://ojs.uph.edu/index.php/FaSTJST/article/view/10886

Pemanfaatan Kitosan Kepiting Bakau (*Scylla serrata)* dan Ion Ag^+ dalam Pembuatan Lapisan Antibakteri pada *Casing Handphone*

Adolf Parhusip [1*], Esli Yunita Sari [2*], Donna Calistalia Ruslim [3], Jessica Adelia Tiono [4]
[1]Teknologi Pangan, Universitas Pelita Harapan, Tangerang, 15811, Indonesia
[2]IPA, SMA Tarakanita Citra Raya, Tangerang, 15710, Indonesia (esli11sari79@gmail.com)
[3]IPA, SMA Tarakanita Citra Raya, Tangerang, 15710, Indonesia (donnalia29@gmail.com)
[4]IPA, SMA Tarakanita Citra Raya, Tangerang, 15710, Indonesia (jessicaadellia15@gmail.com)

ABSTRACT

Casing handphone berfungsi melindungi *handphone* dari kotoran dan risiko kerusakan, namun juga berpotensi menjadi media pertumbuhan bakteri seperti *Staphylococcus aureus*. Untuk mengatasi masalah tersebut, dikembangkan lapisan antibakteri pada *casing handphone* yang terdiri dari epoxy resin dengan kombinasi kitosan *Scylla serrata* dan ion Ag^+ dari $AgNO_3$ sebagai agen antibakteri. Penelitian ini bertujuan untuk mengetahui efektivitas kitosan *Scylla serrata* dan ion Ag^+ dalam lapisan antibakteri serta menentukan rasio perbandingan terbaik dalam menghambat pertumbuhan *Staphylococcus aureus*. Penelitian dilakukan secara *in vitro* menggunakan metode difusi agar sumuran pada media *Nutrient Agar*. Larutan kitosan–$AgNO_3$ sebanyak 75 µL dengan rasio (C:Ag^+) 0:1, 1:0, 1:1, 2:1, dan 1:2 diuji terhadap bakteri. Epoxy resin dengan etanol absolut 99,9% digunakan sebagai kontrol negatif, sedangkan amoksisilin 100 ppm sebagai kontrol positif. Zona hambat diukur dalam satuan milimeter dan dianalisis menggunakan uji normalitas, homogenitas, Oneway ANOVA, dan Games-Howell. Hasil menunjukkan bahwa rasio 0:1 dan 1:0 memiliki daya hambat tertinggi, sedangkan kombinasi kitosan–Ag^+ paling efektif pada rasio 1:1.

ARTICLE INFO

Keywords:
Ag^+ ion; antibakteri; difusi agar sumur; kitosan; *Scylla serrata*

***Penulis Korespondensi:**
adolf.parhusip@uph.edu
esli11sari79@gmail.com

Article history:
Submitted 5 Feb 2026
Revised 26 Feb 2026
Accepted 11 Mar 2026
Online Available 17 Apr 2026
Published 20 May 2026

1. Pendahuluan

Perkembangan teknologi komunikasi telah menjadikan *handphone* sebagai perangkat yang tidak terpisahkan dari aktivitas manusia sehari-hari. Intensitas penggunaan *handphone* yang tinggi menyebabkan perangkat ini sering bersentuhan langsung dengan tangan, wajah, serta berbagai permukaan lingkungan. Kondisi tersebut menjadikan *handphone*, khususnya bagian *casing*, berpotensi menjadi media akumulasi dan transmisi mikroorganisme patogen. Berbagai penelitian melaporkan bahwa *handphone* dapat terkontaminasi oleh beragam bakteri, termasuk bakteri patogen yang berisiko menimbulkan gangguan kesehatan pada manusia [1].

Studi sebelumnya menunjukkan bahwa tingkat kontaminasi bakteri pada *handphone* tergolong tinggi. Gashaw *et al.* [1] melaporkan bahwa lebih dari 90% *handphone* yang digunakan oleh tenaga kesehatan terkontaminasi bakteri. Penelitian lain juga mengidentifikasi keberadaan bakteri patogen seperti *Staphylococcus aureus*, *Escherichia coli*, *Bacillus* sp., dan *Streptococcus* sp. pada permukaan *handphone* [2]. Keberadaan bakteri tersebut menjadi perhatian serius karena *Staphylococcus aureus* diketahui dapat menyebabkan berbagai infeksi, mulai dari infeksi kulit hingga infeksi sistemik dengan tingkat keparahan yang bervariasi [3].

Sebagai upaya untuk melindungi *handphone* dari kerusakan fisik, penggunaan *casing* menjadi hal yang umum dilakukan [4]. Namun, di sisi lain, *casing handphone* juga dapat berperan sebagai reservoir mikroorganisme apabila tidak dibersihkan secara rutin [5]. Oleh karena itu, diperlukan inovasi yang tidak hanya berfungsi melindungi *handphone* secara mekanis, tetapi juga mampu menghambat pertumbuhan bakteri pada permukaannya. Salah satu pendekatan yang dapat diterapkan adalah pengembangan lapisan antibakteri pada *casing handphone*.

Ion perak (Ag^+) dan kitosan merupakan dua bahan yang telah banyak dilaporkan memiliki aktivitas antibakteri yang baik. Ion Ag^+ diketahui mampu merusak struktur sel bakteri melalui interaksi dengan protein dan asam nukleat, sehingga menghambat metabolisme dan menyebabkan kematian sel [6] [7]. Sementara itu, kitosan merupakan polisakarida kationik hasil deasetilasi kitin yang banyak diperoleh dari limbah cangkang krustasea. Kitosan memiliki aktivitas antibakteri yang berkaitan dengan

FaST - Jurnal Sains dan Teknologi, Vol. 10, No. 1, Mei 2026
e-ISSN 2598-9596
DOI: https://doi.org/10.19166/fastjst.v10i1.10886
Available online at: https://ojs.uph.edu/index.php/FaSTJST/article/view/10886

keberadaan gugus amina bermuatan positif yang dapat berinteraksi dengan dinding sel bakteri bermuatan negatif [8].

Indonesia sebagai negara maritim memiliki potensi besar dalam pemanfaatan sumber daya laut, termasuk kepiting bakau (*Scylla serrata*). Produksi kepiting bakau yang tinggi menghasilkan limbah cangkang dalam jumlah besar yang belum dimanfaatkan secara optimal. Limbah tersebut berpotensi diolah menjadi kitosan bernilai tambah tinggi dan ramah lingkungan [9]. Pemanfaatan kitosan dari cangkang *Scylla serrata* sebagai agen antibakteri tidak hanya mendukung pengembangan material fungsional, tetapi juga berkontribusi terhadap pengelolaan limbah perikanan.

Beberapa penelitian melaporkan bahwa kombinasi kitosan dan ion Ag^+ dapat menghasilkan aktivitas antibakteri yang lebih baik dibandingkan penggunaan tunggal masing-masing komponen [6], [10]. Namun, efektivitas sistem kitosan–Ag^+ sangat dipengaruhi oleh rasio perbandingan kedua komponen tersebut. Perbedaan konsentrasi dan viskositas larutan dapat memengaruhi kemampuan difusi senyawa aktif ke dalam media dan sel bakteri [8][11]. Hingga saat ini, penelitian mengenai penggunaan kombinasi kitosan *Scylla serrata* dan ion Ag^+ dalam bentuk lapisan antibakteri pada *casing handphone*, khususnya dengan variasi rasio perbandingan yang berbeda, masih terbatas.

Berdasarkan uraian tersebut, penelitian ini bertujuan untuk mengevaluasi efektivitas kitosan *Scylla serrata* dan ion Ag^+ sebagai agen antibakteri dalam lapisan berbasis epoxy resin terhadap pertumbuhan *Staphylococcus aureus*. Selain itu, penelitian ini juga bertujuan untuk menentukan rasio perbandingan kitosan dan ion Ag^+ yang paling optimal dalam menghasilkan daya hambat antibakteri. Hasil penelitian ini diharapkan dapat menjadi dasar pengembangan material lapisan antibakteri yang aplikatif, ramah lingkungan, dan bernilai tambah bagi industri *casing handphone*.

2. Metode Penelitian

2.1 Alat dan Bahan

Alat yang digunakan dalam penelitian ini meliputi cawan Petri disposable berdiameter 90 mm (Onemed), spiritus, laminar air flow, autoklaf, vortex, mikropipet, mikrotip 1 mL dan 5 mL, erlenmeyer 250 mL, magnetic stirrer, alu dan mortar, botol kaca, tabung ulir, serta digital caliper. Seluruh alat digunakan untuk mendukung proses sterilisasi, pencampuran larutan, penanaman bakteri, serta pengukuran diameter zona hambat pada pengujian antibakteri.

Bahan yang digunakan dalam penelitian ini terdiri atas kitosan sebanyak 100 gram, resin epoxy, larutan $AgNO_3$ dengan konsentrasi 20 ppm, asam asetat 1%, etanol absolut 99,9%, amoksisilin, akuades, garam fisiologis, media Plate Count Agar (PCA), Nutrient Agar (NA), Nutrient Broth (NB), serta alkohol 70%. Seluruh bahan tersebut digunakan dalam pembuatan lapisan antibakteri, persiapan larutan uji, serta pelaksanaan uji aktivitas antibakteri terhadap *Staphylococcus aureus*.

2.2 Metode Penelitian

Penelitian dilaksanakan pada Mei–Oktober 2025 di SMA Tarakanita Citra Raya dan Universitas Pelita Harapan. Penelitian ini dilakukan secara in vitro untuk menguji aktivitas antibakteri lapisan berbasis epoxy resin dengan agen aktif kitosan *Scylla serrata* dan ion Ag^+ (dari $AgNO_3$) terhadap *Staphylococcus aureus* menggunakan metode difusi agar sumuran. Perlakuan berupa variasi rasio kitosan: Ag^+ yaitu 1:0, 0:1, 1:1, 2:1, dan 1:2, disertai kontrol negatif dan kontrol positif, total 5 cawan petri. Setiap cawan petri dibuat 6 sumuran (4 ulangan perlakuan dengan rasio sama, 1 kontrol negatif, 1 kontrol positif). Seluruh alat dan bahan disterilkan menggunakan *autoclave* selama 15 menit pada suhu 121°C. Sebelum digunakan di dalam *Laminar Air Flow*, seluruh alat dan bahan disemprot alkohol.

2.2.1 Pembuatan larutan kitosan 1%

Kitosan (DD 96%) ditimbang 1 g dan dimasukkan ke botol kaca steril. Kitosan dilarutkan dalam 30 mL asam asetat, dikocok hingga larut, kemudian ditambahkan 70 mL akuades. Larutan dihomogenkan menggunakan *magnetic stirrer* pada suhu 50°C.

2.2.2 Pencampuran kitosan dan $AgNO_3$

Larutan disiapkan dengan variasi rasio kitosan: Ag^+ sebagai berikut.

(a) Rasio 1:1: 10 mL kitosan + 10 mL $AgNO_3$, diaduk perlahan 30 menit dengan *magnetic stirrer*.
(b) Rasio 2:1: 20 mL kitosan + 10 mL $AgNO_3$, diaduk perlahan 30 menit.

FaST - Jurnal Sains dan Teknologi, Vol. 10, No. 1, Mei 2026
e-ISSN 2598-9596
DOI: https://doi.org/10.19166/fastjst.v10i1.10886
Available online at: https://ojs.uph.edu/index.php/FaSTJST/article/view/10886

(c) Rasio 1:2: 10 mL kitosan + 20 mL $AgNO_3$, diaduk perlahan 30 menit.
(d) Rasio 1:0 dan 0:1: masing-masing 10 mL larutan kitosan dan 10 mL AgNO3 dimasukkan ke erlenmeyer terpisah.

2.2.3 Pencampuran dengan epoxy resin (lapisan antibakteri)

Sebanyak 2g epoxy resin dilarutkan dalam 10 mL etanol, lalu diaduk kuat selama 1 jam menggunakan *magnetic stirrer*. Selama pengadukan, larutan kitosan–$AgNO_3$ (atau kitosan saja/$AgNO_3$ saja) diteteskan ke dalam larutan epoxy secara bertahap hingga tercampur.

2.2.4 Pembuatan larutan kontrol

Kontrol negatif dibuat dari 2g epoxy resin yang dilarutkan dalam 10 mL etanol dan diaduk kuat selama 1 jam. Kontrol positif dibuat dengan menggerus 10 mg amoksisilin hingga halus, kemudian dilarutkan dalam 100 mL akuades steril sehingga diperoleh konsentrasi 100 ppm.

2.2.5 Persiapan suspensi bakteri *Staphylococcus aureus*

Sebanyak 1 mL suspensi bakteri diambil dari tabung ulir. Pengenceran pertama (10^{-1}) dilakukan dengan menambahkan 1 mL suspensi ke dalam 9 mL larutan garam fisiologis. Pengenceran kedua (10^{-2}) dilakukan dengan memindahkan 1 mL dari pengenceran pertama ke tabung kedua berisi 9 mL larutan garam fisiologis. Seluruh tahap dilakukan aseptis di dalam *Laminar Air Flow*.

2.2.6 Inokulasi bakteri pada media

Sebanyak 1 mL suspensi *S. aureus* pengenceran 10^{-2} dimasukkan ke masing-masing 5 cawan petri steril, kemudian ditambahkan 20 mL Nutrient Agar (NA) dan dicampurkan perlahan dengan gerakan membentuk pola angka delapan hingga homogen. Media dibiarkan memadat sempurna secara aseptis di dalam *Laminar Air Flow*.

2.2.7 Uji antibakteri metode difusi agar sumuran

Pembuatan sumuran dilakukan dengan melubangi media agar yang telah memadat menggunakan pipet steril berdiameter 6 mm. Pada setiap cawan petri dibuat enam sumuran yang terdiri atas empat sumuran untuk ulangan perlakuan, satu sumuran sebagai kontrol negatif, dan satu sumuran sebagai kontrol positif. Selanjutnya, masing-masing larutan perlakuan dengan rasio 1:0, 0:1, 1:1, 2:1, dan 1:2 serta larutan kontrol dimasukkan ke dalam sumuran sebanyak 75 µL menggunakan mikropipet secara perlahan untuk mencegah tumpahan. Cawan kemudian diinkubasi pada suhu 37°C selama 24 jam. Setelah inkubasi, zona bening (zona hambat) yang terbentuk pada media Nutrient Agar diukur menggunakan digital caliper dan dinyatakan dalam satuan milimeter (mm).

2.2.8 Analisis data

Data diameter zona hambat dianalisis menggunakan uji normalitas dan uji homogenitas. Selanjutnya dilakukan uji One-way ANOVA, dan bila terdapat perbedaan signifikan dilanjutkan dengan uji lanjut Games–Howell.

3. Hasil dan Pembahasan

3.1 Hasil Uji Antibakteri

Uji daya antibakteri larutan kitosan *Scylla serrata* dan ion Ag^+ dengan perbandingan (C:Ag^+) sebesar 0:1, 1:0, 1:1, 1:2, dan 2:1 terhadap *Staphylococcus aureus* dilakukan dengan pengulangan sebanyak 4 kali. Hasil uji antibakteri dapat dilihat pada **Tabel 1**. Biakan bakteri *Staphylococcus aureus* dalam media Nutrient Agar yang telah diberi perlakuan difusi sumur dengan larutan kitosan *Scylla serrata* dan ion Ag^+ tercampur resin epoxy menunjukkan pembentukan zona bening di sekitar sumuran. Besarnya daya antibakteri larutan kitosan *Scylla serrata* dan ion Ag^+ diketahui melalui pengukuran diameter zona bening yang diukur dengan satuan milimeter (mm).

FaST - Jurnal Sains dan Teknologi, Vol. 10, No. 1, Mei 2026
e-ISSN 2598-9596
DOI: https://doi.org/10.19166/fastjst.v10i1.10886
Available online at: https://ojs.uph.edu/index.php/FaSTJST/article/view/10886

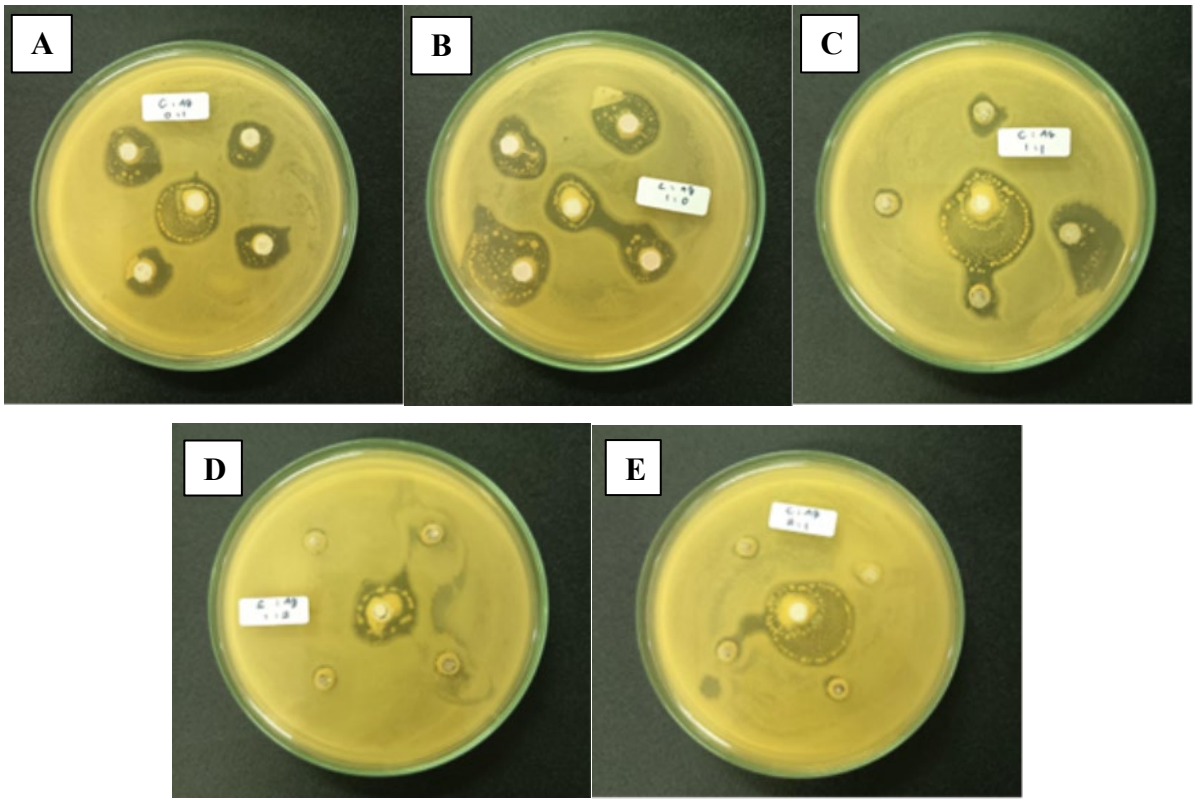

Gambar 1. Aktivitas antibakteri larutan kitosan Scylla serrata dan ion Ag^+ terhadap *Staphylococcus aureus* pada media Nutrient Agar berdasarkan zona hambat: (A) 0:1, (B) 1:0, (C) 1:1, (D) 1:2, (E) 2:1.

Tabel 1. Diameter zona bening pertumbuhan *Staphylococcus aureus* dengan perlakuan larutan kitosan *Scylla serrata* dan ion Ag^+, dan kontrol pada media Nutrient Agar

No	Perlakuan/Kontrol	Diameter zona bening (mm) 1	Diameter zona bening (mm) 2	Diameter zona bening (mm) 3	Diameter zona bening (mm) 4	Mean (mm)
1.	Kontrol Negatif	16,75	19,13	26,53	26,5	22,23
2.	Perbandingan (C:Ag+) 0:1	13,7	17,33	13,6	15,28	14,98
3.	Perbandingan (C:Ag+) 1:0	22,88	17,48	15,43	16,8	18,15
4.	Perbandingan (C:Ag+) 1:1	8	11,95	21,2	10,05	12,8
5.	Perbandingan (C:Ag+) 1:2	7,73	6,33	6,8	7,55	7,10
6.	Perbandingan (C:Ag+) 2:1	7,93	6,5	8,03	6,3	7,19
7.	Kontrol Positif	41,68	54,03	44,68	54,1	48,62

3.2 Analisis Statistik

Data yang diperoleh tersebut dianalisis menggunakan uji normalitas untuk mengetahui tingkat distribusi data yang diperoleh. Jika data yang diperoleh terbukti memiliki tingkat distribusi normal, data akan dianalisis lebih lanjut dengan uji Oneway ANOVA dan Post Hoc Test.

3.2.1 Uji Normalitas

Tingkat distribusi data diuji dengan uji normalitas sebelum perbedaan antar variabel yang terdapat pada data dapat diuji menggunakan uji Oneway ANOVA. Hasil analisis distribusi data menurut uji normalitas pada **Tabel 2**. Diketahui bahwa semua kelompok perlakuan memiliki nilai signifikansi lebih dari 0,05. Melalui hasil tersebut, data percobaan dinyatakan terdistribusi secara normal. Keputusan ini telah memenuhi syarat untuk Uji Oneway ANOVA, yaitu data wajib terdistribusi secara normal.

FaST - Jurnal Sains dan Teknologi, Vol. 10, No. 1, Mei 2026
e-ISSN 2598-9596
DOI: https://doi.org/10.19166/fastjst.v10i1.10886
Available online at: https://ojs.uph.edu/index.php/FaSTJST/article/view/10886

Tabel 2. Hasil Uji Normalitas

Hasil Uji Normalitas						
	Kolmogorov-Smirnov			Shapiro-Wilk		
Perlakuan	Statistic	df	Sig	Statistic	df	Sig
Rasio 1:0	.331	4	.	.855	4	.242
Rasio 0:1	.268	4	.	.873	4	.308
Rasio 1:1	.308	4	.	.865	4	.279
Rasio 2:1	.290	4	.	.807	4	.116
Rasio 1:2	.253	4	.	.921	4	.544
Negatif	.301	4	.	.827	4	.160
Positif	.301	4	.	.828	4	.163

Ket: Sig. > 0.05 maka data dinyatakan terdistribusi normal
Sig. < 0.05 maka data dinyatakan terdistribusi tidak normal
a. Lilliefors Significance Correction.

3.2.2 Uji Homogenitas

Homogenitas data diuji dengan uji homogenitas sebelum dapat diuji menggunakan uji ANOVA. Hasil analisis distribusi data menurut uji normalitas pada **Tabel 3**.

Tabel 3. Hasil Uji Homogenitas

Hasil Uji Homogenitas				
Dasar Perhitungan	**Levene Statistic**	**df1**	**df2**	**Sig.**
Based on Mean	6.260	6	21	<.001
Based on Median	3.332	6	21	.018
Based on Median and with adjusted df	3.332	6	6.611	.075
Based on trimmed mean	5.671	6	21	.001

Ket: Sig. > 0.05 maka data dinyatakan terdistribusi normal
Sig. < 0.05 maka data dinyatakan terdistribusi tidak normal

Nilai signifikansi *Based on Median and with adjusted df* yang lebih besar dari 0,05 menunjukkan bahwa varians data antar kelompok tidak homogen, sehingga asumsi homogenitas tidak terpenuhi dan analisis parametrik tidak dapat langsung digunakan.

3.2.3 Uji Oneway ANOVA

Perbedaan variabel data diuji dengan uji Oneway ANOVA dengan interval kepercayaan 95%. Setelah dilakukan input data dan analisis, diperoleh output pada **Tabel 4**.

Tabel 4. Hasil Uji ANOVA

ANOVA					
Hasil	Sum of Squares	df	Mean Square	F	Sig.
Between Groups	4894.998	6	815.833	49.482	<.001
Within Groups	346.236	21	16.487		
Total	5241.234	27			

Ket: Sig. > 0.05 maka data dinyatakan terdistribusi normal
Sig. < 0.05 maka data dinyatakan terdistribusi tidak normal

Dari tabel hasil Uji Oneway ANOVA di atas, diketahui bahwa kelompok percobaan memiliki nilai signifikansi kurang dari 0.05. Melalui hasil tersebut, data percobaan dinyatakan memiliki perbedaan signifikan.

FaST - Jurnal Sains dan Teknologi, Vol. 10, No. 1, Mei 2026
e-ISSN 2598-9596
DOI: https://doi.org/10.19166/fastjst.v10i1.10886
Available online at: https://ojs.uph.edu/index.php/FaSTJST/article/view/10886

3.1.4 Uji Post Hoc

Uji Oneway ANOVA adalah uji yang hanya mampu menganalisis data untuk mengetahui ada atau tidaknya perbedaan signifikan di antara semua variabel data tanpa menampilkan perlakuan yang berbeda secara spesifik [12]. Untuk mengetahui perbedaan signifikan di antara variabel data satu dengan yang lain, diperlukan Uji Post Hoc. Dalam penelitian ini, Uji Post Hoc menurut Games-Howell dilakukan untuk menganalisis perbedaan signifikan antara variabel data.

Tabel 5. Hasil Uji Post Hoc (Games-Howell)

(I) Perlakuan	(J) Perlakuan	Mean Difference (I-J)	Std. Error	Sig.	95% Confidence Interval Lower Bound	95% Confidence Interval Upper Bound
Rasio 1:0	Rasio 0:1	3.17000	1.85288	.640	-5.4527	11.7927
	Rasio 1:1	5.34750	3.34075	.692	-9.9958	20.6908
	Rasio 2:1	10.95750	1.69716	.029	1.7533	20.1617
	Rasio 1:2	11.04500	1.66646	.032	1.5893	20.5007
	Negatif	-4.08000	3.00563	.805	-17.3760	9.2160
	Positif	-30.47500	3.59431	.005	-47.4167	-13.5333
Rasio 0:1	Rasio 1:0	-3.17000	1.85288	.640	-11.7927	5.4527
	Rasio 1:1	2.17750	3.04193	.982	-14.1263	18.4813
	Rasio 2:1	7.78750	.96644	.006	3.1735	12.4015
	Rasio 1:2	7.87500	.93263	.009	3.1059	12.6441
	Negatif	-7.25000	2.66956	.297	-21.1459	6.6459
	Positif	-33.64500	2.31840	.007	-51.7251	-15.5649
Rasio 1:1	Rasio 1:0	-5.34750	3.34075	.692	-20.6908	9.9958
	Rasio 0:1	-2.17750	3.04193	.982	-18.4813	14.1263
	Rasio 2:1	5.61000	2.94967	.574	-11.4636	22.6836
	Rasio 1:2	5.69750	2.93211	.560	-11.5619	22.9509
	Negatif	-9.42750	3.85409	.319	-25.6107	6.7557
	Positif	-35.82250	4.32888	.002	-53.9243	-17.7207
Rasio 2:1	Rasio 1:0	-10.95750	1.69716	.029	-20.1617	-1.7533
	Rasio 0:1	-7.78750	.96644	.006	-12.4015	-3.1735
	Rasio 1:1	-5.61000	2.94967	.574	-22.6836	11.4636
	Rasio 1:2	.08750	.56300	1.000	-2.3495	2.5245
	Negatif	-15.03750	2.56393	.047	-29.7168	-.3582
	Positif	-41.43250	3.23403	.005	-60.2603	-22.6047
Rasio 1:2	Rasio 1:0	-11.04500	1.66646	.032	-20.5007	-1.5893
	Rasio 0:1	-7.87500	.93263	.009	-12.6441	-3.1059
	Rasio 1:1	-5.69750	2.93211	.560	-22.9569	11.5619
	Rasio 2:1	-.08750	.56300	1.000	-2.5245	2.3495
	Negatif	-15.12500	2.54371	.048	-30.0100	-.2400
	Positif	-41.52000	3.21802	.005	-60.5207	-22.5193
Negatif	Rasio 1:0	4.08000	3.00563	.805	-9.2160	17.3760
	Rasio 0:1	7.25000	2.66956	.297	-6.6459	21.1459
	Rasio 1:1	9.42750	3.85409	.319	-6.7557	25.6107
	Rasio 2:1	15.03750	2.56393	.047	.3582	29.7168
	Rasio 1:2	15.12500	2.54371	.048	.2400	30.0100
	Positif	-26.39500	4.07583	.007	-43.7181	-9.0719
Positif	Rasio 1:0	30.47500	3.59431	.005	13.5333	47.4167

FaST - Jurnal Sains dan Teknologi, Vol. 10, No. 1, Mei 2026
e-ISSN 2598-9596
DOI: https://doi.org/10.19166/fastjst.v10i1.10886
Available online at: https://ojs.uph.edu/index.php/FaSTJST/article/view/10886

Rasio 0:1	33.64500	3.31840	.007	15.5649	51.7251
Rasio 1:1	35.82250	4.32888	.002	17.7207	53.9243
Rasio 2:1	41.43250	3.23403	.005	22.6047	60.2603
Rasio 1:2	41.52000	3.21802	.005	22.5193	60.5207
Negatif	26.39500	4.07583	.007	9.0719	43.7181

Ket: Sig. > 0.05 maka data dinyatakan terdistribusi normal
Sig. < 0.05 maka data dinyatakan terdistribusi tidak normal

Dari hasil Uji Oneway Post Hoc (Games-Howell) pada **Tabel 5**, diketahui bahwa kelompok percobaan memiliki nilai signifikansi kurang dari 0.05. Melalui hasil tersebut, data percobaan dinyatakan memiliki perbedaan signifikan.

3.3 Pembahasan Hasil

Berdasarkan hasil uji antibakteri yang telah diperoleh dan diolah secara statistik, diketahui bahwa data terdistribusi secara normal sehingga uji Oneway ANOVA yang memiliki normalitas data sebagai syarat pengujian. Uji Oneway ANOVA merupakan uji parametric yang berfungsi untuk mengetahui ada atau tidaknya perbedaan antar variabel independen dalam data.

Uji Oneway ANOVA dilakukan pada 7 variabel yaitu larutan kitosan-$AgNO_3$ dengan rasio perbandingan (C:$AgNO_3$) 0:1, 1:0, 1:1, 1:2, 2:1, kontrol negatif dan kontrol positif. Melalui uji tersebut, diperoleh hasil analisis berupa nilai Sig. < 0.05 (tabel 4). Nilai Sig. tersebut lebih kecil daripada probabilitas 0.05 sehingga data dinyatakan memiliki perbedaan signifikan. Keputusan yang diambil terhadap data di atas adalah ketujuh populasi dinyatakan tidak identik satu sama lain (data diameter zona bening tiap kelompok perlakuan berbeda secara signifikan)[13].

Hasil uji Oneway ANOVA tidak dapat menunjukkan perbedaan yang ada antara satu kelompok dengan kelompok yang lain secara independen. Oleh karena itu, diperlukan uji Post Hoc untuk mengetahui perbedaan 2 variabel yang bersifat independen. Jenis uji yang digunakan adalah uji Games-Howell.

Hasil uji Games-Howell terhadap 2 variabel independen yang tampak pada tabel 5 menunjukkan bahwa terdapat perbedaan signifikan antara kelompok perlakuan 2:1 dan 1:2 dengan kontrol negatif. Namun, hal tersebut disebabkan oleh kelompok perlakuan 2:1 dan 1:2 memiliki efektivitas yang lebih rendah daripada kontrol negatif. Kontrol negatif sendiri memiliki zona bening, hal ini disebabkan oleh adanya penggunaan ethanol absolut 99%. Ethanol sendiri dikatakan efektif sebagai zat antibakteri, termasuk terhadap *Staphylococcus aureus* [12]. Namun, ethanol pada kontrol negatif tidak mampu untuk membunuh bakteri secara maksimal. Terlihat dari pertumbuhan kembali bakteri di dalam zona bening tersebut. Ini mengindikasikan adanya penurunan aktivitas antibakteri dari kontrol negatif dalam 24 jam masa inkubasi [14].

Berdasarkan hasil uji Games-Howell, semua kelompok perlakuan memiliki perbedaan secara nyata dengan kelompok positif. Analisis peneliti terhadap kelompok percobaan 0:1, 1:0, 1:1, 1:2, dan 2:1 telah menunjukkan adanya potensi antibakteri yang lebih besar pada kelompok percobaan 0:1 dan 1:0. Ini ditunjukkan dari adanya zona bening yang paling besar di antara lainnya, dan bakteri yang tumbuh kembali cenderung lebih sedikit dibandingkan kelompok percobaan lain [15]. Dari hasil tersebut, dapat dinyatakan juga bahwa kitosan atau ion Ag^+ memiliki daya hambat yang lebih tinggi terhadap pertumbuhan bakteri dalam perlakuan tunggal. Hasil ini tidak sinergis dengan hasil yang didapatkan dalam penelitian [6] yang menemukan adanya daya hambat pertumbuhan bakteri yang lebih baik dari komposit kitosan-Ag. Perbedaan hasil ini menunjukkan bahwa efektivitas sistem kitosan–Ag^+ sangat bergantung pada konsentrasi, viskositas, dan metode formulasi yang digunakan. Menurut [6], konsentrasi kitosan berpengaruh terhadap viskositas larutan yang akhirnya menyebabkan degradasi pada daya hambat terhadap *Staphylococcus aureus*. Semakin tinggi viskositas larutan, semakin lemah daya hambat terhadap bakteri.

Di antara ketiga variasi rasio perbandingan kitosan-$AgNO_3$, rasio perbandingan 1:1 adalah rasio perbandingan yang menghasilkan daya hambat antibakteri tertinggi berdasarkan nilai mean (mm). Idealnya, kitosan dapat menjadi stabilisator bagi ion Ag^+. Namun, kitosan juga dapat membatasi difusi ion Ag+ ke dalam sel bakteri [7]. Larutan dengan rasio perbandingan 2:1 dan 1:2 mengeluarkan daya hambat yang lebih rendah daripada larutan dengan rasio perbandingan 1:1 karena adanya pengaruh kitosan terhadap difusi ion Ag+.

FaST - Jurnal Sains dan Teknologi, Vol. 10, No. 1, Mei 2026
e-ISSN 2598-9596
DOI: https://doi.org/10.19166/fastjst.v10i1.10886
Available online at: https://ojs.uph.edu/index.php/FaSTJST/article/view/10886

Berdasarkan pengamatan secara kualitatif, diketahui bahwa daya hambat larutan kitosan-Ag+ dengan rasio perbandingan 1:0, 0:1, dan 1:1 tergolong kuat. Sedangkan daya hambat larutan kitosan-Ag+ dengan rasio perbandingan 2:1 dan 1:2 tergolong menengah [6].

4. Kesimpulan dan Saran

Kitosan *Scylla serrata* dan ion Ag+ menghambat pertumbuhan *Staphylococcus aureus* secara signifikan sebagai zat aktif dalam lapisan antibakteri. Hal ini dikarenakan diameter zona hambat kelompok percobaan kitosan-$AgNO_3$, kitosan, dan $AgNO_3$ menunjukkan perbedaan secara nyata terhadap kontrol positif. Dapat dilihat melalui hasil Uji Post Hoc, yaitu nilai signifikansi antara kontrol positif dengan kelima variasi rasio perbandingan kurang dari 0,05, yang menandakan adanya perbedaan yang signifikan. Rasio kitosan *Scylla serrata* dan ion Ag^+ pada kelompok percobaan 1:0, 0:1, dan 1:1 terbukti memberikan efek penghambatan yang signifikan terhadap pertumbuhan *Staphylococcus aureus*. Penghambatan terbesar diperoleh pada rasio 0:1, dengan rata-rata diameter zona hambat sebesar 18,15 mm, menunjukkan efektivitas antibakteri yang lebih tinggi dibandingkan rasio lainnya.

Berdasarkan hasil penelitian ini, diharapkan peneliti selanjutnya dapat mengkaji lebih dalam mengenai alasan kelompok perlakuan dengan rasio 1:0 dan 0:1 menunjukan diameter zona hambat yang lebih luas dibandingkan dengan ketiga variasi rasio perbandingan kitosan-$AgNO_3$ lainnya. Selain itu, perlu dilakukan eksplorasi terhadap metode pencampuran yang mampu menghasilkan larutan yang lebih homogen, serta pencarian bahan alternatif lain yang berpotensi memberikan efektivitas antibakteri yang lebih optimal.

Ucapan Terimakasih

Kami mengucapkan terima kasih yang sebesar-besarnya kepada Kepala Sekolah SMA Tarakanita Citra Raya, Tangerang yang telah memberikan kesempatan untuk mengikuti OPSI (Olimpiade Penelitian Siswa Indonesia). Ucapan terima kasih juga disampaikan kepada Kaprodi Teknologi Pangan dan tim laboran di Laboratorium Mikrobiologi, Universitas Pelita Harapan atas bantuan dan fasilitas yang diberikan selama pelaksanaan penelitian.

Daftar Referensi

[1] M. Gashaw, M. Abtew, and A. Addis, "Prevalence and antimicrobial susceptibility pattern of bacteria isolated from mobile phones of health care professionals working in Gondar town health centers," *Journal of Environmental and Public Health*, vol. 2014, Art. no. 205074, 2014. doi: 10.1155/2014/205074.

[2] A. Rahman, I. Hardi, and A. Baharuddin, "Identifikasi bakteri *Staphylococcus* sp. pada handphone dan analisis praktik personal hygiene," *Window of Health*, vol. 1, no. 1, pp. 40–47, 2018.

[3] M. U. E. Sanam, A. I. R. Detha, and N. K. Rohi, "Detection of antibacterial activity of lactic acid bacteria isolated from Sumba mare's milk against *Bacillus cereus*, *Staphylococcus aureus*, and *Escherichia coli*," *Journal of Advanced Veterinary and Animal Research*, vol. 9, no. 1, p. 53, 2022. doi: 10.5455/javar.2022.i568.

[4] S. S. M. Talabani and A. Taifor, "Simulation the effect of impact on the mobile cover using SolidWorks analysis," *ZANCO Journal of Pure and Applied Sciences*, vol. 31, no. s3, 2019, doi: 10.21271/ZJPAS.31.s3.6.

[5] T. Sadiq, A. Arikan, T. Sanlidag, E. Guler, and K. Suer, "Big concern for public health: Microbial contamination of mobile phones," *Journal of Infection in Developing Countries*, vol. 15, no. 6, pp. 798–804, 2021, doi: 10.3855/jidc.13708.[6] M. Potara, E. Jakab, A. Damert, O. Popescu, V. Canpean, and S. Astilean, "Synergistic antibacterial activity of chitosan–silver nanocomposites on *Staphylococcus aureus*," *Nanotechnology*, vol. 22, no. 13, p. 135101, 2011. doi: 10.1088/0957-4484/22/13/135101.

[7] J. Florencia, "Menilik manfaat ion perak dalam membunuh bakteri," KlikDokter, 2017. [Online]. Available: https://www.klikdokter.com

[8] F. Nurainy, S. Rizal, and Y. Yudiantoro, "Pengaruh konsentrasi kitosan terhadap aktivitas antibakteri dengan metode difusi agar (sumur)," *Jurnal Teknologi Industri dan Hasil Pertanian*, vol. 13, no. 2, pp. 117–123, 2008.

[9] M. Ambari, "Kepiting dan rajungan: Enak rasanya, unggulan ekspor Indonesia, bagaimana keberlanjutannya?" Mongabay Indonesia, 2024. [Online]. Available: https://mongabay.co.id

[10] C.-J. Yao, S.-J. Yang, M.-J. Shieh, and T.-H. Young, "Development of a chitosan–silver nanocomposite/β-1,3-glucan/hyaluronic acid composite as an antimicrobial system for wound healing," *Polymers*, vol. 17, no. 3, p. 350, 2025. doi: 10.3390/polym17030350.

[11] R. Riski and F. J. Sami, "Formulasi krim anti jerawat dari nanopartikel kitosan cangkang udang windu (*Penaeus monodon*)," *Jurnal Farmasi UIN Alauddin Makassar*, vol. 3, no. 4, pp. 1–6, 2017.
[12] C. Wendakoon, P. Calderon, and D. Gagnon, "Evaluation of selected medicinal plants extracted in different ethanol concentrations for antibacterial activity against human pathogens," *Journal of Medicinally Active Plants*, vol. 1, no. 2, pp. 60–68, 2012.
[13] A. W. Lestari, Z. Marlita, V. Sefiya, and I. A. Prasetyo, "Analysis of variance (ANOVA): Concept, steps, and its application in data analysis," *J. Sintesis*, vol. 6, no. 1, 2025, doi: 10.56399/jst.v6i1.283.
[14] N. B. A. Prasetya, Ngadiwiyana, Ismiyarto, and P. R. Sarjono, "Synthesis and study of antibacterial activity of polyeugenol," *IOP Conference Series: Materials Science and Engineering*, vol. 509, no. 1, Art. no. 012101, 2019, doi: 10.1088/1757-899X/509/1/012101.
[15] G. E. C. Alouw, Fatimawali, and J. S. Lebang, "Uji aktivitas antibakteri ekstrak etanol daun kersen (*Muntingia calabura* L.) terhadap bakteri *Staphylococcus aureus* dan *Pseudomonas aeruginosa* dengan metode difusi sumuran," *Pharmacy Medical Journal*, vol. 5, no. 1, pp. 36–45, 2022, doi: 10.35799/pmj.v5i1.41430

FaST - Jurnal Sains dan Teknologi, Vol. 10, No. 1, Mei 2026
e-ISSN 2598-9596
DOI: https://doi.org/10.19166/fastjst.v10i1/10932
Available online at: https://ojs.uph.edu/index.php/FaSTJST/article/view/10932

Assessment of Rainwater Quality from Rainwater Storage in Ende, East Nusa Tenggara Province, Indonesia

Yohanes Erik Kurniawan Nggae[1)], Intan Supraba[2)], Radianta Triatmadja[2*)]
[1]Department of Civil Engineering, Faculty of Science and Technology, Universitas Pelita Harapan, Tangerang, Indonesia
[21]Department of Civil and Environmental Engineering, Faculty of Engineering, Universitas Gadjah Mada, Yogyakarta, Indonesia

ABSTRACT

Using rainwater as an alternative water source requires careful attention to its quality, particularly in simple storage systems. This study aims to analyze changes in the physical, chemical, and microbiological quality of rainwater stored in a tank over a specified period, as well as the effects of maintenance practices on rainwater harvesting systems. The research methodology involved collecting samples of untreated rainwater and rainwater stored in a tank over four weeks. Physical parameters analyzed included color, turbidity, and total dissolved solids (TDS); chemical parameters included pH; and microbiological parameters included total coliforms and *Escherichia coli*. The results indicate that poor roof surface and gutter system cleanliness led to increased turbidity and noticeable changes in rainwater color. Following roof and gutter cleaning, improvements in the physical quality of the stored rainwater were observed. However, an anomaly in turbidity occurred during the third week, reaching 52 NTU. TDS values decreased throughout the storage period, while the pH of the rainwater remained within a neutral range. From a microbiological perspective, the concentrations of total coliforms and *E. coli* decreased significantly over the storage period, presumably due to limited nutrient availability and unfavourable environmental conditions for bacterial growth. The boiling process was effective in reducing bacterial concentrations; however, total coliforms and *E. coli* were still detected at levels of 11 CFU/100 mL and 4.4 CFU/100 mL, respectively. These findings demonstrate that stored rainwater requires further treatment prior to use, particularly for potable purposes.

ARTICLE INFO

Keywords: alternative water source; microbiological quality; rainwater; rainwater quality; rainwater storage.
***Corresponding author**: intan.supraba@ugm.ac.id

Article history:
Submitted 22 Feb 2026
Revised 13 Apr 2026
Accepted 15 Apr 2026
Online Available 17 Apr 2026
Published 20 May 2026

1. Introduction

Rainwater is one of the sources of raw water for a clean water supply derived from surface water [1]. The use of rainwater is common in regions experiencing water scarcity during the dry season. Rainwater harvesting can be considered relatively simple and accessible to most communities, as rainwater falling on rooftops is collected through gutters, conveyed by pipes, and subsequently stored in tanks. Typically, the tank inlet is equipped with a water filter to prevent debris and sediment from entering the storage tank, as well as a water purification unit to ensure the collected water meets the required quality standards for a clean water supply [2].

Many countries have utilized rainwater as a source of raw water to meet clean water demands. One country that has extensively adopted rainwater not only as a raw water source but also for potable purposes is Australia [3]. Most regions in Australia have introduced regulations or policies promoting rainwater harvesting, primarily to reduce dependence on centralized water supply utilities. This approach is critical given that Australia is one of the driest continents on Earth, with continuously increasing air temperatures that have led to widespread depletion of surface water and groundwater resources. For example, the state of Queensland enforces regulations requiring new residential buildings with roof areas of at least 100 m² to install rainwater harvesting systems with a minimum storage capacity of 5 kL.

Related studies on the use of rainwater as a raw water source have also been conducted in Jordan, a country that experiences severe water scarcity during the dry season [4]. These studies demonstrated that approximately 15 m³/year of rainwater can be harvested from a single household roof in Jordan, equivalent to about 5.6% of the total domestic water supply in 2005, which largely depended on groundwater resources. In most regions of the American continent, rainwater is primarily used for non-potable purposes, such as hygiene activities (toilet flushing, laundry, and irrigation), with limited use for drinking water. This is because rainwater collected from rooftops and stored in ponds or tanks requires appropriate treatment before use for potable purposes [5].

FaST - Jurnal Sains dan Teknologi, Vol. 10, No. 1, Mei 2026
e-ISSN 2598-9596
DOI: https://doi.org/10.19166/fastjst.v10i1/10932
Available online at: https://ojs.uph.edu/index.php/FaSTJST/article/view/10932

Rainwater has also been utilized as a source of raw water in several regions of Indonesia. A study conducted by Krisnayanti *et al*. [6] in Kupang Town demonstrated that the minimum rainwater storage capacity, calculated using the water balance method, ranges from 26.59 to 44.10 m³ per household. This capacity was shown to reduce reliance on the municipal water supply (PDAM) by 30.57% and to significantly decrease household expenditures on clean water. Another study by Purwantoro *et al*. [7] in Panggang District, Gunungkidul Regency, examined patterns of household water resource utilization and estimated the appropriate size of rainwater harvesting systems. The results indicated relatively high rainfall conditions, with five dry months and six wet months annually. The required storage volume was determined by multiplying daily water demand by the duration of the dry season. The potential volume of harvestable rainwater was estimated by multiplying the effective roof catchment area by the average monthly rainfall and the runoff coefficient of the roofing material.

The quality of rainwater as a raw water source for a clean water supply generally complies with the standards stipulated in the Indonesian Ministry of Health Regulation (Permenkes) No. 32 of 2017; however, most measurements of rainwater quality indicate a tendency toward acidic pH values that do not meet the prescribed quality standards [8–10]. According to Maryono [11] , the acidic nature of rainwater in Indonesia is mainly due to high atmospheric carbon dioxide concentrations, which react with water vapor to form carbonic acid, a weak acid. Rainwater with a pH range of 5.0 to 6.0 is generally considered safe for use and poses no significant health risks. Nonetheless, bacterial contamination remains a critical concern, requiring appropriate treatment before it can be used for clean water purposes [12,13].

Hamilton *et al*. [12] identified several factors influencing the presence of bacteria in rooftop-harvested rainwater storage tanks, including meteorological factors (wind direction and speed), catchment location, climatic conditions, organic matter accumulation in gutters, the presence of animal feces or animals around the roof area, water volume and retention time within the tank, as well as the condition of the roof and storage system. In addition, the presence of *Escherichia coli* in untreated rainwater is presumed to be associated with bioaerosol events, in which pathogenic microorganisms attached to aerosol particles are deposited with rainfall. Rahayu *et al*. [14] reported that *E. coli* is a member of the coliform group of bacteria that can survive and persist in the digestive tracts of humans and animals. The growth and survival of *E. coli* are strongly influenced by environmental conditions, including temperature, pH, and osmotic pressure. The optimal temperature for *E. coli* growth is approximately 37 °C, with a minimum generation time (doubling time) of about 30 minutes. *E. coli* is also capable of surviving under acidic conditions, within a pH range of 2.5 to 4.6.

This study aims to analyze changes in the physical, chemical, and microbiological quality of rainwater stored in a tank over a specified period, and to evaluate the effects of maintenance practices on the rainwater harvesting system. The research process began with the collection of samples of untreated rainwater and rainwater stored in the tank, followed by an assessment of roof and gutter conditions, the implementation of cleaning procedures for the rainwater harvesting system, and periodic monitoring of water quality through physical, chemical, and microbiological parameter testing throughout the storage period.

2. Methodology

2.1 Tools and Materials

A simple rainwater storage installation requires a set of materials designed to ensure the effective collection, conveyance, and storage of rainwater. The main component is a 1,300-liter storage tank that serves as the reservoir for roof runoff. Rainwater is collected through 6-inch gutters equipped with gutter outlets and gutter guards, allowing for controlled flow while minimizing the entry of large debris such as leaves and twigs.

The water conveyance system employs PVC pipes with varying diameters 4 inches, 2 inches, and ¾ inch adjusted to meet the required flow rate and pressure at different sections of the system. Larger-diameter pipes are used in the upstream section to accommodate relatively high runoff discharge, after which the pipe size is gradually reduced using reducing sockets from 4 inches to 2 inches and from 2 inches to ¾ inch. Pipe fittings, including 2-inch elbow (L) joints and 2-inch tee (T) joints, are utilized to control flow direction and branching, allowing the installation configuration to be adapted to site-specific conditions.

FaST - Jurnal Sains dan Teknologi, Vol. 10, No. 1, Mei 2026
e-ISSN 2598-9596
DOI: https://doi.org/10.19166/fastjst.v10i1/10932
Available online at: https://ojs.uph.edu/index.php/FaSTJST/article/view/10932

Flow regulation and the use of harvested rainwater are facilitated by installing valves and ¾-inch faucets, enabling users to control outflow from the storage tank according to demand. In addition, a plastic float ball combined with a wire is used as a preliminary filter (pre-filter) to retain floating debris before the water enters the tank. The integration of these components results in a rainwater harvesting system that is simple, cost-effective, and easy to implement, while still supporting water conservation efforts and sustainable water resource management. The rainwater storage system was installed in Kota Raja Subdistrict, Ende Utara District, at coordinates 8.836498° S, 121.6479562° E. The installation of the rainwater harvesting system is shown in **Fig. 1**.

Figure 1. Rainwater Harvesting System

2.2 Research Methods

Data analysis methods were applied to evaluate changes in rainwater quality across the collection, conveyance, and storage processes within the rainwater harvesting (RWH) system. The initial stage involved planning the installation of the RWH system by considering roof conditions, gutter configuration, rainwater flow direction, and storage tank capacity, ensuring that the system adequately represented actual rainwater utilization practices. Subsequently, the RWH system was installed at the predetermined location in accordance with the planned design, ensuring consistent rainwater collection and conveyance throughout the observation period.

Water sampling was conducted in stages to capture variations in rainwater quality at each process phase. The samples included rainwater collected prior to roof contact, rainwater after runoff from the roof surface, and rainwater stored in the RWH system. Sampling of stored rainwater was carried out periodically from the first to the fourth week of storage to observe changes in water quality resulting from storage processes, sedimentation, and potential contamination. All samples were collected following standard water sampling procedures to minimize contamination and ensure analytical accuracy. The rainwater samples analyzed comprised untreated rainwater (R0), roof-runoff rainwater (R1), first-flush rainwater collected in a 1 m pipe (RX), and rainwater stored in a tank (R2). Following the sampling process, water quality testing was conducted weekly over four weeks after a rainfall event, during which no additional rainwater entered the storage system. This approach enabled the isolation of external variables and allowed for a focused assessment of the natural purification processes occurring within the tank until the water quality met the established clean water standards.

All water samples were analyzed at the Regional Health Laboratory of Ende Regency using standardized water quality testing methods. The analyzed parameters included physical, chemical, and microbiological indicators, and the results were compared with relevant water quality standards. The test results were analyzed descriptively and comparatively to assess differences in water quality across

FaST - Jurnal Sains dan Teknologi, Vol. 10, No. 1, Mei 2026
e-ISSN 2598-9596
DOI: https://doi.org/10.19166/fastjst.v10i1/10932
Available online at: https://ojs.uph.edu/index.php/FaSTJST/article/view/10932

process stages and changes over the storage period. Based on these analyses, recommendations were formulated regarding the suitability of harvested rainwater for non-potable domestic use, as well as the potential development of additional treatment systems to enable safer, more sustainable use of rainwater.

3. Results and Discussion

During the first rainfall event, rainwater samples were collected and analyzed at the Regional Health Laboratory of Ende Regency. The results of the water quality analysis are presented in **Table 1**. The findings indicate that all tested rainwater samples failed to meet the required standards for color, turbidity, total coliforms, and *Escherichia coli*. Rainwater that had passed over the roof exhibited total dissolved solids (TDS) values exceeding the permissible limits, whereas rainwater collected prior to roof contact showed TDS concentrations below 300 mg/L. The observed deterioration in rainwater quality can be attributed to several factors.

First, the poor condition of the roof surface and gutters, which conveyed rainwater into the storage tank, significantly affected water quality. Prolonged periods without rainfall following system installation led to the accumulation of leaf litter on the roof and in the gutters. Rainwater mixed with decaying leaves led to increased turbidity and noticeable changes in water color. Turbidity is closely associated with suspended and dissolved solids, while water color is related to TDS, suspended solids, and turbidity levels. Elevated TDS values are influenced by the presence of dissolved organic and inorganic compounds, as well as plankton or microorganisms in the water [15]. High concentrations of total coliforms and *E. coli* may result from bacterial contamination originating from roof surfaces or leaf debris, as well as from bioaerosol deposition processes [12]. The condition of the roof prior to cleaning is shown in **Fig. 2**, while a representative sample of water collected from the storage tank is presented in **Fig. 3**.

Figure 2. The condition of the roof prior to cleaning

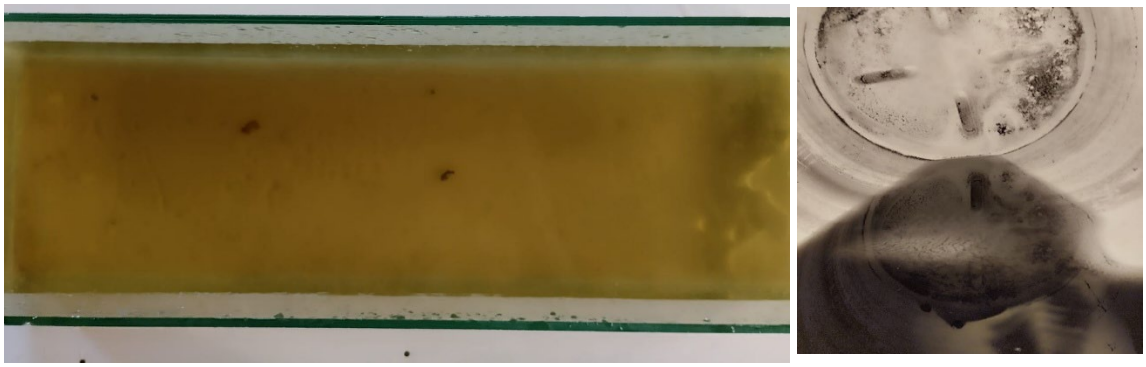

Figure 3. Rainwater from the storage prior to cleaning

FaST - Jurnal Sains dan Teknologi, Vol. 10, No. 1, Mei 2026
e-ISSN 2598-9596
DOI: https://doi.org/10.19166/fastjst.v10i1/10932
Available online at: https://ojs.uph.edu/index.php/FaSTJST/article/view/10932

Second, the quality of untreated rainwater samples may be poor, depending on the timing of the rainfall event and the environmental sanitation conditions at the sampling location. Precipitation patterns play a critical role in determining water quality within storage tanks. Short-duration rainfall events often result in higher concentrations of dissolved substances because of their limited volume. In contrast, prolonged precipitation results in significant dilution, lowering the overall concentration of dissolved materials [16, 17]. Maryono *et al*. [11] suggested that rainwater should be collected only after the first 5–10 minutes of a rainfall event. The initial runoff, commonly referred to as the "first flush," is believed to have inferior quality due to mixing with atmospheric pollutants and airborne particles. It should be noted that the rainwater samples analyzed in this study were collected from the first rainfall event following the installation of the rainwater harvesting system.

Subsequently, the roof and gutter system were cleaned, and overhanging branches were trimmed to reduce the accumulation of leaf debris on the roof and in the gutters, which could obstruct the flow of rainwater into the storage tank. The rainwater storage tank was also cleaned to prevent contamination from previously stored water. Rainwater harvesting was then conducted during the subsequent rainfall event, and the collected water was stored for four weeks to assess changes in rainwater quality during storage. Rainwater was collected from a single rainfall event only and was not supplemented by subsequent rainfall. Water quality testing was carried out at the beginning of the first week (R4), the second week (R5), the third week (R6), and the fourth week (R7) of storage. The cleaned conditions of the roof, gutters, storage tank, and the outflow from the cleaned storage tank are presented in **Fig. 4**.

Figure 4. Condition of the roof, the storage tank after cleaning, and the condition of the water inside the storage tank

The results of the water quality analysis are presented in **Table 2**. The findings indicate an increase in color intensity in rainwater stored in the rainwater storage tank. As discussed previously, water color is closely associated with dissolved solids, suspended solids, and turbidity. Based on the cross-sectional configuration of the installed rainwater harvesting system, rainwater enters the storage tank from the roof located above the tank, while water intended for use is withdrawn through a tap positioned near the bottom of the tank. The observed increase in color in stored rainwater may be attributed to particles, chemical compounds, bacteria, plankton, or even algae that enter the tank with the rainwater.

FaST - Jurnal Sains dan Teknologi, Vol. 10, No. 1, Mei 2026
e-ISSN 2598-9596
DOI: https://doi.org/10.19166/fastjst.v10i1/10932
Available online at: https://ojs.uph.edu/index.php/FaSTJST/article/view/10932

Table 1 Rainwater quality prior to roof cleaning

No	Location			Parameter									
	Latitude	Longitude	Sample Code	Odor	Taste	Color (TCU)	Turbidity (NTU)	Temperature (°C)	TDS (mg/L)	pH	Salinity (mg/L)	Total Coliform (CFU/100 mL)	E. coli (CFU/100 mL)
1	-8,8365	121,648	R0	Odorless	Tasteless	28	12	24°C	75	7,9	0	>2400	120
2	-8,8365	121,648	R1	Odorless	Tasteless	26	30	24°C	320	7,9	0	>2400	150
3	-8,8365	121,648	R2	Odorless	Tasteless	24	34	25°C	380	7,8	0	>2400	210
4	-8,8365	121,648	RX	Odorless	Tasteless	46	52	24°C	230	7	0	>2400	210

Table 2 Rainwater quality following roof cleaning

No	Location			Parameter									
	Latitude	Longitude	Sample Code	Odor	Taste	Color (TCU)	Turbidity (NTU)	Temperature (°C)	TDS (mg/L)	pH	Salinity (mg/L)	Total Coliform (CFU/100 ml)	E. coli (CFU/100 ml)
1	-8,8365	121,648	RX2	Odorless	Tasteless	115	10	24°C	41	7,3	0	>2400	240
2	-8,8365	121,648	R3	Odorless	Tasteless	0	0	23°C	16	7,6	0	>2400	240
3	-8,8365	121,648	R4	Odorless	Tasteless	0	0	23°C	21	7,4	0	>2400	240
4	-8,8365	121,648	R5	Odorless	Tasteless	25	2	28,9°C	11	7,6	0	93	7,5
5	-8,8365	121,648	R6	Odorless	Tasteless	30	52	27°C	17	7,5	0	28	11
6	-8,8365	121,648	R7	Odorless	Tasteless	70	2	28°C	9	7,8	0	11	7
7	-8,8369	121,6515	RP	Odorless	Tasteless	0	0	24°C	21	7,8	0	>2400	240

FaST - Jurnal Sains dan Teknologi, Vol. 10, No. 1, Mei 2026
e-ISSN 2598-9596
DOI: https://doi.org/10.19166/fastjst.v10i1/10932
Available online at: https://ojs.uph.edu/index.php/FaSTJST/article/view/10932

The color value of rainwater during the first week of storage complied with the Indonesian Ministry of Health Regulation (Permenkes) No. 2 of 2023, whereas the values measured in subsequent weeks exceeded the prescribed standard. The trend in changes in rainwater color is illustrated in **Fig. 5**.

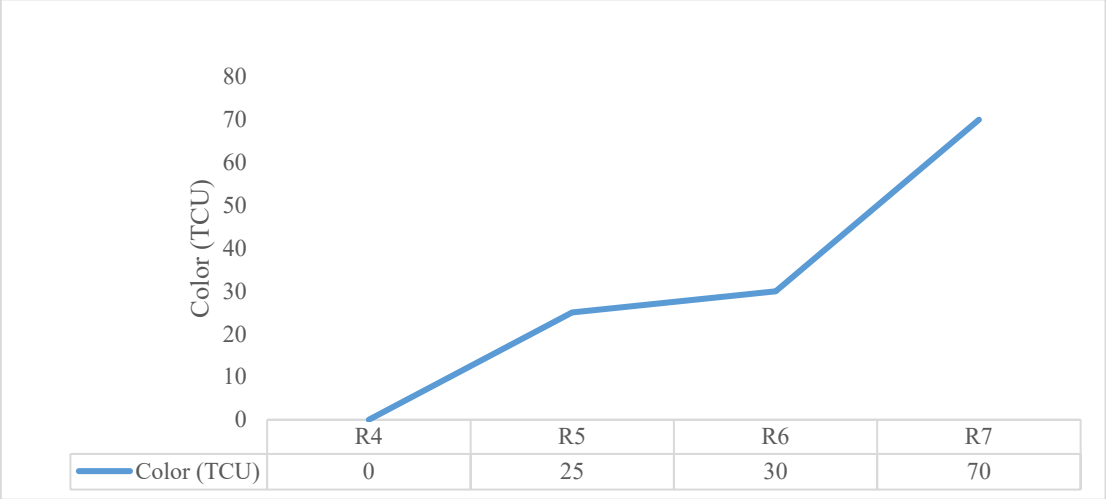

Figure 5. Color of rainwater in the storage tank from week 1 to week 4

Rainwater turbidity may originate from total suspended solids (TSS) or particles transported from the roof into the storage tank. Turbidity levels in the rainwater storage tank showed an anomaly in the third-week sample, when turbidity increased sharply to 52 NTU. This unusually high value may have resulted from sampling error, such as disturbance of the tank prior to sampling. Such a disturbance could resuspend settled particles at the bottom of the tank, temporarily increasing turbidity. Dispersion in water can explain the increase in suspended particles and turbidity within a storage system. Dispersion refers to the movement of particles within a fluid from their initial positions to new locations [18]. Larger particles tend to move more rapidly than smaller particles, and the type of fluid also influences the rate of particle transport in water [19].

Particles carried into the tank with rainwater may originate from an unclean metal roof or poorly maintained gutters. These particles are initially transported from the water surface toward the bottom of the tank, where they gradually settle over time. Consequently, water stored in the tank over a given period will contain particles that slowly sediment to the bottom. Turbidity in stored rainwater increases with the presence and resuspension of suspended particles within the storage system. Turbidity values during the first, second, and fourth weeks of storage complied with the Indonesian Ministry of Health Regulation (Permenkes) No. 2 of 2023, whereas the sample collected in the third week exceeded the allowable standard. The turbidity results are presented in **Fig. 6**.

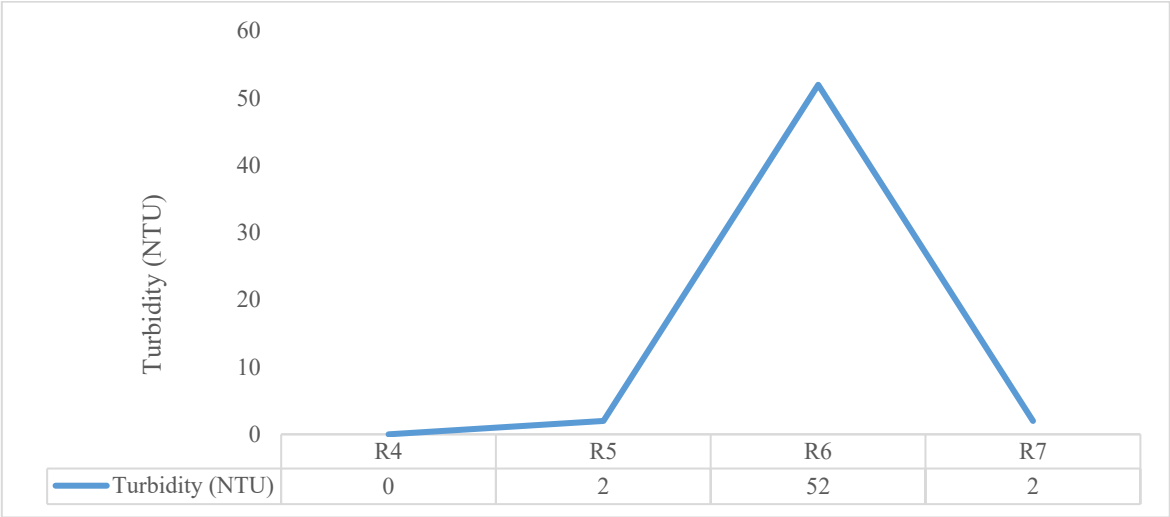

Figure 6. Turbidity of rainwater in the storage tank from week 1 to week 4

FaST - Jurnal Sains dan Teknologi, Vol. 10, No. 1, Mei 2026
e-ISSN 2598-9596
DOI: https://doi.org/10.19166/fastjst.v10i1/10932
Available online at: https://ojs.uph.edu/index.php/FaSTJST/article/view/10932

The total dissolved solids (TDS) values of rainwater stored in the rainwater harvesting tank decreased over the storage period. TDS in stored rainwater may originate from dissolved particles leached from galvanized or metal roofing materials, as well as from residual debris on the roof that is transported and dissolved during rainfall events. Previous studies have shown that roof material quality significantly influences the quality of rainwater collected in storage systems, with chemical parameters—particularly metal concentrations—being the most affected. Galvanized or zinc roofs tend to leach more particles into rainwater compared to clay tile roofs [20]. Furthermore, rainwater collected from corroded roofs exhibits higher TDS values than rainwater harvested from non-corroded roofing surfaces [21].

Therefore, both roof cleanliness and roof material type should be carefully considered in rainwater harvesting applications. The use of appropriate roofing materials combined with regular roof maintenance can substantially improve the quality of stored rainwater. In addition, the surface of the storage material and its placement close to sunlight support the growth of biofilms and trigger the release of organic substances, which cause fluctuations in the TDS of the water [22, 23]. All measured TDS values from the first to the fourth week of storage complied with the Indonesian Ministry of Health Regulation (Permenkes) No. 2 of 2023. The TDS results are presented in **Fig. 7**.

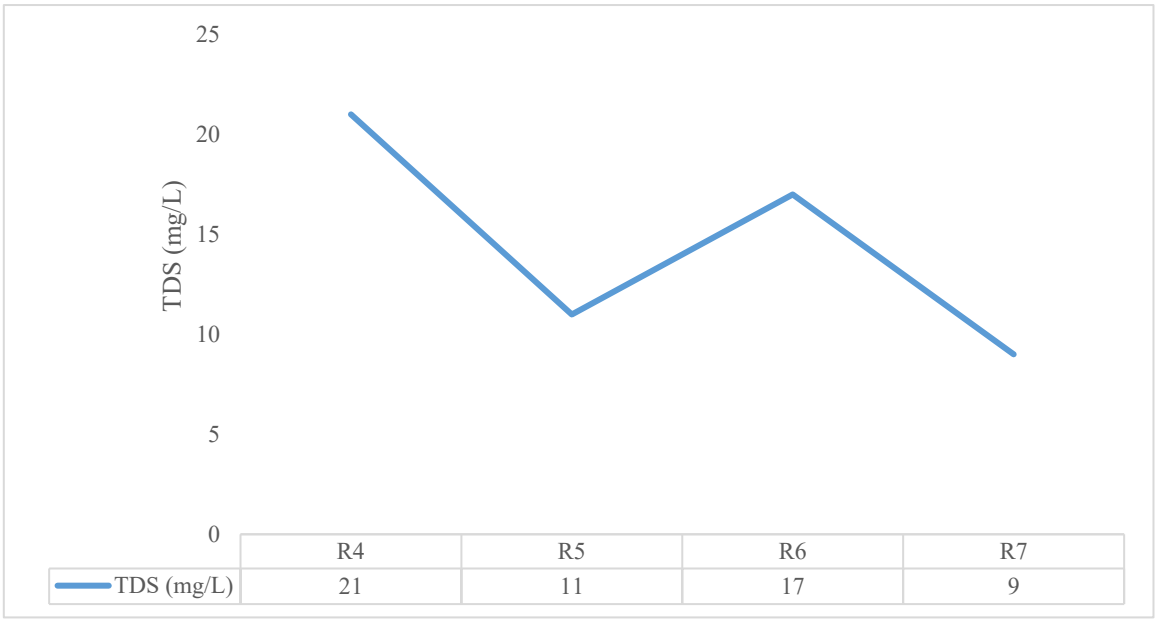

Figure 7. TDS of rainwater in the storage tank from week 1 to week 4

The pH values of the stored rainwater remained within normal conditions, approximately neutral at pH 7. According to the Indonesian Ministry of Health Regulation (Permenkes) No. 2 of 2023, acceptable pH values for water quality range from 6.5 to 8.0. The measured pH values of rainwater samples from the first to the fourth week of storage ranged from 7.4 to 7.8, indicating compliance with the established standard. An increase in water pH may be attributed to changes in dissolved carbon dioxide (CO_2) concentration, as lower CO_2 levels result in higher [24]. Furthermore, the type of storage tank material, such as plastic, can alter the water's pH due to the leaching of chemical additives and the influx of carbon dioxide from the air [22, 25]. The pH variation over the storage period is illustrated in **Fig. 8**.

FaST - Jurnal Sains dan Teknologi, Vol. 10, No. 1, Mei 2026
e-ISSN 2598-9596
DOI: https://doi.org/10.19166/fastjst.v10i1/10932
Available online at: https://ojs.uph.edu/index.php/FaSTJST/article/view/10932

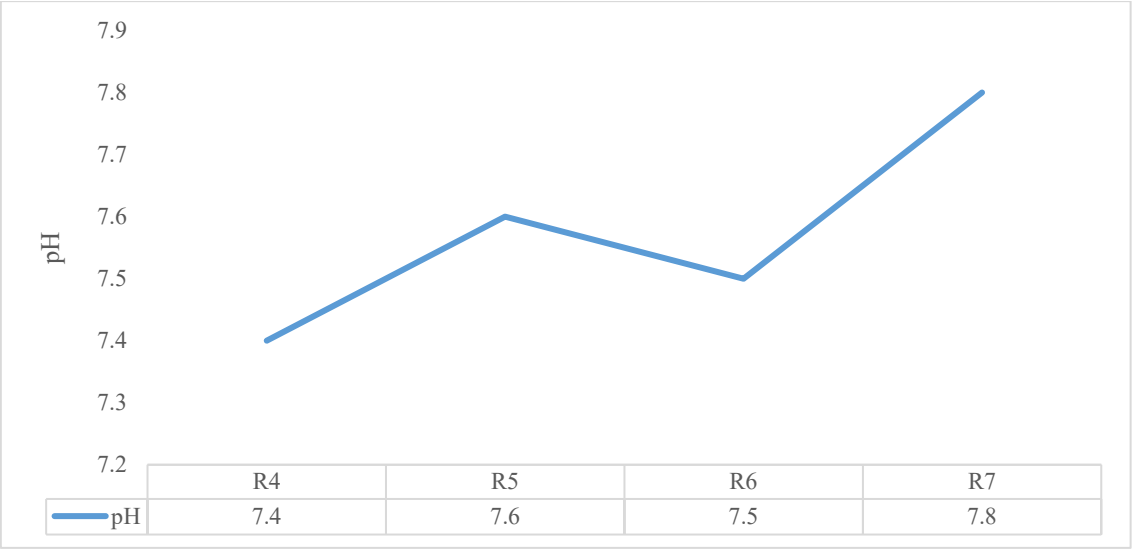

Figure 8. pH of rainwater in the storage tank from week 1 to week 4

Bacteria present in rainwater stored in rainwater harvesting tanks may originate from roof cleanliness, the presence of insects or birds around the roof area and surrounding environmental sanitation conditions that allow aerosol deposition near the [12, 26]. Rainwater samples collected after roof contact (R3) and first-flush rainwater captured in the initial collection pipe (RX2) exhibited high abundances of total coliforms and *Escherichia coli*. These conditions indicate that the rainwater stored in the tank originated from runoff passing through surfaces that served as potential bacterial reservoirs. The concentrations of total coliforms and *E. coli* in the storage tank at the beginning of the first week of sampling (R4) were identical to those measured in rainwater from the first roof runoff and the first-flush sample collected in the pipe.

In addition, rainwater samples collected directly from rainfall near a livestock enclosure without roof contact (RP) also showed high abundances of total coliforms and *E. coli*. This finding suggests that aerosol deposition events can also significantly influence rainwater quality. Over the 4-week storage period, total coliform and *E. coli* concentrations in the rainwater storage tank declined substantially. The trends in bacterial reduction are presented in **Fig. 9** and **Fig. 10**. Previous studies have reported that *E. coli* concentrations in surface water can decrease by up to 50% within 1.5 to 3 days, while total coliform concentrations decrease by 50% within approximately 0.9 days [27]. These reductions may be attributed to decreases in temperature, limited availability of organic carbon in the water, and variations in sunlight intensity, which affect bacterial survival.

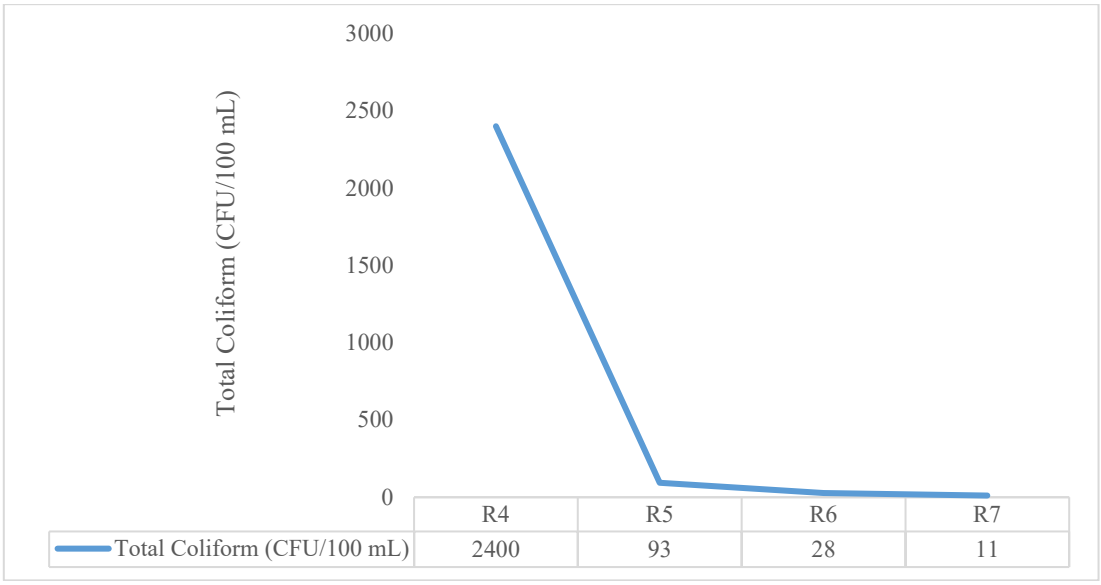

Figure 9. Total Coliform of rainwater in the storage tank from week 1 to week 4

FaST - Jurnal Sains dan Teknologi, Vol. 10, No. 1, Mei 2026
e-ISSN 2598-9596
DOI: https://doi.org/10.19166/fastjst.v10i1/10932
Available online at: https://ojs.uph.edu/index.php/FaSTJST/article/view/10932

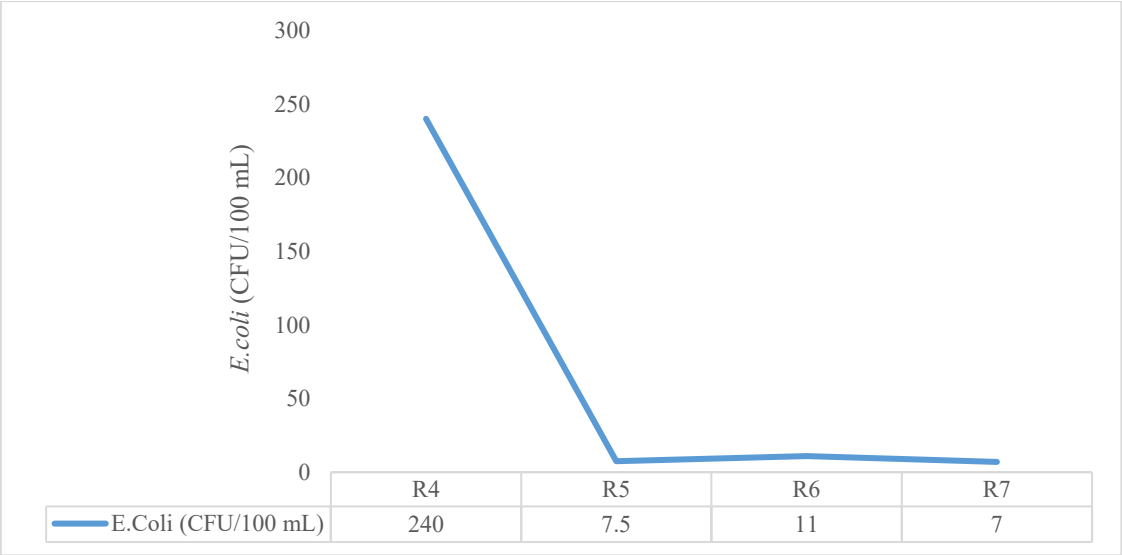

Figure 10. *E. coli* of rainwater in the storage tank from week 1 to week 4

The decrease in total coliforms and *E. coli* concentrations in stored rainwater may also be associated with limited nutrient availability and unfavorable environmental conditions within the storage system. Such conditions may induce bacterial dormancy or inactivity. Dormancy is defined as a physiological state in which bacterial cells remain viable and metabolically active but are unable to grow under prevailing environmental conditions [28]. A study by Gao *et al.* [29] from Harvard University found that, to survive harsh environmental conditions, bacteria may enter a dormant state by forming spores and developing protective layers around the cell. This protective structure enables bacteria to survive in nutrient-free environments and protects them from cellular damage caused by extreme temperatures, ultraviolet radiation, harsh chemicals, and antibiotics. However, when spores detect favorable environmental conditions and nutrient availability, they can shed their protective layers and reactivate metabolic activity. The spores referred to in this context are endospores, which function as bacterial survival mechanisms under extreme and unfavorable conditions rather than as part of vegetative growth or genetic reproduction processes [30].

Dormant bacteria exhibit greater antibiotic resistance than metabolically active bacteria. Following antibiotic exposure, dormant bacteria may resuscitate and resume growth when environmental conditions become favorable and sufficient nutrients are available. Dormant bacteria are difficult to detect using conventional laboratory microbiological techniques because, during dormancy, bacterial cells often undergo morphological changes from rod-shaped to coccoid forms. Actively detectable bacteria are typically rod-shaped. Moreover, during dormancy, bacteria lose intracellular components such as proteins and other molecules essential for routine cellular functions, including respiration and metabolism, making them less detectable through standard microbiological assays [28], [31].

This study did not measure water temperature within the storage tank or quantify nutrient availability in the stored rainwater to assess correlations with bacterial dormancy directly. Instead, the study further examined changes in the quality of stored rainwater following boiling treatment (RB) using a household electric water heater. The boiled rainwater sample was collected at the beginning of the second week of storage. The results showed that, although the rainwater had been boiled, total coliforms and *E. coli* were still detected at concentrations of 11 CFU/100 mL and 4.4 CFU/100 mL, respectively. Prior to boiling, the rainwater contained 93 CFU/100 mL of total coliforms and 7.5 CFU/100 mL of *E. coli*. Heating is one method that can damage bacterial DNA, leading to bacterial inactivation or death [32]. Previous studies have reported that bacteria generally cannot survive heating at 75 °C [33] and *that E. coli* is inactivated at approximately 70 °C [34]. However, these studies were conducted under sterile laboratory conditions rather than in household settings. Therefore, the persistence of *E. coli* in boiled rainwater samples may be attributed to environmental hygiene conditions or contamination associated with the boiling container itself. The thermal resistance of total coliforms and *E. coli* warrants further investigation to better their survival under extreme temperature conditions. Such studies could

provide valuable recommendations for the effectiveness of conventional rainwater treatment methods, such as boiling, in ensuring safe water use.

4. Conclusion

Based on the study results, the physical and chemical parameters of rainwater stored in the storage tank were strongly influenced by roof conditions, gutter cleanliness, rainfall timing, and surrounding environmental hygiene. The presence of organic debris, such as leaves and twigs, on the roof and in the gutters was shown to contribute to increased turbidity and changes in rainwater color. Maintenance measures, including roof and gutter cleaning and vegetation trimming around the building, were effective in improving the physical quality of rainwater through natural sedimentation during storage. In addition, the chemical characteristics of the stored rainwater remained relatively stable, with pH values within the neutral range and a decreasing trend in dissolved substances, suggesting water quality stabilization during storage.

From a microbiological perspective, the stored rainwater still showed potential contamination indicators, although their abundance tended to decrease with more extended storage. This reduction is likely influenced by limited nutrient availability and unfavorable environmental conditions within the storage tank, causing bacteria to enter a dormant state. Nevertheless, the detection of bacteria even after heat treatment indicates that boiling alone does not fully guarantee the microbiological safety of harvested rainwater. Therefore, rainwater stored in tanks still requires additional treatment before use, particularly for drinking, to ensure it is safe and compliant with health standards.

References

[1] R. Triatmadja, Teknik Penyediaan Air Minum Perpipaan, Yogyakarta: Gadjah Mada University Press, 2021.
[2] A. Maryono, Memanen Air Hujan, Yogyakarta: Gadjah Mada University Press, 2022.
[3] C. E. Chubaka, H. Whiley, J. W. Edwards, and K. E. Ross, "A Review of Roof Harvested Rainwater in Australia," *J. Environ. Public Health*, vol. 2018, 2018. https://doi.org/10.1155/2018/6471324.
[4] F. A. Abdulla and A. W. Al-Shareef, "Roof rainwater Harvesting Systems for Household Water Supply in Jordan," *Desalination*, vol. 243, no. 1–3, pp. 195–207, 2009. https://doi.org/10.1016/j.desal.2008.05.013.
[5] C. M. Silva, V. Sousa, and N. V. Carvalho, "Evaluation of Rainwater Harvesting in Portugal : Application to Single-Family Residences," *"Resources, Conserv. Recycl.*, vol. 94, pp. 21–34, 2015. https://doi.org/10.1016/j.resconrec.2014.11.004.
[6] D. S. Krisnayanti, Y. T. Yosafath, J. J. S. Pah, K. Air, K. Air, and N. Air, "Efisiensi Pemanfaatan Air dengan Sarana Penampungan Air Hujan Pada Rumah Warga Kota Kupang," vol. VIII, no. 2, pp. 165–178, 2019.
[7] U. Purwantoro, Suhadi; Sudarsono, Agus; Hador, "Pola Pemanfaatan Air Hujan di Kecamatan Panggang Gunung Kidul," *Geomedia*, vol. 4 Nomor 2, 2006. https://doi.org/10.21831/gm.v4i2.17939
[8] M. I. Diviantama, "Sistem Otomatis untuk Menjaga Kestabilan pH Air pada Rainwater Tank," *Tenik Inform.*, vol. 8, no. 2, pp. 3551–3563, 2021.
[9] L. S. Pasaribu, N. Bafdal, and E. Suryadi, "Kajian Kualitas Air dan Volume Pemanenan Air Hujan Sistem Atap Pada Greenhouse Academic Leadership Grant," *Pros. Semin. Nas. ...*, vol. 4, no. 1, pp. 198–204, 2020.
[10] A. R. Asnaning, Surya, and A. E. Saputra, "Uji Kualitas Air Hujan Hasil Filtrasi untuk Penyediaan Air Bersih," *Pros. Semin. Nas. PengembanganTeknologi Pertan. VII*, no. 2016, pp. 288–293, 2018.
[11] A. Maryono, S. Nuranto, P. T. S. Sembada, and H. T. B. M. Petrus, "GAMA-RainFilter: a Modified Rainwater Harvesting Technique to Meet The Demand of Clean Water in Indonesia," *Int. J. Hydrol. Sci. Technol.*, vol. 13, no. 1, pp. 1–22, 2022. https://doi.org/10.1504/ijhst.2022.119272.
[12] K. Hamilton *et al.*, "A Global Review of The Microbiological Quality and Potential Health Risks Associated With Roof-Harvested Rainwater Tanks," *npj Clean Water*, no. August 2018, 2019. https://doi.org/10.1038/s41545-019-0030-5.
[13] M. De Kwaadsteniet and P. H. Dobrowsky, "Domestic Rainwater Harvesting : Microbial and Chemical Water Quality and Point-of-Use Treatment Systems," 2013.

https://doi.org/10.1007/s11270-013-1629-7.
[14] E. K. Winiati P. Rahayu, Siti Nurjanah, Escherichia Coli: Patogenitas, Analisis dan Kajian Risiko. Bogor: IPB Press, 2018.
[15] Y. Hanifah and Widyastuti, "Kajian Kualitas Air Sungai Konteng Sebagai Sumber Air Baku PDAM Tirta Darma Unit Gamping, Kabupaten Sleman," *J. Bumi Indones.*, vol. 6, no. 1, pp. 1–10, 2017.
[16] A. Chowdhury, P. Egodawatta, and J. McGree, "Pattern-Based Assessment of the Influence of Rainfall Characteristics on Urban Stormwater Quality," *Water Sci. Technol.*, vol. 87, no. 9, pp. 2292–2303, 2023. https://doi.org/10.2166/wst.2023.125.
[17] W. Zhang, X. Zhang, J. Fan, Z. Shi, Y. Zhao, and S. Li, "Runoff Pollution Characterization and First Flush Effect of Urban Roof Catchment," *Desalin. Water Treat.*, vol. 119, pp. 262–266, 2018. https://doi.org/10.5004/dwt.2018.22061.
[18] L. K. Clark, M. H. Dibenedetto, N. T. Ouellette, and J. R. Koseff, "Dispersion of Finite-Size, Non-Spherical Particles by Waves and Currents," *J. Fluid Mech.*, vol. 954, pp. 1–10, 2023. https://doi.org/10.1017/jfm.2022.968.
[19] L. Eitzen, A. S. Ruhl, and M. Jekel, "Particle Size and Pre-Treatment Effects on Polystyrene Microplastic Settlement in Water: Implications for Environmental Behavior and Ecotoxicological Tests," *Water (Switzerland)*, vol. 12, no. 12, pp. 1–12, 2020. https://doi.org/10.3390/w12123436.
[20] J. Y. Lee, G. Bak, and M. Han, "Quality of Roof-Harvested Rainwater-Comparison of Different Roofing Materials," *Environ. Pollut.*, vol. 162, pp. 422–429, 2012. https://doi.org/10.1016/j.envpol.2011.12.005.
[21] K. Anuar, A. Ahmad, and S. Sukendi, "Analisis Kualitas Air Hujan Sebagai Sumber Air Minum Terhadap Kesehatan Masyarakat (Studi Kasus di Kecamatan Bangko Bagansiapiapi)," *Din. Lingkung. Indones.*, vol. 2, no. 1, p. 32, 2015. https://doi.org/10.31258/dli.2.1.p.32-39.
[22] F. A.-R. Muhsin and H. H. M. Al-Tabatabai, "The Effect of Different Types of Drinking Water Plastic Tanks Used at Homes on Water Quality: A Study of Various Samples under Standard Conditions," *South East. Eur. J. Public Heal.*, pp. 785–791, 2024. https://doi.org/10.70135/seejph.vi.1484.
[23] A. Javed, H. Amjad, I. Hashmi, and W. Miran, "Investigating the Influence of Tank Material and Residual Chlorine on The Proliferation of Bacterial Biofilm Growth in the Drinking Water Storage Systems," *J. Water Sanit. Hyg. Dev.*, vol. 15, no. 4, pp. 305–321, 2025. https://doi.org/10.2166/washdev.2025.285.
[24] K. Supriatna, Mohhamd Mahmudi; Muhammad Musa, "Model pH dan Hubungannya dengan Parameter Kualitas Air pada Tambak Intensif Udang Vaname (*Litopenaeus Vannamei*) di Banyuwangi Jawa Timur," *JFMR-Journal Fish. Mar. Res.*, vol. 4, no. 3, pp. 368–374, 2020. https://doi.org/10.21776/ub.jfmr.2020.004.03.8.
[25] O. S. D. Hima Bindu, G. V. K. S. V. Prasad, and R. Al-Fatlawy, "Effect of Water Storage Tank Material on Quality of Water with Storage Period," *E3S Web Conf.*, vol. 529, 2024. https://doi.org/10.1051/e3sconf/202452903010.
[26] R. Kaushik, R. Balasubramanian, and A. A. de la Cruz, "Influence of Air Quality on the Composition of Microbial Pathogens in Fresh Rainwater," *Appl. Environ. Microbiol.*, vol. 78, no. 8, pp. 2813–2818, 2012. https://doi.org/10.1128/AEM.07695-11.
[27] J. P. S. Cabral, "Water Microbiology. Bacterial Pathogens and Water," *Int. J. Environ. Res. Public Health*, vol. 7, no. 10, pp. 3657–3703, 2010. https://doi.org/10.3390/ijerph7103657.
[28] S. Wagley, "Novel Detection Methods for Dormant Bacteria in Seafood," *Res. Featur.*, no. 134, 2021. https://doi.org/10.26904/rf-134-1417.
[29] Y. Gao *et al.*, "Bacterial Spore Germination Receptors are Nutrient-Gated Ion Channels," *Science (80-.).*, vol. 380, no. 6643, pp. 387–391, 2023. https://doi.org/10.1126/science.adg9829.
[30] S. Van Vliet, "Bacterial Dormancy: How to Decide When to Wake Up," *Curr. Biol.*, vol. 25, no. 17, pp. R753–R755, 2015. https://doi.org/10.1016/j.cub.2015.07.039.
[31] B. R. Mohapatra and M. T. La Duc, "Detecting the Dormant: A Review of Recent Advances in Molecular Techniques for Assessing the Viability of Bacterial Endospores," *Appl. Microbiol. Biotechnol.*, vol. 97, no. 18, pp. 7963–7975, 2013. https://doi.org/10.1007/s00253-013-5115-3.
[32] B. N. Muhammad, Z. Fadli, and R. Risandiansyah, "Perbandingan Isolasi DNA Bakteri Escherichia coli dengan Metode Heat Treatment dan Filter Based Kit Berdasarkan Nilai Limit of Detection dan

Limit of Quantification," *J. Kedoketeran Komuniitas*, vol. 8, no. 2, pp. 66–73, 2020.

[33] J. Van Kessel *et al.*, "Time and Temperature Requirements for Heat Inactivation of Pathogens to be Applied to Swine Transport Trailers," *J. Swine Heal. Prod.*, vol. 29, no. 1, pp. 19–28, 2021. https://doi.org/10.54846/jshap/1193.

[34] C. James, R. Dixon, L. Talbot, S. J. James, N. Williams, and B. A. Onarinde, "Assessing the Impact of Heat Treatment of Food on Antimicrobial Resistance Genes and Their Potential Uptake by Other Bacteria—A Critical Review," *Antibiotics*, vol. 10, no. 12, 2021. https://doi.org/10.3390/antibiotics10121440.

FaST - Jurnal Sains dan Teknologi, Vol. 10, No. 1, Mei 2026
e-ISSN 2598-9596
DOI: https://doi.org/10.19166/fastjst.v10i1/10895
Available online at: https://ojs.uph.edu/index.php/FaSTJST/article/view/10895

Sistem Monitoring *Schedule Compliance* untuk Pengendalian *Shortage* Material pada Proses Produksi Extruder Ban

Daffa Aji Firmansyah [1)], Priskila Christine Rahayu [1*)]
[1]Program Studi Teknik Industri, Universitas Pelita Harapan, Tangerang, Indonesia

ABSTRACT

Schedule compliance management for extruder machines in manufacturing environments is often still performed manually, leading to reporting delays, recording errors, and limited visibility of schedule adherence and material readiness. This study aims to develop a digital-based schedule compliance monitoring system to improve the effectiveness of production schedule control, material availability tracking, and detection of non-conforming schedules. The system was developed using the Rapid Application Development (RAD) approach, which includes requirement planning, system design (use case diagram, data flow diagram, and entity relationship diagram), prototype development, and implementation testing in an operational environment. The proposed system integrates production schedule data, material usage, material shortage information, and compliance status into a centralized dashboard displaying real-time performance and compliance indicators. Testing results show a significant reduction in monitoring time from 38.63 minutes in the manual system to 0.61 minutes using the proposed system, resulting in a time efficiency improvement of 98.42%. Furthermore, the system enhances information transparency, decision-making speed, and reporting accuracy. Therefore, the developed system is effective in supporting data-driven operational control in manufacturing production processes.

ARTICLE INFO

Keywords: schedule compliance; shortage; extruder machine, monitoring system; rapid application development

***Corresponding author:**
priskila.christine@uph.edu

Article history:
Submitted 12 Feb 2026
Revised 10 Apr 2026
Accepted 17 Apr 2026
Online Available 7 May 2026
Published 20 May 2026

1. Pendahuluan

Kepatuhan terhadap jadwal produksi (*schedule compliance*) merupakan salah satu indikator kinerja logistik yang krusial dalam sistem produksi, khususnya pada lingkungan manufaktur dengan kompleksitas tinggi. Schmidt menunjukkan bahwa pencapaian *schedule compliance* yang tinggi dipengaruhi oleh kombinasi variabel kontrol pada sistem produksi *job shop*, seperti waktu aman (*safety time*) dan distribusi keterlambatan proses [1]. Model kuantitatif yang mereka kembangkan membuktikan bahwa pengendalian variabel-variabel tersebut tidak hanya berdampak pada ketepatan waktu produksi, tetapi juga pada tingkat persediaan barang jadi dan kinerja pengiriman dalam rantai pasokan.

Piontek menambahkan bahwa potensi peningkatan *schedule compliance* juga ditentukan oleh kebijakan pengurutan pekerjaan (*dispatching rules*), khususnya pengurutan berdasarkan tanggal jatuh tempo operasi paling awal [2]. Penelitian tersebut mengidentifikasi lima parameter utama yang memengaruhi peluang peningkatan kepatuhan jadwal, yaitu penyimpangan urutan input, tingkat *Work in Progress* (WIP), jumlah operasi, tingkat pertukaran urutan yang direncanakan dalam *throughput* pesanan, serta jumlah mesin paralel. Temuan ini menegaskan bahwa *schedule compliance* merupakan hasil interaksi antara pengendalian aliran material, struktur sistem produksi, dan kebijakan operasional.

Namun, pendekatan tersebut umumnya masih menitikberatkan pada model sistem dan simulasi, sementara faktor manusia dalam implementasi keputusan penjadwalan belum banyak diintegrasikan. Celah ini dijelaskan lebih lanjut dalam studi kasus pada industri semikonduktor mengenai *operator dispatching compliance* [3]. Penelitian tersebut menunjukkan bahwa meskipun sistem telah menghasilkan urutan prioritas pekerjaan secara optimal, operator sering melakukan deviasi karena pertimbangan praktis seperti jarak fisik lot, kemudahan pengambilan material, atau upaya meminimalkan waktu menganggur mesin. Rata-rata tingkat kepatuhan operator hanya sekitar 75%, yang berarti seperempat keputusan produksi menyimpang dari rekomendasi sistem. Temuan ini menegaskan bahwa performa sistem penjadwalan bersifat *socio-technical*, dipengaruhi oleh interaksi antara sistem informasi dan perilaku manusia.

Perspektif kepatuhan juga diperluas dalam ranah kebijakan ketenagakerjaan. Lambert menganalisis implementasi regulasi penjadwalan kerja di tingkat lokal dan menemukan bahwa kepatuhan terhadap aturan penjadwalan sangat dipengaruhi oleh praktik manajerial, budaya organisasi,

FaST - Jurnal Sains dan Teknologi, Vol. 10, No. 1, Mei 2026
e-ISSN 2598-9596
DOI: https://doi.org/10.19166/fastjst.v10i1/10895
Available online at: https://ojs.uph.edu/index.php/FaSTJST/article/view/10895

serta model bisnis yang berorientasi biaya [4]. Variasi praktik antar tempat kerja menunjukkan bahwa keberadaan sistem atau aturan saja tidak menjamin kepatuhan; diperlukan mekanisme pengawasan, pelatihan, dan dukungan sistem yang memudahkan pelaksanaan regulasi. Studi ini memperkuat pemahaman bahwa compliance dalam konteks penjadwalan—baik tenaga kerja maupun produksi—memerlukan integrasi antara sistem formal dan praktik operasional di lapangan.

Pendekatan serupa terlihat dalam penelitian tata kelola dan kepatuhan pada industri jasa pelabuhan BUMN di Indonesia. Sitompul menunjukkan bahwa faktor *risk management* dan *regulatory compliance* memiliki pengaruh signifikan dalam pencegahan potensi fraud, sementara aspek tata kelola formal tidak selalu berdampak langsung [5]. Temuan ini menegaskan bahwa efektivitas compliance sangat bergantung pada sistem pengendalian operasional dan mekanisme pemantauan risiko yang berjalan secara nyata, bukan sekadar keberadaan struktur kebijakan. Konsep ini relevan dengan pengendalian *schedule compliance*, di mana sistem monitoring operasional menjadi elemen penting dalam memastikan implementasi jadwal berjalan sesuai rencana.

Dalam praktik industri manufaktur, tantangan terhadap *schedule compliance* semakin meningkat seiring bertambahnya variasi produk. Variasi produk muncul sebagai respons terhadap kebutuhan pasar yang dinamis dan perkembangan teknologi, namun di sisi lain menambah kompleksitas perencanaan dan pengendalian produksi. Kondisi ini menyebabkan peningkatan risiko keterlambatan, ketidakseimbangan aliran material, serta potensi kekurangan material (*shortage*). Oleh karena itu, *schedule compliance* tidak hanya berfungsi sebagai indikator kinerja operasional, tetapi juga sebagai mekanisme pengendalian risiko produksi dan jaminan pemenuhan kebutuhan pelanggan.

PT ABC merupakan perusahaan manufaktur otomotif yang memproduksi ban kendaraan dengan struktur material yang terdiri atas material bertulang (*reinforced material*) dan tidak bertulang (*non-reinforced material*). Di antara seluruh komponen penyusun ban, material *sidewall* memiliki tingkat variasi paling tinggi akibat karakteristik kustomisasi dan rendahnya *common use* antarproduk. Tingginya variasi ini meningkatkan kompleksitas penjadwalan produksi serta frekuensi pergantian jadwal pada setiap *shift*. Kondisi tersebut berdampak langsung pada kestabilan *schedule compliance* dan ketersediaan material.

Data perusahaan periode 2022–2024 menunjukkan bahwa rata-rata *schedule compliance* material *sidewall* telah melampaui 80%, namun target *shortage* sebesar 0,30% belum tercapai. Analisis menggunakan *scatter diagram* pada **Gambar 1**, menunjukkan korelasi negatif yang kuat antara *schedule compliance* dan *shortage*, dengan persamaan garis tren $y = -0{,}0458x + 0{,}0462$dan koefisien determinasi $R^2 = 0{,}9325$. Hasil ini mengindikasikan bahwa peningkatan *schedule compliance* berkontribusi signifikan terhadap penurunan tingkat *shortage*. Berdasarkan temuan tersebut, manajemen PT ABC menetapkan target peningkatan *schedule compliance* hingga 95%.

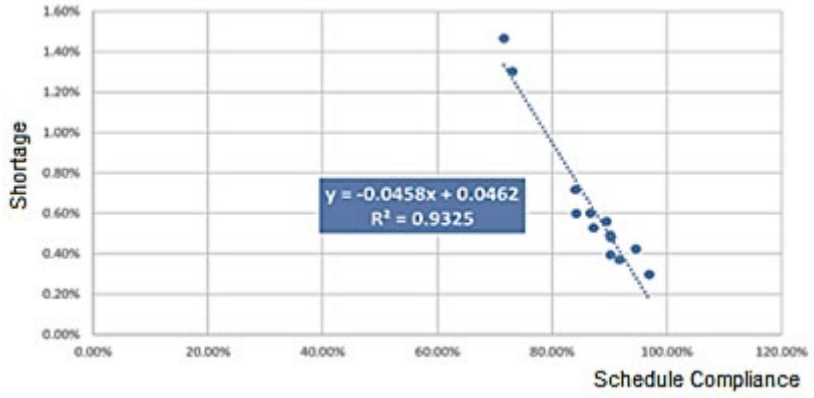

Gambar 1 Diagram Scatter Data *Schedule Compliance* dan *Shortage* PT ABC Periode 2022-2024

Meskipun berbagai penelitian telah membahas faktor-faktor yang memengaruhi *schedule compliance*, sebagian besar masih berfokus pada aspek model konseptual dan simulasi. Studi berbasis data operasional aktual yang mengintegrasikan *schedule compliance* dengan pengendalian *shortage* material pada komponen bervariasi tinggi masih terbatas. Oleh karena itu, penelitian ini bertujuan mengembangkan sistem monitoring *schedule compliance* berbasis VBA - Excel yang mampu mengidentifikasi penyebab deviasi jadwal secara cepat dan akurat.

FaST - Jurnal Sains dan Teknologi, Vol. 10, No. 1, Mei 2026
e-ISSN 2598-9596
DOI: https://doi.org/10.19166/fastjst.v10i1/10895
Available online at: https://ojs.uph.edu/index.php/FaSTJST/article/view/10895

2. Metode

Penelitian dilaksanakan secara bertahap, diawali observasi lapangan serta pengumpulan data historis dan data performa sistem. Data tersebut digunakan untuk memahami kondisi aktual *schedule compliance* serta permasalahan operasional pada mesin *extruder*.

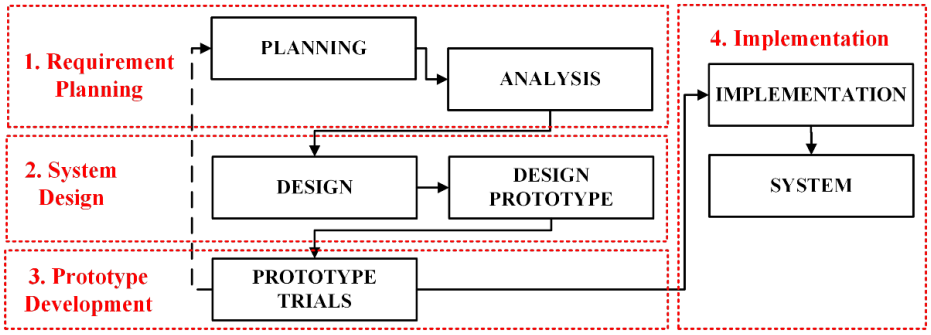

Gambar 2 Diagram Alur Metode *Rapid Application Development*

Pengembangan sistem dilakukan menggunakan metode *Rapid Application Development* (RAD) sebagaimana ditunjukkan pada **Gambar 2**. Metode ini dipilih karena menekankan siklus pengembangan yang cepat dan fleksible melalui pembuatan prototipe serta pemanfaatan umpan balik pengguna secara berkelanjutan [6]. Rangkaian kegiatan penelitian diawali tahap pertama *Requirement Planning*, yang bertujuan mengidentifikasi kebutuhan sistem melalui analisis kondisi eksisting. Pada tahap ini dilakukan evaluasi sistem *schedule compliance* saat ini menggunakan pendekatan SWOT (*Strengths, Weaknesses, Opportunities, Threats*) untuk mengidentifikasi kekuatan, kelemahan, peluang, dan ancaman dalam proses monitoring yang berjalan. Hasil analisis ini menjadi dasar perumusan kebutuhan fungsional dan non-fungsional sistem. Tahap kedua adalah *System Design*. Pada tahap ini dilakukan perancangan sistem secara konseptual dan logis, meliputi: 1) Pemodelan kebutuhan sistem dalam bentuk *Use Case Diagram* dan spesifikasi kebutuhan dalam tabel deskriptif. 2) Pemodelan proses menggunakan *Data Flow Diagram* (DFD) untuk menggambarkan aliran data antarproses dalam sistem monitoring dan 3) Pemodelan data menggunakan *Entity Relationship Diagram* (ERD) yang telah melalui proses normalisasi untuk memastikan integritas dan efisiensi struktur basis data. Selanjutnya pada tahap ketiga *Prototype Development* dilakukan implementasi hasil rancangan ke dalam bentuk prototipe aplikasi berbasis VBA - Excel. Tahap ini mencakup pengembangan antarmuka pengguna, modul input data, proses perhitungan indikator *schedule compliance*, serta penyajian laporan dan visualisasi laporan. Tahap terakhir adalah *Implementation and Testing*. Pada tahap ini prototipe yang telah dikembangkan diuji coba pada lingkungan operasional untuk mengevaluasi kesesuaian fungsi sistem terhadap kebutuhan pengguna. Tahap ini meliputi pengujian fungsional, validasi hasil perhitungan, serta evaluasi kemudahan penggunaan (*usability*). Umpan balik dari pengguna digunakan untuk melakukan penyempurnaan sistem sebelum diterapkan secara penuh.

3. Hasil dan Diskusi

3.1 *Requirement Planning*

Perusahaan saat ini menggunakan sistem manual untuk memantau kepatuhan terhadap berbagai regulasi. Sistem ini mengandalkan proses pencatatan dan pelaporan yang dilakukan secara berkala oleh bagian produksi. Namun, pendekatan manual tersebut memiliki sejumlah keterbatasan, antara lain potensi kesalahan manusia, tidak tersedianya pemantauan secara *real-time*, serta keterbatasan dalam akses dan pengolahan data secara cepat. Proses penyusunan laporan *schedule compliance* di PT ABC terdiri atas beberapa tahapan. Tahap awal adalah pengumpulan data produksi harian dari bagian produksi. Data tersebut kemudian dianalisis untuk mengidentifikasi ketidaksesuaian jumlah produk dalam tiga kategori, yaitu jumlah terbuat kurang dari rencana (*size under production)*, size *over production*, dan *unproduced size*. Selanjutnya, laporan disusun dengan memuat ringkasan ketidaksesuaian, analisis penyebab, serta rekomendasi tindakan korektif. Laporan yang telah disusun, kemudian melalui proses pemeriksaan dan validasi internal sebelum disampaikan kepada manajemen dan departemen terkait. Tahap akhir adalah

FaST - Jurnal Sains dan Teknologi, Vol. 10, No. 1, Mei 2026
e-ISSN 2598-9596
DOI: https://doi.org/10.19166/fastjst.v10i1/10895
Available online at: https://ojs.uph.edu/index.php/FaSTJST/article/view/10895

pemantauan berkala terhadap pelaksanaan tindakan perbaikan untuk memastikan efektivitasnya serta melakukan evaluasi hasil perbaikan tersebut.

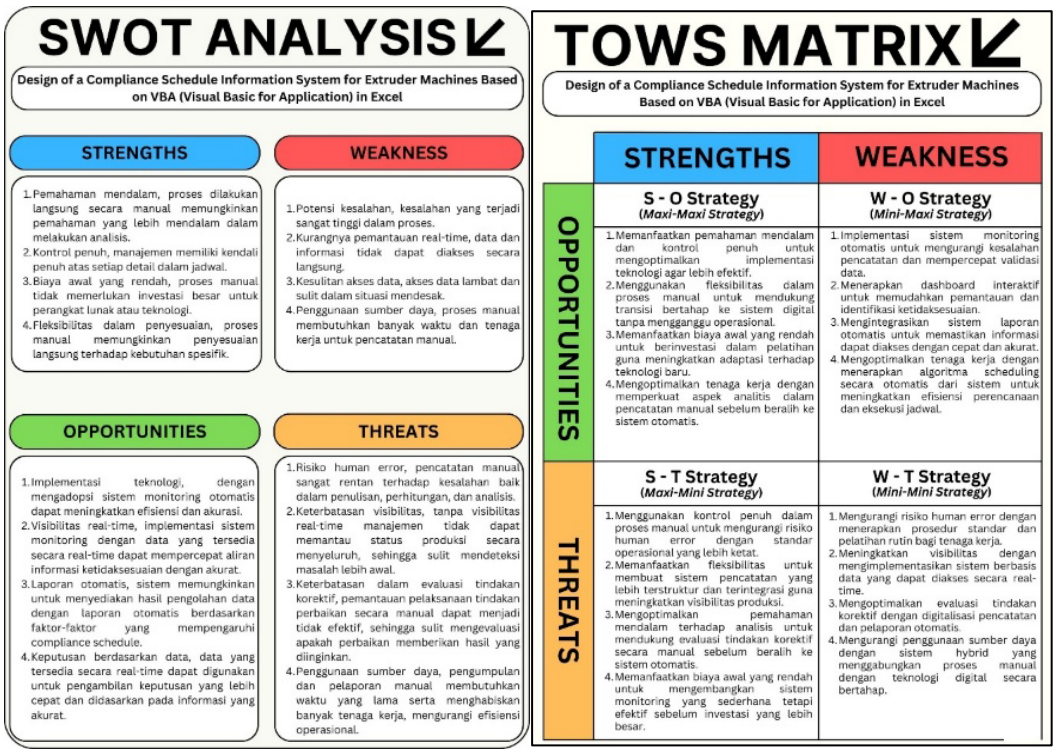

Gambar 3 Hasil Analisis SWOT

Hasil evaluasi terhadap sistem maual dengan metode analisis SWOT pada **Gambar 3** menunjukkan bahwa posisi perusahaan berada pada kuadran WO (*Weaknesses-Opportunities*) sehingga dipilih strategi *Mini-Maxi* yang berfokus pada meminimalkan kelemahan internal dengan memanfaatkan peluang eksternal yang tersedia [7]. Strategi yang direkomendasikan adalah pemanfaatan peluang teknologi untuk meminimalkan kelemahan sistem manual. Implementasi sistem monitoring otomatis akan mengurangi kesalahan pencatatan dan mempercepat validasi data. Keterbatasan visibilitas dapat diatasi melalui dashboard *real-time*, sementara beban kerja administratif dapat ditekan melalui otomasi proses pelaporan. Integrasi data historis juga mendukung perencanaan produksi yang lebih efisien dan eksak.

Dengan demikian diketahui kebutuhan fungsional sistem yang akan dirancang adalah sistem mampu menghitung, memonitor, dan melaporkan *schedule compliance* serta *shortage.* Selain itu, kebutuhan non-fungsional sistem adalah sistem dapat digunakan dengan cepat, memberikan informasi yang akurat, mudah digunakan, dan dapat mendukung pencapaian target kinerja produksi.

3.2 *System Design*

Sesuai dengan metode RAD, proses perancangan sistem dilakukan secara kolaboratif dan iteratif. Pada tahap ini melibatkan pemangku kepentingan, termasuk pengguna akhir dan pengembang, yang bekerja bersama dalam sesi intensif untuk merancang dan mengembangkan prototipe sistem. Tujuannya adalah untuk memastikan bahwa sistem yang dikembangkan memenuhi kebutuhan pengguna secara tepat dan cepat [8].

FaST - Jurnal Sains dan Teknologi, Vol. 10, No. 1, Mei 2026
e-ISSN 2598-9596
DOI: https://doi.org/10.19166/fastjst.v10i1/10895
Available online at: https://ojs.uph.edu/index.php/FaSTJST/article/view/10895

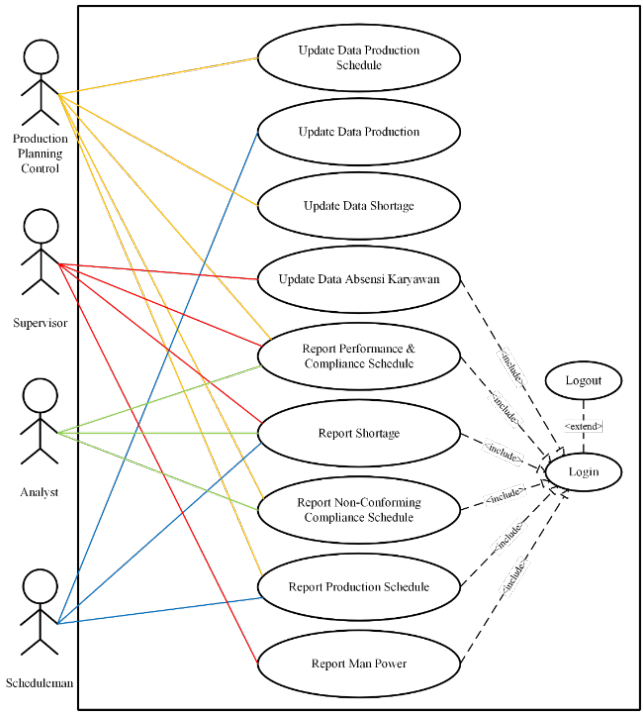

Gambar 4 Use Case Diagram

Rancangan sistem dimulai dengan pemodelan kebutuhan sistem dalam bentuk *use case* diagram pada **Gambar 4** [9,10]. Sistem yang akan dirancang, diperlukan untuk memantau kesesuaian pelaksanaan produksi terhadap jadwal, ketersediaan material, serta dukungan sumber daya manusia. Sistem akan menghasilan berbagai laporan kinerja operasional. Untuk itu seluruh pengguna wajib melalui proses Login sebelum mengakses fungsi sistem dan mengakhiri sesi melalui Logout. Relasi garis putus-putus menuju Login menunjukkan bahwa hampir semua *use case* memiliki ketergantungan autentikasi. Terdapat empat aktor utama, yaitu 1) *Production Planning Control* (PPC) yang berperan dalam pengelolaan data utama yang berkaitan dengan jadwal dan realisasi produksi, 2) *Supervisor* yang berfokus pada pemantauan operasional serta evaluasi kinerja produksi dan ketidaksesuain jadwal, 3) *Analyst* yang bertanggung jawab terhadap analisis data performa produksi, khususnya terakit keptuhan jadwal dan kekurangan material, dan 4) *Scheduler* berperan dalam penyusunan dan evaluasi jadwal produksi serta analisis kebutuhan tenaga kerja. *Use case* diagram dilengkapi dengan use case tabel untuk memperjelas kebutuhan proses di dalam sistem yang akan dirancang [11].

Berdasarkan *use case* tabel, dirancang pemodelan aliran dan pengolahan data dalam sistem, dalam bentuk DFD pada **Gambar 5**. Sistem terdiri dari 5 penyimpanan data (*data storage*), yaitu 1) data *schedule* produksi (jadwal produksi yang direncanakan), 2) data real produksi (data hasil produksi aktual), 3) data *shortage* material (catatan kejadian kekurangan material), 4) data absensi karyawan (data kehadiran tenaga kerja produksi), dan 5) data *schedule compliance* (hasil perhitungan tingkat kepatuhan jadwal). Sistem berfungsi sebagai pusat pengolahan data operasional yang berasal dari berbagai bagian produksi, kemudian mengubahnya menjadi informasi monitoring dan laporan manajerial.

FaST - Jurnal Sains dan Teknologi, Vol. 10, No. 1, Mei 2026
e-ISSN 2598-9596
DOI: https://doi.org/10.19166/fastjst.v10i1/10895
Available online at: https://ojs.uph.edu/index.php/FaSTJST/article/view/10895

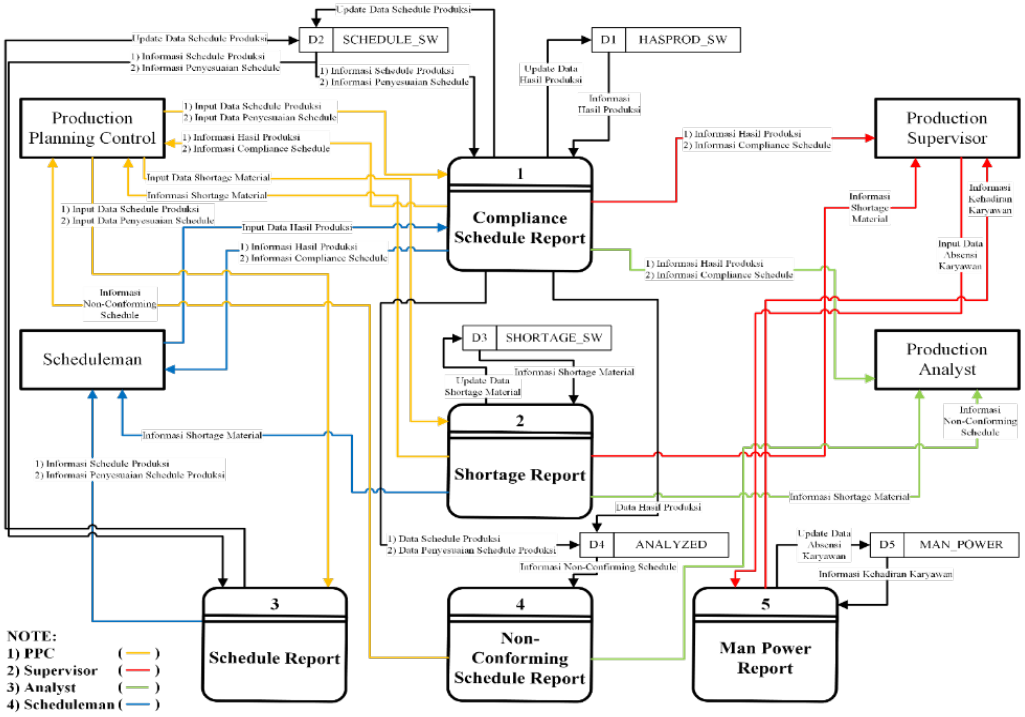

Gambar 5 Data Flow Diagram

Selanjutnya dilakukan pemodelan tempat penyimpanan data dalam bentuk ERD pada **Gambar 6**. Melalui proses normalisasi untuk memastikan data diatur dengan benar, meminimalkan redundansi, dan mengoptimalkan integritas data, terdapat tujuh kumpulan data (entitas) yang saling terhubung [12,13].

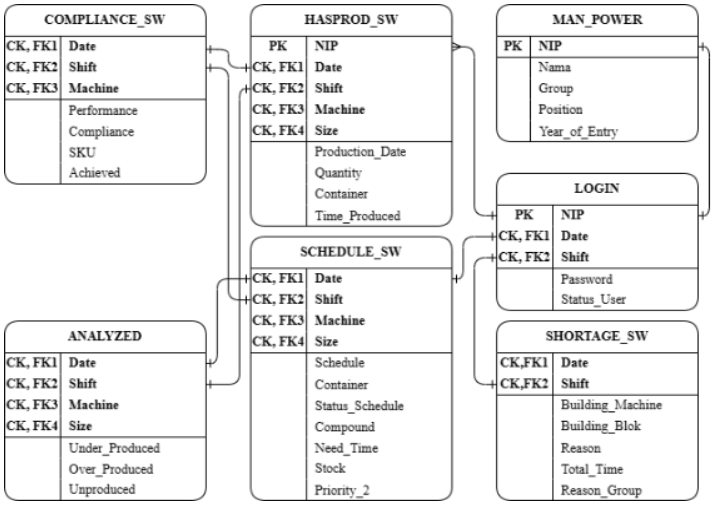

Gambar 6 Entity Relationship Diagram Ternormalisasi

3.3 Prototype Development

Prototipe aplikasi hasil pengembangan sistem monitoring *schedule compliance* berbasis VBA_Excel ditunjukkan pada **Gambar 7**. Antar muka dirancang sebagai panel kendali operasional yang memungkinkan pengguna memantau kinerja produksi secara ringkas, cepat dan visual. Proses pengembangan prototipe melalui lima kali iterasi dengan pengguna, agar sesuai dengan kebutuhan dan keinginan pengguna [14,15].

FaST - Jurnal Sains dan Teknologi, Vol. 10, No. 1, Mei 2026
e-ISSN 2598-9596
DOI: https://doi.org/10.19166/fastjst.v10i1/10895
Available online at: https://ojs.uph.edu/index.php/FaSTJST/article/view/10895

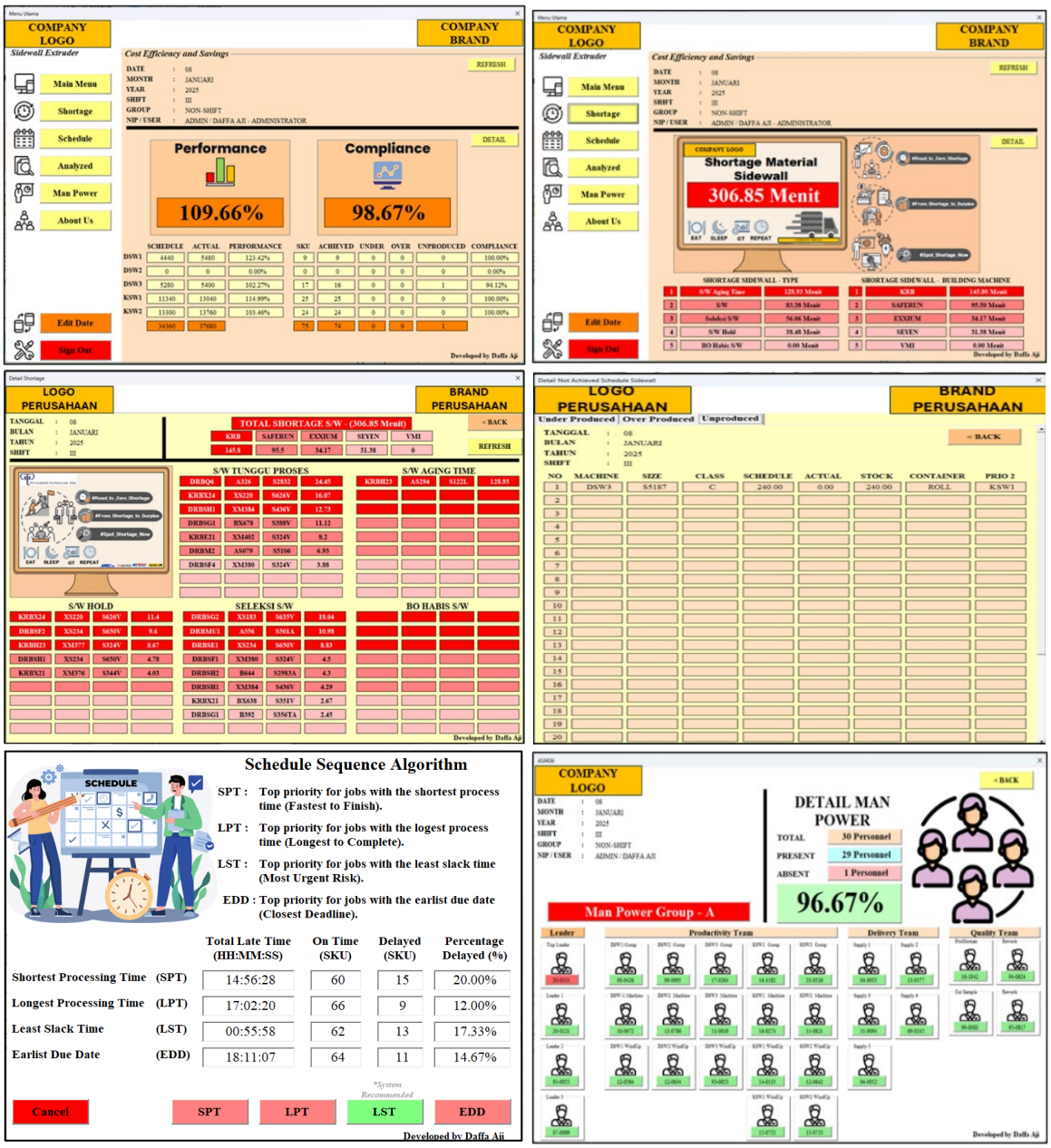

Gambar 7 Prototipe Sistem Monitoring Schedule Compliance

3.4 Implementation and Testing

Prototipe akhir diimplementasikan pada kegiatan operasional perusahaan sebagai uji coba *blackbox* oleh 30 pengguna meliputi keempat jenis aktor. Uji coba menggunakan 19 skenario yang mencakup fitur login, date picker, dashboard form *schedule compliance, shortage, schedule, about us, analyzed, man power, man power analysis*, dan *logout*. Hasil uji coba menunjukkan bahwa semua menu dan user interface pada aplikasi dapat digunakan. Kemudian dilakukan pengukuran keberhasilan sistem dalam bentuk kuisioner yang diisi oleh pengguna meliputi enam dimensi keberhasilan sebuah sistem informasi dari Delone dan McLean, dengan hasil seperti pada **Tabel 1** [16,17].

Tabel 1 Rekapitulasi Pengujian Delone dan McLean

Dimensi	Nilai Aktual	Nilai Ideal	% Keberhasilan
Kualitas Sistem	433	450	96,2
Kualitas Informasi	416	450	92,4
Kualitas Layanan	411	450	91,3
Penggunaan	409	450	90,9
Kepuasan Pengguna	417	450	92,7
Kebermanfaatan	394	450	87,6
Rata-rata	413,3	450	91,9

FaST - Jurnal Sains dan Teknologi, Vol. 10, No. 1, Mei 2026
e-ISSN 2598-9596
DOI: https://doi.org/10.19166/fastjst.v10i1/10895
Available online at: https://ojs.uph.edu/index.php/FaSTJST/article/view/10895

Setelah implementasi sistem padfa 33 siklus operasional, proses monitoring dan pelaporan dapat dilakukan secara langsung sehingga memungkinkan deteksi dini terhadap deviasi jadwal dan percepatan penangganan masalah. Hasil evaluasi menunjukkan bahwa sistem tidak hanya meningkatkan *schedule compliance* dan menurunkan shortage (**Tabel 2)**, tetapi juga mengoptimalkan alokasi sumber daya.

Tabel 2 Perbandingan Performa Sistem

Item Evaluasi	Target	Sistem Manual	Sistem Otomatis
Schedule Compliance	95%	84,27%	92.65%
Shortage	0,30%	0,75%	0.39%

Sistem otomatisasi juga meningkatkan efisiensi pemanfaatan tenaga kerja dengan mengurangi aktivitas manual yang berulang dalam pengolahan data, validasi, dan *monitoring*. Berdasarkan pengukuran waktu terhadap 33 proses pembuatan laporan (setelah uji normalitas dan keseragaman data), rata-rata waktu pada sistem manual adalah 38,63 menit, sedangkan pada sistem otomatis hanya 0,61 menit. Hal ini menunjukkan efisiensi waktu dan biaya tenaga kerja sebesar 98,43%.

4. Kesimpulan

Pengembangan sistem monitoring *schedule compliance* mesin extruder menggunakan pendekatan Rapid Application Development terbukti mampu meningkatkan efektivitas pengendalian jadwal produksi secara terintegrasi. Sistem ini mengimplementasikan konsep *smart monitoring* dengan menggabungkan data jadwal produksi, pemakaian material, kondisi *material shortage*, serta status *non-conforming schedule* ke dalam satu dashboard terpusat yang menyajikan indikator kinerja secara *real-time*. Pendekatan ini sejalan dengan prinsip *Manufacturing Execution System* (MES) dan *digital factory monitoring* dalam kerangka *Industry 4.0*, yang menekankan visibilitas operasional dan integrasi data lintas proses produksi.

Hasil implementasi menunjukkan peningkatan efisiensi waktu yang signifikan, dari 38,63 menit pada metode manual menjadi 0,61 menit pada sistem otomatis (efisiensi 98,42%). Selain itu, sistem meningkatkan akurasi data dan mempercepat proses pengambilan keputusan berbasis data (*data-driven decision making*), yang merupakan karakteristik utama dalam *production scheduling analytics*. Dengan demikian, digitalisasi monitoring tidak hanya memberikan perbaikan operasional, tetapi juga mendukung transformasi menuju sistem manufaktur yang lebih adaptif, responsif, dan berbasis teknologi.

Daftar Pustaka

[1] M. Schmidt, S. Bertsch, and P. Nyhuis, “Schedule compliance operating curves and their application in designing the supply chain of a metal producer,” *Production Planning & Control*, vol. 25, no. 2, pp. 123–133, 2014, https://doi.org/10.1080/09537287.2013.782947.

[2] A. Piontek and H. Lödding, “Determining the potential to improve schedule compliance,” *Procedia CIRP*, vol. 63, pp. 477–482, 2017, https://doi.org/10.1016/j.procir.2017.03.127.

[3] B. Waschneck, T. Altenmüller, T. Bauernhansl, and A. Kyek, “Case study on operator compliance to scheduling decisions in semiconductor manufacturing,” in *Proc. IEEE Int. Conf. Automation Science and Engineering (CASE)*, Munich, Germany, 2018, pp. 649–652, https://doi.org/10.1109/COASE.2018.8560395.

[4] S. J. Lambert and A. Haley, “Implementing work scheduling regulation: Compliance and enforcement challenges at the local level,” *ILR Review*, vol. 74, no. 5, pp. 1231–1257, 2021, doi: 10.1177/00197939211031227.

[5] Y. B. P. Sitompul, “Governance, risk management, compliance on preventing potential fraud in Indonesian state-owned port service industry,” *Indonesian Journal of Multidisciplinary Science*, vol. 3, no. 7, 2024, https://doi.org/10.55324/ijoms.v3i6.846.

[6] A. Dennis, B. H. Wixom, and R. M. Roth, *Systems Analysis and Design*, 8th ed. Hoboken, NJ, USA: John Wiley & Sons, 2021.

[7] B. Skotnicka-Zasadzień, M. Zasadzień, and W. Grebski, “Application of TOWS/SWOT analysis as an element of strategic management on the example of a manufacturing company,” *Scientific Papers of Silesian University of Technology, Organization and Management Series*, pp. 541–551, 2023, https://doi.org/10.29119/1641-3466.2023.189.34.

[8] R. Delima, H. Santosa, and J. Purwadi, "Development of Dutatani website using Rapid Application Development," *International Journal of Information Technology and Electrical Engineering*, vol. 1, no. 2, pp. 36–44, 2017, https://doi.org/10.22146/ijitee.28362.

[9] Y. R. Rizcha and S. Yaakub, "Sistem informasi manajemen sumber daya manusia pada Universitas Muhammadiyah Jambi," *Jurnal Manajemen Sistem Informasi*, vol. 8, no. 1, pp. 78–93, 2023, https://doi.org/10.33998/jurnalmsi.2023.8.1.765.

[10] N. Selamat and R. Ibrahim, "Similarity syntax rules between DFD and UML diagrams," *International Journal of Advanced Trends in Computer Science and Engineering*, vol. 8, no. 3, pp. 786–794, 2019, https://doi.org/10.30534/ijatcse/2019/70832019.

[11] M. N. Mornie *et al.*, "Visualisation of user stories to UML use case diagram," *Journal of Advanced Research in Applied Sciences and Engineering Technology*, vol. 63, no. 3, pp. 68–80, 2025, https://doi.org/10.37934/araset.63.3.6880.

[12] Z. F. Azzahra and A. D. Anggoro, "Analisis teknik entity-relationship diagram dalam perancangan database: Sebuah literature review," *Intech*, vol. 3, no. 2, pp. 70–74, 2022, https://doi.org/10.54895/intech.v3i2.1682.

[13] K. Hingorani, D. Gittens, and N. Edwards, "Reinforcing database concepts by using entity relationships diagrams (ERD) and normalization together for designing robust databases," *Issues in Information Systems*, vol. 18, no. 1, pp. 148–155, 2017, https://doi.org/10.48009/1_iis_2017_148-155.

[14] O. B. Y. Lisyafa and A. M. Sayuti, "Design of inventory monitoring information system of office equipment and supplies at BAZNAS City of Bandung based on macro Excel (VBA)," *Business Analytics and System Innovations*, vol. 3, no. 1, pp. 1–12, 2024, https://doi.org/10.62201/abaj.v3i1.343.

[15] A. N. Adiya, D. L. Anggraeni, and I. Albana, "Analisa perbandingan penggunaan metodologi pengembangan perangkat lunak (Waterfall, Prototype, Iterative, Spiral, Rapid Application Development (RAD))," *Merkurius: Jurnal Riset Sistem Informasi dan Teknik Informatika*, vol. 2, no. 4, pp. 122–134, 2024, https://doi.org/10.61132/merkurius.v2i4.148.

[16] M. Zen, Irwan, Hafni, and M. D. P. Ananda, "Implementasi dan pengujian menggunakan metode BlackBox testing pada sistem informasi tracer study," *Bulletin of Computer Science Research*, vol. 4, no. 4, pp. 327–340, 2024, https://doi.org/10.47065/bulletincsr.v4i4.359.

[17] Rulinawaty *et al.*, "Investigating the influence of the updated DeLone and McLean information system (IS) success model on the effectiveness of learning management system (LMS) implementation," *Cogent Education*, vol. 11, no. 1, 2024, https://doi.org/10.1080/2331186X.2024.2365611.

FaST - Jurnal Sains dan Teknologi, Vol.10, No. 1, Mei 2026
e-ISSN 2598-9596
DOI: https://doi.org/10.19166/fastjst.v10i1/10891
Available online at: https://ojs.uph.edu/index.php/FaSTJST/article/view/10891

Analisis Risiko Beban Kerja dengan Metode NIOSH *Lifting Equation* dan *Rapid Entire Body Assessment* pada Aktivitas *Dumping* Aditif di PT X

Dani Hermawan [1)], Agustina Christiani [1*)].
[1]Program Studi Teknik Industri, Universitas Pelita Harapan, Tangerang, Indonesia

ABSTRACT

Additive dumping activities at PT X are characterized by manual, repetitive lifting of sacks and frequent bending postures, which may increase the risk of developing Musculoskeletal Disorders (MSDs). Based on the results of the Cornell Musculoskeletal Discomfort Questionnaire (CMDQ), the predominant area of reported discomfort was the lower back. This study aimed to evaluate workload risks using the NIOSH Lifting Equation and the Rapid Entire Body Assessment. The initial assessment indicated a high-risk lifting task, with a Composite Lifting Index of 1.1307, exceeding the recommended threshold of 1.00, and a REBA score of 10, signifying a high level of risk. An ergonomic intervention involving the implementation of a Manual Hydraulic Stacker Forklift was proposed to elevate the initial load to waist height, thereby improving worker posture. Simulation results of the proposed intervention demonstrated a reduction in the lifting index to 0.88 and a substantial decrease in the REBA score to 3, corresponding to a low-risk category. These findings underscore the effectiveness of material handling equipment in mitigating musculoskeletal risk factors.

ARTICLE INFO

Keywords: Additive Dumping; CMDQ; Musculoskeletal disorders (MSDs); NIOSH Lifting Equation; Rapid Entire Body Assessment (REBA)

***Corresponding author**:
agustina.christiani@uph.edu

Article history:
Submitted 6 Feb 2026
Revised 19 Apr 2026
Accepted 27 Apr 2026
Online Available 7 May 2026
Published 20 May 2026

1. Pendahuluan

Kesehatan kerja merupakan pilar utama dalam menjaga produktivitas dan kesejahteraan karyawan melalui pendekatan preventif yang menyelaraskan kemampuan fisik pekerja dengan lingkungan kerjanya. Salah satu instrumen krusial dalam mencapai hal ini adalah penerapan ergonomi, yaitu studi interaksi manusia dengan sistem kerjanya untuk mencegah gangguan kesehatan [1]. Di industri manufaktur petrokimia, seperti PT X yang merupakan produsen bijih plastik terbesar di Indonesia, aspek ergonomi menjadi sangat vital mengingat adanya proses manual dan berulang yang menuntut kinerja fisik, salah satunya adalah aktivitas dumping aditif, yaitu proses pencampuran bahan tambahan ke dalam resin yang melibatkan pengangkatan manual (*manual handling*) karung aditif ke dalam *dump station* secara berulang dan posisi membungkuk dalam durasi waktu tertentu.

Kondisi di lapangan menunjukkan bahwa aktivitas dumping aditif pada produk HF 10 TQ dilakukan secara rutin setiap 8 jam dengan durasi sekitar 30 menit per sesi yang dilakukan oleh 3 orang operator dengan 2 operator sebagai *dumper* dan 1 operator bertugas membersihkan sampah kemasan aditif. Beban kerja fisik yang repetitif dengan posisi membungkuk ini menimbulkan keluhan subjektif berupa nyeri pinggang dan punggung di kalangan operator, yang merupakan indikasi awal dari *Musculoskeletal Disorders* (MSDs). Berdasarkan data International Labour Organization (ILO), cedera punggung akibat pengangkatan material yang tidak ergonomis merupakan penyebab utama kecelakaan kerja di sektor industri [2]. Namun, di PT X sendiri, risiko ergonomi pada aktivitas spesifik ini belum terukur secara ilmiah, sehingga menciptakan ancaman laten yang dapat berdampak pada kesehatan jangka panjang pekerja jika tidak segera ditangani.

Untuk mengatasi permasalahan tersebut, penelitian ini dilakukan dengan mengidentifikasi risiko MSDs menggunakan *Cornell Musculoskeletal Discomfort Questionnaire (CMDQ)* untuk mendapatkan wawasan subjektif dari pekerja mengenai bagian tubuh yang mengalami sakit atau nyeri [3] serta mengintegrasikan dua metode evaluasi ergonomi yang diakui secara internasional, yaitu NIOSH *Lifting Equation* dan *Rapid Entire Body Assessment* (REBA). Melalui NIOSH *Lifting Equation*, dilakukan perhitungan *Recommended Weight Limit* (RWL) dan *Lifting Index* (LI) untuk menentukan ambang batas beban yang aman, sementara metode REBA digunakan untuk menganalisis risiko postur tubuh operator

FaST - Jurnal Sains dan Teknologi, Vol.10, No. 1, Mei 2026
e-ISSN 2598-9596
DOI: https://doi.org/10.19166/fastjst.v10i1/10891
Available online at: https://ojs.uph.edu/index.php/FaSTJST/article/view/10891

secara keseluruhan selama bekerja. Metode ini telah diakui secara internasional sebagai standar untuk menilai risiko cedera punggung akibat pengangkatan manual, dengan mempertimbangkan faktor seperti jarak angkat, frekuensi, dan postur tubuh [4-6]. Dengan menggabungkan hasil CMDQ, pendekatan NIOSH dan REBA, penelitian ini bertujuan untuk menganalisis risiko beban kerja pada aktivitas *dumping* aditif secara menyeluruh serta merancang solusi ergonomis yang tepat guna mengurangi potensi cedera dan meningkatkan keselamatan pekerja.

Penelitian terdahulu mengenai risiko ergonomi pada aktivitas manual material handling umumnya berfokus pada dua pendekatan utama, yaitu analisis batas aman pengangkatan menggunakan *NIOSH Lifting Equation* dan analisis postur kerja menggunakan REBA. Beberapa penelitian terdahulu [7-13] menekankan identifikasi risiko pengangkatan manual menggunakan parameter RWL dan LI, namun belum mengintegrasikan analisis postur tubuh secara menyeluruh. Sebaliknya, Hamdy dan Zalisman (2018) serta Faudy dan Sukanta (2022) menunjukkan efektivitas REBA dalam mengidentifikasi postur berisiko dan mengevaluasi usulan perbaikan, tetapi belum menggabungkannya dengan analisis kuantitatif batas aman beban angkat [14, 15]. Oleh karena itu, masih terdapat celah penelitian pada kajian ergonomi yang mengintegrasikan keluhan subjektif pekerja, analisis risiko pengangkatan dengan tugas bervariasi (*multi-task)*, dan analisis postur kerja secara simultan pada aktivitas dumping aditif di industri petrokimia. Penelitian ini mengisi celah tersebut melalui penggunaan CMDQ, NIOSH Lifting Equation dengan *Composite Lifting Index*, serta REBA, kemudian memvalidasi usulan intervensi melalui simulasi. Dengan demikian, kebaruan penelitian ini terletak pada pendekatan evaluasi ergonomi yang terintegrasi, berbasis aktivitas multi-variasi, dan disertai simulasi perbaikan yang terukur.

2. Metode Penelitian

Metode penelitian mengacu pada pendekatan sistematis berupa tahapan yang dilakukan dalam melakukan penelitian, dengan tahapan sebagai berikut:

1. Penelitian Pendahuluan
   Penelitian pendahuluan dilakukan dengan cara observasi langsung pada aktivitas *dumping* aditif dan wawancara langsung dengan operator mengenai tantangan dan kendala dalam melakukan aktivitas tersebut.
2. Perumusan Masalah
   Permasalahan utamanya adalah posisi operator yang membungkuk saat melakukan aktivitas *dumping* aditif sehingga tidak aman bagi pekerja. Operator sering mengeluh sakit pinggang dan punggung yang berbahaya dari sisi kesehatan jangka panjang serta dapat menyebabkan cedera muskuloskeletal.
3. Penentuan Tujuan Penelitian
   Tujuan penelitian ini adalah menganalisis risiko beban kerja pada aktivitas *dumping* aditif secara terukur dan memberikan rekomendasi untuk mengurangi potensi cedera sehingga dapat meningkatkan kenyamanan operator.
4. Studi Literatur.
   Pada langkah ini akan dilakukan studi literatur dengan mencari dan mempelajari teori-teori yang sesuai dengan topik penelitian mengenai beban kerja pada aktivitas manual handling sebagai informasi pendukung atau dasar dalam penelitian ini.
5. Pengumpulan Data
   Pengumpulan data dilakukan melalui observasi langsung, wawancara operator, penyebaran kuesioner CMDQ, serta pengukuran data variabel untuk perhitungan *lifting index* dan analisis REBA. Data yang diperlukan mencakup data berat dan ukuran karung aditif, jarak horizontal dan vertikal pengangkatan, sudut putar, frekuensi dan durasi pengangkatan serta foto postur pekerja saat melakukan pengangkatan.
6. Pengolahan Data
   Tahap ini meliputi pengolahan data kuesioner CMDQ untuk menentukan tingkat ketidaknyamanan operator, perhitungan *Recommended Weight Limit* (RWL) dan *Composite Lifting Index* (CLI), serta analisis postur kerja menggunakan metode REBA berdasarkan foto postur pekerja.
7. Analisis dan Pembahasan
   Pada tahap ini dicari solusi serta usulan perbaikan berdasarkan hasil perhitungan CLI dan skor REBA. Analisis berfokus pada identifikasi faktor dominan penyebab risiko tinggi, pengajuan

FaST - Jurnal Sains dan Teknologi, Vol.10, No. 1, Mei 2026
e-ISSN 2598-9596
DOI: https://doi.org/10.19166/fastjst.v10i1/10891
Available online at: https://ojs.uph.edu/index.php/FaSTJST/article/view/10891

usulan perbaikan yang efektif, serta perbandingan nilai *lifting index* dan skor REBA sebelum dan sesudah perbaikan.

8. Kesimpulan dan Saran
   Kesimpulan dibuat untuk menjawab tujuan utama penelitian, yaitu mengevaluasi risiko beban kerja pada aktivitas *dumping* aditif. Dalam tahap ini juga dituliskan keterbatasan penelitian serta saran yang mencakup rekomendasi terhadap perusahaan serta usulan untuk penelitian di masa mendatang agar menghasilkan solusi yang lebih komprehensif.

3. Hasil dan Pembahasan

3.1 *Cornell Musculoskeletal Discomfort Questionnaire (CMDQ)*

Pada tahap awal dilakukan survei dengan menggunakan CMDQ terhadap 8 operator dumping aditif produk HF 10 TQ. Berdasarkan hasil pengolahan CMDQ diketahui bahwa punggung bawah merupakan bagian tubuh yang paling dominan mengalami keluhan dengan skor total 220 dan persentase sebesar 62,86%. Keluhan lain yang juga muncul meliputi punggung atas sebesar 11,43%, bahu kanan dan kiri masing-masing 8,57%, serta pinggul/pantat 5,71%. Temuan ini mengindikasikan bahwa aktivitas pengangkatan aditif secara manual sangat berisiko menyebabkan gangguan *musculoskeletal*, dengan fokus risiko utama pada area punggung bawah.

3.2 Perhitungan *Composite Lifting Index (CLI)*

Berikutnya dilakukan pengumpulan data meliputi ukuran spesifik beberapa elemen yang berhubungan dengan aktivitas *dumping* aditif, meliputi ketinggian meja *dump station* yaitu 80 cm sebagai *vertical destination*, dimensi panjang, lebar, tinggi dari masing-masing karung aditif, pengukuran ketinggian masing-masing tumpukan aditif sebagai *vertical origin*. Terdapat total 72 karung yang terbagi ke dalam empat tumpukan aditif seperti dapat dilihat pada **Gambar 1**.

Gambar 1 Tumpukan karung aditif untuk Produk HF 10 TQ

Pengumpulan data selanjutnya dilakukan dengan mengukur dimensi horizontal dan vertikal pengangkatan, sudut putar tubuh, kategori *coupling* untuk menilai kualitas pegangan, serta frekuensi dan durasi pengangkatan. Hasil pengukuran untuk pengangkatan 72 karung aditif dikelompokkan menjadi 11 variasi tugas berdasarkan perbedaan ketinggian vertikal origin dengan rentang 25-105 cm, seperti dapat dilihat pada **Tabel 1**.

FaST - Jurnal Sains dan Teknologi, Vol.10, No. 1, Mei 2026
e-ISSN 2598-9596
DOI: https://doi.org/10.19166/fastjst.v10i1/10891
Available online at: https://ojs.uph.edu/index.php/FaSTJST/article/view/10891

Tabel 1 Data pengukuran variabel untuk perhitungan CLI

Task No.	Object Weight (kg)		Hand Location (cm)				Vertical Distance	Asymmetric		Frequency Rate	Duration (hrs)	Object Coupling	Jumlah karung	Waktu per taks
			Origin		Destination			Origin	Dest.					
	L(avg)	L(max)	H	V	H	V	D	A	A	F		C		
1	7,56	12,5	45	25	45	90	65	50°	40°	0,15	<1	Fair	4	1,44
2	7,56	12,5	45	30	45	95	65	50°	40°	0,46	<1	Fair	12	4,33
3	7,56	12,5	45	35	45	90	55	50°	40°	0,15	<1	Fair	4	1,44
4	7,56	12,5	45	40	45	90	50	50°	40°	0,04	<1	Fair	1	0,36
5	7,56	12,5	45	45	45	95	50	50°	40°	0,42	<1	Fair	11	3,97
6	7,56	12,5	45	45	45	90	45	50°	40°	0,15	<1	Fair	4	1,44
7	7,56	12,5	45	55	45	90	35	50°	40°	0,19	<1	Fair	5	1,81
8	7,56	12,5	45	60	45	95	35	50°	40°	0,31	<1	Fair	8	2,89
9	7,56	12,5	45	75	45	95	20	50°	40°	0,31	<1	Fair	8	2,89
10	7,56	12,5	45	90	45	95	5	50°	40°	0,31	<1	Fair	8	2,89
11	7,56	12,5	45	105	45	95	10	50°	40°	0,27	<1	Fair	7	2,53
										2,77			72	26,00

Berdasarkan data pada **Tabel 1**, dilakukan perhitungan *multipliers* dan CLI untuk menilai risiko kumulatif dari seluruh tugas pengangkatan manual menggunakan NIOSH *equation* untuk *multi-task lifting job* seperti dapat dilihat pada **Tabel 2** dan **Tabel 3**.

Tabel 2 Perhitungan *Multipliers* dan FIRWL, STRWL, FILI, STLI

Task No.	LC	HM	VM	DM	AM	CM	FIRWL	FM	STRWL	FILI= L/FIRWL	STLI= L/STRWL	NewTask No.	F Cum	FM_i
1	23	0,56	0,85	0,89	0,84	0,95	7,71	1,00	7,71	16,219	0,9812	2	0,62	0,9631
2	23	0,56	0,87	0,89	0,84	0,95	7,84	0,97	7,64	15,938	0,9901	1	0,46	0,9738
3	23	0,56	0,88	0,90	0,84	0,95	8,09	1,00	8,09	15,447	0,9346	3	0,77	0,9538
4	23	0,56	0,90	0,91	0,84	0,95	8,30	1,00	8,30	15,052	0,9106	5	1,23	0,9331
5	23	0,56	0,91	0,91	0,84	0,95	8,44	0,98	8,26	14,804	0,9161	4	1,19	0,9342
6	23	0,56	0,91	0,92	0,84	0,95	8,54	1,00	8,54	14,643	0,8859	6	1,39	0,9285
7	23	0,56	0,94	0,95	0,84	0,95	9,09	1,00	9,09	13,748	0,8318	7	1,58	0,9227
8	23	0,56	0,96	0,95	0,84	0,95	9,24	0,99	9,14	13,533	0,8276	8	1,89	0,9134
9	23	0,56	1,00	1,00	0,84	1,00	10,73	0,99	10,62	11,646	0,7123	11	2,77	0,8869
10	23	0,56	0,96	1,00	0,84	1,00	10,25	0,99	10,14	12,195	0,7458	10	2,46	0,8961
11	23	0,56	0,91	1,00	0,84	1,00	9,77	0,99	9,70	12,798	0,7797	9	2,15	0,9054

Tabel 3 Perhitungan CLI

Rumus	Hasil
$STLI_1$	0,9901
$FILI_2$ x $(1/FM_{1,2} - 1/FM_1) = DLI_2$	0,0186
$FILI_3$ x $(1/FM_{1,2,3} - 1/FM_{1,2}) = DLI_3$	0,0155
$FILI_4$ x $(1/FM_{1,2,3,4} - 1/FM_{1,2,3}) = D\ LI_4$	0,0326
$FILI_5$ x $(1/FM_{1,2,3,4,5} - 1/FM_{1,2,3,4}) = D\ LI_5$	0,0020
$FILI_6$ x $(1/FM_{1,2,3,4,5,6} - 1/FM_{1,2,3,4,5}) = D\ LI_6$	0,0078
$FILI_7$ x $(1/FM_{1,2,3,4,5,6,7} - 1/FM_{1,2,3,4,5,6}) = D\ LI_7$	0,0093
$FILI_8$ x $(1/FM_{1,2,3,4,5,6,7,8} - 1/FM_{1,2,3,4,5,6,7}) = D\ LI_8$	0,0148
$FILI_9$ x $(1/FM_{1,2,3,4,5,6,7,8,9} - 1/FM_{1,2,3,4,5,6,7,8}) = D\ LI_9$	0,0125
$FILI_{10}$ x $(1/FM_{1,2,3,4,5,6,7,8,9,10} - 1/FM_{1,2,3,4,5,6,7,8,9}) = D\ LI_{10}$	0,0139
$FILI_{11}$ x $(1/FM_{1,2,3,4,5,6,7,8,9,10,11} - 1/FM_{1,2,3,4,5,6,7,8,9,10}) = D\ LI_{11}$	0,0135
CLI	**1,1307**

Hasil akhir CLI pada **Tabel 3** adalah 1,1307. Nilai CLI > 1,00 menunjukkan bahwa beban kerja pengangkatan aditif secara keseluruhan melebihi batas yang disarankan oleh NIOSH dan berpotensi menimbulkan risiko cedera bagi pekerja dan memerlukan intervensi ergonomi untuk mengurangi risiko cedera tersebut.

3.3 Pengolahan Data Metode REBA

Berdasarkan hasil observasi terhadap aktivitas *dumping* aditif, pengangkatan tumpukan paling bawah teridentifikasi sebagai postur paling ekstrem dengan risiko cedera tertinggi. Oleh karena itu, postur tersebut dipilih sebagai sampel untuk dianalisis lebih lanjut menggunakan metode REBA guna

FaST - Jurnal Sains dan Teknologi, Vol.10, No. 1, Mei 2026
e-ISSN 2598-9596
DOI: https://doi.org/10.19166/fastjst.v10i1/10891
Available online at: https://ojs.uph.edu/index.php/FaSTJST/article/view/10891

menentukan tingkat urgensi intervensi. Pengukuran sudut untuk analisis REBA dapat dilihat pada **Gambar 2**.

Gambar 2 Pengukuran sudut postur kerja pengangkatan karung aditif

Berdasarkan hasil pengukuran sudut pada **Gambar 2**, maka dilakukan penilaian skor postur kerja seperti dapat dilihat pada **Gambar 3**.

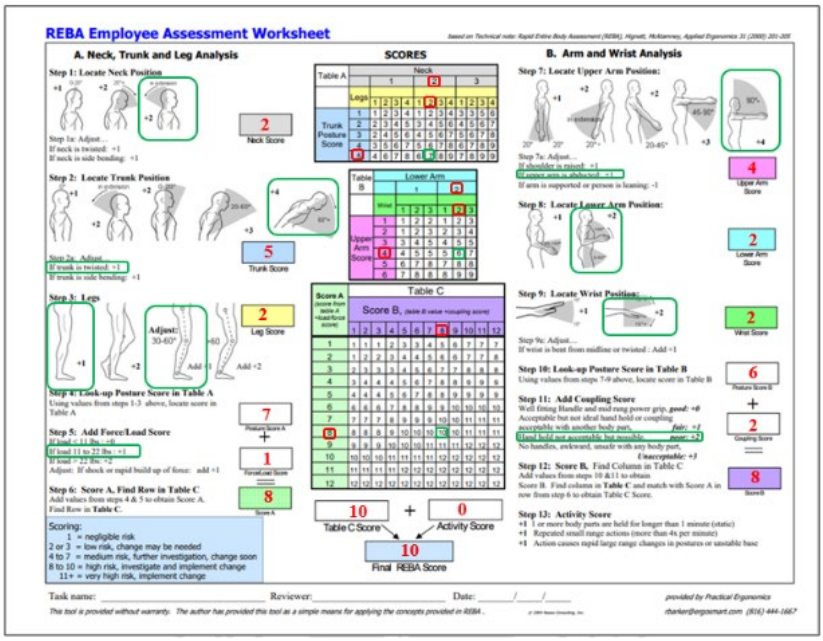

Gambar 3 *Worksheet* REBA postur *dumping* aditif kondisi awal

Berdasarkan REBA worksheet pada gambar 3 dapat disimpulkan bahwa postur kerja aktivitas *dumping* aditif tersebut memiliki risiko tinggi terhadap kesehatan *musculoskeletal*, dengan skor akhir REBA=10. Skor ini mengindikasikan bahwa perubahan perlu segera diimplementasikan untuk mencegah cedera serius.

3.4 Usulan Perbaikan

Berdasarkan hasil evaluasi menggunakan kedua metode ergonomi tersebut, ditemukan bahwa aktivitas *dumping* aditif saat ini berada pada kategori risiko tinggi dan perlu segera dilakukan intervensi. Perbaikan dilakukan dengan mengevaluasi nilai *multiplier* paling kecil pada perhitungan RWL yang menyebabkan LI tinggi, Mengingat jarak horizontal tangan saat pengangkatan karung tidak dapat dikurangi karena pengangkatan dilakukan oleh 2 orang operator, maka perbaikan difokuskan pada jarak vertikal yaitu dengan menyamakan ketinggian antara posisi *origin* dan *destination*. Salah satu solusi praktis untuk menjaga tumpukan aditif pada ketinggian konstan adalah dengan penggunaan alat bantu *Manual Hydraulic Stacker Forklift* seperti yang ditunjukkan pada **Gambar 4**.

FaST - Jurnal Sains dan Teknologi, Vol.10, No. 1, Mei 2026
e-ISSN 2598-9596
DOI: https://doi.org/10.19166/fastjst.v10i1/10891
Available online at: https://ojs.uph.edu/index.php/FaSTJST/article/view/10891

Gambar 4 *Manual Hydraulic Stacker Forklift*

Gambar 5 menunjukkan simulasi penggunaan *Manual Hydraulic Stacker Forklift* yang memungkinkan pengaturan ketinggian tumpukan aditif secara dinamis agar selalu sejajar dengan meja *dump station* di ketinggian 80 cm pada berbagai tumpukan karung. Rekayasa teknik ini secara efektif mengeliminasi aktivitas membungkuk dan pengangkatan beban dari posisi rendah, sehingga operator dapat mempertahankan postur tubuh tegap sempurna selama proses dumping berlangsung sehingga stasiun kerjanya menjadi *proper work design.*

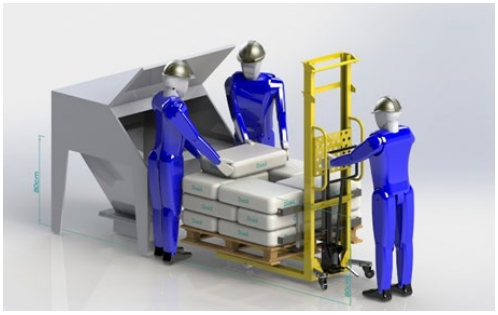

Tumpukan keempat

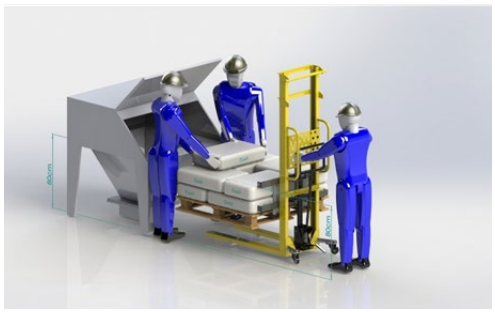

Tumpukan ketiga

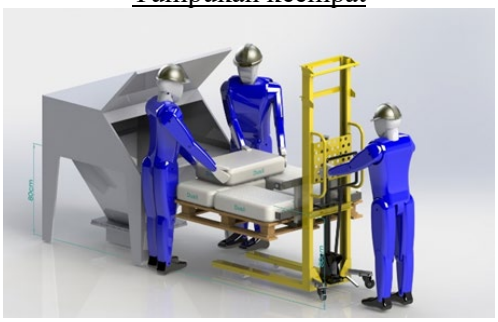

Tumpukan kedua

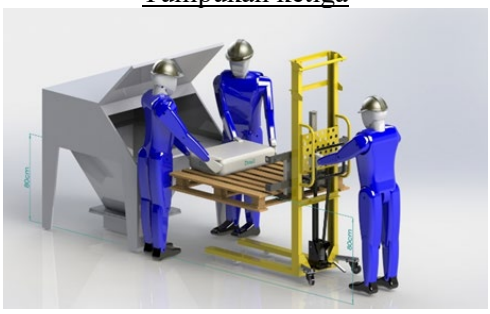

Tumpukan pertama

Gambar 5 Simulasi pengangkatan dumping aditif pada berbagai ketinggian tumpukan

3.5 Analisis *lifting index* setelah perbaikan

Setelah dilakukan simulasi maka *vertical origin* untuk setiap tumpukan berada pada ketinggian yang sama dengan *vertical destination* yaitu ketinggian *dump station*. Hal ini berarti sudah tidak ada variasi tugas, sehingga untuk perhitungan *Recommended Weight Limit* (RWL) dan *Lifting Index* (LI) digunakan perhitungan *single task lifting job*. Berdasarkan **Gambar 6**, dapat dilihat bahwa hasil perhitungan *lifting index* adalah 0,88 untuk posisi *origin* dan 0,84 untuk posisi *destination*, yang berarti pekerjaan pengangkatan aman untuk pekerja (LI < 1).

FaST - Jurnal Sains dan Teknologi, Vol.10, No. 1, Mei 2026
e-ISSN 2598-9596
DOI: https://doi.org/10.19166/fastjst.v10i1/10891
Available online at: https://ojs.uph.edu/index.php/FaSTJST/article/view/10891

JOB ANALYSIS WORKSHEET

STEP 1. Measure and Record Task Variables

Object Weight (kg)		Hand Location (cm)				Vertical Distance (cm)	Asymmetric Angle (degrees)		Frequency Rate (lifts/min)	Duration (hrs)	Object Coupling
		Origin		Destination			Origin	Dest.			
L(avg)	L(max)	H	V	H	V	D	A	A	F		C
7,56	12,5	45	95	45	95	95-95 = 0	50°	40°	2,77	26 min	Fair

STEP 2. Determine the multipliers and Compute the RWL's

RWL = LC x HM x VM x DM x AM x FM x CM

ORIGIN RWL = 23 x 0,56 x 0,94 x 1 x 0,84 x 0,89 x 0,95 = 8,59 kg

DESTINATION RWL = 23 x 0,56 x 0,94 x 1 x 0,87 x 0,89 x 0,95 = 8,92 kg

STEP 3. Compute the LIFTING INDEX

ORIGIN LIFTING INDEX = object weight (L) / RWL = 7,56 / 8,59 = 0,88

DESTINATION LIFTING INDEX = object weight (L) / RWL = 7,56 / 8,92 = 0,84

Gambar 6 *Worksheet* perhitungan RWL dan LI setelah perbaikan

3.6 Analisis REBA setelah Perbaikan

Analisis REBA dengan simulasi pengukuran sudut postur tubuh berdasarkan usulan perbaikan dapat dilihat pada **Gambar 7**. Analisis postur pekerja dilakukan dengan menggunakan REBA *worksheet* seperti dapat dilihat pada **Gambar 8**. Berdasarkan gambar 8 dapat disimpulkan bahwa postur kerja aktivitas *dumping* aditif pada operator memiliki risiko rendah terhadap cedera muskuloskeletal, dengan skor REBA akhir 3.

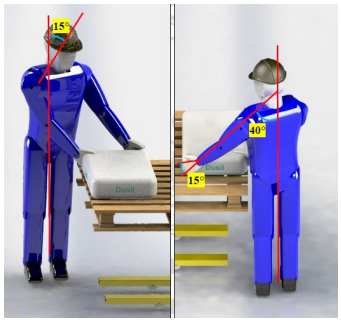

Gambar 7 Pengangkatan karung aditif dengan *hydraulic stacker*

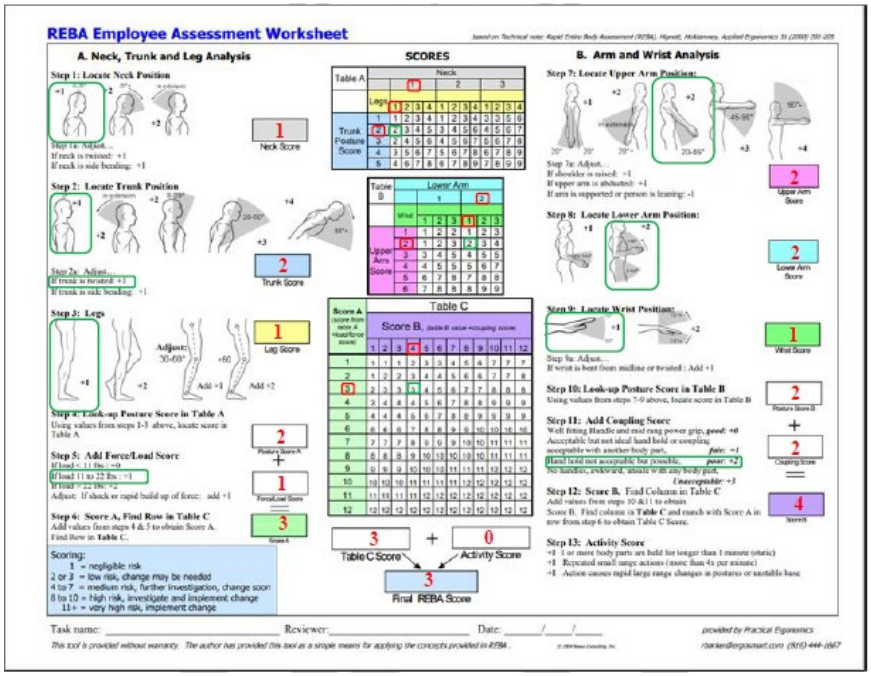

Gambar 8 *Worksheet* REBA postur *dumping* aditif dengan penggunaan *hydraulic stacker*

FaST - Jurnal Sains dan Teknologi, Vol.10, No. 1, Mei 2026
e-ISSN 2598-9596
DOI: https://doi.org/10.19166/fastjst.v10i1/10891
Available online at: https://ojs.uph.edu/index.php/FaSTJST/article/view/10891

3.7 Evaluasi usulan perbaikan

Berdasarkan hasil simulasi, penggunaan *Manual Hydraulic Stacker Forklift* pada aktivitas *dumping* aditif diketahui dapat memitigasi risiko ergonomi tanpa mengganggu produktivitas. Dari sisi ergonomi, alat ini berhasil menurunkan nilai *Composite Lifting Index* (CLI) dan skor REBA. Perbaikan ini secara objektif menyelesaikan keluhan *musculoskeletal* akibat postur membungkuk yang sebelumnya terkonfirmasi melalui kuesioner CMDQ.

Dari aspek operasional, penggunaan alat ini dipastikan tidak menambah waktu siklus karena pengoperasiannya dilakukan secara paralel oleh operator ketiga yang sebelumnya bertugas untuk membersihkan sampah karung. Dengan pembagian tugas ini, proses *dumping* tetap berjalan kontinu tanpa jeda pengaturan ketinggian, sehingga efisiensi kerja meningkat. Meskipun demikian, perubahan sistem ini menimbulkan konsekuensi berupa penambahan beban kerja operasional bagi operator pembersihan yang kini bertanggung jawab penuh atas pengoperasian *Manual Hydraulic Stacker Forklift* tersebut.

4. Keterbatasan penelitian

Pada penelitian ini, cakupan analisis postur kerja dibatasi hanya untuk 8 operator dumping aditif produk HF 10 TQ yang merupakan produk dengan jumlah aditif terbanyak dan paling sering diproduksi pada lantai produksi polipropilen *train 1.* Analisis REBA hanya dilakukan untuk postur pengangkatan yang paling ekstrem, yaitu pengangkatan karung aditif pada tumpukan pertama (tumpukan paling bawah). Analisis terhadap usulan perbaikan dilakukan dengan menggunakan simulasi perangkat lunak *SolidWorks* karena realisasi pengadaan alat bantu *hydraulic stacker* manual mengalami penundaan terkait kelangkaan bahan baku pembuatan biji plastik. Pada penelitian ini tidak dibahas faktor kelelahan jangka panjang, variasi individu dan faktor lingkungan kerja.

5. Kesimpulan dan Saran

Penelitian menyimpulkan bahwa aktivitas *dumping* aditif pada kondisi awal di PT X memiliki risiko beban kerja fisik yang tinggi dan berbahaya. Berdasarkan kuesioner CMDQ, keluhan muskuloskeletal didominasi oleh area punggung bawah (62,86%), yang diperkuat oleh analisis ergonomi dengan nilai *Composite Lifting Index* (CLI) sebesar 1,1307 dan skor REBA mencapai 10. Sebagai solusi, diusulkan penggunaan alat bantu *Manual Hydraulic Stacker Forklift* yang secara simulasi terbukti efektif memitigasi risiko tersebut. Simulasi menunjukkan bahwa alat ini mampu menempatkan beban pada ketinggian ideal dan menghilangkan gerakan membungkuk, sehingga menurunkan nilai *Lifting Index* secara signifikan menjadi 0,88 (*origin*) dan 0,84 (*destination*), serta menurunkan skor REBA ke level 3 (risiko rendah). Untuk mengatasi keterbatasan penelitian, jumlah operator yang menjadi responden dapat ditingkatkan agar lebih mewakili keseluruhan operator dumping aditif. Selain itu, usulan perbaikan diharapkan dapat diimplementasikan agar dapat dievaluasi efektivitasnya dalam menurunkan tingkat ketidaknyamanan operator dan risiko cedera muskuloskeletal. Untuk penelitian selanjutnya dapat diperhitungkan faktor kelelahan jangka panjang, variasi individu dan faktor lingkungan kerja.

Daftar Pustaka

[1] W. Macdonald and J. Oakman, “Requirements for more effective prevention of work-related musculoskeletal disorders,” *BMC Musculoskelet. Disord.*, vol. 16, no. 1, p. 293, Dec. 2015, https://doi.org/10.1186/s12891-015-0750-8.

[2] X. Ding *et al.*, “Prevalence and risk factors of work-related musculoskeletal disorders among emerging manufacturing workers in Beijing, China,” *Front. Med. (Lausanne).*, vol. 10, Oct. 2023, https://doi.org/10.3389/fmed.2023.1289046.

[3] J. M. Astete-Cornejo and J. R. Asencios-Hidalgo, “Validation of the Cornell Musculoskeletal Discomfort Questionnaires in textile workers in Peru,” *Rev Bras Med Trab*. Vol.21, no. 4, Feb 2024, https://doi.org/10.47626/1679-4435-2023-1029.

[4] Waters et al, “Efficacy of the Revised NIOSH Lifting Equation to Predict Risk of Low Back Pain Due to Manual Lifting,” *JOEM*, vol. 53, Sep. 2011.

[5] NIOSH, *Applications manual for the Revised NIOSH lifting equation*, No. 94-110. U.S. Department of Health and Human Services, Centers for Disease Control and Prevention, 1991.

[6] M. Hita-Gutiérrez, M. Gómez-Galán, M. Díaz-Pérez, and A. J. Callejón-Ferre, "An Overview of REBA Method Applications in the World," *Int J Environ Res Public Health*., vol. 17, no. 8, Apr 2020, https://doi.org/10.3390/ijerph17082635.

[7] D. P. Mayangsari, S. Sunardi, and T. Tranggono, "Analisis Risiko Ergonomi Pada Pekerjaan Mengangkat di Bagian Gudang Bahan Baku PT. AAP Dengan Metode NIOSH Lifting Equation," *JUMINTEN*, vol. 1, no. 3, pp. 91–103, May 2020, https://doi.org/10.33005/juminten.v1i3.109.

[8] N. H. Kamarudin, S. A. Ahmad, Mohd. K. Hassan, R. Mohd Yusuff, and S. Z. Md Dawal, "A Review of the NIOSH Lifting Equation and Ergonomics Analysis," *Advanced Engineering Forum*, vol. 10, pp. 214–219, Dec. 2013, https://doi.org/10.4028/www.scientific.net/AEF.10.214.

[9] Andianingsari et al., "Pengukuran ergonomi metode Recommended Weight Limit (RWL) dan Lifting Index (LI) di PT X," *IMTechno: Journal of Industrial Management and Technology*, vol. 3, pp. 110–114, 2022.

[10] D. Lesmana, "Analisis Beban Kerja menggunakan Metode Recommended Weight Limit dan Lifting Index," *J. Teknol.*, pp. 21–26, Jun. 2022, https://doi.org/10.35134/jitekin.v12i1.66.

[11] Pradita et al., "Analisis dan perbaikan manual material handling mengangkat beban galon dengan metode Recommended Weight Limit dan Lifting Index (NIOSH) di Depot Sri Water," *TALENTA Conference Series: Energy and Engineering (EE)*, vol. 7, pp. 1065–1072, 2024.

[12] R. A. Ratriwardhani, "Analisa aktivitas pengangkatan dengan metode Recommended Weight Limit (RWL)," *Medical Technology and Public Health Journal*, vol. 3, pp. 96–100, 2019.

[13] D. Fitriani, N. Amanda, N. M. Dewantari, A. S. Mariawati, L. Herlina, dan A. Umyati, "Pengukuran Beban Kerja Fisik dengan Menggunakan Metode NIOSH (*National Institute of Occupational Safety and Health*) Pada Kegiatan Mengangkut Beras Di Pasar Kranggot - Cilegon," *JOSEAM*, vol. 3, no. 2, Dec 2024, pp. 79-84.

[14] M. I. Hamdy and S. Zalisman, "Analisa Postur Kerja dan Perancangan Fasilitas Penjemuran Kerupuk yang Ergonomis Menggunakan Metode Analisis Rapid Entire Body Assessment (REBA) dan Antropometri," *Jurnal Sains, Teknologi dan Industri*, vol. 16, no. 1, p. 57, Dec. 2018, https://doi.org/10.24014/sitekin.v16i1.5388.

[15] M. K. Faudy and S. Sukanta, "Analisis Ergonomi Menggunakan Metode REBA Terhadap Postur Pekerja pada Bagian Penyortiran di Perusahaan Bata Ringan," *Go-Integratif : Jurnal Teknik Sistem dan Industri*, vol. 3, no. 01, pp. 47–58, May 2022, https://doi.org/10.35261/gijtsi.v3i01.6540.

FaST - Jurnal Sains dan Teknologi, Vol.10, No. 1, Mei 2026
e-ISSN 2598-9596
DOI: https://doi.org/10.19166/fastjst.v10i1/10892
Available online at: https://ojs.uph.edu/index.php/FaSTJST/article/view/10892

Analisis Sistem Antrian di Indomaret Fresh Bitung dengan Pendekatan Teori Antrian dan Simulasi

Nanda Dwi Putra Purba[1], Sylvia[1*], Rifqi Bilal Kumara[1], Yoga Rendika[1], Yoga Putranto[1], Nuryudha Darmawan[1]
[1]Program Studi Teknik Industri, Universitas Pelita Harapan, Tangerang, Indonesia

ABSTRACT

This study analyzes the performance of the cashier queueing system at Indomaret Fresh Bitung using observational data on inter-arrival times and service times, integrated with simulation modeling. The data collected indicate that customer inter-arrival times follow an exponential distribution. The analysis demonstrates that shorter inter-arrival times substantially increase waiting times and server utilization. During peak hours, an average inter-arrival time of 1.21 minutes results in an average waiting time of 0.769 minutes and a server utilization rate of 60%, indicating that the cashier operates near maximum capacity. In contrast, during non-peak hours, a longer average inter-arrival time of 1.832 minutes reduces system workload, leading to a shorter average waiting time of 0.341 minutes and increasing the probability of server idleness to 62.5%. Combined simulation results reveal a relatively balanced operational condition with an overall utilization level of 50%. Overall, the findings confirm that shorter inter-arrival times increase the likelihood of queue formation; therefore, optimal resource allocation during peak periods is necessary to maintain service efficiency.

ARTICLE INFO

Keywords: Queueing Theory; Inter-arrival Time; Service Time; Simulation modeling; Waiting Time.

***Corresponding author**:
sylvia.apandi@gmail.com

Article history:
Submitted 9 Feb 2026
Revised 17 Apr 2026
Accepted 23 Apr 2026
Online Available 7 May 2026
Published 20 May 2026

1. Pendahuluan

Gerai ritel modern di Indonesia terus mengalami perkembangan seiring dengan perubahan kebutuhan dan preferensi konsumen. Fenomena ini memberikan manfaat ekonomi, seperti peningkatan konsumsi domestik, pembukaan lapangan kerja, dan pemasukan pajak [1]. Salah satu bentuk inovasi tersebut adalah format Indomaret Fresh, yang memperluas konsep minimarket konvensional dengan menyediakan produk segar, bahan makanan, serta ragam produk yang lebih lengkap. Format ini bertujuan untuk memberikan pengalaman belanja yang lebih komprehensif sebagai pusat pemenuhan kebutuhan sehari-hari *(one-stop shopping),* sehingga berpotensi meningkatkan volume kunjungan dan durasi berbelanja pelanggan, khususnya pada periode waktu sibuk seperti sore hari dan akhir pekan.

Peningkatan jumlah pelanggan secara langsung berdampak pada kompleksitas pengelolaan sistem pelayanan. Salah satu aspek operasional yang krusial dalam lingkungan ritel adalah sistem antrian pada titik pelayanan kasir. Efisiensi operasional mengacu pada kemampuan suatu organisasi untuk melakukan tugas-tugasnya dengan seefisien mungkin, mengoptimalkan penggunaan sumber daya, dan menghasilkan hasil yang diinginkan dalam waktu sesingkat mungkin [2]. Sistem antrian yang tidak efisien dapat menyebabkan waktu tunggu yang panjang, menurunkan tingkat kepuasan pelanggan, serta berdampak negatif terhadap persepsi kualitas pelayanan dan loyalitas pelanggan. Berbagai penelitian di sektor ritel menunjukkan bahwa keterbatasan kapasitas pelayanan dan pengelolaan antrian yang kurang optimal dapat memicu ketidakpuasan pelanggan dan menurunkan loyalitas. Jumlah kasir *(server)* yang optimal diperlukan untuk memberikan pelayanan yang efektif dan efisien [3].

Kepuasan pelanggan dalam konteks ritel sangat dipengaruhi oleh kualitas layanan, termasuk kecepatan pelayanan, keramahan petugas kasir, dan efisiensi proses transaksi. Meskipun Indomaret Fresh Bitung memiliki tingkat penilaian yang relatif tinggi berdasarkan ulasan pelanggan, terdapat indikasi bahwa aspek pelayanan di titik kasir, khususnya terkait sistem antrian, masih berpotensi menimbulkan ketidakpuasan. Pengalaman di berbagai gerai ritel serupa menunjukkan bahwa permasalahan seperti waktu tunggu yang lama, jumlah kasir yang tidak sebanding dengan jumlah pelanggan pada jam sibuk, serta keterlambatan pelayanan sering menjadi keluhan utama pelanggan. Nilai ulasan Indomaret Fresh Bitung di *Google review* adalah 4,4 dengan total 247 ulasan [4] di mana beberapa keluhan mengenai pelayanan kasir lambat dan lamanya antrian.

FaST - Jurnal Sains dan Teknologi, Vol.10, No. 1, Mei 2026
e-ISSN 2598-9596
DOI: https://doi.org/10.19166/fastjst.v10i1/10892
Available online at: https://ojs.uph.edu/index.php/FaSTJST/article/view/10892

Kasir adalah tempat pelayanan penting di minimarket karena seluruh transaksi diproses pada bagian kasir. Tingginya variasi waktu kedatangan pelanggan, terutama pada jam sibuk, sering menyebabkan antrian dan meningkatnya waktu tunggu. Kondisi ini dapat menurunkan kepuasan pelanggan serta efisiensi operasional toko. Untuk memahami masalah tersebut, analisis sistem antrian diperlukan karena mampu menggambarkan hubungan antara waktu kedatangan dan waktu pelayanan. Antrian terbentuk dalam sistem ketika waktu layanan dan tingkat kedatangan bervariasi. Model antrian sederhana memberikan wawasan tentang bagaimana variabilitas waktu kedatangan dan waktu pelayanan menyebabkan kemacetan. Memahami hal ini sangat penting untuk desain dan pengelolaan berbagai sistem produksi dan layanan [5].

Berbagai penelitian sebelumnya menunjukkan bahwa teori antrian dapat digunakan untuk mengevaluasi kinerja pelayanan kasir. Penelitian oleh [6] pada Hyperstore Supermarket menemukan bahwa pola kedatangan pelanggan memengaruhi panjang antrian dan kapasitas kasir yang optimal. Studi lain oleh [7] di Supermarket Cool Tomohon menunjukkan bahwa pada jam puncak terjadi lonjakan antrian yang signifikan dan kapasitas kasir perlu disesuaikan dengan kondisi lapangan. Penelitian dan analisa antrian dengan model single channel di Supermarket Ngagel juga menunjukan sistem berjalan cukup efisien, namun peningkatan volume pelanggan dapat menyebabkan antrian menumpuk. Oleh karena itu, disarankan untuk menambah titik layanan atau meningkatkan manajemen antrian guna menjaga efisiensi dan kenyamanan layanan [8]. Analisa antrian pelayanan kasir Indomaret Aek menggunakan single channel-single phase menunjukan sistem M/M/1 memiliki tingkat utilitas yang tinggi sehingga menyebabkan waktu tunggu dan panjang antrian yang besar **[9]**. Penelitian di PT Tri Arga Travel [10] menggunakan bilangan acak dari *Linear Congruential Generator (LCG)* digunakan untuk memprediksi tingkat lonjakan penumpang pada tahun berikutnya dengan memanfaatkan data penumpang tahun sebelumnya untuk memberikan rekomendasi untuk memprediksi tingkat lonjakan penumpang dan juga membantu meningkatkan layanan kepada calon penumpang PT. Tri Arga Travel. Penelitian studi kasus Bank PLC di Anyigba, Kogi State, Nigeria menggunakan model antrian eksponensial untuk mengevaluasi *single* dan *multi server* [11].

Berdasarkan temuan tersebut, penelitian ini bertujuan untuk menganalisis sistem antrian di Indomaret Fresh Bitung guna mengevaluasi efisiensi operasional pelayanan pelanggan dengan memperhitungkan rata-rata waktu antri (tunggu), utilitas server, dan kemungkinan (probabilitas) pelanggan menunggu. Secara khusus, penelitian ini bertujuan untuk mengkaji pola kedatangan pelanggan, distribusi waktu pelayanan di kasir, disiplin antrian yang diterapkan, serta kecukupan jumlah saluran pelayanan (kasir). Hasil penelitian ini diharapkan dapat memberikan rekomendasi berbasis data untuk mengoptimalkan kinerja antrian, mengurangi rata-rata waktu tunggu, serta meningkatkan kepuasan pelanggan dan kualitas pelayanan di Indomaret Fresh Bitung.

2. Metode Penelitian

Penelitian ini menggunakan pendekatan simulasi sistem antrian *(queueing simulation)* berbasis data empiris yang diperoleh dari observasi langsung di lokasi penelitian. Metodologi penelitian terdiri atas tiga tahapan utama, yaitu:

1. Pengambilan data waktu antar kedatangan pelanggan *(interarrival time)* dan waktu pelayanan *(service time)*,
2. Analisis distribusi statistik menggunakan statistik histogram dengan aplikasi excel untuk menentukan model probabilitas yang sesuai, dan
3. Simulasi sistem antrian menggunakan *Linear Congruential Generator (LCG)* untuk menggenerasi bilangan acak dan parameter distribusi hasil analisis dengan menggunakan software excel.

Penelitian dilakukan pada sistem antrian riil yang diamati secara langsung di lokasi yang telah ditentukan. Objek penelitian adalah sistem antrian satu server *(single server)* pada lokasi riil, yaitu Indomaret Fresh Bitung, Kabupaten Tangerang. Pengamatan dilakukan pada dua kondisi waktu operasional, yaitu: jam normal, dan jam sibuk. Penentuan periode jam sibuk dan jam normal dilakukan berdasarkan pola tingkat kunjungan pelanggan (popular times) pada fitur *Google Maps Review*. Berdasarkan informasi tersebut, periode sekitar pukul 18.00 WIB diidentifikasi sebagai jam sibuk, sedangkan sekitar pukul 21.00 WIB ditetapkan sebagai jam normal karena tingkat kunjungan yang

FaST - Jurnal Sains dan Teknologi, Vol.10, No. 1, Mei 2026
e-ISSN 2598-9596
DOI: https://doi.org/10.19166/fastjst.v10i1/10892
Available online at: https://ojs.uph.edu/index.php/FaSTJST/article/view/10892

relatif lebih rendah. Data yang dikumpulkan pada jam sibuk dan jam normal sebanyak 107 observasi dengan masing-masing waktu antar kedatangan dan waktu pelayanan. Data interarrival time dan service time disajikan dalam bentuk tabel pada file Microsoft Excel, masing-masing pada lembar (sheet) terpisah untuk jam normal dan jam sibuk. Karakteristik operasional sistem antrian sebagian besar ditentukan oleh dua sifat statistik, yaitu distribusi probabilitas waktu antar kedatangan dan distribusi probabilitas waktu pelayanan [12]. Analisis distribusi dilakukan untuk menentukan distribusi probabilitas yang paling sesuai bagi waktu antar kedatangan dan waktu pelayanan, pada masing-masing kondisi waktu (jam normal dan jam sibuk) berdasarkan karakteristik bentuk histogram. Histogram adalah alat untuk merepresentasikan distribusi nilai variabel kontinu [13]. Kemudian dilakukan simulasi menggunakan bilangan acak *Linear Congruential Generator (LCG)*, transformasi invers berdasarkan distribusi waktu antar kedatangan dan waktu pelayanan untuk melakukan simulasi 40 pelanggan. Dari simulasi dilakukan perhitungan indikator kinerja sistem antrian yaitu rata-rata waktu menunggu, probabilitas pelanggan menunggu, probabilitas kasir menganggur, probabilitas kasir sibuk, rata-rata waktu pelayanan, rata-rata waktu antar kedatangan, rata-rata waktu menunggu untuk pelanggan yang menunggu, rata-rata waktu pelanggan di dalam sistem, dan kesimpulan kinerja sistem antrian.

3. Hasil dan Pembahasan

Grafik pertama (**Gambar 1**) menunjukkan distribusi waktu antar kedatangan pelanggan di jam normal. Berdasarkan histogram tersebut, dapat terlihat bahwa sebagian besar kedatangan terjadi pada interval waktu yang sangat pendek, yaitu antara 0 hingga 2 menit, dengan frekuensi kemunculan tertinggi. Interval berikutnya, yaitu 2 hingga 4 menit, tetap memiliki frekuensi yang cukup tinggi, meskipun lebih rendah daripada interval pertama. Sementara itu, interval di atas 4 menit memiliki frekuensi yang sangat kecil hingga mendekati nol, yang menunjukkan bahwa jeda kedatangan yang panjang jarang terjadi dalam sistem ini. Pola distribusi yang semakin menurun dari kiri ke kanan menunjukkan kecenderungan bahwa data antar kedatangan mengikuti karakteristik distribusi eksponensial, yang umum digunakan untuk memodelkan waktu antar kedatangan pada sistem antrian dengan sifat kedatangan acak namun intensitas relatif tinggi. Distribusi eksponensial sering digunakan untuk menjelaskan fenomena yang terjadi secara acak dalam waktu dan tempat, dengan kecepatan konstan .

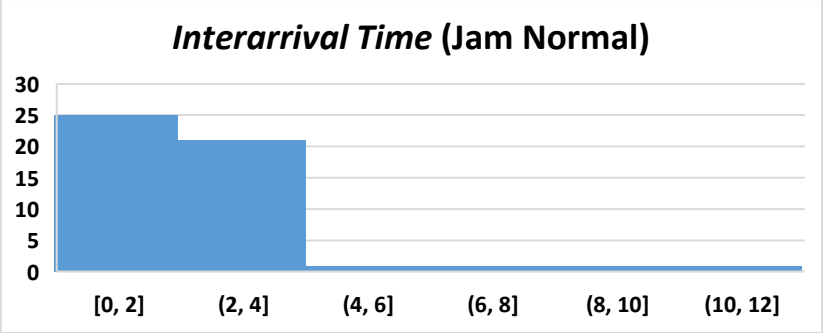

Gambar 1 Waktu Antar Kedatangan pada Jam Normal

Grafik kedua (**Gambar 2**) menampilkan distribusi waktu pelayanan di jam normal. Histogram menunjukkan bahwa waktu pelayanan didominasi oleh interval 0,27 hingga 1,03 menit dengan frekuensi tertinggi, sehingga menggambarkan bahwa sebagian besar proses layanan berlangsung sangat cepat. Interval berikutnya, yaitu 1,03 hingga 1,79 menit, memiliki frekuensi yang lebih rendah namun tetap signifikan, sementara interval di atas rentang tersebut menunjukkan frekuensi yang semakin kecil hingga mendekati nol. Pola distribusi tersebut mengindikasikan bahwa waktu layanan mengikuti distribusi eksponensial. Karakteristik ini sesuai dengan sistem layanan cepat yang jarang mengalami waktu pelayanan ekstrem, sehingga distribusi tersebut tepat digunakan untuk memodelkan waktu layanan dalam simulasi antrian.

FaST - Jurnal Sains dan Teknologi, Vol.10, No. 1, Mei 2026
e-ISSN 2598-9596
DOI: https://doi.org/10.19166/fastjst.v10i1/10892
Available online at: https://ojs.uph.edu/index.php/FaSTJST/article/view/10892

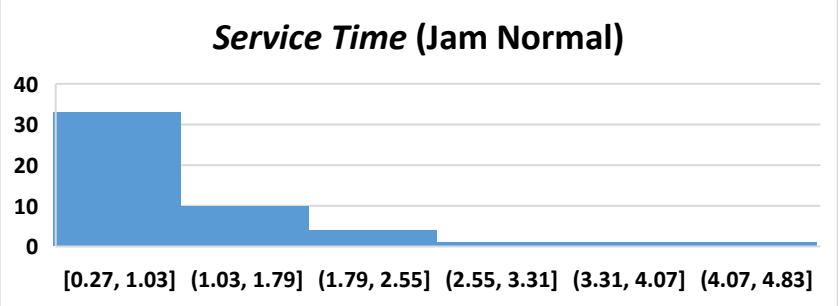

Gambar 2 Waktu Layanan pada Jam Normal

Grafik ketiga (**Gambar 3**) menggambarkan distribusi waktu antar kedatangan pelanggan pada jam sibuk. Dari histogram terlihat bahwa interval waktu antar kedatangan yang paling sering muncul berada pada rentang 0 hingga 0,86 menit, dengan frekuensi tertinggi sekitar 26 kejadian. Hal ini menunjukkan bahwa pada jam sibuk, pelanggan datang dalam interval yang sangat singkat, sehingga sistem menerima arus kedatangan yang padat. Interval berikutnya, yaitu 0,86 hingga 1,72 menit, memiliki frekuensi yang masih cukup besar yaitu sekitar 18 kejadian. Sementara itu, frekuensi terus menurun pada interval 1,72 hingga 3,44 menit, dan menjadi sangat rendah pada rentang 3,44 hingga 4,3 menit. Pola ini menunjukkan bahwa waktu antar kedatangan pada jam sibuk cenderung terkonsentrasi pada nilai-nilai kecil dan menurun secara eksponensial, suatu karakteristik yang umum pada proses kedatangan acak dengan intensitas tinggi pada sistem antrian.

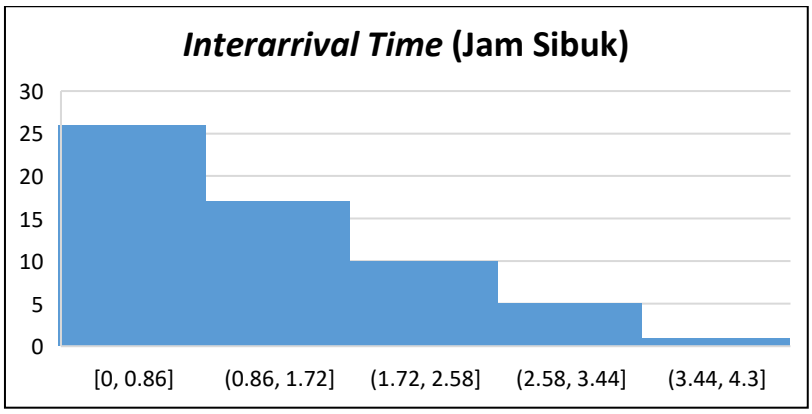

Gambar 3 Waktu Antar Kedatangan pada Jam Sibuk

Grafik keempat (**Gambar 4**) menunjukkan distribusi waktu layanan pada jam sibuk. Histogram memperlihatkan bahwa interval waktu layanan yang paling banyak terjadi adalah pada rentang 0,26 hingga 0,8 menit, dengan frekuensi tertinggi sekitar 26 kejadian. Hal ini mengindikasikan bahwa proses pelayanan pada jam sibuk cenderung berlangsung sangat cepat. Interval 0,8 hingga 1,34 menit memiliki frekuensi paling sering kedua, sekitar 20 kejadian, sementara interval di atasnya— 1,34 hingga 2,42 menit—menunjukkan penurunan signifikan dalam frekuensi, dengan hanya sekitar 7 hingga 5 kejadian. Pada rentang di atas 2,42 menit, frekuensi mendekati nol. Distribusi yang menurun dengan nilai dominan di rentang kecil ini menunjukkan bahwa waktu layanan juga memiliki kecenderungan mengikuti distribusi eksponensial, yang sesuai dengan karakteristik pelayanan cepat pada sistem antrian satu server di kondisi beban tinggi**.**

FaST - Jurnal Sains dan Teknologi, Vol.10, No. 1, Mei 2026
e-ISSN 2598-9596
DOI: https://doi.org/10.19166/fastjst.v10i1/10892
Available online at: https://ojs.uph.edu/index.php/FaSTJST/article/view/10892

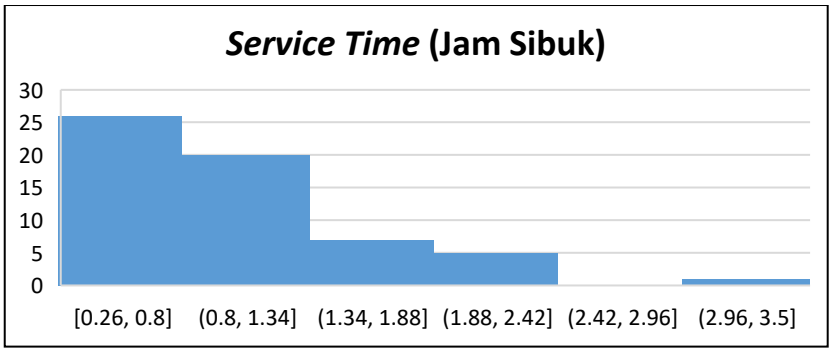

Gambar 4 Waktu Layanan pada Jam Sibuk

Hasil pengumpulan data dan grafik menunjukan perbedaan yang jelas antara kinerja antrian pada jam sibuk dan jam normal. Data yang telah melalui proses pembersihan menggunakan metode QUARTILE.INC di mana *outlier* dibersihkan dari data. Di jam normal, dari 49 data pelanggan, untuk waktu antar kedatangan ada 3 outlier dan waktu pelayanan ada 4 data outlier yang dibersihkan. Setelah data outlier dikeluarkan, maka didapatkan rata-rata waktu antar kedatangan di jam normal adalah 1,827 menit dan rata-rata waktu pelayanan adalah 0,752 menit. Sementara di jam sibuk, dari 58 data pelanggan tidak ada outlier untuk waktu antar kedatangan dan 3 data outlier untuk waktu pelayanan. Dengan data outlier dikeluarkan maka rata-rata waktu antar kedatangan di jam sibuk adalah 1,207 menit dan rata-rata waktu pelayanan adalah 0,871 menit.

Analisis dalam penelitian ini dilakukan menggunakan pendekatan *simulation-based modeling*, dengan cara membangkitkan bilangan acak untuk transformasi invers waktu antar kedatangan dan waktu pelayanan melalui metode *Linear Congruential Generator (LCG).* Banyak sistem sangat kompleks, sehingga model matematika yang valid untuk sistem tersebut juga kompleks. Dalam hal ini, model harus dipelajari melalui simulasi yang menjalankan model secara numerik untuk input yang dimaksud untuk melihat bagaimana input tersebut memengaruhi ukuran kinerja output [14]. Bilangan acak yang dibangkitkan adalah pseudorandom karena pembangkitannya menggunakan operasi matematika dan bilangan acak yang dibangkitkan memenuhi distribusi tertentu [15]. Metode LCG dimanfaatkan untuk menghasilkan deret bilangan acak yang berdistribusi seragam (0,1) [16], dan merupakan generator bilangan acak yang karena tidak memerlukan komputasi yang besar. Berikut persamaan untuk memperoleh deret bilangan bulat Z:

$$Z_i = (aZ_{i-1} + c) \bmod(m) \tag{1}$$

Di mana:

a = multiplier
c = increment constant
m = modulus constant
Z_i = urutan bilangan bulat Z_0 adalah benih awal. nilai Zi dibatasi oleh $0 \leq Zi \leq m - 1$ dan terdistribusi secara seragam dalam kasus diskrit.

Dari nilai Z_i kemudian dicari nilai U_i dengan persamaan sebagai berikut:

$$U_i = Z_i / m \tag{2}$$

yang selanjutnya dilakukan transformasi invers ke dalam distribusi eksponensial menggunakan persamaan:

$$\mathbf{x = -\beta \cdot \ln(1 - u)} \tag{3}$$

Di mana:

U = bilangan acak dari LCG
β = rata-rata waktu antar kedatangan atau pelayanan
X = nilai waktu antar kedatangan atau waktu pelayanan

FaST - Jurnal Sains dan Teknologi, Vol.10, No. 1, Mei 2026
e-ISSN 2598-9596
DOI: https://doi.org/10.19166/fastjst.v10i1/10892
Available online at: https://ojs.uph.edu/index.php/FaSTJST/article/view/10892

Simulasi dilakukan dengan menggunakan menggunakan LCG (dengan nilai a= 21, c= 9, m= 512, dengan benih awal Zo untuk waktu intearrival time = 21 dan Zo untuk waktu service time = 77) dan transformasi distribusi eksponensial untuk jam normal dan jam sibuk untuk 40 pelanggan seperti dapat dilihat di **Tabel 1** dan **Tabel 2**.

Tabel 1 Simulasi Antrian Indomaret Fresh Bitung di Jam Normal Menggunakan Excel

$\beta_{interarrival\ time}$	1.827	Menit/Pelanggan	α	21	M	512	$Z1_0$ 21
$\beta_{service\ time}$	0.752	Menit/Pelanggan	c	9			$Z2_0$ 77

i	Arrival To Indomart			Service Time			Simulation Logic						
	Stream 1	Random Number	Interarrival Time	Stream 1	Random Number	Service Time	Customer Number	Arrival Time	Begin Service Time	Service Time	Depature Time	Time Queque	Time In System
	$Z1_i$	$U1_i$	$X1_i$	$Z2_i$	$U2_i$	$X2_i$	1	2	3	4	5	6	7
0	21		Exp	77									
1	450	0.879	3.859	90	0.176	0.146	1	3.859	3.859	0.146	4.005	0	0.146
2	243	0.475	1.177	363	0.709	0.928	2	5.036	5.036	0.928	5.964	0	0.928
3	504	0.984	7.555	464	0.906	1.778	3	12.591	12.591	1.778	14.369	0	1.778
4	353	0.689	2.134	25	0.049	0.038	4	14.725	14.725	0.038	14.763	0	0.038
5	254	0.496	1.252	22	0.043	0.033	5	15.977	15.977	0.033	16.01	0	0.033
6	223	0.436	1.046	471	0.92	1.899	6	17.023	17.023	1.899	18.922	0	1.899
7	84	0.164	0.327	172	0.336	0.308	7	17.35	18.922	0.308	19.23	1.572	1.88
8	237	0.463	1.136	37	0.072	0.056	8	18.486	19.23	0.056	19.286	0.744	0.8
9	378	0.738	2.447	274	0.535	0.576	9	20.933	20.933	0.576	21.509	0	0.576
10	267	0.521	1.345	131	0.256	0.222	10	22.278	22.278	0.222	22.5	0	0.222

Tabel 2 Simulasi Antrian Indomaret Fresh Bitung di Jam Sibuk Menggunakan Excel

$\beta_{interarrival\ time}$	1.207	Menit/Pelanggan	α	21	M	512	$Z1_0$ 21
$\beta_{service\ time}$	0.871	Menit/Pelanggan	c	9			$Z2_0$ 77

i	Arrival To Indomart			Service Time			Indomart Logic						
	Stream 1	Random Number	Interarrival Time	Stream 1	Random Number	Service Time	Customer Number	Arrival Time	Begin Service Time	Service Time	Depature Time	Time Queque	Time In System
	$Z1_i$	$U1_i$	$X1_i$	$Z2_i$	$U2_i$	$X2_i$	1	2	3	4	5	6	7
0	21		Exp	77									
1	450	0.879	2.549	90	0.176	0.169	1	2.549	2.549	0.169	2.718	0	0.169
2	243	0.475	0.778	363	0.709	1.075	2	3.327	3.327	1.075	4.402	0	1.075
3	504	0.984	4.991	464	0.906	2.059	3	8.318	8.318	2.059	10.377	0	2.059
4	353	0.689	1.41	25	0.049	0.044	4	9.728	10.377	0.044	10.421	0.649	0.693
5	254	0.496	0.827	22	0.043	0.038	5	10.555	10.555	0.038	10.593	0	0.038
6	223	0.436	0.691	471	0.92	2.2	6	11.246	11.246	2.2	13.446	0	2.2
7	84	0.164	0.216	172	0.336	0.357	7	11.462	13.446	0.357	13.803	1.984	2.341
8	237	0.463	0.75	37	0.072	0.065	8	12.212	13.803	0.065	13.868	1.591	1.656
9	378	0.738	1.617	274	0.535	0.667	9	13.829	13.868	0.667	14.535	0.039	0.706
10	267	0.521	0.888	131	0.256	0.258	10	14.717	14.717	0.258	14.975	0	0.258

Pada jam sibuk, proses simulasi menghasilkan rata-rata waktu tunggu sebesar 0,769 menit, jauh lebih tinggi dibandingkan simulasi jam normal yang hanya mencapai 0,341 menit. Perbedaan ini terjadi akibat nilai rata-rata kedatangan yang lebih pendek pada jam sibuk (1,21 menit per pelanggan), sehingga jumlah permintaan layanan meningkat dan menambah antrian.

Sebaliknya, simulasi jam normal menunjukkan bahwa nilai waktu antar kedatangan yang lebih panjang (1,832 menit) menghasilkan beban kerja kasir yang lebih rendah. Hal ini menyebabkan waktu tunggu menurun dan persentase kasir menganggur meningkat hingga 62,5%. Tabel 3 menunjukan hasil simulasi secara keseluruhan.

Tabel 3 Hasil Simulasi Antrian Indomaret Fresh Bitung

	Hasil Simulasi		
	Jam Sibuk (sekitar jam 18:00)	Jam Normal (sekitar jam 21.00)	Gabungan Jam Sibuk & Normal
Rata-rata Waktu Antar Kedatangan	1.21	1.832	1.521
Rata-rata Waktu Pelayanan	0.782	0.675	0.729
Rata- rata Waktu Antri	0.769	0.341	0.473
Waktu Dalam Sistem	1.551	1.016	1.202
% Kasir Menganggur *(idle)*	40%	62.5%	50%
% Kasir Sibuk	60%	37.5%	50%

Hasil simulasi dengan memberikan pola yang konsisten dengan perilaku sistem antrian nyata: semakin pendek waktu antar kedatangan, semakin tinggi peluang terjadinya antrian. Hasil simulasi di

FaST - Jurnal Sains dan Teknologi, Vol.10, No. 1, Mei 2026
e-ISSN 2598-9596
DOI: https://doi.org/10.19166/fastjst.v10i1/10892
Available online at: https://ojs.uph.edu/index.php/FaSTJST/article/view/10892

jam sibuk menunjukkan bahwa sistem antrian Indomaret di jam sibuk cukup sibuk, dengan sekitar 60% pelanggan harus menunggu dan tingkat kesibukan kasir juga sekitar 60%. Meskipun demikian, waktu tunggu pelanggan tetap singkat, rata-rata hanya 0,77 menit. Waktu pelayanan cukup baik (0,782 menit), sehingga kasir bekerja cukup efisien. Secara keseluruhan, pelanggan menghabiskan sekitar 1.55 menit di dalam sistem, menunjukkan proses layanan yang cepat. Karena tingkat kedatangan lebih rendah dari kemampuan pelayanan, sistem berada dalam kondisi stabil dan tidak berpotensi menyebabkan antrian yang berlebihan. Di jam normal, sistem antrian berada pada kondisi ringan dengan tingkat pelanggan yang harus menunggu hanya 37,5%, menandakan kapasitas pelayanan masih optimal. Rata-rata waktu tunggu pelanggan hanya 0.341 menit, dan bagi pelanggan yang memang menunggu, durasinya tetap singkat yaitu sekitar 0,908 menit. Waktu pelayanan rata-rata (0,675 menit) sehingga kinerja server efisien. Secara keseluruhan, pelanggan hanya menghabiskan sekitar 1,016 menit di dalam sistem, sehingga proses pelayanan berjalan sangat cepat, tidak menimbulkan penumpukan antrian, dan server masih memiliki kapasitas cadangan untuk menghadapi peningkatan kedatangan pelanggan.

4. Kesimpulan

Berdasarkan hasil observasi lapangan dan pemodelan simulasi menggunakan *Linear Congruential Generator (LCG)* dan transformasi invers distribusi eksponensial, dapat disimpulkan bahwa kinerja sistem antrian sangat dipengaruhi oleh variasi waktu kedatangan pelanggan. Jam sibuk menunjukkan kondisi beban tertinggi, ditandai dengan rata-rata waktu antar kedatangan yang lebih pendek (1,21 menit) serta tingkat utilisasi server sebesar 60%. Kondisi ini menyebabkan meningkatnya waktu tunggu dalam antrian hingga 0,769 menit dan waktu total dalam sistem mencapai 1,551 menit. Hal tersebut menunjukkan bahwa pada jam sibuk, kasir beroperasi mendekati kapasitas optimalnya sehingga potensi penumpukan antrian lebih besar.

Sebaliknya, pada jam normal, waktu antar kedatangan lebih panjang (1,832 menit) sehingga beban kerja server jauh lebih rendah. Hal ini berdampak pada menurunnya waktu tunggu menjadi 0,341 menit dan meningkatnya *idle server* hingga 62,5%. Kondisi ini menggambarkan bahwa kapasitas layanan lebih dari cukup untuk menangani permintaan pada jam normal.

Pada simulasi data gabungan, nilai performansi berada di antara kedua kondisi tersebut, dengan utilisasi 50%, waktu tunggu 0,473 menit, dan waktu total dalam sistem 1,202 menit. Hasil ini menunjukkan bahwa rata-rata operasional harian berada pada kondisi stabil tanpa indikasi kelebihan beban.

Penelitian ini memiliki keterbatasan dalam hal pengambilan data dilakukan pada sebanyak 107 observasi pada bulan Agustus sampai November 2025 sehingga distribusi kedatangan maupun pelayanan hanya merefleksikan distribusi pada periode tersebut. Secara keseluruhan, penelitian ini membuktikan bahwa semakin pendek waktu antar kedatangan, semakin tinggi potensi terjadinya antrian, yang sepenuhnya konsisten dengan teori dasar antrian. Metode generasi bilangan acak menggunakan LCG dan transformasi invers eksponensial di dalam simulasi menunjukan bahwa pelayanan Indomaret Fresh Bitung masih di dalam kapasitas yang sesuai dengan waktu antar kedatangan dan operasional pelayanan pelanggan efisien. Penelitian ini juga menegaskan pentingnya pengaturan sumber daya pada jam sibuk untuk meminimalkan waktu tunggu pelanggan, misalnya melalui penambahan kapasitas layanan secara fleksibel atau manajemen distribusi beban *server* di jam sibuk atau ketika terjadinya antrian panjang untuk meningkatkan kualitas pelayanan dan kepuasan pelanggan.

Daftar Pustaka

[1] D. Meliana, J. Riswati, and D. Astuti, “Analisis Perkembangan Bisnis Ritel di Indonesia,” *Journal of Business Economics and Management*, vol. 01, pp. 235–243, 2025.
[2] G. Darmawan, A. P. Sari, A. Hudzaifa, et al., Efisiensi Operasional dengan ProModel: Panduan Teori Antrian. Kaizen Media Publishing, Des. 2023.
[3] M. Arianto, Efektivitas Sistem Antrian Layanan Kasir (Studi Kasus pada Toko Retail ABC di Bandung) – Dalam Bentuk Buku Karya Ilmiah, 2024. [Online]. Available: repositori Telkom University. Diakses: 6 Feb 2026.
[4] “Indomaret Fresh Bitung Ulasan,” Google Search. [Online]. Available: Google Search – Indomaret Fresh Bitung Ulasan. Diakses: 6 Feb 2026.

[5] W. J. Hopp, "Single Server Queueing Models," in *Building Intuition: Insights from Basic Operations Management Models and Principles*, T. J. Chhajed Dilip and Lowe, Ed., Boston, MA: Springer US, 2008, pp. 51–79. https://doi.org/10.1007/978-0-387-73699-0_4
[6] B. L. V Bataona, A. E. L. Nyoko, and N. P. Nursiani, "Analisis Sistem Antrian dalam Optimalisasi Layanan di Supermarket Hyperstore," *Journal of Management: Small and Medium Enterprises (SMEs)*, vol. 12, no. 2, pp. 225–237, Sep. 2020, https://doi.org/10.35508/jom.v12i2.2695
[7] I. C. B. C. Chan, M. S. Paendong, and T. Manurung, "Analisis Antrian pada 'Supermarket Cool' Tomohon Menggunakan Teori Antrian untuk Menentukan Pelayanan yang Optimal," *d'Cartesian*, vol. 12, no. 1, pp. 26–34, Jun. 2023, https://doi.org/10.35799/dc.12.1.2023.48046
[8] L. D. Dhae, D. J. Aquilan, I. G. A. S. Deviyanti, and P. E. Yuliana, "Analisis Antrian dengan Model Single Channel Single Phase: Studi Kasus Supermarket Ngagel," *Jurnal Teknik Industri Terintegrasi (JUTIN)*, vol. 9, no. 1, pp. 1042–1047, Jan. 2026, https://doi.org/10.31004/jutin.v9i1.55305.
[9] Q. U. N. Liu and H. Chen, "Optimization of J supermarket cashier service system based on M/M/c model," *ACM International Conference Proceeding Series*, pp. 478–484, Apr. 2022, https://doi.org/10.1145/3535782.3535846
[10] D. Mardiati, "Simulasi Monte Carlo dalam Memprediksi Tingkat Lonjakan Penumpang," 2020, https://doi.org/10.37034/infeb.vi0.49
[11] K. Daramola, Abubakar Yahaya, and Umar Kabir Abdullahi, "Evaluating Single and Multi-Server Exponential Queuing Models: A Case Study of Access Bank PLC in Anyigba, Kogi State, Nigeria," *Malaysian Journal of Science and Advanced Technology*, pp. 482–488, Nov. 2024, https://doi.org/10.56532/mjsat.v4i4.360
[12] F. S. Hillier and G. J. Lieberman, *Introduction to Operations Research*, Seventh edition. in McGraw-Hill Series in Industrial Engineering and Management Science. Boston: McGraw-Hill, 2001.
[13] C. Heumann, Michael, and S. Shalabh, *Introduction to Statistics and Data Analysis Introduction to Statistics and Data Analysis Introduction to Statistics and Data Analysis*. South Africa: Springer, 2016. https://doi.org/10.1007/978-3-319-46162-5
[14] A. M. Law, *Simulation modeling and analysis*. McGraw-Hill Education, 2015.
[15] "Membangkitkan Bilangan Acak Metode Linear Congruential Generator (LCG)," HMJ Statistika FMIPA UNM. Diakses: 6 Feb 2026.
[16] C. Harrell, B. K. Ghosh, and R. Bowden, *Simulation Using ProModel*. New York, NY, USA: McGraw-Hill/Higher Education, 2004.

FaST - Jurnal Sains dan Teknologi, Vol.10, No. 1, Mei 2026
e-ISSN 2598-9596
DOI: https://doi.org/10.19166/fastjst.v10i1/10897
Available online at: https://ojs.uph.edu/index.php/FaSTJST/article/view/10897

Design of a Two-Point Temperature Monitoring System on a Heating Medium Based on Arduino Mega 2560 and IoT

Nataly Wisnu Anggara*1), Mario Gracio Anduinta Rhizma1)
[1]Electrical Engineering Study Program, Universitas Pelita Harapan, Tangerang, Indonesia

ABSTRACT

This research aims to design a two-point temperature monitoring system using 2 DS18B20 sensors on a heating medium using DS18B20 sensors controlled by an Arduino Mega 2560 and integrated with Internet of Things (IoT) technology. The measured data are processed by the microcontroller and transmitted via the ESP8266 module to the Firebase platform, then displayed on a smartphone application and recorded as historical data. The experimental results show that the DS18B20 sensors are able to read temperature changes linearly within the tested temperature range of approximately 27°C to 67°C and can follow the temperature increase trend of the heating medium. To improve measurement accuracy, calibration was performed using a linear regression method with a surface thermocouple as the reference instrument. After calibration, the measurement error was significantly reduced to 2.90% at the upper measurement point and 2.66% at the lower measurement point, indicating that the system is more representative for monitoring temperature changes at two measurement locations. The proposed demonstrates decent performance as an IoT-based temperature monitoring prototype, making it suitable for small-scale heating applications and educational purposes.

ARTICLE INFO

Keywords: Arduino Mega 2560, Firebase, IoT, DS18B20 thermocouple sensor, prototype

*** Corresponding author**:
mario.rhizma@uph.edu

Article history:
Submitted 11 Feb 2026
Revised 2 May 2026
Accepted 7 May 2026
Online Available 7 May 2026
Published 20 May 2026

1. Introduction

Rapid technological advancement has driven industrial systems to shift from conventional manual operations toward automated and more efficient processes. In manufacturing industries, process stability, particularly temperature control, plays a critical role in maintaining product quality and reducing defects.

Research on temperature monitoring using microcontrollers [1-3] has been extensively conducted, employing devices such as the AT89C51 [4], Arduino Uno [5-6], and Arduino Mega [7-9]. This study focuses on the use of an Arduino Mega in a two-point temperature monitoring system. The dual-sensor temperature control method can be applied in various contexts [10]; in this prototype project, it is specifically would be implemented to monitor the heating medium temperature in the production process of automotive components, specifically in the Am-Tube curing section.

In the curing process of automotive components, temperature deviation can significantly affect mechanical properties and product reliability. Conventional monitoring methods often rely on indirect parameters or manual measuring, which are unable to represent real-time temperature conditions during machine operation. This limitation increases the risk of undetected process deviations. Therefore, this study proposes the development of a real time temperature monitoring and alarm system based on Internet of Things (IoT) technology.

The use of IoT technologies for monitoring temperatures in enclosed spaces and environmental conditions has been widely explored [11-12]. Likewise, the DS18B20 temperature sensor has been extensively utilized for temperature measurements in various applications [13-17]. The proposed system is expected to improve process visibility, reduce measurement errors, and support data-driven evaluation of temperature stability.

2. System Framework and Research Methodology

2.1 System Overview

The proposed system is designed as an IoT-based temperature monitoring platform consisting of sensing, processing, communication, and visualization layers as shown on **Figure 1**.

FaST - Jurnal Sains dan Teknologi, Vol.10, No. 1, Mei 2026
e-ISSN 2598-9596
DOI: https://doi.org/10.19166/fastjst.v10i1/10897
Available online at: https://ojs.uph.edu/index.php/FaSTJST/article/view/10897

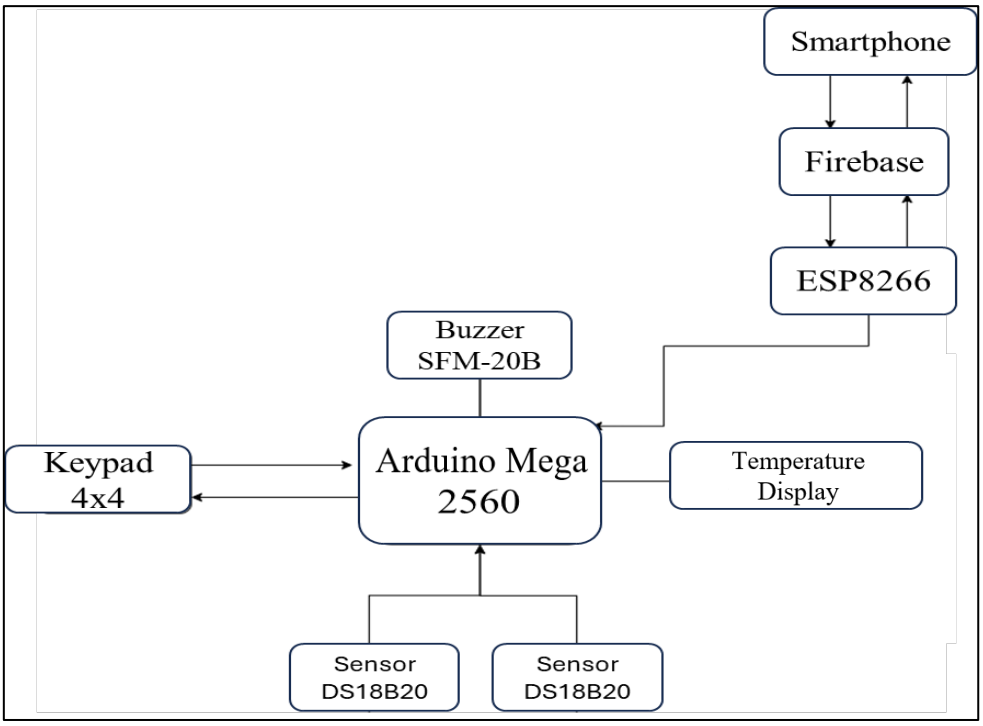

Figure 1 Block diagram of IoT-based temperature monitoring system

Temperature data are acquired using digital sensors, processed by a microcontroller, transmitted through a wireless module, and displayed in real time via mobile application and cloud database. As shown on **Figure 2**, the keypad functions to provide commands to the LCD in accordance with predefined settings. In this study, the commands configured in the operating system are as follows:

1. Button A displays the actual temperature of the upper and lower sensors.
2. Button B displays the Top Mold parameters.
3. Button C displays the Bottom Mold parameters.
4. Button D displays the Alarm parameters (continuous flip-flop mode).
5. The "#" button functions to reset the alarm. After the keypad is pressed, a display appears prompting the user to enter the reset code, which is 0000.

The buzzer functions as an alarm when the temperature exceeds the predetermined threshold, while the actual measured temperature is displayed on 20x4 LCD Display, and also on user smartphone.

Figure 2 20x4 LCD Display with keypad for display commands

FaST - Jurnal Sains dan Teknologi, Vol.10, No. 1, Mei 2026
e-ISSN 2598-9596
DOI: https://doi.org/10.19166/fastjst.v10i1/10897
Available online at: https://ojs.uph.edu/index.php/FaSTJST/article/view/10897

2.2 Hardware Configuration

Table 1 Hardware components specification

No.	Components	Detail
1.	Computer	Windows 10, Intel Core i5, RAM 16GB, SSD 512 GB
2.	Arduino Module	ATmega 2560
3.	Thermocouple Module	MAX6675
4.	Wi-Fi Module	ESP8266
5.	Relay	
6.	Keypad	4x4
7.	Temperature Sensor	DS18B20
8.	Buzzer	SFM-20B
9.	LCD	20 x 4
10.	Smartphone	Android Operating System
11.	Android Software	Kodular

The hardware system consists of DS18B20 digital temperature sensors for temperature measurement, an Arduino Mega 2560 as the main processing unit, and an ESP8266 Wi-Fi module for data transmission. The sensors provide digital temperature readings, which are periodically processed by the microcontroller before being sent to the cloud database. The relays are used to control external loads such as system cooling fans or warning indicator lights.

2.3 Software Architecture

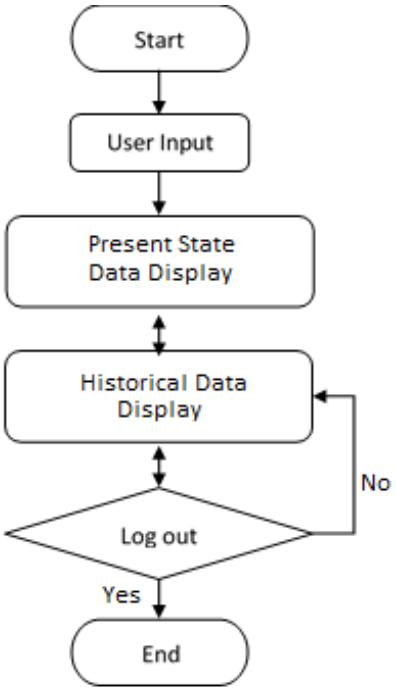

Figure 3 Flowchart of temperature monitoring and alarm system

The flowchart of software architecture is shown on **Figure 3**. The software system includes firmware developed using Arduino IDE, a Firebase Realtime Database for cloud-based data storage, and a mobile application developed using Kodular as the user interface. Google Spreadsheets is utilized for historical data logging and further analysis. The application allows users to monitor temperature conditions in real time and review historical data remotely.

2.4 Temperature Measurement and Calibration Method

Temperature readings obtained from the DS18B20 sensors are initially treated as raw data. To improve measurement accuracy, a calibration process is applied using linear regression with a thermocouple

FaST - Jurnal Sains dan Teknologi, Vol.10, No. 1, Mei 2026
e-ISSN 2598-9596
DOI: https://doi.org/10.19166/fastjst.v10i1/10897
Available online at: https://ojs.uph.edu/index.php/FaSTJST/article/view/10897

surface sensor as the reference instrument. The calibration equation is expressed as:

$$T = aX + b \tag{1}$$

where **X** represents the raw sensor reading, and **a** and **b** are regression coefficients obtained from experimental data. The calibrated temperature values are then used for monitoring, alarm triggering, and data logging.

3. Results and Discussion

3.1 Real-Time Monitoring Performance

The developed system demonstrates the capability to display temperature data in real time through a mobile application interface, as shown on **Figure 4**. Data transmission from the microcontroller to the cloud database occurs continuously during system operation, enabling users to monitor temperature conditions remotely. This feature provides better visibility of temperature behavior compared to manual measurement methods, which only capture data at specific moments. The real-time monitoring capability allows early detection of abnormal temperature conditions, supporting faster decision-making and improving overall system reliability.

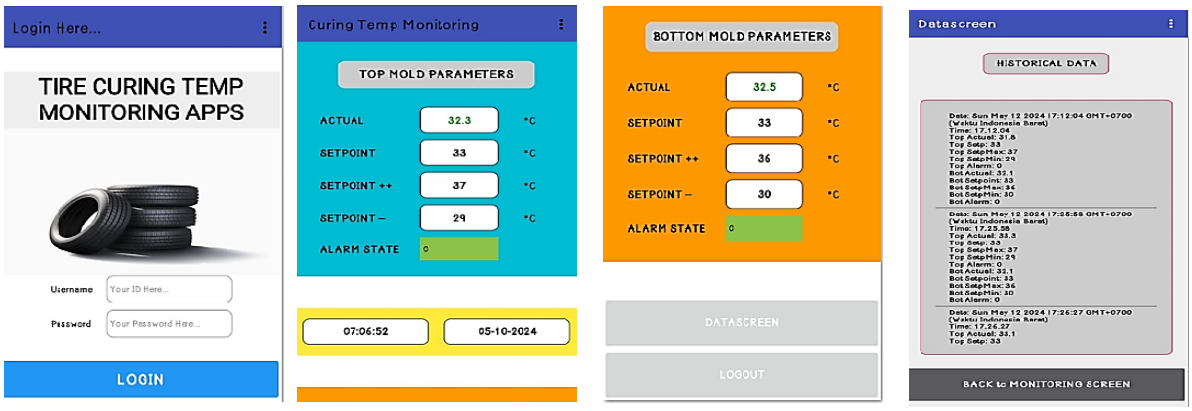

Figure 4 Mobile application interface for real-time temperature monitoring

3.2 Temperature Measurement Results Before Calibration

The initial measurement results indicate discrepancies between the temperature values measured by the DS18B20 sensors and the thermocouple surface reference. These differences are observed throughout the measurement duration and become more pronounced during periods of rapid temperature change.

The deviation is mainly caused by differences in sensor response characteristics and measurement principles. The DS18B20 sensor exhibits a slower response compared to the thermocouple surface, resulting in lag during dynamic temperature variations. This initial measurement is shown on **Figure 4**.

3.3 Error Analysis Before Calibration

In this experiment, the test medium for sensor accuracy testing consisted of an aluminium plate heated using a heat source. Two DS18B20 sensors were attached to the aluminium surface using aluminium foil to ensure adequate thermal contact, and were positioned adjacent to a surface thermocouple used as the reference measurement instrument. The two sensors were positioned approximately 5 cm apart, and the data were sampled at 1 second intervals for 200 datasets. The test was conducted to compare the readings of the DS18B20 sensors with the surface thermocouple, as well as to evaluate the system's accuracy before and after calibration.

Error analysis before calibration shows relatively high percentage errors for both upper and lower sensor readings. The highest error values occur at the beginning of the measurement process, where temperature changes rapidly. In this condition, small absolute differences between sensor readings and reference values can lead to large percentage errors. These results is displayed on **Figure 5**, confirm that

FaST - Jurnal Sains dan Teknologi, Vol.10, No. 1, Mei 2026
e-ISSN 2598-9596
DOI: https://doi.org/10.19166/fastjst.v10i1/10897
Available online at: https://ojs.uph.edu/index.php/FaSTJST/article/view/10897

raw DS18B20 sensor data are not sufficiently accurate for applications requiring precise temperature measurement without calibration. The R^2 coefficient for upper sensor is 0.964, and 0.968 for lower sensor. The two sensors show a strong linear relationship with time, but the average error of the upper sensor reached **6.05%**, while the lower sensor showed an average error of **5.35%**. This error must be improved for better accuracy.

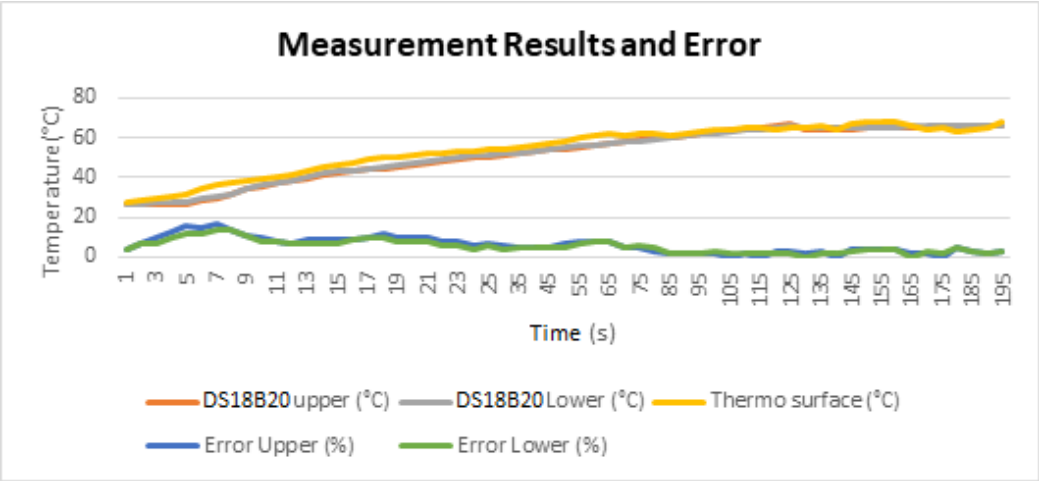

Figure 5 Temperature measurement results before calibration

3.4 Results After Linear Regression Calibration

After applying linear regression calibration, the corrected temperature values show improved agreement with the thermocouple surface reference. The calibration process reduces systematic deviations by adjusting raw sensor readings using regression coefficients obtained from experimental data.

Based on the results, the average measurement error decreases significantly after calibration, as shown on **Figure 6**. This reduction indicates that the linear regression method effectively enhances the accuracy of the temperature monitoring system.

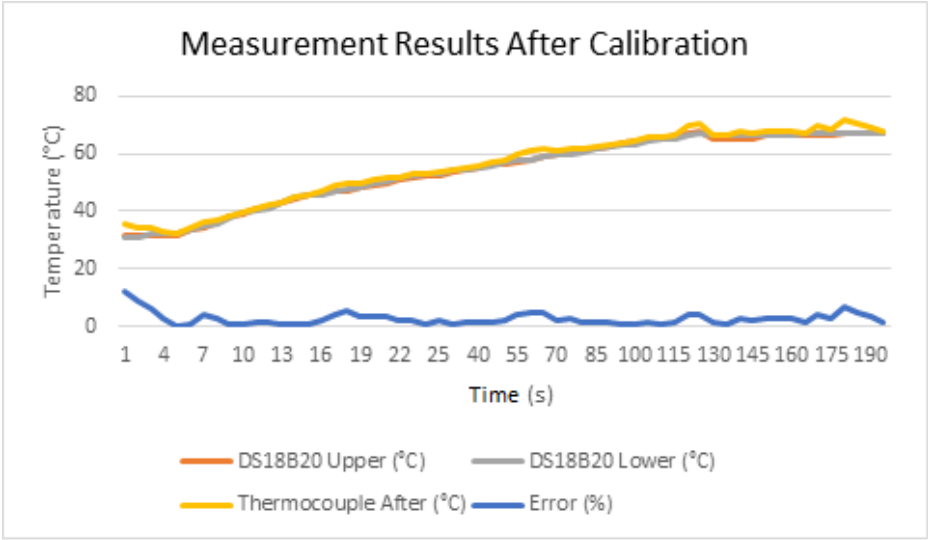

Figure 6 Temperature and error results after linear regression calibration

The R^2 coefficient improved for the two sensors, the R^2 of the upper sensor is 0.982, and 0.984 for lower sensor. The average error of the upper sensor decreased to **2.90%**, while the lower sensor error was reduced to **2.66%**.

3.5 Discussion

The experimental results demonstrate that calibration is essential when using general-purpose digital

temperature sensors for monitoring applications that require higher accuracy. Although the DS18B20 sensor is not specifically designed for surface temperature measurement, linear regression calibration significantly improves its measurement performance.

However, minor discrepancies remain during rapid temperature transitions due to the inherent response characteristics of the sensor. For industrial-scale implementation requiring fast response and high accuracy, industrial-grade sensors such as thermocouples are recommended.

The subsequent temperature readings are transmitted via the ESP8266 module to a Firebase database and displayed in a monitoring application developed using Kodular. The data transmission process operates periodically at 1 second interval, enabling users to monitor temperature variations in real time through a smartphone.

4. Conclusion

This study has successfully developed a prototype of an IoT-based temperature monitoring and alarm system capable of providing real-time temperature data through a mobile application. The integration of digital temperature sensors, a microcontroller platform, cloud database, and mobile interface enable continuous monitoring and remote access to temperature information. The experiment results indicate that the uncalibrated DS18B20 sensors exhibit relatively high measurement errors when compared to the thermocouple surface reference. Before calibration, the average error of the upper sensor reached **6.05%**, while the lower sensor showed an average error of **5.35%**. These results confirm that direct sensor readings are not sufficient for applications requiring higher accuracy.

After applying linear regression calibration, a significant improvement in measurement accuracy was achieved. The average error of the upper sensor decreased to **2.90%**, while the lower sensor error was reduced to **2.66%**. This reduction demonstrates that the proposed calibration method minimizes systematic measurement deviations and enhances the reliability of the monitoring system.

Although minor discrepancies remain during rapid temperature changes due to inherent sensor response characteristics, the developed system is suitable as a prototype IoT-based monitoring solution. Further improvements can be achieved by employing industrial-grade sensors and control devices for implementation in real industrial environments.

Acknowledgement

The author would like to express gratitude to Universitas Pelita Harapan for the academic support provided during this research. Appreciation is also extended to all parties who contributed to the completion of this study through technical assistance, guidance, and constructive feedback.

References

[1] B. Li and J.H. Lei, "Design of Industrial Temperature Monitoring System Based on Single Chip Microcontroller," *2011 International Conference on Computer Science and Service System (CSSS)*, Nanjing, 2011, pp. 342-344, https://doi.org/10.1109/CSSS.2011.5974595.

[2] S. Ponnusamy, R. Samikannu, B. A. Tlhabologo, W. Ullah and S. Murugesan, “Design and Development of Microcontroller-Based Temperature Monitoring and Control System for Power Plant Generators,” *IOP Conference Series: Materials Science and Engineering*, Volume 1055, International Virtual Conference on Robotics, Automation, Intelligent Systems and Energy (IVC RAISE 2020) 15th December 2020, Erode, India https://doi.org/10.1088/1757-899X/1055/1/012158

[3] D. K. Fisher, H. Kebede, “A Low-Cost Microcontroller-Based System to Monitor Crop Temperature and Water Status,” *Computers and Electronics in Agriculture*, Volume 74, Issue 1, 2010, Pages 168-173, ISSN 0168-1699, https://doi.org/10.1016/j.compag.2010.07.006.

[4] H. Zhu and L. Bai, "Temperature Monitoring System Based on AT89C51 Microcontroller," *2009 IEEE International Symposium on IT in Medicine & Education*, Jinan, China, 2009, pp. 316-320, https://doi.org/10.1109/ITIME.2009.5236408.

[5] K.K. Khaing, K. S. Raju, G.R. Sinha, W.Y. Swe, “Automatic Temperature Control System Using Arduino,” *Proceedings of the Third International Conference on Computational Intelligence and Informatics*, 2020, Advances in Intelligent Systems and Computing, vol 1090. Springer, Singapore. https://doi.org/10.1007/978-981-15-1480-7_18

[6] J. Hubbart, T. Link, C. Campbell, and D. Cobos, "Evaluation of a Low-Cost Temperature Measurement System for Environmental Applications," 2005, *Hydrological Processes* Vol. 19 Issue 7: 1517-1523. https://doi.org/10.1002/hyp.5861

[7] A. Indriani, Hendra, and Y. Witanto, "Error of Assembly Microcontroller Arduino Mega and ATmega in the Control of Temperature for Heating and Cooling System," *AMM*, vol. 842, pp. 324–328, Jun. 2016, https://doi.org/10.4028/www.scientific.net/amm.842.324.

[8] P. Megantoro, A. A. Bagus, H. F. A. Kusuma, S. A. Reina, M. Fadhilah, "Automation System of Temperature Calibrator for Room Thermostat Using Arduino Mega256," *Proceedings of the International Conference on Advanced Technology and Multidiscipline (ICATAM 2024)*, 2024. https://doi.org/10.2991/978-94-6463-566-9_14

[9] M. K. Fadzly, Yiling, M. F. Rosli, T. Amarul and M. S. M. Effendi, "Smart Air Quality Monitoring System Using Arduino Mega," *Materials Science and Engineering*, Volume 864, 2nd Joint Conference on Green Engineering Technology & Applied Computing 2020 4-5 February 2020, Bangkok, Thailand. https://doi.org/10.1088/1757-899X/864/1/012215

[10] X. Gao, Q. Ma, X. Sun, J. Wang and S. Li, "Research on a Dual-Closed-Loop Temperature Control Method and System Based on Dual Sensors for Infrared Object Simulation," *IEEE Sensors Journal*, vol. 19, no. 23, pp. 11553-11561, 1 Dec.1, 2019, https://doi.org/10.1109/JSEN.2019.2935555.

[11] M. A. Muslim, R. A. Setyawan, A. Basuki, A. A. Razak, F. P. Hario and E. Fernando, "IOT Based Climate Monitoring System," *Earth and Environmental Science*, *Volume 746, 3rd International Conference on Life and Applied Sciences for Sustainable Rural Development (ICLAS-SURE 2020)*, November 18-19, 2020 Central Java, Indonesia. https://doi.org/10.1088/1755-1315/746/1/012044

[12] R. F. Maulana, M. A. Ramadhan, W. Maharani and M. I. Maulana, "Rancang Bangun Sistem Monitoring Suhu dan Kelembapan Berbasis IOT Studi Kasus Ruang Server ITTelkom Surabaya," *Indonesian Journal of Multidisciplinary on Social and Technology*, 2023, 1(3), 224–231. https://doi.org/10.31004/ijmst.v1i3.169

[13] R. Saha, S. Biswas, S. Sarmah, S. Karmakar and P. Das, "A Working Prototype Using DS18B20 Temperature Sensor and Arduino for Health Monitoring," *SN Computer Science Vol.2*, article number 33, 2021. https://doi.org/10.1007/s42979-020-00434-2

[14] Y. X. Wu, D. Liu, and X. H. Kuang, "A Temperature Detecting System Based on DS18B20," *Advanced Materials Research*, vol. 328–330, pp. 1806–1809, Sept. 2011, https://doi.org/10.4028/www.scientific.net/amr.328-330.1806.

[15] R. A. Koestoer, Y. A. Saleh, I. Roihan, Harinaldi, "A Simple Method for Calibration of Temperature Sensor DS18B20 Waterproof in Oil Bath Based on Arduino Data Acquisition System," *AIP Conference Proceedings,* 25 January 2019; 2062 (1): 020006. https://doi.org/10.1063/1.5086553

[16] S. Budijono and Felita, "Smart Temperature Monitoring System Using ESP32 and DS18B20," *Earth and Environmental Science, Volume 794, 4th International Conference on Eco Engineering Development*, 10-11 November 2020, Banten, Indonesia, https://doi.org/10.1088/1755-1315/794/1/012125

[17] A. N. Fathoni, N. Hudallah, R. D. M. Putri, K. Khotimah, T. Rijanto and M. Ma'arif, "Design Automatic Dispenser for Blind People based on Arduino Mega using DS18B20 Temperature Sensor," *2020 Third International Conference on Vocational Education and Electrical Engineering (ICVEE)*, Surabaya, Indonesia, 2020, pp. 1-5, https://doi.org/10.1109/ICVEE50212.2020.9243254

FaST - Jurnal Sains dan Teknologi, Vol.10, No. 1, Mei 2026
e-ISSN 2598-9596
DOI: https://doi.org/10.19166/fastjst.v10i1/10492
Available online at: https://ojs.uph.edu/index.php/FaSTJST/article/view/10492

Asesmen Kualitas RTH Publik Menggunakan Indeks Vegetasi di Taman Hutan Raya Ir. H. Djuanda Kota Bandung

Raden Muhammad Alwan Faris Fadlirullah[1)], Adytia Heru Nugraha[1)],
Ammar Muhammad Nabil[1)], Yulia Asyiawati[1*)]

[1]Perencanaan Wilayah dan Kota Universitas Islam Bandung, Bandung, Indonesia

ABSTRACT

Urban forest ecosystems are increasingly subject to significant anthropogenic pressures; however, the resulting ecological responses often exhibit a delayed manifestation. The Ir. H. Djuanda Forest Park (Tahura) serves as a vital urban conservation area in Bandung, Indonesia, which has experienced a massive surge in tourist volume. This study aims to analyze the "lag effect" of visitor pressure on vegetation quality dynamics over the 2015–2025 period. A descriptive quantitative approach was employed, integrating spatial analysis via Google Earth Engine (GEE) to extract Normalized Difference Vegetation Index (NDVI) values from Sentinel-2A satellite imagery. Statistical analyses, including Spearman correlation and linear regression, were conducted with time-lag intervals ranging from 0 to 5 years to identify the relationship between annual visitor numbers and the extent of high-density vegetation. The findings reveal no significant correlation at lag 0 ($\rho = -0.12$; $p > 0.05$). Conversely, a significant negative correlation emerged at lag 3 ($\rho = -0.61$; $p < 0.05$) and reached its peak at lag 5 ($\rho = -0.78$; $p < 0.01$). These results demonstrate a threshold of vegetation resistance, where physical degradation only becomes spectrally manifest after several years of cumulative disturbance. This study recommends the implementation of visitor management policies based on environmental carrying capacity that incorporate temporal variables to ensure the long-term sustainability of the Tahura Ir. H. Djuanda ecosystem.

ARTICLE INFO

Keywords: Anthropogenic Pressure, Delayed Response (Lag Effect), Google Earth Engine, NDVI, Vegetation Dynamics

***Corresponding author**:
yulia.asyiawati@unisba.ac.id

Article history:
Submitted 5 Feb 2026
Revised 25 Apr 2026
Accepted 7 May 2026
Online Available 7 May 2026
Published 20 May 2026

1. Pendahuluan

Urbanisasi menyebabkan pergeseran penggunaan lahan yang signifikan, hilangnya keanekaragaman hayati, dan fragmentasi ekologis. Hal ini juga memberikan kontribusi pada berbagai bentuk polusi dan memperburuk dampak perubahan iklim, terutama efek panas perkotaan [1]. Urbanisasi merupakan salah satu fenomena transformasi sosial-ekonomi terbesar di era modern yang membawa implikasi signifikan terhadap lingkungan perkotaan. Pertumbuhan kota yang pesat, didorong oleh peningkatan populasi, industrialisasi, dan ekspansi penggunaan lahan, telah menyebabkan perubahan mendasar pada sistem ekologis perkotaan [1], [2]. Perubahan tutupan lahan dan fragmentasi habitat akibat tekanan antropogenik ini berisiko menurunkan kemampuan ekosistem dalam menyimpan stok karbon dan mengancam keragaman flora endemik yang menjadi identitas kawasan [3]. Ruang Terbuka Hijau (RTH), khususnya dalam bentuk hutan kota, bukan sekadar pelengkap estetika kota, melainkan komponen esensial dalam menjaga keseimbangan ekologis melalui penyediaan jasa ekosistem (*ecosystem services*) yang komprehensif. Jasa ini mencakup fungsi regulasi iklim mikro, pendukung biodiversitas, penyediaan sumber daya, hingga fungsi budaya melalui rekreasi spiritual dan edukasi [4], [5]. Secara spesifik, keberadaan kanopi pohon yang rapat berperan vital dalam memitigasi efek *Urban Heat Island* (UHI) dengan menurunkan suhu permukaan melalui proses evapotranspirasi dan peneduhan [6].

Di Indonesia, fenomena degradasi kualitas lingkungan perkotaan semakin nyata, termasuk di Kota Bandung yang kini menghadapi tantangan serius akibat pemanasan lokal dan penurunan kualitas udara. Sebagai pusat aktivitas ekonomi di Jawa Barat, Kota Bandung mengalami tekanan pembangunan yang mengakibatkan sulitnya pemenuhan kuantitas RTH sesuai amanat regulasi tata ruang [7], sehingga memberikan dampak pada degradasi ekosistem alami dan hilangnya keanekaragaman hayati secara progresif. Salah satu Ruang Terbuka Hijau publik yang terdapat di Kota Bandung adalah Taman Hutan Raya (Tahura) Ir. H. Djuanda berfungsi sebagai “paru-paru kota" yang dapat memitigasi efek pemanasan global melalui proses sekuestrasi karbon yang signifikan [8], sehingga dapat menjaga resiliensi ekologi

FaST - Jurnal Sains dan Teknologi, Vol.10, No. 1, Mei 2026
e-ISSN 2598-9596
DOI: https://doi.org/10.19166/fastjst.v10i1/10492
Available online at: https://ojs.uph.edu/index.php/FaSTJST/article/view/10492

kota dan menyediakan layanan ekosistem vital bagi masyarakat [9]. Keberadaan struktur vegetasi yang sehat dan padat dalam sistem ini merupakan indikator utama keberhasilan pengelolaan lingkungan perkotaan yang adaptif terhadap perubahan iklim [9]. Tahura Djuanda diharapkan mampu mempertahankan integritas vegetasi yang tinggi untuk menjalankan fungsi hidrologis dan perlindungan tanah, sembari memberikan layanan jasa ekosistem budaya berupa rekreasi alam yang berkelanjutan bagi masyarakat [10].

Fakta empiris di lapangan menunjukkan adanya potensi benturan kepentingan yang signifikan antara fungsi konservasi dengan dan intensitas kegiatan manusia, terutama pasca-pandemi, di mana kebutuhan masyarakat akan interaksi langsung dengan lingkungan hijau (biophilia) meningkat untuk melakukan atraksi wisata alam, termasuk di Tahura Djuanda Tingginya minat masyarakat terhadap wisata alam di Tahura Djuanda membawa konsekuensi pada tekanan lingkungan [11]. Peningkatan jumlah wisatawan yang tidak diimbangi dengan manajemen daya dukung (*carrying capacity*) dapat memicu fragmentasi habitat, pemadatan tanah, dan penurunan vitalitas vegetasi [12]. Degradasi kualitas vegetasi dan reduksi tutupan hijau di kawasan urban secara empiris memberikan implikasi sosio-ekologis yang signifikan, yang mencakup penurunan indeks kenyamanan publik serta pengikisan identitas visual lanskap kota [13]. Dari penelitian yang sudah dilakukan sebelumnya mengindikasikan bahwa kondisi ekologis mayoritas hutan kota (RTH) di Kota Bandung masih berada di bawah standar baku, baik dari aspek densitas vegetasi maupun diversitas spesiesnya [7]. Hal ini dapat dilihat dari kondisi Tahura Djuanda dengan luas 527,03 ha mengalami tekanan sosio-ekologis yang dapat mengancam keberlanjutan fungsi lingkungannya. Intervensi manusia, yang termanifestasi melalui ekspansi jalur setapak ilegal dan pemadatan tanah, teridentifikasi memicu fragmentasi spasial dan mendegradasi kualitas kesehatan vegetasi di kawasan tersebut [14].

Celah riset saat ini berakar pada minimnya kerangka monitoring yang mensinergikan data biofisik dengan tekanan antropogenik secara spasial menjadi celah pengetahuan utama dalam studi ini. Hal tersebut terefleksi dari kurangnya literatur yang mengevaluasi secara spasial mengenai dampak dinamika kunjungan wisatawan terhadap kesehatan vegetasi di Tahura Ir. H. Djuanda. Studi mengenai Tahura Ir. H. Djuanda hingga kini umumnya terbatas pada inventarisasi stok karbon pada tipe tegakan tertentu [8] maupun kajian deskriptif mengenai manajemen pariwisata [11]. Belum ditemukan penelitian komprehensif yang secara khusus mengaplikasikan teknologi penginderaan jauh untuk mengidentifikasi pola hubungan antara intensitas kunjungan wisatawan dan penurunan kualitas hijau secara longitudinal (*time-series*). Meskipun pemetaan kerapatan vegetasi telah banyak menerapkan teknik Forest Canopy Density (FCD) [12], indeks Normalized Difference Vegetation Index (NDVI) memiliki sensitivitas yang lebih tinggi dalam mendeteksi respons klorofil terhadap tekanan lingkungan. Fakta mengenai fluktuasi puncak wisatawan pada periode tertentu memang telah tersedia [15], namun bagaimana fenomena ini berimplikasi pada degradasi vegetasi secara temporal belum tereksplorasi secara mendalam melalui integrasi data penginderaan jauh. Melalui analisis respons spektral klorofil, Normalized Difference Vegetation Index (NDVI) dapat menghasilkan akurasi signifikan dalam mendeteksi gejala stres vegetasi secara preventif, sehingga dapat mengidentifikasi dan memantau kondisi kesehatan tanaman sebelum terjadinya degradasi fisik yang tampak secara visual [16].

Penelitian ini didorong oleh kekhawatiran atas penurunan kualitas vegetasi Tahura yang berdampak luas terhadap ekosistem Kota Bandung. Mengacu pada korelasi signifikan antara kerapatan vegetasi berbasis NDVI dan cadangan karbon [8], degradasi vegetasi akibat aktivitas wisatawan berisiko menurunkan efektivitas mitigasi polusi dan pengaturan suhu lingkungan secara langsung. Dengan demikian, sinkronisasi antara data kunjungan dan kondisi biofisik lahan melalui asesmen berkala menjadi instrumen navigasi kebijakan yang sangat relevan dalam menjaga resiliensi ekosistem perkotaan [17]. Topik ini sangat relevan mengingat urgensi pencapaian target SDG 11 terkait pembangunan kota berkelanjutan [18], [19]. Ketidakmampuan dalam mengawasi kesehatan vegetasi di objek konservasi seperti Tahura Djuanda akan memperkuat kerentanan iklim urban serta menurunkan standar kualitas hidup akibat hilangnya fungsi penyaringan polutan alami [13]. Konsekuensinya, asesmen berbasis bukti ilmiah diperlukan untuk mensinergikan orientasi ekonomi pariwisata dengan prinsip keberlanjutan ekosistem.

Distingsi fundamental penelitian ini dibandingkan dengan kajian terdahulu terletak pada pemosisian variabel antropogenik, khususnya densitas wisatawan yang berfungsi sebagai determinan utama dalam pemodelan nilai Normalized Difference Vegetation Index (NDVI) di kawasan Taman Hutan Raya (Tahura). Studi ini melampaui sekadar pemetaan kondisi eksis dengan memformulasikan

FaST - Jurnal Sains dan Teknologi, Vol.10, No. 1, Mei 2026
e-ISSN 2598-9596
DOI: https://doi.org/10.19166/fastjst.v10i1/10492
Available online at: https://ojs.uph.edu/index.php/FaSTJST/article/view/10492

model penilaian kualitas yang mampu mengidentifikasi degradasi vegetasi secara spasial pada area terdampak beban aktivitas wisata yang eksesif. Pendekatan ini mengonstruksi perspektif dinamis mengenai interaksi antara aktivitas manusia dan integritas ekosistem, yang menjadi instrumen krusial bagi perencanaan wilayah dan kota berkelanjutan [20]. Penelitian ini menyajikan pendekatan baru dalam pemetaan kualitas vegetasi dengan mengintegrasikan jumlah wisatawan menggunakan analisis spasial berbasis NDVI di Tahura Ir. H. Djuanda Kota Bandung. Melalui metode ini, korelasi antara konsentrasi aktivitas manusia dan penurunan kualitas vegetasi dapat diidentifikasi, sehingga tersedianya basis data spasial yang krusial untuk pengembangan kebijakan zonasi konservasi yang lebih preventif dan protektif terhadap ekosistem hutan kota.

Penelitian ini diarahkan untuk mengasesmen integritas vegetasi di Tahura Ir. H. Djuanda dengan mengolaborasikan metode penginderaan jauh dan analisis korelasi jumlah pengunjung. Melalui pendekatan multidimensi, penelitian ini berupaya memetakan pola spasial kualitas RTH serta merumuskan hubungan kausalitas antara intensitas aktivitas pariwisata dengan fluktuasi kesehatan vegetasi. Secara akademis, studi ini berkontribusi pada khazanah perencanaan wilayah dalam konteks manajemen RTH yang resilien; sementara secara praktis, hasil penelitian ini berfungsi sebagai basis data fundamental dalam menyusun regulasi pengelolaan kegiatan pariwisata pada kualitas vegetasi, agar dapat menjaga keberlanjutan layanan hutan kota di Kota Bandung

2. Metode dan Hasil Penelitian

2.1 Lokasi Penelitian

Penelitian ini dilakukan di kawasan Taman Hutan Raya (Taman Hutan Raya) Ir. H. Djuanda. Secara geografis, Taman Hutan Raya Ir. H. Djuanda terletak pada koordinat 107° 30' Bujur Timur dan 6° 52' Lintang Selatan. Kawasan ini memanjang dari arah selatan ke utara, mulai dari Dago Pakar di Kota Bandung hingga Maribaya di Lembang, Kabupaten Bandung Barat **(Gambar 1)**. Elevasi kawasan bervariasi secara signifikan, mulai dari ±770 mdpl di bagian selatan (lembah Sungai Cikapundung) hingga mencapai ±1.350 mdpl di bagian utara (wilayah Maribaya/Lembang).

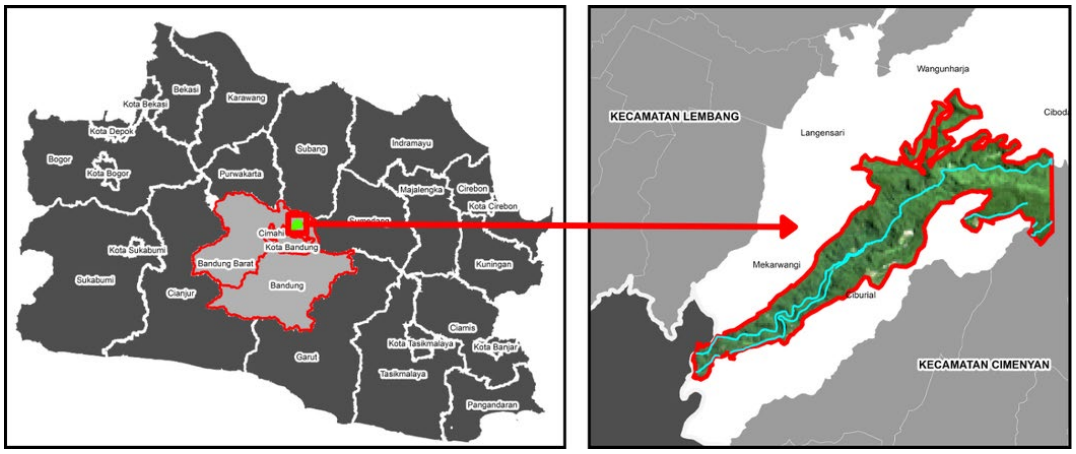

Gambar 1. Lokasi studi berada di Taman Hutan Raya Ir. H. Djuanda, Provinsi Jawa Barat.

Topografi wilayah didominasi oleh bentuk lahan perbukitan struktural dan vulkanik dengan lereng yang bervariasi dari agak curam hingga sangat terjal. Sungai Cikapundung membelah kawasan ini, menciptakan lembah sungai (*river valley*) yang dalam dan menjadi habitat penting bagi vegetasi riparian serta satwa liar. Berdasarkan aspek administrasi pemerintahan, Taman Hutan Raya Ir. H. Djuanda meliputi wilayah:

1. Desa Ciburial, Kecamatan Cimenyan di Kabupaten Bandung;
2. Desa Mekarwangi, Langensari, dan Cibodas di Kecamatan Lembang, Kabupaten Bandung Barat;
3. Kelurahan Dago, Kecamatan Coblong di Kota Bandung.

Taman Hutan Raya Ir. H. Djuanda dulunya merupakan hutan lindung yang mengalami alih fungsi menjadi taman hutan raya pada tahun 1985. Kawasan ini didominasi oleh hutan sekunder campuran

FaST - Jurnal Sains dan Teknologi, Vol.10, No. 1, Mei 2026
e-ISSN 2598-9596
DOI: https://doi.org/10.19166/fastjst.v10i1/10492
Available online at: https://ojs.uph.edu/index.php/FaSTJST/article/view/10492

dengan tegakan pinus, mahoni, puspa, dan berbagai jenis pohon lokal lainnya (Ibrahim Miftahulhuda dkk., 2019), Kawasan ini merupakan rumah bagi koleksi tumbuhan alami maupun buatan, baik alami dari Indonesia ataupun tumbuhan dari luar negeri dengan jumlah vegetasi tidak kurang dari 100.000-an pohon, yang terdiri dari 108 famili dan 524 spesies. Koleksi ini mencakup jenis tanaman asli maupun introduksi. Lokasi ini dipilih secara purposif karena memiliki fungsi ekologis ganda yaitu sebagai kawasan konservasi dan destinasi wisata alam yang mengalami tekanan lingkungan akibat aktivitas wisata yang meningkat setiap tahunnya.

2.2 Data Penelitian

Data yang digunakan dalam penelitian mencakup dua variabel utama, yaitu jumlah pengunjung tahunan yang diperoleh dari Dinas Kehutanan Provinsi Jawa Barat dalam bentuk data tahunan dan Luasan vegetasi hijau dengan kerapatan tinggi (NDVI tinggi) yang diperoleh melalui analisis citra satelit Landsat dengan resolusi spasial 30 meter menggunakan Google Earth Engine (GEE) dan ArcMap 10.8 untuk mengubah data raster menjadi data numerik. Data citra diambil untuk periode 2015–2025 dan telah melalui proses koreksi dasar (*cloud masking*) sehingga siap digunakan untuk analisis vegetasi.

2.3 Pengolahan NDVI dan Klasifikasi Vegetasi

Indeks vegetasi dihitung menggunakan metode Normalized Difference Vegetation Index (NDVI), yaitu transformasi spektral yang memanfaatkan perbedaan reflektansi antara kanal inframerah dekat (*near-infrared*/NIR) dan kanal merah (*red*) untuk mengidentifikasi kondisi vegetasi. Secara matematis, NDVI dinyatakan sebagai rasio antara selisih dan jumlah kedua kanal tersebut, sebagaimana dirumuskan pada **Persamaan 1** [21].

$$\boldsymbol{NDVI = \frac{(NIR - red)}{(NIR + red)}} \quad (1)$$

Proses pengambilan citra dilakukan menggunakan Google Earth Engine dengan tahapan preprocessing berupa *cloud masking* dan komposit citra tahunan. Nilai NDVI kemudian diklasifikasikan kedalam lima kelas kategori kerapatan vegetasi [22] seperti pada **Tabel 1**. Data citra tersebut kemudian diekspor kedalam ArcMap 10.8 untuk mendapatkan data luasan kelas vegetasi dalam satuan hektar. Dalam penelitian ini, analisis difokuskan pada kelas vegetasi tinggi sebagai indikator utama kondisi ekosistem.

Tabel 1. Klasifikasi Kelas Kerapatan Vegetasi [22]

Klasifikasi	Kerapatan Tutupan
-1<NDVI<-0,03	Lahan tidak bervegetasi
-0,03<NDVI<0,15	Kehijauan Sangat Rendah
0,15<NDVI<0,25	Kehijauan Rendah
0,25<NDVI<0,35	Kehijauan Sedang
0,35<NDVI<1	Kehijauan Tinggi

2.4 Variabel dan Analisis Data

Penelitian ini menggunakan dua variabel utama, yaitu jumlah pengunjung sebagai variabel independen dan luas vegetasi tinggi pada NDVI sebagai variabel dependen. Analisis dilakukan menggunakan pendekatan *time-series* dengan mempertimbangkan efek keterlambatan (*lag*).

Analisis statistik meliputi:

- Korelasi Spearman untuk mengidentifikasi hubungan antar variabel
- Analisis *lag* untuk melihat keterlambatan respon vegetasi (lag 0–6 tahun)
- Regresi linear sederhana untuk mengukur besarnya pengaruh jumlah pengunjung terhadap vegetasi

Pengolahan data spasial dilakukan menggunakan Google Earth Engine, sedangkan analisis statistik dilakukan menggunakan IBM SPSS Statistics.

FaST - Jurnal Sains dan Teknologi, Vol.10, No. 1, Mei 2026
e-ISSN 2598-9596
DOI: https://doi.org/10.19166/fastjst.v10i1/10492
Available online at: https://ojs.uph.edu/index.php/FaSTJST/article/view/10492

2.5 Hasil dan Pembahasan

2.5.1 Dinamika Vegetasi Terhadap Jumlah Kunjungan

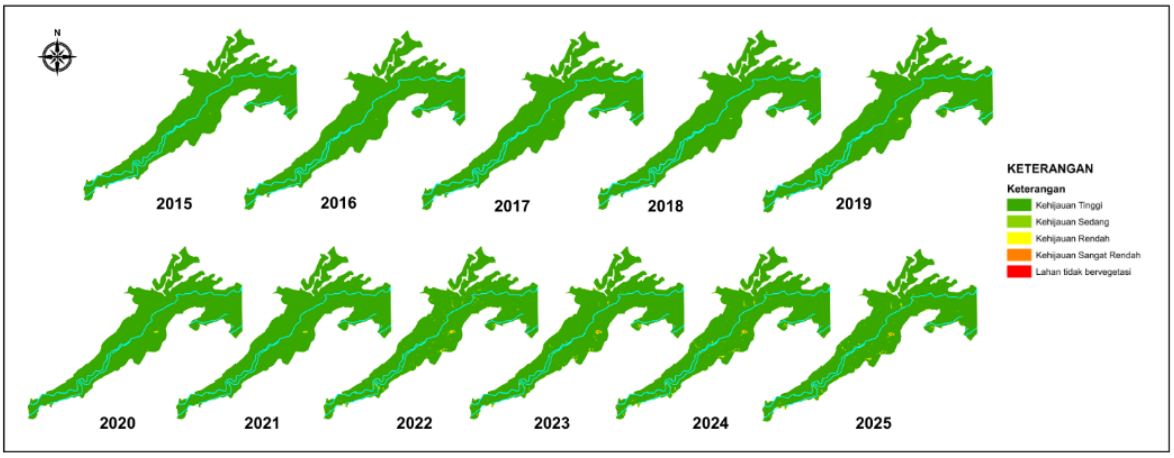

Gambar 2. Peta Kerapatan Vegetasi Taman Hutan Raya Ir. H. Djuanda, Provinsi Jawa Barat.

Tabel 2. Luasan Lahan Menurut Klasifikasi NDVI (ha)

Tahun	Lahan Tak Bervegetasi	Sangat Rendah	Rendah	Sedang	Tinggi	TOTAL
2015	0,000	0,001	0,016	0,650	602,612	603,279
2016	0,000	0,017	0,000	0,001	603,262	603,280
2017	0,000	0,272	0,035	0,304	602,668	603,280
2018	0,000	0,001	0,016	0,183	603,080	603,280
2019	0,000	0,038	0,470	1,299	601,473	603,280
2020	0,003	0,026	0,329	0,606	602,315	603,280
2021	0,001	0,004	0,322	0,585	602,368	603,280
2022	0,003	0,422	2,301	17,024	583,444	603,194
2023	0,000	0,494	2,555	18,413	581,818	603,280
2024	0,000	0,451	1,652	9,363	591,814	603,280
2025	0,000	0,464	1,856	11,318	589,640	603,279

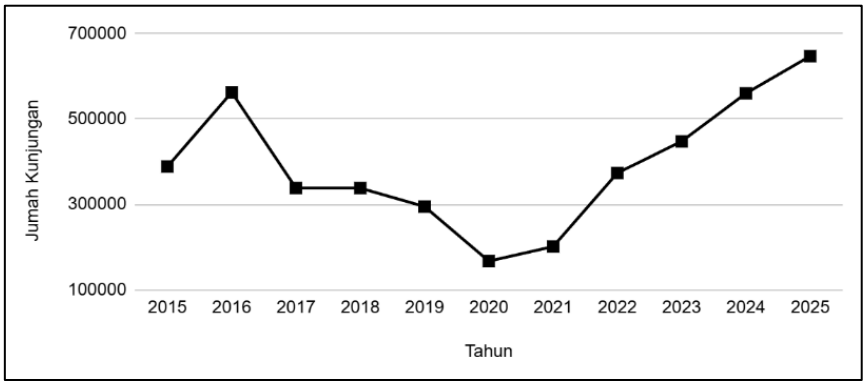

Gambar 3. Tren Pengunjung Taman Hutan Raya Ir. H. Djuanda, Provinsi Jawa Barat.

Tabel 3. Jumlah Pengunjung Taman Hutan Raya Ir. H Djuanda, Provinsi Jawa Barat.

Tahun	Jumlah Kunjungan
2015	388.436
2016	562.189
2017	338.096
2018	338.033
2019	294.946
2020	167.183
2021	201.251
2022	373.448
2023	447.488

FaST - Jurnal Sains dan Teknologi, Vol.10, No. 1, Mei 2026
e-ISSN 2598-9596
DOI: https://doi.org/10.19166/fastjst.v10i1/10492
Available online at: https://ojs.uph.edu/index.php/FaSTJST/article/view/10492

Tahun	Jumlah Kunjungan
2024	559.836
2025	646.989

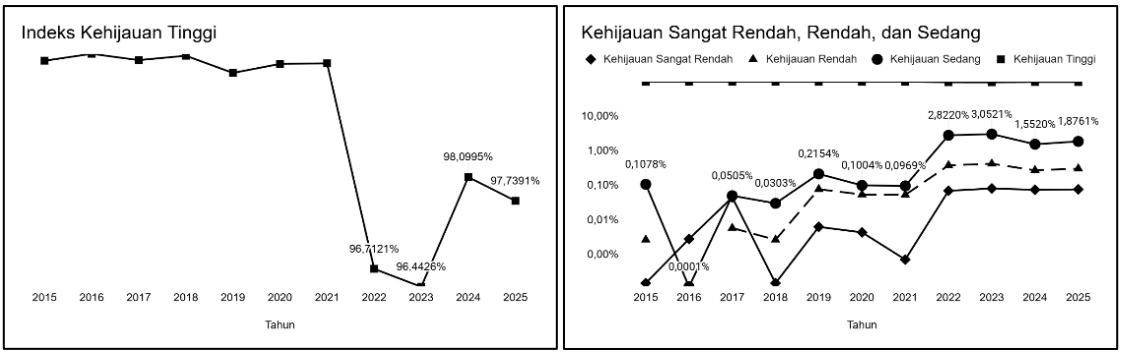

Gambar 4. Tren Indeks Vegetasi di Taman Hutan Raya Ir. H. Djuanda, Provinsi Jawa Barat.

Berdasarkan hasil pengolahan citra **(Tabel 2)**, diperoleh bahwa kelas kehijauan tinggi secara konsisten mendominasi luas area setiap tahunnya dengan rata-rata lebih dari 5,9 juta m² dari total luas kawasan ±6,03 juta m². Dominasi ini mengindikasikan bahwa sebagian besar area konservasi masih berada dalam kondisi vegetatif yang baik **(Gambar 2)**. Namun, terjadi kecenderungan penurunan vegetasi pada periode dengan peningkatan jumlah pengunjung **(Gambar 3)**, meskipun pada beberapa tahun tertentu terlihat adanya pemulihan vegetasi pada tahun 2023 **(Gambar 4)** yang diasumsikan akibat penurunan jumlah kunjungan pada masa pandemi COVID-19 tahun 2020 **(Tabel 3)**. Dinamika fluktuatif tetap terjadi pada kelas-kelas kehijauan rendah hingga sedang, yang merepresentasikan area yang sensitif terhadap perubahan lingkungan dan aktivitas antropogenik.

2.5.2 Analisis Korelasi *Lag* dan Analisis Regresi

Analisis hubungan antara jumlah pengunjung dan luas vegetasi tinggi dilakukan menggunakan uji korelasi Pearson dan analisis regresi linear sederhana. Uji Pearson digunakan untuk mengukur kekuatan dan arah hubungan linear antara kedua variabel, dengan nilai koefisien korelasi (r) berkisar antara -1 hingga +1. Nilai positif menunjukkan hubungan searah, sedangkan nilai negatif menunjukkan hubungan berlawanan. Selain itu, dilakukan uji signifikansi menggunakan nilai *p-value* untuk menentukan apakah hubungan yang ditemukan signifikan secara statistik. Dalam penelitian ini, tingkat signifikansi yang digunakan adalah $\alpha = 0,05$.

Untuk mengidentifikasi adanya efek tertunda (*delayed effect*), digunakan pendekatan *lagged correlation* dengan menggeser data deret waktu *(time-series shifting*). Variabel jumlah pengunjung digeser ke depan (*forward shift*) terhadap variabel vegetasi dengan interval *lag* 0 hingga 6 tahun. *Lag* 0 menunjukkan hubungan pada tahun yang sama, sedangkan *lag* 1 hingga *lag* 6 menunjukkan hubungan antara jumlah pengunjung pada tahun sebelumnya dengan kondisi vegetasi pada tahun berikutnya.

Proses pembentukan variabel *lag* dilakukan menggunakan fitur *Create Time Series* pada perangkat lunak IBM SPSS Statistics, sehingga dihasilkan variabel baru (misalnya *Lag*_1, *Lag*_2, hingga *Lag*_6) yang merepresentasikan jumlah pengunjung pada periode sebelumnya **(Tabel 4)**. Selanjutnya, masing-masing variabel *lag* diuji korelasinya terhadap luas vegetasi tinggi untuk mengidentifikasi waktu keterlambatan respon vegetasi terhadap tekanan antropogenik.

FaST - Jurnal Sains dan Teknologi, Vol.10, No. 1, Mei 2026
e-ISSN 2598-9596
DOI: https://doi.org/10.19166/fastjst.v10i1/10492
Available online at: https://ojs.uph.edu/index.php/FaSTJST/article/view/10492

Tabel 4. Hasil Pergeseran Data Jumlah Kunjungan

Tahun	Jumlah Pengunjung	Luas Kerapatan Vegetasi Tinggi	*Lag* 1	*Lag* 2	*Lag* 3	Lag..(n)	*Lag* 6
2015	388436	6.026.120.000	-	-	-		-
2016	562189	6.032.620.000	388436.00	-	-		-
2017	338096	6.026.680.000	562189.00	388436.00	-		-
2018	338033	6.030.800.000	338096.00	562189.00	388436.00		-
2019	294946	6.014.730.000	338033.00	338096.00	562189.00		-
2020	167183	6.023.150.000	294946.00	338033.00	338096.00	**.. (n)**	-
2021	201251	6.023.680.000	167183.00	294946.00	338033.00		388436.00
2022	373448	5.834.440.000	201251.00	167183.00	294946.00		562189.00
2023	447488	5.818.180.000	373448.00	201251.00	167183.00		338096.00
2024	559836	5.918.140.000	447488.00	373448.00	201251.00		338033.00
2025	646989	5.896.400.000	559836.00	447488.00	373448.00		294946.00

Tabel 5. Hasil Uji Korelasi antara Jumlah Pengunjung dan Luas Kerapatan Vegetasi Tinggi (2015–2025)

Lag time	Spearman's ρ	Arah Hubungan	p-value	N	Interpretasi
0 tahun	–0,018	Negatif lemah	0,960	10	Tidak signifikan
1 tahun	–0,183	Negatif sedang	0,637	9	Awal efek antropogenik
2 tahun	–0,524	Negatif kuat	0,183	8	Efek mulai terlihat
3 tahun	–0,714	Negatif kuat	0,071	7	Puncak degradasi vegetasi
4 tahun	–0,771	Negatif kuat	0,072	6	*Delayed effect* masih bertahan
5 tahun	–0,300	Negatif lemah	0,624	5	Efek mulai hilang
6 tahun	+0,400	Positif lemah	0,600	4	Pemulihan vegetasi alami

Hasil uji korelasi menunjukkan bahwa hubungan antara jumlah pengunjung dan luas vegetasi tidak muncul secara langsung pada tahun yang sama (lag 0). Hubungan mulai terlihat pada lag ke-2 dan puncaknya pada *lag* ke-3 dengan nilai koefisien korelasi sebesar –0,714, yang menunjukkan hubungan negatif dengan kekuatan moderat **(Tabel 5)** sementara pada *lag* ke-4 mulai menunjukkan pelemahan.

Selain itu, dilakukan analisis regresi linear sederhana pada *lag* 1 hingga *lag 4* untuk mengukur besarnya pengaruh jumlah pengunjung terhadap perubahan vegetasi. Model regresi digunakan untuk menghitung koefisien determinasi (R^2) dan menguji signifikansi hubungan melalui uji F dan nilai p-value. Seluruh analisis statistik dilakukan menggunakan IBM SPSS Statistics, sedangkan pengolahan data spasial dilakukan menggunakan Google Earth Engine.

Tabel 6. Hasil Uji Regresi NDVI terhadap Jumlah Pengunjung (*Lag* 0–6)

Lag time	R^2	β(JP)	Sig. (Model)	Interpretasi
0 tahun	0.134	–0.34	0.818	Model tidak signifikan
1 tahun	0.296	–0.53	0.591	Awal efek antropogenik
2 tahun	0.346	–0.68	0.597	NDVI menurun setelah 2 tahun
3 tahun	0.680	–0.80	0.275	*Delayed effect* maksimum
4 tahun	0.662	–0.66	0.461	Efek masih bertahan
5 tahun	0.303	–1.62	0.921	Efek melemah
6 tahun	1.000	+2.37	—	*Overfit*, tidak valid

Hasil analisis regresi pada lag ke-3 menunjukkan bahwa jumlah pengunjung mampu menjelaskan sebesar 68% variasi luas vegetasi tinggi (R^2 = 0,680). Nilai signifikansi sebesar 0,275 menunjukkan bahwa model mendekati signifikan, namun belum memenuhi batas signifikansi statistik konvensional **(Tabel 6)**. Hasil ini sejalan dengan analisis korelasi Spearman yang menunjukkan hubungan negatif

FaST - Jurnal Sains dan Teknologi, Vol.10, No. 1, Mei 2026
e-ISSN 2598-9596
DOI: https://doi.org/10.19166/fastjst.v10i1/10492
Available online at: https://ojs.uph.edu/index.php/FaSTJST/article/view/10492

dengan kekuatan moderat pada lag ke-3 ($\rho = -0{,}714$), yang mengindikasikan adanya hubungan antara tekanan pengunjung dan penurunan vegetasi.

Secara keseluruhan, pola hubungan yang tidak muncul pada lag awal (lag 0–2) namun mulai terlihat pada lag ke-3 menunjukkan adanya efek tertunda (*delayed effect*) akibat aktivitas wisata. Hal ini mengindikasikan bahwa dampak aktivitas wisata terhadap vegetasi tidak terjadi secara langsung, melainkan muncul setelah periode waktu tertentu sebagai akibat akumulasi tekanan antropogenik.

Namun demikian, jumlah observasi yang relatif terbatas ($n \approx 10$) menjadi salah satu keterbatasan utama penelitian ini dan berpengaruh terhadap tingkat signifikansi statistik yang diperoleh. Oleh karena itu, hasil penelitian ini lebih tepat diinterpretasikan dalam konteks signifikansi ekologis dibandingkan signifikansi statistik semata. Selain itu, meskipun hubungan terkuat muncul pada lag yang lebih tinggi, penelitian ini menekankan lag ke-3 sebagai model utama karena jumlah data yang lebih besar dan hasil yang lebih stabil secara statistik. Sebagai pendukung tambahan dalam menjelaskan pola keterlambatan respon vegetasi maka disajikan seperti pada **Gambar 5** yang memvisualisasikan deret waktu (*time-series*) antara NDVI dan jumlah pengunjung untuk memperkuat interpretasi ini.

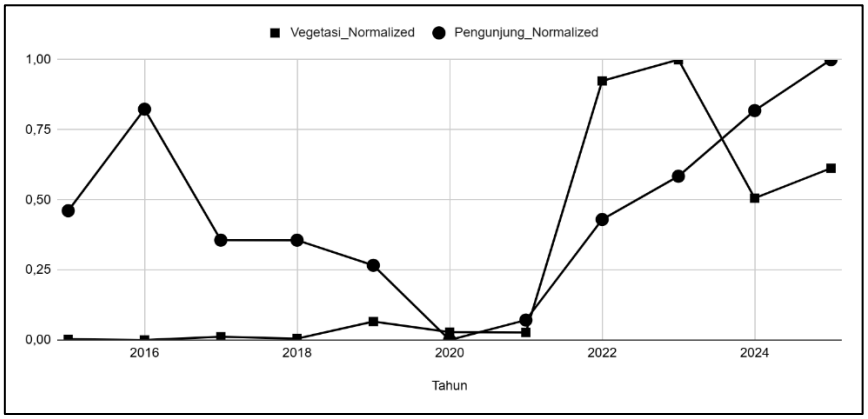

Gambar 5. Tren Jumlah Kunjungan (*Normalized*) dan Luasan Vegetasi Kelas Tinggi (*Normalized*)

Tabel 7. Hasil Normalisasi Data Agregat (2015–2025)

Tahun	Vegetasi_Normalized	Pengunjung_Normalized
2015	0,002798794261	0,4611301234
2016	0	0,8232619017
2017	0,01155950146	0,3562127193
2018	0,00492371526	0,3560814162
2019	0,06587536208	0,2662805384
2020	0,02800909411	0
2021	0,02686069027	0,07100369733
2022	0,9242093861	0,4298924982
2023	1	0,5842048661
2024	0,5060302391	0,8183578363
2025	0,6127500828	1

Normalisasi data agregat dilakukan untuk mengubah seluruh nilai data ke dalam rentang 0 hingga 1, sehingga perbandingan langsung antara variabel dengan skala yang berbeda dapat dilakukan tanpa menyebabkan distorsi matematis. Hasil normalisasi **(Tabel 7)** menunjukkan bahwa nilai 1 menandakan titik maksimum sepanjang periode observasi (kondisi paling tinggi dari suatu variabel), sedangkan nilai 0 merepresentasikan kondisi terendah (kondisi paling menurun atau terdegradasi).

Berdasarkan hasil normalisasi data agregat antara jumlah kunjungan wisata dan luasan vegetasi tinggi, diperoleh pola temporal yang menunjukkan adanya keterkaitan yang bersifat tertunda (*delayed effect*). Nilai *normalized* pada variabel jumlah pengunjung mencapai angka 0 pada kunjungan wisata tahun 2020, sedangkan nilai *normalized* pada variabel luasan vegetasi baru mencapai angka 1 dengan selisih waktu sekitar tiga tahun setelahnya atau tahun 2023. Hal ini mengindikasikan adanya jeda waktu

FaST - Jurnal Sains dan Teknologi, Vol.10, No. 1, Mei 2026
e-ISSN 2598-9596
DOI: https://doi.org/10.19166/fastjst.v10i1/10492
Available online at: https://ojs.uph.edu/index.php/FaSTJST/article/view/10492

(*ecological lag*) dimana dampak tekanan antropogenik terhadap vegetasi baru muncul setelah periode akumulasi stres ekologis selama kurang lebih tiga tahun.

2.5.4 Pembahasan dan Implikasi

Temuan penelitian ini menunjukkan adanya *delayed effect*, di mana vegetasi merespons tekanan antropogenik setelah beberapa tahun. Pola ini menunjukkan bahwa ekosistem memiliki kemampuan resiliensi dalam jangka pendek, namun dapat mengalami penurunan apabila tekanan berlangsung secara terus-menerus. Implikasi dari hasil ini adalah perlunya pengelolaan jumlah pengunjung secara lebih adaptif, dengan mempertimbangkan dampak jangka panjang terhadap kondisi vegetasi. Selain itu, hasil ini juga menunjukkan pentingnya penggunaan analisis berbasis waktu (*time-series*) dalam evaluasi kondisi ekosistem hutan kota.

Hasil normalisasi selanjutnya digunakan dalam analisis *forecasting* (peramalan) untuk memproyeksikan tren pertumbuhan kedua variabel hingga tahun 2030. Metode yang digunakan mengacu pada model regresi polinomial derajat kedua (*second-order polynomial regression*), yang dipilih karena mampu menggambarkan perubahan pola naik–turun yang tidak linear pada sistem ekologis. Hasil *forecasting* **(Gambar 6)** menunjukkan bahwa tren jumlah pengunjung cenderung meningkat secara berkelanjutan hingga tahun 2030, dengan potensi mencapai puncak baru yang melampaui periode pra-pandemi. Sebaliknya, garis proyeksi vegetasi tinggi menunjukkan kecenderungan menurun setelah tahun 2025 dan melewati batas garis 0,0 pada rentang tahun 2027–2028.

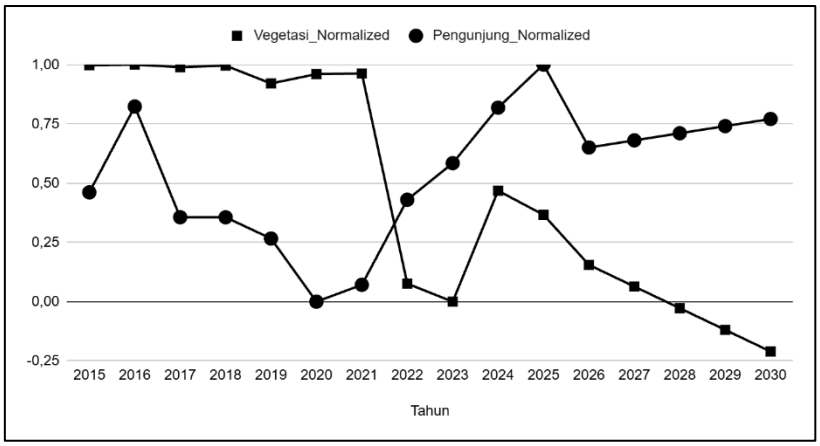

Gambar 6. Proyeksi Dinamika Vegetasi Kelas Tinggi dan Jumlah Kunjungan

Secara matematis, kondisi $\boldsymbol{x' = 0}$ pada hasil normalisasi menandakan bahwa nilai aktual vegetasi telah mencapai titik minimum ekologis sepanjang periode analisis. Artinya, jika tren ini berlanjut tanpa intervensi, maka pada tahun 2027–2028 luasan vegetasi tinggi diperkirakan turun di bawah ambang batas keseimbangan ekologis, dan kawasan tersebut akan mengalami pergeseran kelas vegetasi dari kategori tinggi menjadi kategori sedang.

Kecenderungan ini juga diperkuat oleh hasil *forecasting* pada grafik vegetasi sedang **(Gambar 7)**, dimana garis proyeksi menembus nilai 1,0 pada periode yang sama (pertengahan 2027–2028). Kondisi ini secara ekologis menggambarkan bahwa vegetasi sedang akan meluas karena terjadi *class transition* dari vegetasi tinggi yang mengalami degradasi. Dengan kata lain, penurunan kelas vegetasi tinggi berbanding lurus dengan ekspansi vegetasi sedang akibat tekanan kumulatif dari aktivitas wisata yang meningkat.

FaST - Jurnal Sains dan Teknologi, Vol.10, No. 1, Mei 2026
e-ISSN 2598-9596
DOI: https://doi.org/10.19166/fastjst.v10i1/10492
Available online at: https://ojs.uph.edu/index.php/FaSTJST/article/view/10492

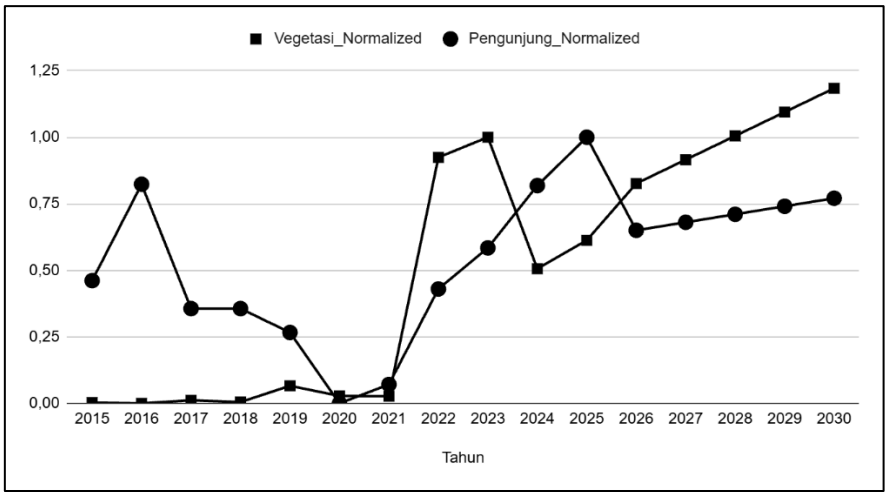

Gambar 7. Proyeksi Dinamika Vegetasi Kelas Sedang dan Jumlah Kunjungan

Temuan ini memberikan dasar penting bagi perencanaan pengelolaan kawasan konservasi berbasis waktu (*temporal-based management*). Tahun 2027–2028 dapat diidentifikasi sebagai titik kritis ekologis (*ecological tipping point*) yang perlu diantisipasi melalui kebijakan pembatasan jumlah kunjungan tahunan. Jika tidak dilakukan pengendalian intensitas wisata, maka penurunan kualitas vegetasi diperkirakan akan berlanjut hingga melewati ambang minimum yang dapat dipulihkan secara alami.

Selisih waktu sekitar tiga tahun antara puncak aktivitas wisata dan penurunan vegetasi menggambarkan fase akumulasi stres ekologis, yang kemudian diikuti oleh fase penurunan yang cepat (*decline phase*). Berdasarkan model proyeksi hingga 2030, jika tren peningkatan wisata berlanjut tanpa pengaturan, maka nilai vegetasi hijau akan turun di bawah titik degradasi ($V < 0$) pada pertengahan 2027–2028, dan berpotensi menimbulkan pergeseran kelas vegetasi tinggi menjadi vegetasi sedang.

Langkah akhir dari penelitian ini adalah menentukan ambang batas optimal jumlah kunjungan tahunan (*annual visitor threshold*) berdasarkan model proyeksi, agar garis vegetasi tinggi tetap berada di atas nilai normalisasi 0. Penentuan ambang batas ini akan menjadi dasar dalam perumusan strategi pengendalian kapasitas wisata (*ecological carrying capacity*) yang memastikan keseimbangan antara aktivitas rekreasi dan kelestarian vegetasi.

Untuk memahami batas kemampuan ekosistem dalam menahan tekanan wisata, dilakukan pemodelan regresi linear sederhana antara jumlah pengunjung dan nilai *vegetasi normalized* berdasarkan data periode 2015–2030. Hasil model menunjukkan hubungan negatif yang kuat, dengan **Persamaan 2,**

$$\boldsymbol{V = 1.1007 - 1.6692P} \quad (2)$$

Dimana (V = nilai vegetasi hijau dalam skala normalisasi) dan (P = nilai jumlah pengunjung dalam skala normalisasi). Koefisien negatif menandakan bahwa setiap peningkatan aktivitas wisata berkontribusi langsung pada penurunan kualitas vegetasi. Dengan mensubstitusikan $\boldsymbol{V = 0}$ (batas degradasi ekologis), diperoleh nilai $\boldsymbol{P = 0.6599}$ pada skala normalisasi. Ketika nilai ini dikonversikan kembali ke satuan aktual menggunakan formula *min–max scaling*, diperoleh:

$$\boldsymbol{P} \text{ aktual} = \mathbf{167,183 + 0.6599 \times (646,989 - 167,183) = 659,927} \quad (3)$$

Hasilnya, ambang batas kunjungan tahunan (*visitor threshold*) yang dapat ditoleransi tanpa menyebabkan penurunan kelas vegetasi adalah ±659.927 pengunjung per tahun **(Persamaan 3)**, setara dengan ±54,994 pengunjung perbulan; atau ±1.833 pengunjung perharinya. Angka ini merupakan batas maksimum yang masih dapat diterima tanpa menyebabkan penurunan signifikan pada indeks vegetasi tinggi. Jika jumlah pengunjung tahunan melebihi batas ini secara berturut-turut selama dua hingga tiga tahun, maka sistem vegetasi akan memasuki fase ketidakseimbangan yang sulit dipulihkan secara alami. Ketika nilai vegetasi *normalized* mendekati 0.25, maka mekanisme pembatasan kunjungan perlu segera diterapkan sebagai fase peringatan dini (*early warning stage*).

Secara ekologis, nilai vegetasi *normalized* = 0 merepresentasikan titik kritis dimana vegetasi tinggi telah kehilangan sebagian besar fungsi ekologis utamanya, termasuk penyerapan karbon, peneduhan,

FaST - Jurnal Sains dan Teknologi, Vol.10, No. 1, Mei 2026
e-ISSN 2598-9596
DOI: https://doi.org/10.19166/fastjst.v10i1/10492
Available online at: https://ojs.uph.edu/index.php/FaSTJST/article/view/10492

dan pengaturan mikroklimat. Ketika jumlah kunjungan melampaui batas tersebut, sistem vegetasi tidak lagi mampu melakukan regenerasi alami dengan kecepatan yang seimbang terhadap tingkat gangguan.

3. Kesimpulan dan Rekomendasi

Hasil penelitian ini menunjukkan bahwa dinamika vegetasi di kawasan konservasi perkotaan tidak hanya dipengaruhi oleh faktor iklim, tetapi lebih kuat dikendalikan oleh aktivitas antropogenik yang terjadi secara berulang dan berskala masif. Berdasarkan analisis deret waktu terhadap data jumlah pengunjung dan nilai *Normalized Difference Vegetation Index* (NDVI) selama periode 2015–2025, ditemukan bahwa hubungan antara jumlah pengunjung dan NDVI bersifat negatif kuat pada jeda waktu (*lag time*) dua hingga empat tahun. Hal ini menandakan adanya dampak ekologis tertunda (*delayed anthropogenic impact*) dari peningkatan aktivitas wisata terhadap luasan vegetasi dengan kerapatan tinggi. Model regresi terbaik terdapat pada *lag* tiga tahun dengan nilai R^2 sebesar 0.680 dan koefisien βJP –0.80, yang mengindikasikan bahwa sekitar 68% variasi NDVI tiga tahun kemudian dapat dijelaskan oleh variabel jumlah pengunjung, dengan kontribusi terbesar berasal dari tekanan wisata.

Tekanan antropogenik memiliki pengaruh jangka menengah yang kuat, dengan efek penurunan vegetasi yang muncul dua hingga tiga tahun setelah peningkatan aktivitas wisata dan bertahan hingga empat tahun sebelum proses pemulihan alami vegetasi mulai terjadi. Hasil ini memperkuat teori *Human–Environment Interaction* dan *Delayed Ecological Response* yang menjelaskan bahwa gangguan ekologis akibat aktivitas manusia tidak selalu langsung terlihat, tetapi muncul secara bertahap seiring waktu. Secara keseluruhan, penelitian ini menegaskan bahwa aktivitas manusia merupakan salah satu faktor perubahan vegetasi dengan indeks tinggi di kawasan konservasi perkotaan. Fenomena penurunan NDVI dengan *delayed effect* memperlihatkan bahwa dampak antropogenik tidak hanya bersifat langsung, tetapi juga kumulatif, sehingga diperlukan strategi pengelolaan yang memperhitungkan periode waktu pemulihan ekologis (*ecological recovery window*).

Berdasarkan hasil analisis kuantitatif dan proyeksi hingga tahun 2030, diperoleh bahwa jumlah pengunjung maksimum yang masih dapat ditoleransi oleh ekosistem vegetasi tinggi di Tahura Ir. H. Djuanda tanpa melampaui batas degradasi ekologis adalah 659.927 pengunjung per tahun. Nilai ini menandai batas atas kapasitas ekologis yang perlu dijaga agar sistem vegetasi tidak mengalami penurunan kelas ke vegetasi sedang pada periode kritis 2027–2028. Maka disarankan agar pengelola kawasan menetapkan kebijakan pembatasan kunjungan berbasis daya dukung ekologis dengan menerapkan sistem kuota tahunan yang adaptif. Kebijakan ini dapat diintegrasikan ke dalam mekanisme perizinan kunjungan berbasis data spasial dan waktu, dimana jumlah pengunjung harian dan bulanan disesuaikan dengan kondisi vegetasi. Selain itu, perlu dikembangkan sistem pemantauan vegetasi berbasis NDVI secara periodik untuk mendeteksi lebih dini perubahan vegetasi dan mengevaluasi efektivitas program konservasi. Strategi adaptif seperti penutupan temporer area wisata, pembentukan zona pemulihan vegetasi, dan integrasi data spasial ke dalam sistem pengambilan keputusan dapat membantu menjaga keberlanjutan fungsi ekologis kawasan.

Dari sisi akademik, penelitian ini memberikan kontribusi terhadap penguatan teori *delayed anthropogenic impact* pada ekosistem konservasi tropis. Namun, keterbatasan penelitian ini terletak pada resolusi temporal data NDVI tahunan dan jumlah observasi yang relatif sedikit, sehingga pengaruh jangka pendek *(intra-annual)* belum sepenuhnya terdeteksi. Berdasarkan hasil uji korelasi Spearman, hubungan antara jumlah pengunjung dan NDVI menunjukkan pola negatif kuat pada jeda waktu dua hingga empat tahun ($\rho = -0{,}595$ hingga $-0{,}771$) dengan nilai p-value mendekati signifikan ($p \approx 0{,}072$). Meskipun belum signifikan secara statistik, pola hubungan yang konsisten ini menunjukkan signifikansi ekologis yang kuat, mencerminkan adanya efek *delayed ecological response* akibat tekanan wisata terhadap vegetasi. Ketidaksignifikanan statistik diduga disebabkan oleh keterbatasan jumlah observasi tahunan (n=10), sehingga hasil ini lebih tepat diinterpretasikan sebagai *ecologically meaningful correlation* daripada *statistically significant correlation*. Penelitian selanjutnya disarankan untuk menggunakan data dengan resolusi temporal yang lebih tinggi, seperti MODIS atau Sentinel-2, serta mengintegrasikan variabel sosial-ekologis lain seperti indeks kenyamanan termal, kepadatan vegetasi spesifik jenis, dan aktivitas pembangunan fisik secara spasial. Pendekatan tersebut diharapkan dapat memberikan pemahaman yang lebih komprehensif tentang dinamika vegetasi di kawasan konservasi perkotaan dan memperkuat dasar ilmiah bagi kebijakan konservasi adaptif yang berkelanjutan.

Kebijakan Penggunaan Generative Artificial Intelligence (AI)

Penggunaan Generative Artificial Intelligence (AI) dalam penelitian ini hanya terbatas sebagai alat bantu dalam menemukan referensi yang relevan dalam penelitian. AI tidak digunakan dalam perumusan ide penelitian, pengolahan data, analisis, maupun penarikan kesimpulan.

Penulis menggunakan ChatGPT (OpenAI) untuk membantu perbaikan bahasa dan struktur kalimat. Seluruh isi, analisis, dan hasil penelitian sepenuhnya menjadi tanggung jawab penulis.

Referensi

[1] J. B. Patel and Z. Raval, "The Impacts of Urbanization on Ecological Systems: A Comprehensive Study of the Complex Challenges Arising from Rapid Urban Growth," *Research Review Journal of Indian Knowledge Systems*, vol. 1, no. 1, pp. 1–10, Jun. 2024, https://doi.org/10.31305/rrjiks.2024.v1.n1.001.

[2] X. Bai *et al.*, "Linking Urbanization and the Environment: Conceptual and Empirical Advances," 2017, https://doi.org/10.1146/annurev-environ.

[3] B. L. T. Ii, E. F. Lambin, and A. Reenberg, "The emergence of land change science for global environmental change and sustainability," 2007. [Online]. Available: www.pnas.orgcgidoi10.1073pnas.0704119104

[4] I. A. Abdul Samad, Z. M. Baharuddin, and H. H. Md Jani, "Evaluation of Ecosystem Services Contributions on Urban Forests in Kuala Lumpur," *Journal of Architecture, Planning and Construction Management*, vol. 14, no. 1, Jun. 2024, https://doi.org/10.31436/japcm.v14i1.697.

[5] A. Paula Branco do Nascimento, S. Rosana dos Santos, G. Gaudereto, and A. Lucia Casteli Figueiredo Gallardo, "Gerenciamento de Cidades Os serviços ecossistêmicos de espaços verdes urbanos: contribuições para a Agenda 2030."

[6] A. Karimi, P. Pahlavani, and B. Bigdeli, "Land use analysis on land surface temperature in urban areas using a geographically weighted regression and Landsat 8 imagery, a case study: Tehran, Iran," in *International Archives of the Photogrammetry, Remote Sensing and Spatial Information Sciences - ISPRS Archives*, International Society for Photogrammetry and Remote Sensing, Sep. 2017, pp. 117–122. https://doi.org/10.5194/isprs-archives-XLII-4-W4-117-2017.

[7] Kintan Annisa and Weishaguna, "Kajian Kualitas Hutan Kota di Kota Bandung," *Jurnal Riset Perencanaan Wilayah dan Kota*, pp. 1–8, Jul. 2023, https://doi.org/10.29313/jrpwk.v3i1.1805.

[8] M. Ibrahim Miftahulhuda *et al.*, "Estimasi Stok Karbon Taman Hutan Raya Ir H. Djuanda."

[9] S. T. A. Pickett and M. L. Cadenasso, "Advancing urban ecological studies: Frameworks, concepts, and results from the Baltimore Ecosystem Study," in *Austral Ecology*, Apr. 2006, pp. 114–125. https://doi.org/10.1111/j.1442-9993.2006.01586.x.

[10] C. Afrianti *et al.*, "An Assessment of Urban Forest Landscape Services for Green Space Management Improvement in Bandung City, West Java, Indonesia," in *BIO Web of Conferences*, EDP Sciences, Mar. 2024. https://doi.org/10.1051/bioconf/20249404006.

[11] M. Effendi, Nurhayati, and H. S. Arifin, "Strategi Pengelolaan Lanskap Wisata di Perkampungan Budaya Betawi Setu Babakan Jakarta," *Jurnal Lanskap Indonesia*, vol. 16, no. 1, pp. 84–98, Apr. 2024, https://doi.org/10.29244/jli.v16i1.48700.

[12] S. Fahmi *et al.*, "Comparison of Vegetation Canopy Density Mapping in Djuanda Great Forest Park Using FCD And MSARVI Transformation Based on Sentinel-2A Image," Cetak, 2025.

[13] S. A. Shirazi and J. H. Kazmi, "Analysis of socio-environmental impacts of the loss of urban trees and vegetation in Lahore, Pakistan: a review of public perception," Dec. 01, 2016, *Springer Verlag*. https://doi.org/10.1186/s13717-016-0050-8.

[14] U. States, "FRAGSTATS: Spatial Pattern Analysis Program for Quantifying Landscape Structure," 1995.

[15] A. Moh Rifiyan Arief Program Studi Pariwisata Jurusan Ilmu Administasi, "Pengembangan Aktivitas Wisata Di Taman Hutan Raya Ir. H. Djuanda Bandung Jawa Barat."

[16] Compton J. Tucker, "Red and Photographic Infrared Linear Combinations for Monitoring Veqetation," 1978. https://doi.org/10.1016/0034-4257(79)90013-0.

[17] C. Neumann, R. Behling, and G. Weiss, "Biodiversity Change in Cultural Landscapes—The Rural Hotspot Hypothesis," *Ecol. Evol.*, vol. 15, no. 1, Jan. 2025, https://doi.org/10.1002/ece3.70811.

[18] P. Katila, C. J. P. Colfer, W. de Jong, G. Galloway, P. Pacheco, and G. Winkel, *Towards SDG 11: How Urban Greenery Can Help Us Build Sustainable Cities*. Cambridge University Press, 2019. https://doi.org/10.1017/9781108765015.

[19] A. Azmeer, F. Tahir, and S. G. Al-Ghamdi, "Towards SDG 11: How Urban Greenery Can Help Us Build Sustainable Cities," *Front. Young Minds*, vol. 12, Nov. 2024, https://doi.org/10.3389/frym.2024.1419477.

[20] J. F. Dashiell, "Mcgraw-Hill Pusllcatlons In Psychology Fundamental Statistics in Psychology and Education."

[21] S. Huang, L. Tang, J. P. Hupy, Y. Wang, and G. Shao, "A commentary review on the use of normalized difference vegetation index (NDVI) in the era of popular remote sensing," *J. For. Res. (Harbin).*, vol. 32, no. 1, pp. 1–6, Feb. 2021, https://doi.org/10.1007/s11676-020-01155-1.

[22] S. W. Andini, Y. Prasetyo, and A. Sukmono, "Analisis Sebaran Vegetasi Dengan Citra Satelit Sentinel Menggunakan Metode NDVI dan Segmentasi," 2018.

FaST - Jurnal Sains dan Teknologi, Vol.10, No. 1, Mei 2026
e-ISSN 2598-9596
DOI: https://doi.org/10.19166/fastjst.v10i1/10960
Available online at: https://ojs.uph.edu/index.php/FaSTJST/article/view/10960

Pemanfaatan Probiotik *Lactobacillus casei* dan *Lactobacillus plantarum* dalam Yoghurt Berbasis Susu Kacang Arab (*Cicer Arietinum* L.) dengan Perendaman Natrium Bikarbonat dan Penambahan Stevia

Jennifer Felicia Prananto[1], Adolf J. N. Parhusip[1*)]
[1]Program Studi Teknologi Pangan, Universitas Pelita Harapan, Jl. M.H. Thamrin Boulevard 1100
Lippo Village, Karawaci, Tangerang, Indonesia

ABSTRACT

Yogurt is a functional food product rich in probiotics and plays a vital role in maintaining digestive health and the immune system. Animal-based yogurt contains lactose and cholesterol, making it unsuitable for those with lactose intolerance. Therefore, lactose-free, high-protein, and nutrient-rich chickpea milk can be an alternative ingredient for plant-based yogurt. However, chickpea yogurt has quite an unpleasant taste and aroma, as well as a bitter aftertaste due to phenolic compounds and lipoxygenase enzyme activity. This study aims to develop chickpea milk yogurt with optimal sensory and nutritional quality by soaking chickpeas in sodium bicarbonate solution (0, 1, 2, 3%; 8, 16, 24 hours), adding stevia (0.044, 0.088, 0.133%) as a low-calorie sweetener, and using a combination of probiotics Lactobacillus casei and Lactobacillus plantarum (1:0, 2:1, 1:1, 1:2, 0:1) to support fermentation and yogurt stability. The results of the analysis showed that variations in the ratio of bacteria and stevia concentration significantly affected pH, total lactic acid, total LAB, total sugar, and protein, with a formulation of a 1:1 bacterial ratio and 0.088% stevia providing a pH of 4.1±0.04, protein 6.1±0.04%, lactic acid 0.96±0.01%, total sugar 1.65±0.00%, good fermentation efficiency, high LAB viability (9.27±0.04 log CFU/ml), and the highest sensory acceptance. This combination is recommended as the best formulation for chickpea milk yogurt with optimal chemical, microbiological, and sensory qualities.

ARTICLE INFO

Keywords:
Chickpea; Lactobacillus casei; Lactobacillus plantarum; Stevia; Yogurt

***Corresponding author**:
adolf.parhusip@uph.edu

Article history:
Submitted 4 Mar 2026
Revised 5 May 2026
Accepted 6 May 2026
Online Available 13 May 2026
Published 20 May 2026

1. Pendahuluan

Yoghurt merupakan produk pangan kaya probiotik yang bermanfaat bagi kesehatan, terutama dalam meningkatkan pencernaan dan mendukung sistem imun tubuh. Umumnya, yoghurt dibuat dari susu hewani seperti susu sapi yang mengandung kolesterol, lemak jenuh, dan laktosa. Tingginya prevalensi intoleransi laktosa di Indonesia, mencapai 66% pada orang dewasa [1], mendorong potensi lain sebagai alternatif berbasis nabati. Yoghurt nabati dapat dibuat dari biji-bijian atau kacang-kacangan, seperti kedelai, kacang hijau, kacang merah, biji wijen, dan kacang arab [2]. Dalam 100 gram kacang Arab terdapat sekitar 380 kalori yang disertai dengan kandungan gizi yang cukup lengkap, meliputi 20,5 gram protein, 63 gram karbohidrat, 6 gram lemak, dan 12 gram serat. Selain itu, kacang Arab juga kaya akan vitamin dan mineral penting seperti 550 mikrogram asam folat, 99 mikrogram kolin, 4,3 miligram zat besi, 720 miligram kalium, 80 miligram magnesium, 60 miligram kalsium, 3 miligram zinc serta vitamin B, vitamin E, dan vitamin K [3], sedangkan susu kacang arab (*Cicer arietinum* L.) kaya protein dengan kandungan 23,8 g/100 g [4], serta bebas kolesterol dan laktosa [5].

Meskipun memiliki kandungan gizi tinggi, yoghurt kacang arab memiliki kendala rasa dan aroma, seperti langu dan *aftertaste* pahit akibat senyawa fenolik seperti asam fenolat dan tanin [6], serta aktivitas enzim lipoksigenase yang menurunkan mutu gizi dan menyebabkan *off-flavor* [7]. Perendaman kacang arab dalam larutan natrium bikarbonat dapat mengurangi senyawa penyebab rasa langu dengan memodifikasi struktur protein lipoksigenase sehingga lebih mudah terdegradasi. Efektivitas perendaman terhadap mutu sensorik dan fisikokimia yoghurt kacang arab perlu dievaluasi lebih lanjut.

Kultur probiotik *Lactobacillus casei* dan *Lactobacillus plantarum* tidak hanya mendukung fermentasi dan tekstur yoghurt, tetapi juga berperan mereduksi logam berat melalui mekanisme biosorpsi dan akumulasi. Penelitian Parhusip (2025) menunjukkan rasio probiotik *Bifidobacterium* sp. dan *Lactobacillus* sp. efektif sebagai pereduksi logam berat *in vitro*, sehingga penerapannya pada

FaST - Jurnal Sains dan Teknologi, Vol.10, No. 1, Mei 2026
e-ISSN 2598-9596
DOI: https://doi.org/10.19166/fastjst.v10i1/10960
Available online at: https://ojs.uph.edu/index.php/FaSTJST/article/view/10960

yoghurt kacang arab dapat menambah nilai fungsional bagi penderita intoleransi laktosa dan diabetes [8].

Produk yoghurt biasanya diberi pemanis untuk meningkatkan rasa, namun pemanis berkalori tinggi kurang aman bagi penderita diabetes [9]. Stevia, pemanis alami dari Stevia rebaudiana, memiliki efek hipoglikemik dan tidak memengaruhi metabolisme insulin sehingga cocok sebagai pemanis rendah kalori dalam yoghurt kacang arab.

Penelitian sebelumnya membuktikan *Lactobacillus* sp. mampu mereduksi logam berat melalui pengikatan dan penyerapan [10], namun penerapannya pada produk pangan fungsional belum tersedia. Penelitian ini menghadirkan kebaruan dengan memanfaatkan *L. casei* dan *L. plantarum* dalam yoghurt berbasis kacang arab yang diperkaya stevia, mengintegrasikan efektivitas probiotik *in vitro* ke produk pangan fungsional yang bebas laktosa, tinggi protein nabati, ramah bagi penderita diabetes, dan berpotensi mendukung detoksifikasi logam berat.

2. Bahan dan Metode

2.1 Bahan dan Alat

Bahan yang digunakan dalam penelitian ini adalah kacang arab Garbanzo yang dibeli secara online, aquadest, soda kue "Kopoe-Kopoe", susu skim bubuk "Laktona", ekstrak stevia 97% "Nutiver", kultur murni *L. casei*, kultur murni *L. plantarum*, media de Man Rogosa Sharpe Broth (MRSB) "Merck", de Man Rogosa Sharpe Agar (MRSA) "Merck", natrium klorida (NaCl) "Merck", alkohol 70%, pewarna kristal-violet, larutan Iodin, aseton-alkohol, larutan cat Safranin, hidrogen peroksida (H_2O_2) "Smart Lab", sodium dihydrogen fosfat monohidrat ($NaH_2PO_4 \cdot H_2O$) "Smart Lab", dinatrium hidrogen fosfat (Na_2HPO_4) "Smart Lab", indikator fenolftalein 1%, tembaga(II) sulfat pentahidrat (CuSO4·5H2O) "Smart Lab", asam sitrat "Smart Lab", natrium karbonat anhidrat (Na_2CO_3) "Smart Lab", HCl pekat "Smart Lab", kalium iodida (KI) "Smart Lab", asam sulfat (H_2SO_4) "Smart Lab", natrium thiosulfat ($Na_2S_2O_3$) "Smart Lab", *starch indicator,* kalium sulfat (K_2SO_4) "Smart Lab", selenium "Smart Lab", asam borat "Smart Lab", asam linoleat "Smart Lab", Tween-20 "Smart Lab", natrium borat "Smart Lab", natrium hidroksida (NaOH) "Smart Lab".

Alat yang digunakan dalam penelitian ini adalah *steamer*, kompor, *blender*, kain saring, *heater*, termometer, *water bath* "Memmert", timbangan analitik "AS ONE", mikropipet, tip, pipet tetes, mikroskop, bunsen, *tray*, pH meter, cawan petri *disposable*, penjepit kayu, tabung reaksi, jarum ose, *colony counter* "Prio", spidol, gelas beaker "Iwaki", erlenmeyer "Iwaki", labu takar "Iwaki", buret "Iwaki", corong, gelas ukur "Iwaki", pipet volumetric "Iwaki", *rubber bulb*, labu Kjeldahl, alat destilasi "Buchi", batang pengaduk, *kuvet quartz,*, mesin sentrifugasi "Hermle", lemari asam, spektrofotometer UV-vis "DLAB SP-V1000", autoklaf "Gea", inkubator "Memmert", *vortex* "Hwashin", *aluminium foil*, *magnetic stirrer*, *colony counter* "Prio", dan *laminar air flow*.

2.2 Prosedur Penelitian

Prosedur penelitian diawali dengan tahap persiapan kultur dan pembuatan starter yoghurt, pembuatan susu kacang arab, serta pembuatan yoghurt susu kacang arab yang dilanjutkan dengan analisis parameter kimia, mikrobiologi, dan sensori. Pada tahap awal, kultur bakteri *Lactobacillus casei* dan *Lactobacillus plantarum* disiapkan sebagai kultur stok, kemudian disegarkan menjadi kultur kerja menggunakan media MRSB dengan inkubasi pada suhu 37°C selama 24 jam. Kultur kerja selanjutnya diuji kemurniannya melalui pewarnaan Gram dan uji katalase [11] sebelum digunakan sebagai starter yoghurt, yaitu dengan menginokulasikan 10 mL kultur ke dalam 90 mL susu skim yang telah dipanaskan dan diinkubasi pada suhu 37°C selama 24 jam.

Tahap berikutnya adalah pembuatan susu kacang arab dengan dua faktor perlakuan, yaitu konsentrasi natrium bikarbonat (0%, 1%, 2%, dan 3%) serta waktu perendaman (8, 16, dan 24 jam) pada suhu ruang. Setelah perendaman, kacang arab diuji aktivitas enzim lipoksigenase [12], kemudian ditiriskan, dikupas, dikukus, dan ditambahkan air dengan perbandingan 1:8, disaring, serta dipanaskan pada suhu 85–90°C selama 30 menit hingga diperoleh susu kacang arab. Susu yang dihasilkan kemudian digunakan dalam pembuatan yoghurt dengan penambahan susu skim bubuk 10% (b/v) dan ekstrak stevia pada konsentrasi 0,04%, 0,09%, dan 0,13%, kemudian dihomogenkan. Campuran dipanaskan pada suhu 85°C selama 15 menit dan didinginkan hingga 40°C sebelum diinokulasi starter yoghurt sebanyak 3%

FaST - Jurnal Sains dan Teknologi, Vol.10, No. 1, Mei 2026
e-ISSN 2598-9596
DOI: https://doi.org/10.19166/fastjst.v10i1/10960
Available online at: https://ojs.uph.edu/index.php/FaSTJST/article/view/10960

dengan variasi rasio *L. casei* dan *L. plantarum* yaitu 1:0, 1:1, 2:1, 1:2, dan 0:1, lalu diinkubasi pada suhu 37°C selama 16 jam.

Penelitian ini disusun menggunakan rancangan faktorial dengan tiga faktor perlakuan, yaitu konsentrasi natrium bikarbonat, waktu perendaman, dan rasio kultur bakteri, sehingga diperoleh sejumlah kombinasi perlakuan yang masing-masing dilakukan sebanyak tiga kali ulangan. Setiap perlakuan dianalisis terhadap parameter pH [13], total asam tertitrasi [14], total bakteri asam laktat [15], total gula metode Luff Schoorl [16], serta total protein metode Kjeldahl [17], dan dilengkapi dengan uji sensori berupa uji skoring dan hedonik. Data yang diperoleh dianalisis menggunakan analisis sidik ragam (ANOVA) pada taraf kepercayaan 95%, dan apabila terdapat perbedaan nyata dilanjutkan dengan uji lanjut Duncan's Multiple Range Test (DMRT) untuk mengetahui perbedaan antar perlakuan.

3 Hasil dan Pembahasan

3.1 Hasil Identifikasi Probiotik *L. casei* dan *L. Plantarum*

Identifikasi bakteri probiotik *L. casei* dan *L. plantarum* dilakukan melalui pewarnaan Gram, uji morfologi, dan uji katalase. Hasil identifikasi *L. casei* dan *L. plantarum* dapat dilihat pada **Tabel 1**.

Tabel 1. Hasil identifikasi *L. casei* dan *L. plantarum*

Kultur BAL	Pewarnaan Gram	Bentuk	Uji Katalase
L. casei	+	Basil	-
L. plantarum	+	Basil	-

Hasil pewarnaan Gram kultur kerja bakteri *L. casei* dan *L. plantarum* menunjukkan bahwa kedua kultur bakteri tergolong sebagai bakteri Gram positif berdasarkan warna ungu kebiruan pada sel. Perbedaan warna pada hasil uji Gram positif negatif menunjukkan adanya perbedaan struktur pada dinding sel bakteri. Struktur dinding sel bakteri Gram positif memiliki kandungan peptidoglikan yang tebal, berbeda dengan bakteri Gram negatif yang memiliki struktur dinding sel dengan kandungan lipid yang tinggi [18]. Pengamatan morfologi bakteri *L. casei* dan *L. plantarum* menunjukkan bahwa kedua bakteri berbentuk basil, sesuai dengan karakteristik umum *Lactobacillus* [18]. Pada hasil uji katalase, tidak terbentuknya gelembung gas pada kedua isolat bakteri menunjukkan bahwa kedua bakteri merupakan bakteri katalase negative, sesuai dengan sifat bakteri asam laktat *L. casei* dan *L. plantarum.*

3.2 Aktivitas Enzim Lipoksigenase Kacang Arab dengan Perendaman Natrium Bikarbonat

Aktivitas enzim lipoksigenase kacang arab yang telah direndam dalam larutan natrium bikarbonat dengan konsentrasi dan waktu perendaman yang berbeda dapat dilihat pada Gambar 1.

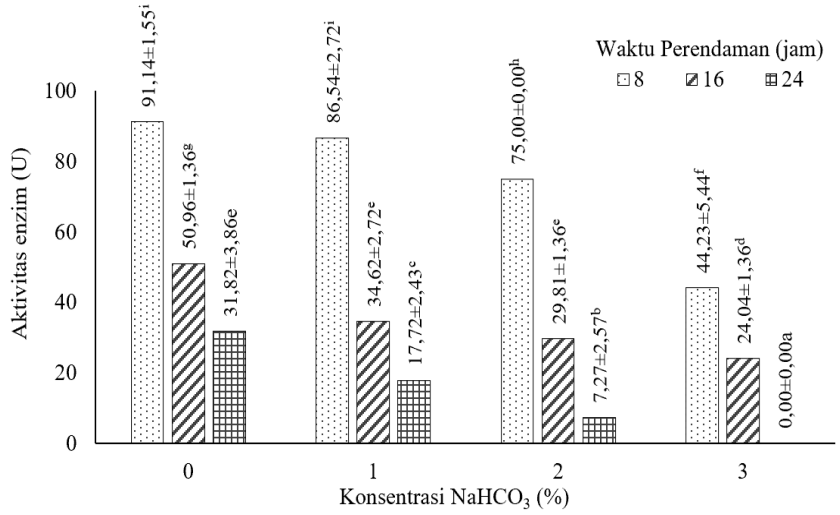

Gambar 1. Hasil uji aktivitas enzim lipoksigenase kacang arab
Keterangan: Perbedaan notasi huruf menunjukkan perbedaan yang signifikan (p≤0,05)

FaST - Jurnal Sains dan Teknologi, Vol.10, No. 1, Mei 2026
e-ISSN 2598-9596
DOI: https://doi.org/10.19166/fastjst.v10i1/10960
Available online at: https://ojs.uph.edu/index.php/FaSTJST/article/view/10960

Aktivitas enzim lipoksigenase-1 pada kacang arab, yang didefinisikan sebagai satu unit enzim (U) setara dengan peningkatan absorbansi 1,0 per menit pada 234 nm, bervariasi antara 0 hingga 91,14 U kacang arab. Aktivitas tertinggi masih terdeteksi pada perlakuan perendaman tanpa penambahan $NaHCO_3$ (0%) selama 8 jam sebesar 91,14±1,55 U, menunjukkan bahwa perlakuan tersebut belum efektif dalam menginaktivasi enzim. Sebaliknya, perendaman selama 24 jam dengan penambahan 3% $NaHCO_3$ menghasilkan aktivitas lipoksigenase yang tidak terdeteksi (0,00±0,00 U), yang mengindikasikan terjadinya inaktivasi enzim akibat perubahan pH dan kerusakan struktur protein enzim oleh paparan basa dalam waktu lama, enzim lipoksigenase memiliki ph aktivasi optimal yang berkisar dari 6 sampai 7 [19]. Inaktivasi lipoksigenase ini berkontribusi pada penurunan rasa kacang atau *beany flavor*, yang umumnya disebabkan oleh pembentukan senyawa karbonil rantai pendek hasil oksidasi asam lemak tak jenuh ganda yang dikatalisis oleh lipoksigenase [20], sehingga perendaman dengan $NaHCO_3$ 3% selama 24 jam dapat dianggap sebagai perlakuan paling efektif untuk memperbaiki mutu sensori yoghurt susu kacang arab.

3.3 Pengaruh Rasio *Starter* Yoghurt dan Konsentrasi Stevia terhadap Yoghurt Susu Kacang Arab

3.3.1 Nilai pH

Nilai pH merupakan salah satu indikator penting untuk menentukan tingkat keasaman dan kualitas produk yoghurt susu kacang arab. Nilai pH yoghurt susu kacang arab pada berbagai rasio *starter L. casei* dan *L. plantarum* serta adanya perbedaan konsentrasi stevia dapat dilihat pada **Gambar 2**.

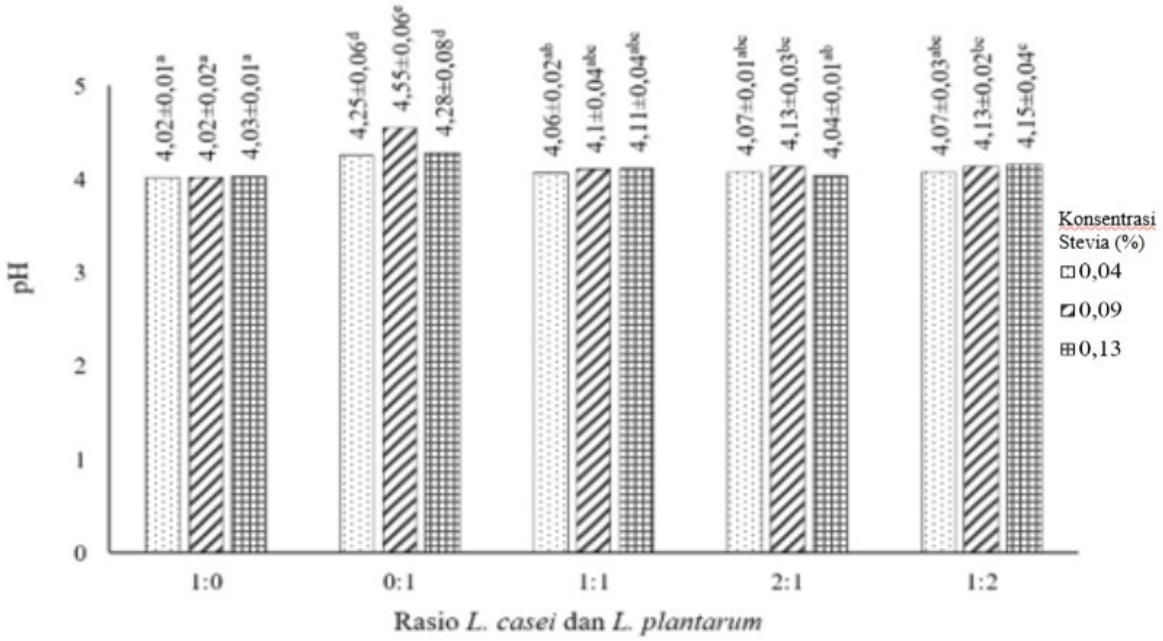

Gambar 2. Grafik nilai pH yoghurt susu kacang arab
Keterangan: Perbedaan notasi huruf menunjukkan perbedaan yang signifikan (p≤0,05)

Nilai pH yoghurt susu kacang arab yang dihasilkan berada pada kisaran 4,01 hingga 4,54, masih sesuai dengan batasan pH ideal produk yoghurt menurut SNI yaitu 3,80-4,50. Nilai pH tertinggi (4,55±0,06) dan terendah (4,02±0,01) diperoleh menunjukkan perbedaan kemampuan bakteri dalam memproduksi asam laktat. *L. plantarum* dinilai lebih efisien pada substrat nabati sehingga dapat mempertahankan pH fermentasi dengan lebih stabil [21], sedangkan *L. casei* cenderung menghasilkan produksi asam lebih intensif sehingga menurunkan pH [22]. Perlakuan terbaik untuk memperoleh pH stabil adalah stevia 0,04% atau 0,09% dengan rasio *starter* 1:0, yang menghasilkan pH 4,02±0,01 dan 4,02±0,02. Kombinasi ini efektif mempertahankan stabilitas protein dan karakteristik yoghurt karena *L. casei* mampu mempercepat penurunan pH pada bahan nabati dengan menghasilkan asam laktat [23]. Karbohidrat dipecah menjadi bentuk monosakarida pada fermentasi asam laktat. Monosakarida diubah menjadi asam laktat dengan bantuan enzim laktase dehidrogenase yang dihasilkan oleh bakteri asam laktat melalui jalur *Embden Meyerhoff Parnas* (EMP). Asam laktat dibentuk melalui jalur EMP, glukosa dirombak menjadi piruvat, lalu diubah menjadi asam laktat dengan bantuan enzim laktase dehidrogenase

FaST - Jurnal Sains dan Teknologi, Vol.10, No. 1, Mei 2026
e-ISSN 2598-9596
DOI: https://doi.org/10.19166/fastjst.v10i1/10960
Available online at: https://ojs.uph.edu/index.php/FaSTJST/article/view/10960

[24]. Metabolisme karbohidrat *L. plantarum* sebagai bakteri homofermentatif melalui jalur EMP seharusnya dapat menunjukkan kemampuan penurunan pH yang lebih baik selama fermentasi dibandingkan dengan *L. casei.*

3.3.2 Total Asam Tertitrasi

Total asam tertitrasi merupakan nilai yang menunjukkan jumlah asam laktat yang terkandung dalam yoghurt. Hasil analisis total asam tertitrasi (TAT) yoghurt susu kacang arab dapat dilihat pada **Gambar 3**.

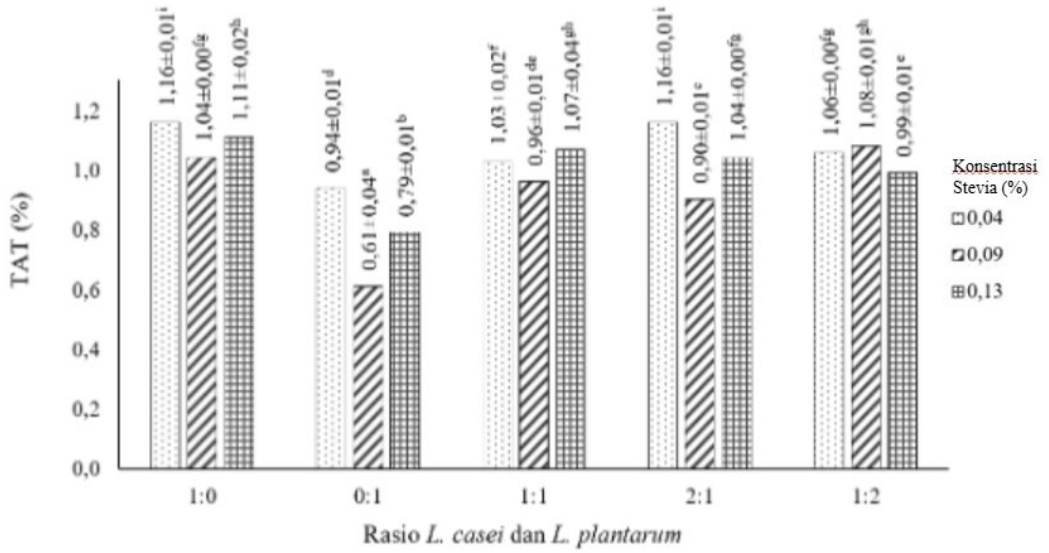

Gambar 3. Grafik total asam tertitrasi yoghurt susu kacang arab
Keterangan: Perbedaan notasi huruf menunjukkan perbedaan yang signifikan (p≤0,05)

Total asam tertitrasi (TAT) menunjukkan kadar asam laktat dalam yoghurt sebagai hasil fermentasi laktosa oleh bakteri asam laktat. Menurut SNI 2981:2009, kadar asam laktat pada yoghurt probiotik yang memenuhi standar berada pada kisaran 0,5-2,0%. Nilai TAT pada yoghurt susu kacang arab berbeda signifikan akibat variasi rasio bakteri *starter* dan konsentrasi stevia. Kadar asam laktat tertinggi terdapat pada yoghurt dengan stevia 0,04% dan rasio *starter* 1:0 atau 2:1 (1,16±0,01 dan 1,16±0,00), sedangkan terendah pada rasio 0:1 dengan stevia 0,09% (0,61 ± 0,04). Penggunaan starter *L. casei* pada yoghurt berbahan dasar nabati memberikan kontribusi besar terhadap pembentukan asam laktat karena aktivitas glikolisisnya yang lebih efisien dibandingkan bakteri lain, namun proses ini dapat terhambat pada konsentrasi stevia 0,10% akibat perubahan tekanan osmotik atau interaksi komponen yang mengganggu sel bakteri dan dikarenakan stevia dapat berperan sebagai antibakteri, antiinflamasi, dan antifungi, sehingga dapat menghambat pertumbuhan bakteri dan asam laktat yang dihasilkan selama proses fermentasi akan berkurang [25]. Berdasarkan analisis statistik, efisiensi fermentasi terbaik dicapai pada penggunaan stevia 0,04% dengan rasio starter 1:0 atau 2:1, yang secara efektif menghasilkan nilai Total Asam Tertitrasi (TAT) maksimum dan keasaman konsisten sesuai standar SNI 2981:2009 tanpa menghambat metabolisme mikroorganisme [21].

3.3.3 Total Bakteri Asam Laktat

Total bakteri asam laktat (BAL) merupakan indikator utama keberhasilan proses fermentasi karena bakteri asam laktat berperan dalam produksi asam laktat, menyebabkan penurunan pH, dan pembentukan karakteristik yoghurt. Jumlah total bakteri asam laktat dihitung dan dinyatakan dalam satuan log CFU/ml. Jumlah bakteri asam laktat terdapat pada yoghurt susu kacang arab dapat dilihat pada **Gambar 4**.

FaST - Jurnal Sains dan Teknologi, Vol.10, No. 1, Mei 2026
e-ISSN 2598-9596
DOI: https://doi.org/10.19166/fastjst.v10i1/10960
Available online at: https://ojs.uph.edu/index.php/FaSTJST/article/view/10960

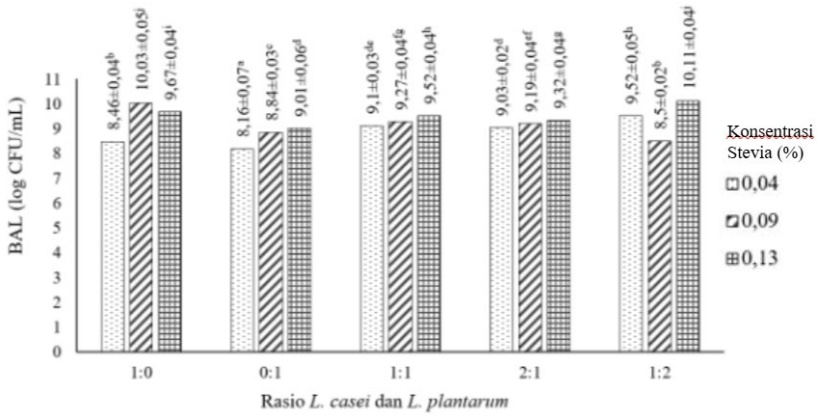

Gambar 4. Grafik total bakteri asam laktat yoghurt susu kacang arab
Keterangan: Perbedaan notasi huruf menunjukkan perbedaan yang signifikan (p≤0,05)

Total bakteri asam laktat (BAL) merupakan indikator utama keberhasilan fermentasi karena berperan dalam produksi asam laktat, penurunan pH, dan pembentukan karakteristik yoghurt. Menurut SNI 2981:2009, yoghurt harus mengandung minimal 10^7 CFU/mL bakteri hidup agar memenuhi standar mikrobiologis. Penggunaan kombinasi kedua isolat bakteri dapat meningkatkan jumlah asam laktat dan populasi BAL secara lebih efektif dibandingkan isolat tunggal dikarenakan jumlah metabolit yang terbentuk diduga menjadi lebih besar dan populasi bakteri asam laktat dapat meningkat [26]. Perbedaan yang terjadi kemungkinan disebabkan kemampuan adaptasi *Lactobacillus plantarum* yang lebih baik pada media fermentasi dengan stevia, meskipun senyawa aktif stevia dapat menghambat pertumbuhan bakteri [27]. Total bakteri asam laktat pada produk yoghurt dapat mengalami penurunan seiring dengan peningkatan konsentrasi stevia karena memiliki senyawa steviosida yang bersifat antibakteri [28]. Stevisoda dapat menghambat pertumbuhan pada bakteri *Streptococcus mutans, Lactobacillus plantarum* dan *Lactobacillus casei* [29]. Namun penggunaan konsentrasi stevia pada konsentrasi rendah (0,025-0,3%) diketahui tidak memberikan efek pada pertumbuhan aktivitas bakteri asam laktat [25].

3.3.4 Total Gula

Total gula pada yoghurt mencakup seluruh kandungan gula dari bahan baku maupun yang terbentuk selama fermentasi, di mana sebagian gula dikonversi oleh bakteri asam laktat menjadi asam laktat dan metabolit lain [25]. Hasil analisis total gula pada yoghurt susu kacang arab dapat dilihat pada **Gambar 5**.

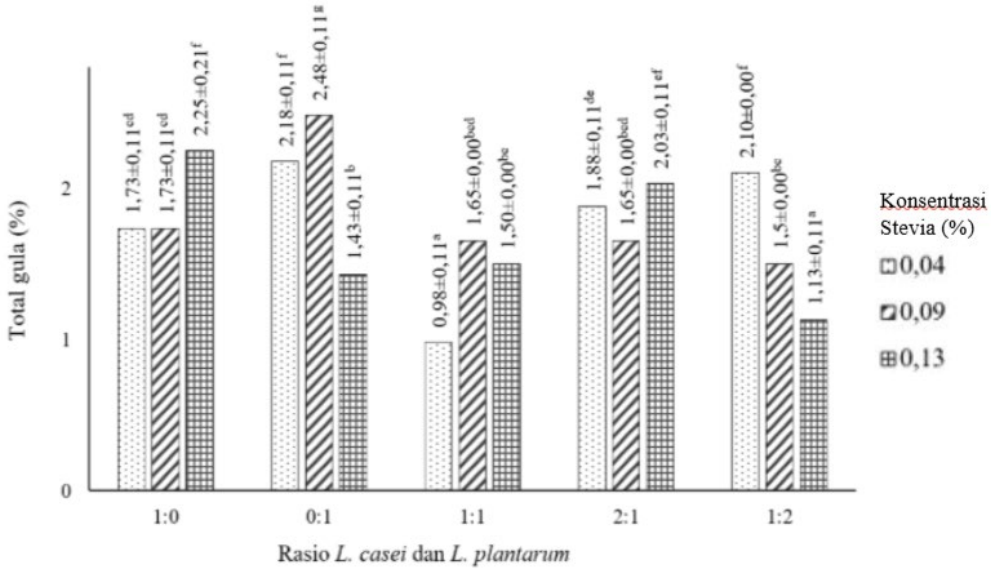

Gambar 5. Grafik total gula yoghurt susu kacang arab
Keterangan: Perbedaan notasi huruf menunjukkan perbedaan yang signifikan (p≤0,05)

FaST - Jurnal Sains dan Teknologi, Vol.10, No. 1, Mei 2026
e-ISSN 2598-9596
DOI: https://doi.org/10.19166/fastjst.v10i1/10960
Available online at: https://ojs.uph.edu/index.php/FaSTJST/article/view/10960

Tingginya total gula pada rasio 0:1 disebabkan *L. plantarum* memanfaatkan karbohidrat lebih lambat, sedangkan sinergi kedua bakteri pada rasio 1:1 mempercepat metabolisme gula, menghasilkan kadar gula terendah [30][31]. Perlakuan rasio 1:1 dengan stevia 0,04% dianggap paling baik karena fermentasi berlangsung paling efisien. Glukosa dimanfaatkan oleh *L. casei* dan *L. plantarum* sebagai sumber energi dan bagian lainnya dimetabolisme lebih lanjut menjadi asam-asam organik, terutama asam laktat. Kandungan gula pada pemanis stevia tidak dapat difermentasi oleh bakteri. Glikosida yang terkandung dalam stevia, seperti rebaudiosida dan steviosida tidak dapat difermentasi oleh bakteri asam laktat [32]. Penambahan stevia dapat menyebabkan jumlah bakteri asam laktat yang terbentuk menjadi lebih sedikit, sehingga gula yang diubah menjadi asam organik semakin berkurang dan sisa gula menjadi lebih banyak [33].

3.3.5 Kadar Protein

Selama proses fermentasi berlangsung, bakteri asam laktat memiliki aktivitas proteolitik yang dapat memecah protein menjadi peptida dan asam amino. Kadar protein yoghurt susu kacang arab dapat dilihat pada **Gambar 6**.

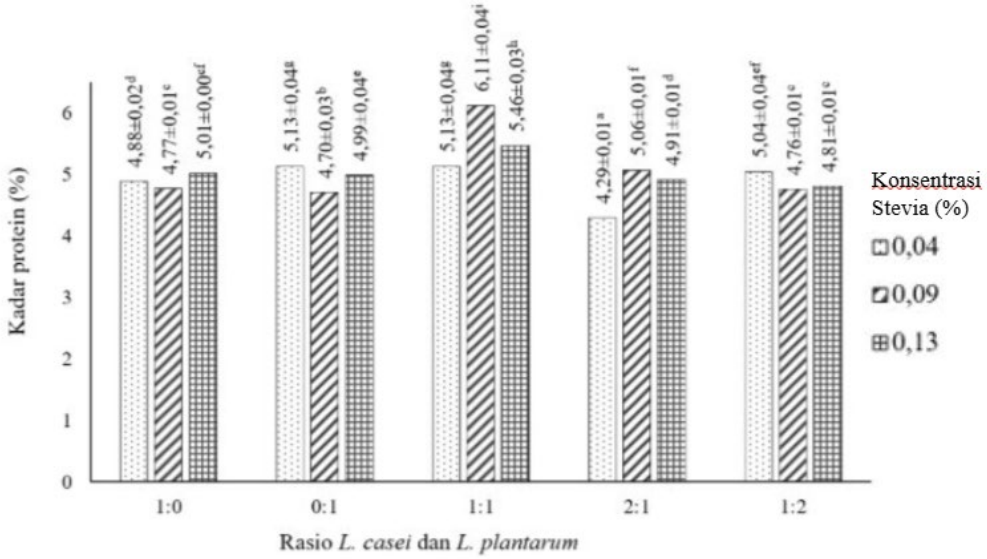

Gambar 6. Grafik kadar protein yoghurt susu kacang arab
Keterangan: Perbedaan notasi huruf menunjukkan perbedaan yang signifikan (p≤0,05)

Total protein pada yoghurt dipengaruhi oleh kandungan protein bahan baku, yaitu susu dan kacang arab, serta aktivitas proteolitik bakteri asam laktat yang memecah protein menjadi peptida dan asam amino, meningkatkan kecernaan dan nilai gizi produk. Kadar protein yoghurt susu kacang arab berbeda signifikan antar perlakuan akibat variasi rasio *L. casei* dan *L. plantarum* serta konsentrasi stevia, dengan seluruh perlakuan memenuhi syarat protein minimum 2,7% menurut SNI 2981:2009. Tingginya kadar protein pada rasio 1:1 disebabkan sinergi kedua spesies BAL dalam aktivitas proteolitik melalui mekanisme komplementaritas sistem proteolitik, di mana efisiensi pemecahan protein tidak hanya bergantung pada jumlah protease, tetapi lebih pada keragaman jenis enzim yang dihasilkan. *L. casei* berperan dominan dalam pemecahan awal protein kompleks melalui protease dinding selnya yang kuat, sementara *L. plantarum* menyediakan spektrum peptidase ekstraseluler yang lebih luas untuk mendegradasi peptida tersebut menjadi asam amino bebas. Kerja sama ini menciptakan efek *cross-feeding*, di mana hasil pemecahan satu spesies menjadi nutrisi bagi spesies lainnya, sehingga metabolisme kedua bakteri menjadi lebih aktif dan optimal dalam membongkar struktur protein kacang arab yang kompleks tanpa terhambat oleh konsentrasi stevia 0,09% [34].

Penggunaan konsentrasi stevia 0,13% pada yoghurt susu kacang arab seharusnya masih berada dalam rentang yang mendukung aktivitas bakteri dan berpotensi menghasilkan kadar protein lebih tinggi seiring dengan meningkatnya konsentrasi stevia. Penggunaan konsentrasi stevia yang rendah hingga sedang, yaitu 0,025% hingga 0,3%, diketahui mampu mendukung pertumbuhan aktivitas bakteri asam laktat seperti proteolisis yang berperan dalam pemecahan protein. Hasil uji kadar protein menunjukkan

FaST - Jurnal Sains dan Teknologi, Vol.10, No. 1, Mei 2026
e-ISSN 2598-9596
DOI: https://doi.org/10.19166/fastjst.v10i1/10960
Available online at: https://ojs.uph.edu/index.php/FaSTJST/article/view/10960

bahwa konsentrasi stevia 0,13% belum menghasilkan yoghurt dengan kadar protein yang paling optimal. Hal tersebut diduga adanya efek stevia terhadap aktivitas bakteri asam laktat seperti terjadinya tekanan osmotik atau perubahan lingkungan fermentasi yang dapat menurunkan efisiensi kerja enzim proteolitik, meskipun konsentrasi tersebut belum berada pada jumlah yang dianggap sebagai antibakteri [25].

3.3.6 Uji Skoring

Uji skoring dilakukan untuk menilai intensitas setiap parameter sensori yoghurt susu kacang arab dan mengetahui pengaruh konsentrasi stevia terhadap karakteristik sensori produk. Uji skoring dilakukan terhadap parameter yang meliputi warna, tekstur, aroma, rasa asam, rasa manis, rasa kacang, dan *aftertaste* yoghurt susu kacang arab. Hasil uji skoring ditunjukkan pada **Tabel 2**. Hasil uji skoring menunjukkan bahwa variasi konsentrasi stevia memberikan pengaruh yang berbeda terhadap parameter sensori yoghurt kacang arab. Parameter warna, tekstur, rasa kacang, dan *aftertaste* tidak menunjukkan perbedaan signifikan ($p>0,05$), yang mengindikasikan bahwa penambahan stevia hingga 0,13% tidak cukup untuk mempengaruhi karakter visual maupun sifat fisik yoghurt [35]. Sebaliknya, parameter aroma, rasa asam, dan rasa manis menunjukkan perbedaan signifikan ($p\leq0,05$). Aroma asam tertinggi diperoleh pada konsentrasi stevia 0,09% dan terendah pada 0,13%, kemungkinan akibat interaksi antara intensitas pemanis dan profil aroma asam yoghurt [36]. Rasa manis meningkat seiring bertambahnya konsentrasi stevia, dengan nilai tertinggi pada 0,13%, sesuai dengan karakter stevia sebagai pemanis berintensitas tinggi [37]. Secara keseluruhan, penambahan stevia terutama mempengaruhi aroma, rasa asam, dan rasa manis, sementara parameter sensori lainnya relatif tidak terpengaruh signifikan, sehingga pemanis berperan penting dalam profil rasa tanpa mengubah sifat fisik dan visual yoghurt susu kacang arab. Konsistensi yoghurt lebih dipengaruhi oleh proses fermentasi dan protein nabati dibandingkan dengan efek pemanis stevia yang bersifat non-kalorik.

Tabel 2. Hasil uji skoring yoghurt susu kacang arab

Parameter	Konsentrasi Stevia		
	0,04%	0,09%	0,13%
Warna	3,24±0,94^{a}	2,92±1,07^{a}	3,16±1,11^{a}
Tekstur	4,3±1,02^{a}	4,08±0,92^{a}	4,2±0,99^{a}
Aroma	3,86±0,95^{a}	4,52±0,71^{b}	3,7±1,02^{a}
Rasa Asam	3,78±1,09^{b}	3,78±1,11^{b}	3,2±1,11^{a}
Rasa Manis	4,04±0,97^{a}	4,52±0,84^{b}	5,24±0,8^{c}
Rasa Kacang	2,6±1,2^{a}	2,38±1,05^{a}	2,76±1,2^{a}
Aftertaste	2,04±0,95^{a}	1,88±0,87^{a}	2,02±1,04^{a}

Keterangan: Perbedaan notasi huruf menunjukkan perbedaan yang signifikan ($p\leq0,05$)
1 = sangat tidak kekuningan; sangat tidak kental; sangat tidak beraroma asam; sangat tidak berasa asam; sangat tidak berasa manis; sangat tidak berasa kacang (*beany*); sangat tidak pahit
6 = sangat kekuningan; sangat kental; sangat beraroma asam; sangat berasa asam; sangat berasa manis; sangat berasa kacang (*beany*); sangat pahit

3.3.7 Uji Hedonik

Uji hedonik dilakukan untuk menilai tingkat kesukaan panelis terhadap yoghurt susu kacang arab sehingga dapat diketahui pengaruh variasi konsentrasi stevia terhadap tingkat penerimaan produk. Penilaian meliputi parameter warna, tekstur, aroma asam, rasa asam, rasa manis, rasa kacang, *aftertaste*, dan kesukaan secara keseluruhan. Hasil uji hedonik yoghurt susu kacang arab dapat dilihat pada **Tabel 3**.

Tabel 3. Hasil uji hedonik yoghurt susu kacang arab

Parameter	Konsentrasi Stevia		
	0,04%	0,09%	0,13%
Warna	5,3±1,04^{a}	5,64±0,85^{a}	5,48±0,91^{a}
Tekstur	5,44±1,16^{a}	5,3±1,28^{a}	5,46±1,23^{a}

FaST - Jurnal Sains dan Teknologi, Vol.10, No. 1, Mei 2026
e-ISSN 2598-9596
DOI: https://doi.org/10.19166/fastjst.v10i1/10960
Available online at: https://ojs.uph.edu/index.php/FaSTJST/article/view/10960

Aroma	4,92±1,37[a]	5,22±1,25[a]	5,1±1,3[a]
Rasa Asam	4,84±1,3[a]	5,32±1,15[a]	4,8±1,5[a]
Rasa Manis	4,96±1,18[a]	5,12±1,29[a]	4,98±1,55[a]
Rasa Kacang	4,68±1,6[a]	5,06±1,5[a]	4,72±1,64[a]
Aftertaste	4,98±1,56[a]	5,44±1,3[a]	5,14±1,63[a]
Keseluruhan	5,02±1,17[a]	5,36±0,96[a]	5,06±1,33[a]

Keterangan: Perbedaan notasi huruf menunjukkan perbedaan yang signifikan (p≤0,05)
1 = sangat tidak suka
7 = sangat suka

Hasil uji hedonik menunjukkan bahwa penambahan stevia pada yoghurt susu kacang arab pada konsentrasi 0,04%, 0,09%, dan 0,13% tidak menimbulkan perbedaan signifikan pada seluruh parameter sensori hedonik, termasuk warna, tekstur, aroma, rasa asam, rasa manis, rasa kacang, *aftertaste*, dan penilaian keseluruhan. Yoghurt dengan stevia 0,09% cenderung memperoleh skor tertinggi pada hampir semua atribut, seperti warna (5,64±0,85[a]), aroma (5,22±1,25[a]), rasa asam (5,32±1,15[a]), rasa manis (5,12±1,29[a]), *aftertaste* (5,44±1,3[a]), dan keseluruhan (5,36±0,96[a]), sedangkan nilai terendah sering ditemukan pada stevia 0,04%. Konsentrasi 0,09% memberikan keseimbangan rasa yang disukai panelis tanpa menimbulkan *aftertaste* yang mengganggu. Stevia sebagai pemanis alami non-kalori tidak mengubah tekstur, konsistensi, atau karakter fisik yoghurt secara signifikan, sehingga penerimaan keseluruhan tetap tinggi [35]. Penggunaan konsentrasi optimal 0,09% efektif sebagai pengganti gula konvensional tanpa merusak karakter sensori yoghurt [38]. Tingkat kemanisan yang sesuai dapat mendukung atribut lain dalam yoghurt susu kacang arab tanpa menimbulkan *aftertaste* mengganggu atau merusak karakteristik alami yoghurt seperti rasa asam.

4. Kesimpulan

Penelitian ini menunjukkan bahwa waktu perendaman kacang arab terbaik untuk menonaktifkan enzim lipoksigenase terdapat pada waktu 24 jam menggunakan kosnentrasi natrium bikarbonat 3%, menunjukkan tidak ada aktivitas enzim lipoksigenase. Variasi rasio *Lactobacillus casei* dan *Lactobacillus plantarum* serta konsentrasi stevia dalam pembuatan yoghurt susu kacang arab memengaruhi karakteristik kimia, mikrobiologis, dan sensori yoghurt. Formulasi dengan rasio bakteri 1:1 dan stevia 0,09% memberikan hasil paling optimal, ditunjukkan oleh pH (4,1±0,04), protein (6,1±0,04%), asam laktat (0,96±0,01%), total gula (1,65±0,00%), efisiensi fermentasi baik, viabilitas BAL tinggi (9,27±0,04 log CFU), serta tingkat penerimaan sensori tertinggi, sehingga kombinasi ini direkomendasikan sebagai formulasi terbaik untuk yoghurt susu kacang arab berkualitas kimia, mikrobiologi, dan sensori optimal.

Ucapan Terimakasih

Ucapan terima kasih disampaikan kepada Lembaga Pengabdian Pada Masyarakat (LPPM) Universitas Pelita Harapan (UPH) atas pendanaan yang diberikan untuk Penelitian Internal dengan nomor kontrak: P-023-DDS-FaST/VII/2025, serta Laboratorium Mikrobiologi - Teknologi Pangan UPH.

Daftar Pustaka

[1] B. Santoso, "Prevalensi Intoleransi Laktosa Pada Orang Dewasa di Indonesia, " *Jurnal Gizi Klinis*, vol. 9, no. 2, hlm. 56–60, 2017.

[2] R. K. Ikhwan, L. Kurniawati, dan N. Suhartatik, "Karakteristik Yoghurt Susu Wijen (Sesamun Indicum L.) dengan Variasi Penambahan Susu Skim," *Jurnal Teknologi dan Industri Pangan*, vol. 3, no. 2, hlm. 95–105, 2018. https://doi.org/10.33061/jitipari.v3i2.2691.

[3] Kemenkes. (2022). 9 Manfaat Kacang Arab yang Sayang untuk Dilewatkan. https://www.alodokter.com/jangan-lewatkan-segudang-manfaat-kacang-arab-ini. (Diakses pada 5 Mei 2026),

[4] T. C. Wallace, "*The Nutritional Value and Health Benefits of Chickpeas and Hummus*," *Nutrients*, vol. 8, no. 12, hlm. 766, 2016. https://doi.org/10.3390/nu8120766.

[5] W. S. U. Roland, L. Pouvreau, J. Curran, F. Van De Velde, dan P. M. T. De Kok, "*Flavor Aspects of Pulse Ingredients*," *Cereal Chemistry*, vol. 94, no. 1, hlm. 58–65, 2017. https://doi.org/10.1094/CCHEM-06-16-0161-FI.

[6] A. A. Ismayasari, Wahyuningsih, dan O. Paramita, "Studi Eksperimen Pembuatan Enting-enting dengan Bahan Dasar Kedelai Sebagai Bahan Pengganti Kacang Tanah," *Food Science and Culinary Education Journal.*, vol. 3, no. 1, 2014. https://doi.org/10.21776/ub.jpa.2021.009.02.4.

[7] A. Randa, Yusmarini, dan Y. Zalfiatri, "Pemanfaatan NaHCO3 dalam Pembuatan Tempe Berbahan Baku Biji Nangka dan Biji Saga," *Jom FAPERTA*, vol. 4, no. 2, 2017.

[8] A. J. N. Parhusip dan Dipakalyano, *"*Kombinasi Probiotik *Bifidobacterium bifidum* dan *Lactobacillus fermentum* untuk Mereduksi Logam Arsen, Kadmium, dan Tembaga*",* 2025.

[9] W.N. Munawaroh dan Indratiningsih, "Produksi *Low Calorie Sweet Bio-yoghurt* dengan Penambahan Ekstrak Daun Stevia (*Stevia Rebaudiana*) Sebagai Pengganti Gula," *Agritech*, vol. 35, no. 4, 2015. 10.22146/agritech.9331

[10] J. N. Bhakta, Y. Munekage, K. Ohnishi, dan B. B. Jana, "Isolation and Identification of Cadmium- and Lead-Resistant Lactic Acid Bacteria for Application as Metal Removing Probiotic," *International Journal of Environmental Science and Technology*, vol. 9, hlm. 433–440, 2012. https://doi.org/10.1007/s13762-012-0049-3.

[11] W. Rahmatullah, E. Novianti, dan A. D. L. Sari, "Identifikasi Bakteri Udara Menggunakan Teknik Pewarnaan Gram," *Jurnal Ilmu Kesehatan Bhakti Setya Medika*, vol. 6, no. 2, hlm. 83–91, 2021. 10.56727/bsm.v6i2.62

[12] S. Ciabotti, A. C. P. Juhász, J. M. G. Mandarino, L. L. Costa, A. D. Corrêa, A. A. Simão, dan E. N. F. Santos, "*Chemical Composition and Lipoxygenase Activity of Soybean* (*Glycine max* L. Merrill.) *Genotypes for Human Consumption with Different Tegument Colours*," *Brazilian Journal Of Food Technology*, vol. 22, hlm. e2018003, 2019. https://doi.org/10.1590/1981-6723.00318.

[13] R. Hidayat, "Total Bakteri Asam Laktat, Nilai pH dan Sifat Organoleptik Drink Yoghurt Dari Susu Sapi yang Diperkaya dengan Ekstrak Buah Mangga," *Animal Agriculture Journal*, vol. 2, no. 1, hlm. 160–167, 2013.

[14] Association of Official Analytical Collaboration (AOAC), *Official Methods of Analysis of AOAC International*, edisi ke-20. Gaithersburg, MD, USA: AOAC International, 2016.

[15] J. M. Jay, *Modern Food Microbiology*, edisi ke-6. Maryland, US: Aspen Publisher, 2000.

[16] Zuhairiah, E. Ginting, D. Romatua, dan F. Fahdi, "Identifikasi Kadar Glukosa dan Sukrosa pada Madu Hutan," *Jurnal Penelitian Farmasi & Herbal*, vol. 1, no. 2, hlm. 5–10, 2019. https://doi.org/10.36656/jpfh.v1i2.62.

[17] *Association of Official Analytical Chemist (AOAC), Official Methods of Analysis, edisi ke-18. United States of America: Association of Official Analytical Chemist, Inc*., 2010.

[18] S. Nurhidayati, Faturrahman, dan M. Ghazali, "Deteksi Bakteri Patogen yang Berasosiasi dengan *Kappaphycus alvarezii* (Doty) Bergejala Penyakit Ice-Ice," *Jurnal Sains Teknologi & Lingkungan*, vol. 1, no. 2, 2015. https://doi.org/10.29303/jstl.v1i2.53

[19] G. N., Inayah, A. Rahamadayanti, A. Argiyanti, R. I. Sukma, B. Supriatno, & S. Anggraeni (2022). Alternatif kegiatan praktikum tingkat SMA: Pengaruh pH terhadap hasil kerja katalase menggunakan respirometer Ganong. *Edukatif: Jurnal Ilmu Pendidikan*, *4*(4), 5501–5510. https://doi.org/10.31004/edukatif.v4i4.3289

[20] E. J. Quinto, P. Jiménez, I. Caro, J. Tejero, J. Mateo, dan T. Girbés, "*Probiotic Lactic Acid Bacteria: A Review,*" *Food and Nutrition Sciences*, vol. 5, hlm. 1765–1775, 2014. https://doi.org/10.4236/fns.2014.518190.

[21] X. Yang, J. Hong, L. Wang, C. Cai, H. Mo, J. Wang, X. Fang, dan Z. Liao, "*Effect of Lactic Acid Bacteria Fermentation on Plant-Based Products,*" *Fermentation*, vol. 10, no. 1, hlm. 48, 2024. https://doi.org/10.3390/fermentation10010048.

[22] A. J. N. Parhusip, J. Fraulencia, Alfredo, E. Kristianto, F. M. N. Sanaky, N. A. Anugrahati, dan C. J. Kurniawan, "*Microencapsulation of Probiotic Lactic Acid Bacteria Using Freeze-Drying with Isolated Whey Protein and Trehalose as Coating Material*," *Jurnal Teknologi & Industri Hasil Pertanian*, vol. 29, no. 1, hlm. 168–175, 2024. https://doi.org/10.23960/jtihp.v29i1

[23] N. A. Usman, K. Suradi, dan J. Gumilar, "Pengaruh Konsentrasi Bakteri Asam Laktat *Lactobacillus plantarum* dan *Lactobacillus casei* Terhadap Mutu Mikrobiologi dan Kimia Mayonnaise Probiotik," *Jurnal Ilmu Ternak*, vol. 18, no. 2, hlm. 79–85, 2018. https://doi.org/10.24198/jit.v18i2.19771.

[24] D. Wahyuningsih, W. W. Hidayah, dan A. L. N. Aminin, "*Jelly Fermented Soy Whey as Antioxidants Source of Alternative Functional Food*," *Jurnal Sains dan Matematika*, vol. 22, no. 3, hlm. 67–71, 2014.

[25] A. V. A. Putri, N. Hafida, dan V. Megawati, "Pengaruh Daya Antibakteri Ekstrak Daun Stevia (*Stevia rebaudiana* Bertoni) pada Konsentrasi 5%, 10%, 20%, 40% dan 80% Terhadap *Streptococcus mutans* (*In Vitro*)," *Jurnal Ilmu Kedokteran Gigi*, 2017. https://doi.org/10.23917/jikg.v13i2.4147

[26] P. A. Retnowati dan J. Kusnadi, "Pembuatan Minuman Probiotik Sari Buah Kurma (*Phoenix dactylifera*) dengan Isolat *Lactobacillus casei* dan *Lactobacillus plantarum,*" *Jurnal Pangan dan Agroindustri*, vol. 2, no. 2, hlm. 70–81, 2014.

[27] Y. Wenda, P. M. Wowor, dan M. A. Leman, "Uji Daya Hambat Ekstrak Daun Stevia *(Stevia rebaudiana* Bertoni M.) Terhadap Pertumbuhan *Staphylococcus aureus* Secara *In Vitro*," *E-GiGi*, vol. 5, no. 1, 2017. https://doi.org/10.35790/eg.5.1.2017.15416.

[28] C. Tandrian, Nurwantoro, dan B. Dwiloka, "Pengaruh Penambahan Pemanis Alami Daun Stevia Terhadap Total Padatan Terlarut, Total Asam, Total Bakteri Asam Laktat, dan Tingkat Kesukaan Cocogurt," *Jurnal Teknologi Pangan*, vol. 8, no. 2, hlm. 30–36, 2024. https://doi.org/10.14710/jtp.2024.30014

[29] M. Kishta-Derani, G. F. Neiva, J. R. Boynton, Y. E. Kim, dan M. Fontana, "*The Antimicrobial Potential of Stevia in an In Vitro Microbial Caries Model*," *American Journal of Dentistry*, vol. 29, no. 2, hlm. 87–92, 2016.

[30] K. Khotimah dan J. Kusnadi, "Aktivitas Antibakteri Minuman Probiotik Sari Kurma (*Phoenix dactilyfera* L.) Menggunakan *Lactobacillus plantarum* dan *Lactobacillus casei*," *Jurnal Pangan dan Agroindustri*, vol. 2, no. 3, hlm. 110–120, 2014.

[31] K. Savijoki, H. Ingmer, dan P. Varmanen, "*Proteolytic Systems of Lactic Acid Bacteria*," *Applied Microbiology and Biotechnology*, vol. 70, no. 4, hlm. 394–406, 2006. https://doi.org/10.1007/s00253-006-0427-1.

[32] A. Limanto, "Stevia, Pemanis Pengganti Gula dari Tanaman *Stevia rebaudiana*," *Jurnal Kedokteran Meditek*, vol. 23, no. 61, 2017. https://doi.org/10.36452/jkdoktmeditek.v23i61.1466.

[33] R. A. Sintasari, J. Kusnadi, dan D. W. Ningtyas, "Pengaruh Penambahan Konsentrasi Susu Skim dan Sukrosa Terhadap Karakteristik Minuman Probiotik Sari Beras Merah," *Jurnal Pangan dan Agroindustri*, vol. 2, no. 3, hlm. 65–75, 2014.

[34] A. I. Juliana, M. Amaro, dan N. Nazaruddin, "Pengaruh Konsentrasi Starter Bakteri *Lactobacillus plantarum* Terhadap Beberapa Komponen Mutu Tepung Porang (*Amorphophallus oncophyllus*)," *Pro Food*, vol. 6, no. 2, hlm. 673–684, 2021. https://doi.org/10.29303/profood.v6i2.136.

[35] B. B. Sembiring, Mardiah, dan M. Z. Fanani, "Glikosida Steviol Sebagai Pemanis Rendah Kalori Berbasis Ekstrak Stevia," *Jurnal Ilmiah Pangan Halal*, vol. 6, no. 2, 2024.

[36] R. Tao dan S. Cho, "*Consumer-Based Sensory Characterization of Steviol Glycosides* (*Rebaudioside* A, D, and M)," *Foods*, vol. 9, no. 8, hlm. 1026, 2020. https://doi.org/10.3390/foods9081026.

[37] R. Silva *et al.*, "*Metabolic Adaptability of Lactobacillus plantarum in Plant-Based Fermentation Systems,*" *Frontiers in Microbiology*, vol. 13, 2022. https://doi.org/10.3389/fmicb.2022.846501

[38] D. Chadha, N. Hamid, K. Kantono, dan M. Marsan, "*Changes In Temporal Sensory Profile, Liking, Satiety, and Postconsumption Attributes of Yogurt with Natural Sweeteners,*" *Journal of Food Science*, vol. 87, no. 7, hlm. 3190–3206, 2022. https://doi.org/10.1111/1750-3841.16224.

FaST - Jurnal Sains dan Teknologi, Vol.10, No. 1, Mei 2026
e-ISSN 2598-9596
DOI: https://doi.org/10.19166/fastjst.v10i1/11083
Available online at: https://ojs.uph.edu/index.php/FaSTJST/article/view/11083

Rancang Bangun Aplikasi Urun Dana Berbasis *Website* Untuk Membeli Dan Membagikan Hasil Panen Petani Kepada Masyarakat Pra-Sejahtera

M. Rikza As-subhy[1)]. Junita[1*)], Marincan Pardede[1)]
[1]Program Studi Teknik Elektro, Universitas Pelita Harapan, Tangerang 15811, Indonesia

ABSTRACT

The Indonesian agricultural sector faces structural problems such as low selling prices, instability in the income of small-scale farmers, waste of harvests, and food in*security* among underprivileged communities. This study developed Bagipanen, a web- and Android-based *crowdfunding* application that integrates a socialfunding model with a mechanism for selling harvests on consignment. The system is designed to connect farmers as commodity providers, donors as funding supporters, and underprivileged communities as beneficiaries. Technically, the application is built using *Laravel* for the web platform and Flutter for the *mobile* platform, and is integrated with the *Midtrans payment gateway*. The research methodology focuses on *software* engineering with the application of *testing* through 25 test scenarios covering unit, integration, *end-to-end* (E2E) *testing* using *Laravel* Dusk, performance, and *security*, with a success rate of 100%. E2E *testing* results showed an average execution time of 5.35 seconds per scenario, while payment *integration testing* showed a failure rate of 0%, an average response time of 320 ms, and successful handling of idempotent *callback*s. Performance *testing* recorded a throughput of 33.96 requests/second with a maximum response time of 850 ms at peak load. *Software* quality analysis showed 87.8% test coverage, 2.3% code duplication, and no critical *security* vulnerabilities were found.

ARTICLE INFO

Keywords: *crowdfunding*, food *security*, flutter, laravel, midtrans

***Corresponding author**:
junita.fti@uph.edu

Article history:
Submitted 17 Apr 2026
Revised 13 May 2026
Accepted 18 May 2026
Online Available 19 May 2026
Published 20 May 2026

1. Pendahuluan

Indonesia sebagai negara agraris menghadapi tantangan struktural pada sektor pertanian yang berdampak langsung pada kesejahteraan petani dan ketahanan pangan nasional. Meskipun kapasitas produksi pangan relatif mencukupi, permasalahan distribusi dan akses menyebabkan terjadinya paradoks pangan, yaitu kelebihan hasil panen di tingkat produsen dan keterbatasan akses di tingkat masyarakat pra-sejahtera [1-4]. Studi terdahulu menunjukkan bahwa permasalahan ketahanan pangan tidak hanya dipengaruhi oleh produksi, tetapi juga oleh efisiensi sistem distribusi dan keterhubungan antar aktor dalam rantai pasok pangan [5, 6].

Pada sisi lain, Indonesia memiliki modal sosial yang kuat berupa budaya gotong royong dan tingkat kedermawanan masyarakat yang tinggi, sebagaimana tercermin dalam *World Giving Index* [7]. Fenomena ini mendorong berkembangnya platform *crowdfunding* digital sebagai sarana penggalangan dana sosial. Penelitian empiris menunjukkan bahwa platform *crowdfunding* mampu mempertemukan produsen dan pendukung secara langsung serta meningkatkan partisipasi publik terhadap isu sosial dan ekonomi [8, 9]. Namun demikian, keberhasilan platform semacam ini sangat bergantung pada tingkat transparansi, kepercayaan pengguna, serta mekanisme tata kelola sistem yang diterapkan [10].

Beberapa studi juga menegaskan bahwa lemahnya pengendalian internal, audit trail, dan asimetri informasi merupakan faktor utama kegagalan platform *crowdfunding* dan agri-*fintech*, terutama pada konteks negara berkembang [10]. Kasus *Crowde* dan *eFishery* menunjukkan bahwa absennya sistem verifikasi digital, pencatatan transaksi yang dapat diaudit, serta ketergantungan pada pelaporan internal membuka celah terjadinya *fraud* dan manipulasi data [11]. Temuan ini memperkuat urgensi penelitian yang tidak hanya berfokus pada fungsi penggalangan dana, tetapi juga pada desain sistem yang aman, terverifikasi, dan dapat diaudit.

Berdasarkan celah penelitian tersebut, studi ini mengusulkan pengembangan platform urun dana hasil panen berbasis web dengan pendekatan rekayasa perangkat lunak terstruktur. Penelitian ini mengisi *gap* dari studi sebelumnya dengan mengintegrasikan mekanisme *crowdfunding* sosial dan fitur titip jual hasil panen dalam satu sistem, disertai integrasi *payment gateway* dan layanan logistik, serta divalidasi melalui pengujian teknis menyeluruh. Pendekatan ini belum banyak dibahas

FaST - Jurnal Sains dan Teknologi, Vol.10, No. 1, Mei 2026
e-ISSN 2598-9596
DOI: https://doi.org/10.19166/fastjst.v10i1/11083
Available online at: https://ojs.uph.edu/index.php/FaSTJST/article/view/11083

pada penelitian terdahulu yang umumnya hanya meninjau *crowdfunding* dari sisi perilaku pengguna atau aspek ekonomi makro [12-14].

2. Metode Penelitian

Penelitian ini menggunakan pendekatan rekayasa perangkat lunak dengan tujuan menghasilkan artefak sistem digital berupa aplikasi urun dana dan titip jual hasil panen berbasis web. Pendekatan ini dipilih karena permasalahan yang dikaji bersifat teknis dan menuntut solusi berbasis perancangan, implementasi, serta pengujian sistem secara terukur. Fokus metode penelitian diarahkan pada tahapan pengembangan sistem, perancangan arsitektur, integrasi layanan eksternal, serta evaluasi kualitas perangkat lunak melalui pengujian terstruktur.

2.1 Metode Pengembangan Sistem

Pengembangan sistem pada penelitian ini mengikuti kerangka *Software Development Life Cycle* (SDLC) dengan model *Waterfall*, yang dipilih karena kebutuhan sistem telah terdefinisi sejak tahap awal dan perubahan selama pengembangan relatif terbatas. Model *Waterfall* memungkinkan setiap tahapan pengembangan terdokumentasi secara sistematis dan tervalidasi melalui pengujian berlapis [15, 16]. Pemilihan model ini juga sejalan dengan studi komparatif SDLC yang menyatakan bahwa pendekatan *plan-driven* lebih sesuai untuk penelitian rekayasa sistem dengan ruang lingkup terkontrol [17, 18].

Pada tahap perancangan sistem, pemodelan dilakukan menggunakan *Unified Modeling Language* (UML) untuk memastikan kebutuhan fungsional diterjemahkan secara konsisten ke dalam arsitektur aplikasi. *Class diagram*, *activity diagram*, dan *sequence diagram* digunakan untuk memodelkan struktur sistem, alur proses bisnis, serta integrasi layanan eksternal [19, 20]. Pendekatan ini bertujuan meminimalkan ketidaksesuaian antara desain konseptual dan implementasi kode, sebagaimana direkomendasikan dalam literatur rekayasa perangkat lunak berbasis model.

Tahap analisis kebutuhan difokuskan pada identifikasi kebutuhan fungsional dan nonfungsional sistem, serta pemetaan peran pemangku kepentingan yang terlibat, yaitu petani, pengelola sistem (admin), dan donatur. Tahap perancangan sistem mencakup perancangan arsitektur aplikasi, pemodelan proses bisnis, rancangan basis data, serta desain integrasi layanan eksternal. Tahap implementasi dilakukan dengan menerjemahkan rancangan tersebut ke dalam kode program, sedangkan tahap pengujian digunakan untuk memverifikasi kesesuaian sistem dengan kebutuhan yang telah ditetapkan.

2.2 Perancangan Arsitektur dan Proses Bisnis Sistem

Arsitektur sistem dirancang menggunakan pendekatan arsitektur terlapis yang memisahkan sistem ke dalam lapisan presentasi, logika bisnis, dan data. Lapisan presentasi diimplementasikan melalui antarmuka web dan *mobile*, lapisan logika bisnis dikembangkan menggunakan *framework Laravel* dengan pola *Model–View–Controller* (MVC), dan lapisan data dikelola menggunakan sistem manajemen basis data relasional MySQL. Pemisahan ini bertujuan meningkatkan modularitas, keterpeliharaan, serta kemudahan pengujian sistem.

Proses bisnis sistem dimodelkan untuk menggambarkan alur interaksi antara aktor dan sistem berdasarkan dua skema layanan utama, yaitu distribusi sosial dan titip jual hasil panen. Pada kedua skema tersebut, petani berperan sebagai pengaju proyek, admin sebagai pihak yang melakukan validasi dan pengawasan, serta donatur sebagai pihak yang melakukan kontribusi atau pembelian. Pemodelan dilakukan menggunakan diagram UML, khususnya *use case* dan *activity diagram*, untuk memastikan alur sistem dapat ditelusuri dan diimplementasikan secara konsisten.

2.3 Perancangan Sistem Dual-Mode

Sistem dirancang dengan pendekatan *dual-mode*, yaitu mode distribusi sosial dan mode titip jual komersial. Mode distribusi sosial memungkinkan hasil panen dialokasikan kepada masyarakat pra-sejahtera, sedangkan mode titip jual memungkinkan donatur membeli hasil panen untuk kebutuhan pribadi. Pendekatan ini diterapkan pada lapisan logika bisnis dengan pemisahan alur transaksi dan status distribusi pada tingkat data, sehingga kedua skema dapat berjalan dalam satu platform tanpa

FaST - Jurnal Sains dan Teknologi, Vol.10, No. 1, Mei 2026
e-ISSN 2598-9596
DOI: https://doi.org/10.19166/fastjst.v10i1/11083
Available online at: https://ojs.uph.edu/index.php/FaSTJST/article/view/11083

memerlukan sistem terpisah. Desain ini memberikan fleksibilitas sistem serta mempermudah pengujian skenario transaksi yang berbeda.

2.4 Perancangan Basis Data dan Integrasi Layanan Eksternal

Perancangan basis data dilakukan menggunakan *Entity Relationship Diagram* (ERD) untuk memodelkan struktur data dan relasi antar entitas utama, seperti pengguna, proyek, transaksi, pembayaran, dan distribusi hasil panen. Perancangan ini bertujuan menjaga integritas data, menghindari redundansi, serta mendukung kebutuhan transaksi dan pelaporan sistem.

Implementasi sistem dilakukan menggunakan *framework Laravel* dengan arsitektur MVC dan dukungan *Object Relational Mapper* (ORM) untuk pengelolaan basis data MySQL. Penggunaan ORM dipilih untuk menjaga konsistensi relasi data dan meningkatkan keterpeliharaan kode, meskipun implikasi kinerja diperhitungkan melalui pengujian terkontrol [21]. Integrasi *payment gateway Midtrans* dan *Application Programming Interface* (API) *RajaOngkir* dilakukan melalui *service layer* berbasis *RESTful API*, dengan mekanisme *callback* asinkron dan validasi respons sebagai bagian dari desain sistem transaksi [22].

Integrasi layanan eksternal dilakukan untuk mendukung fungsi pembayaran dan pengiriman. *Payment gateway Midtrans* digunakan untuk memproses transaksi pembayaran secara aman dan terotomatisasi, sedangkan API *RajaOngkir* digunakan untuk memperoleh data ongkos kirim dan estimasi distribusi. Integrasi dilakukan melalui mekanisme *RESTful API* dengan pertukaran data berbasis JSON, serta dirancang dengan memperhatikan aspek keamanan, reliabilitas, dan idempotensi, khususnya pada mekanisme *callback* pembayaran

2.5 Metode Pengujian Sistem

Pengujian sistem dirancang secara berlapis, meliputi *unit testing*, *integration testing*, dan *end-to-end testing*. Pendekatan ini mengikuti praktik rekayasa perangkat lunak modern yang menekankan verifikasi fungsional sekaligus validasi proses bisnis secara menyeluruh [23, 24]. Pengujian *end-to-end* menggunakan *Laravel Dusk* diterapkan untuk memvalidasi alur kritis sistem dari perspektif pengguna akhir, termasuk proses registrasi, transaksi, dan distribusi hasil panen, sebagaimana direkomendasikan dalam literatur pengujian sistem terintegrasi.

Integration testing difokuskan pada pengujian interaksi antar modul serta komunikasi antara sistem dan layanan eksternal, khususnya pada proses transaksi dan pengelolaan data lintas komponen. *End-to-end testing* dilakukan menggunakan *Laravel* Dusk untuk menguji alur sistem secara menyeluruh dari perspektif pengguna akhir, mulai dari registrasi hingga penyelesaian transaksi. *Performance testing* dilakukan menggunakan *k6* untuk mengevaluasi waktu respons dan stabilitas sistem, sedangkan *security testing* difokuskan pada verifikasi mekanisme keamanan dasar, seperti autentikasi, otorisasi, dan perlindungan terhadap ancaman umum aplikasi web.

3. Hasil dan Pembahasan

Sistem Bagipanen telah diimplementasikan sebagai platform urun dana berbasis *website* yang mendukung dua skema layanan, yaitu distribusi sosial hasil panen dan titip jual hasil panen. Implementasi sistem mencakup modul manajemen proyek hasil panen oleh petani, persetujuan proyek oleh admin, serta transaksi oleh donatur melalui integrasi *payment gateway*. Sistem juga menyediakan dukungan perhitungan ongkos kirim untuk transaksi pengiriman melalui integrasi *RajaOngkir*. Implementasi ini dibangun menggunakan *Laravel* sebagai backend, MySQL sebagai basis data, dan integrasi layanan pihak ketiga pada lapisan *service*. Aplikasi Bagipanen dapat diakses melalui *bagipanen.my.id* dan Aplikasi Android melalui *bit.ly/bagipanen-apk*.

Hasil implementasi menunjukkan bahwa sistem mampu mengelola proses urun dana dan titip jual hasil panen secara terintegrasi, dengan dukungan verifikasi proyek dan pencatatan transaksi otomatis. Integrasi *payment gateway Midtrans* memungkinkan transaksi tercatat secara *real-time* dan dapat direkonsiliasi, yang secara langsung mengurangi risiko manipulasi pembayaran. Temuan ini konsisten dengan studi sebelumnya yang menekankan pentingnya peran pihak ketiga terpercaya dalam meningkatkan kepercayaan pengguna pada platform digital [25].

FaST - Jurnal Sains dan Teknologi, Vol.10, No. 1, Mei 2026
e-ISSN 2598-9596
DOI: https://doi.org/10.19166/fastjst.v10i1/11083
Available online at: https://ojs.uph.edu/index.php/FaSTJST/article/view/11083

3.1 Implementasi Arsitektur Sistem

Implementasi sistem Bagipanen direalisasikan menggunakan arsitektur berlapis yang memisahkan lapisan presentasi, aplikasi, dan data untuk meningkatkan modularitas dan kemudahan pengujian. Arsitektur sistem yang diimplementasikan ditunjukkan pada **Gambar 1**, yang menggambarkan interaksi antara pengguna melalui aplikasi web dan *mobile*, backend berbasis *Laravel*, serta basis data MySQL sebagai penyimpan data utama. Pada arsitektur tersebut, komunikasi antar komponen dilakukan melalui protokol *HTTP/HTTPS* dengan pendekatan *RESTful API*.

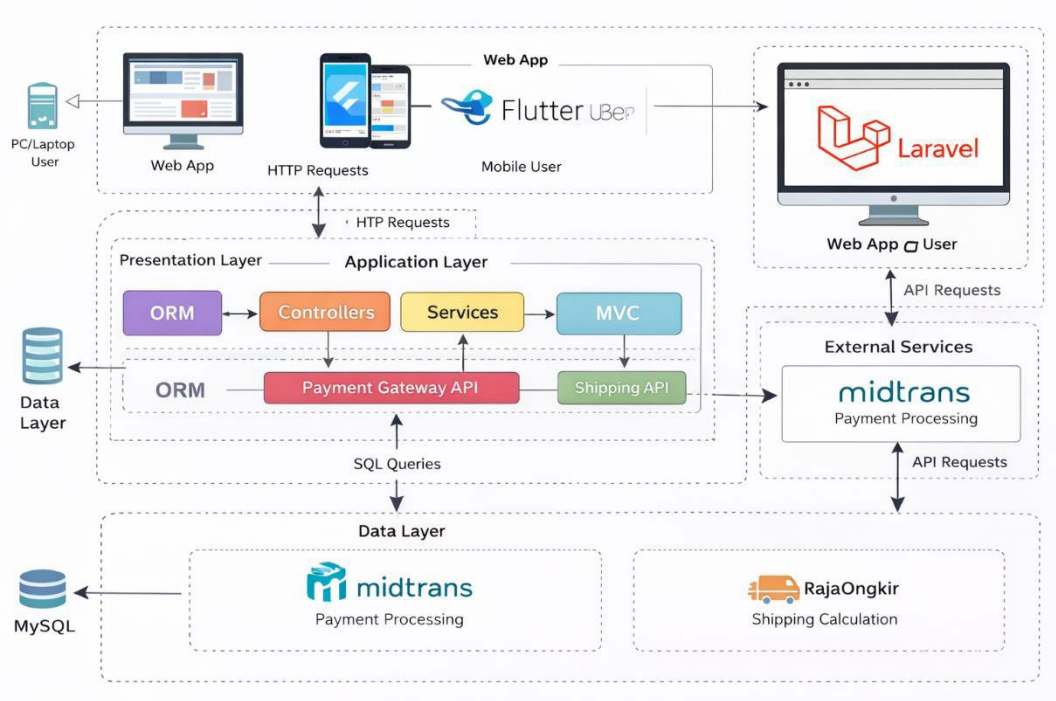

Gambar 1 Arsitektur Sistem

Integrasi layanan eksternal ditempatkan pada lapisan aplikasi melalui *service layer*, sehingga logika bisnis inti tidak bergantung langsung pada implementasi pihak ketiga. Pendekatan ini memungkinkan sistem tetap berjalan secara konsisten meskipun terjadi perubahan atau kegagalan sementara pada layanan eksternal. Struktur ini juga mempermudah proses *integration testing* dan *end-to-end testing* yang dibahas pada bagian selanjutnya.

3.2 Implementasi Proses Bisnis Sistem

Alur proses bisnis utama sistem dimodelkan menggunakan *activity diagram*. Proses bisnis secara menyeluruh ditunjukkan pada **Gambar 2**, yang memperlihatkan interaksi antara tiga aktor utama, yaitu petani, admin, dan donatur. Diagram tersebut menunjukkan bahwa seluruh proyek yang diajukan petani harus melalui proses verifikasi oleh admin sebelum dapat dipublikasikan kepada donatur.

FaST - Jurnal Sains dan Teknologi, Vol.10, No. 1, Mei 2026
e-ISSN 2598-9596
DOI: https://doi.org/10.19166/fastjst.v10i1/11083
Available online at: https://ojs.uph.edu/index.php/FaSTJST/article/view/11083

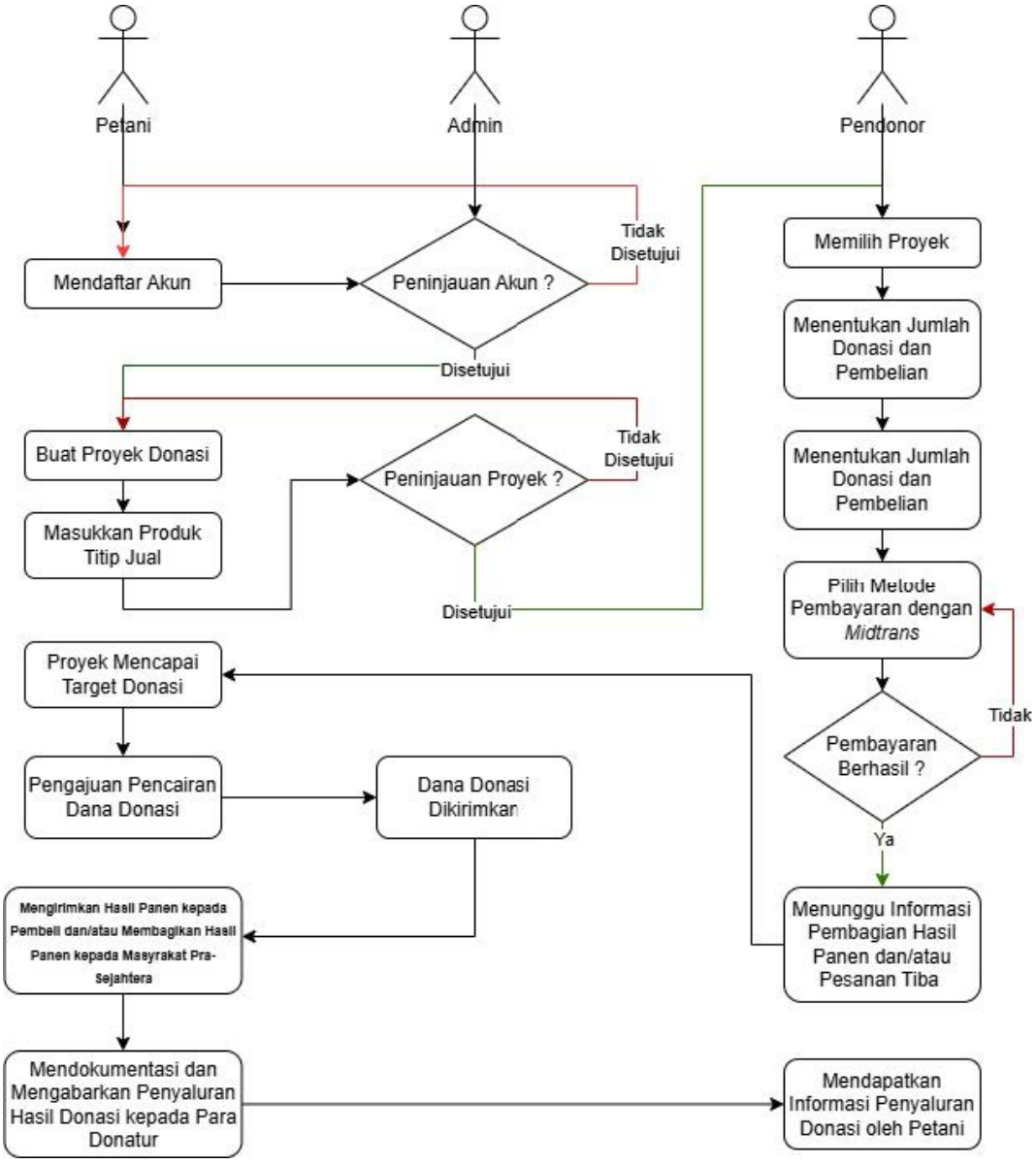

Gambar 2 Proses Bisnis

Pada sistem ini diterapkan dua skema layanan, yaitu distribusi sosial dan titip jual hasil panen. Pada skema distribusi sosial, hasil panen yang didanai akan disalurkan kepada masyarakat pra-sejahtera setelah transaksi berhasil. Sementara itu, pada skema titip jual, donatur dapat membeli hasil panen untuk kebutuhan pribadi dengan mekanisme *checkout* dan pengiriman. Implementasi *dual-mode* ini menjadi pembeda utama Bagipanen dibandingkan platform donasi konvensional.

Secara konseptual, integrasi fitur titip jual dan distribusi sosial pada satu platform memperluas pendekatan *crowdfunding* konvensional yang umumnya hanya berfokus pada donasi. Pendekatan ini sejalan dengan literatur yang menyatakan bahwa model hibrida antara transaksi ekonomi dan tujuan sosial berpotensi meningkatkan keberlanjutan platform dan keterlibatan pengguna [12, 13]. Dengan demikian, hasil penelitian ini tidak hanya memvalidasi implementasi teknis sistem, tetapi juga memperkuat temuan empiris sebelumnya terkait desain platform digital yang berorientasi pada transparansi dan keberlanjutan.

3.3 Implementasi Basis Data dan Relasi Entitas

Perancangan basis data direalisasikan menggunakan MySQL dengan skema relasional yang mengacu pada *Entity Relationship Diagram* (ERD). Struktur relasi antar entitas ditunjukkan pada **Gambar 3**, yang memperlihatkan hubungan antara entitas pengguna, proyek, transaksi donasi, penarikan dana,

FaST - Jurnal Sains dan Teknologi, Vol.10, No. 1, Mei 2026
e-ISSN 2598-9596
DOI: https://doi.org/10.19166/fastjst.v10i1/11083
Available online at: https://ojs.uph.edu/index.php/FaSTJST/article/view/11083

dan pelaporan distribusi. Setiap entitas dirancang dengan kunci utama dan kunci asing untuk menjaga integritas data.

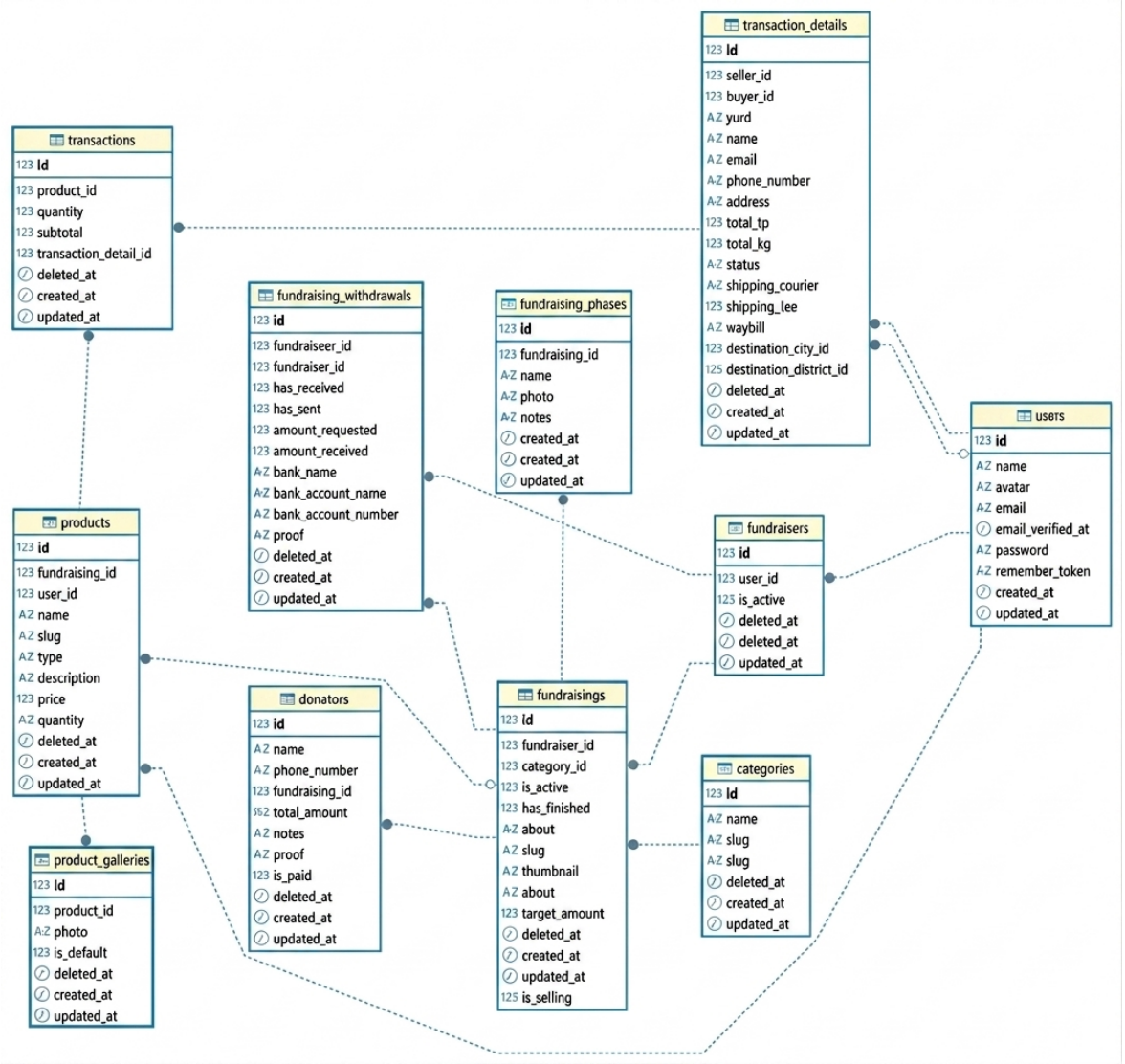

Gambar 3 *Entity Relationship Diagram* bagipanen

Implementasi basis data dilakukan menggunakan migration schema *Laravel* dan *ORM Eloquent*, sehingga relasi antar tabel dapat diakses melalui representasi objek. Pendekatan ini memungkinkan konsistensi antara desain konseptual dan implementasi sistem, serta memudahkan pengujian integrasi basis data yang dilakukan pada tahap pengujian sistem.

3.4 Implementasi Antarmuka Sistem

Hasil implementasi antarmuka sistem ditunjukkan melalui beberapa tampilan utama aplikasi. **Gambar 4** menampilkan halaman *dashboard* donatur yang menyediakan informasi proyek populer, proyek terbaru, serta kategori penggalangan dana. Antarmuka ini dirancang untuk memudahkan pengguna dalam menemukan proyek yang relevan dan meningkatkan keterlibatan pengguna.

FaST - Jurnal Sains dan Teknologi, Vol.10, No. 1, Mei 2026
e-ISSN 2598-9596
DOI: https://doi.org/10.19166/fastjst.v10i1/11083
Available online at: https://ojs.uph.edu/index.php/FaSTJST/article/view/11083

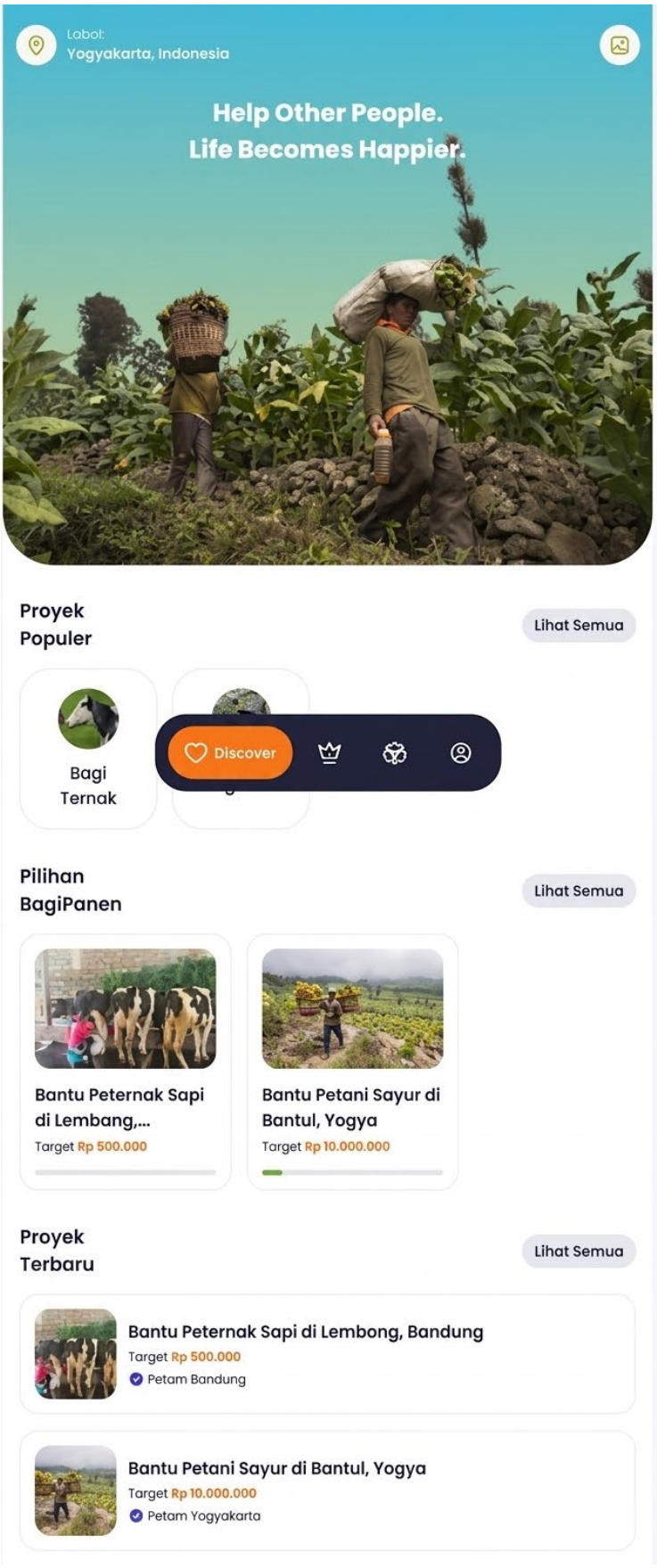

Gambar 4 Halaman *Dashboard* Donatur

FaST - Jurnal Sains dan Teknologi, Vol.10, No. 1, Mei 2026
e-ISSN 2598-9596
DOI: https://doi.org/10.19166/fastjst.v10i1/11083
Available online at: https://ojs.uph.edu/index.php/FaSTJST/article/view/11083

Halaman detail proyek yang ditunjukkan pada **Gambar 5** menyajikan informasi progres pendanaan, deskripsi proyek, dan daftar donatur secara transparan. Selain itu, halaman *checkout* dan pembayaran yang ditunjukkan pada **Gambar 6** memperlihatkan integrasi sistem dengan *payment gateway Midtrans* melalui *embedded payment interface*. Implementasi antarmuka ini mendukung prinsip transparansi dan kemudahan penggunaan yang menjadi faktor penting dalam platform urun dana digital.

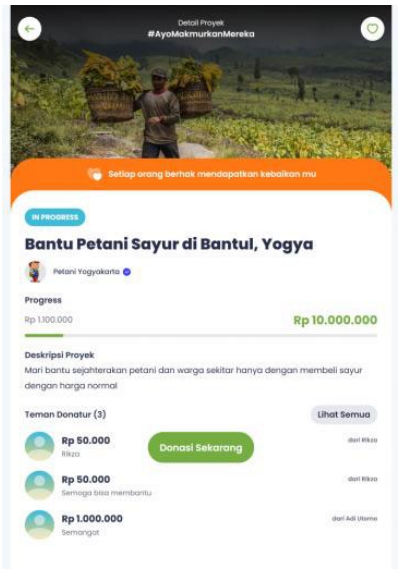

Gambar 1 Detail Proyek

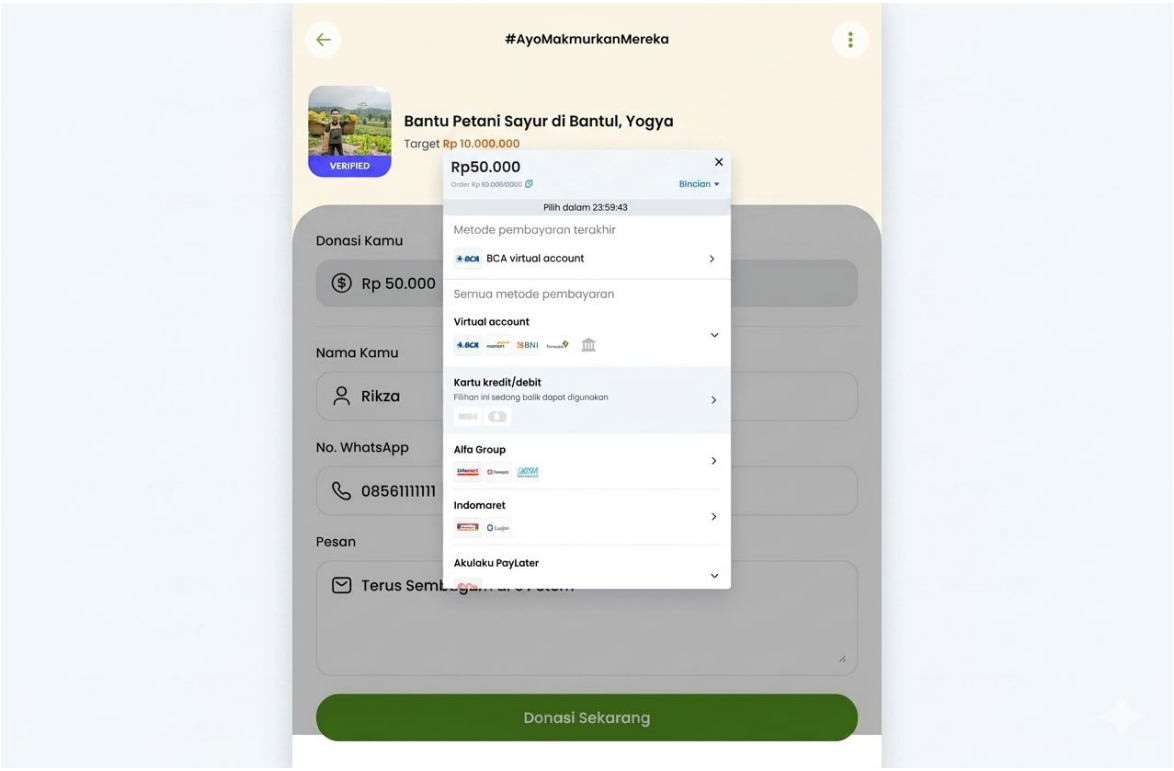

Gambar 6 Implementasi *Midtrans* sebagai *Payment gateway*

3.5 Integrasi *Payment gateway* dan Layanan Pengiriman

Integrasi *payment gateway Midtrans* direalisasikan menggunakan mekanisme *Snap API* dan *callback notification*. Alur integrasi pembayaran ditunjukkan pada **Gambar 7**, yang memperlihatkan proses pembuatan transaksi, pengalihan ke halaman pembayaran, serta penerimaan notifikasi status

FaST - Jurnal Sains dan Teknologi, Vol.10, No. 1, Mei 2026
e-ISSN 2598-9596
DOI: https://doi.org/10.19166/fastjst.v10i1/11083
Available online at: https://ojs.uph.edu/index.php/FaSTJST/article/view/11083

pembayaran secara asinkron. Untuk menjaga konsistensi data, sistem menerapkan mekanisme *idempotent callback* sehingga duplikasi notifikasi tidak menyebabkan pencatatan transaksi ganda.

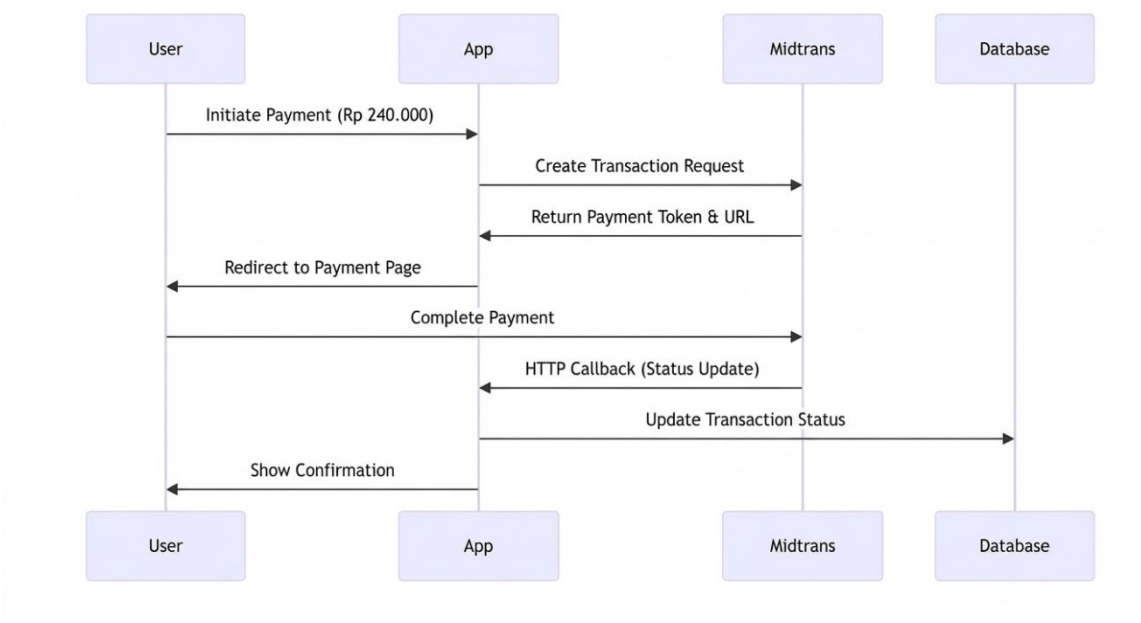

Gambar 7 Sequence Diagram Integrasi *Midtrans*

Selain itu, sistem juga mengintegrasikan API *RajaOngkir* untuk perhitungan ongkos kirim hasil panen. Integrasi ini memungkinkan sistem menghitung biaya pengiriman secara otomatis berdasarkan lokasi asal dan tujuan. Implementasi kedua layanan eksternal ini memperkuat aspek otomasi dan akurasi pada proses transaksi dan distribusi.

3.6 Hasil Pengujian

Pengujian sistem dilakukan pada beberapa tingkat, meliputi *unit testing*, *integration testing*, dan *end-to-end testing*. Contoh implementasi pengujian *end-to-end* menggunakan *Laravel* Dusk ditunjukkan pada **Gambar 8**, yang memverifikasi alur lengkap mulai dari registrasi pengguna hingga proses *checkout* pembayaran. Hasil pengujian menunjukkan bahwa seluruh skenario pengujian dapat dijalankan sesuai dengan alur proses bisnis yang dirancang.

```
public function testCompleteCheckoutProcess() {
        $this->browse(function (Browser $browser) {
            $browser->visit('/login') // 1. Login
              ->type('email', 'test@example.com')
              ->type('password', 'password123')
              ->press('Login')
              ->assertPathIs('/dashboard');
            $browser->visit('/products')
            ->click('@product-1')
            ->assertSee('Detail Product')
            ->type('@quantity-input', '2')
            ->click('@add-to-cart')
            ->assertSee('Produk ditambahkan');
        });
    }
```

Gambar 8 Kode *Testing* dengan Dusk

Ringkasan hasil pengujian sistem disajikan dalam **Tabel 1**, yang menunjukkan bahwa seluruh *test case* berhasil dieksekusi dengan tingkat keberhasilan 100%. Selain itu, pengujian performa menunjukkan bahwa waktu respons sistem berada dalam batas yang dapat diterima untuk aplikasi transaksi daring, sementara pengujian keamanan memastikan perlindungan terhadap serangan umum seperti *CSRF* dan SQL injection.

FaST - Jurnal Sains dan Teknologi, Vol.10, No. 1, Mei 2026
e-ISSN 2598-9596
DOI: https://doi.org/10.19166/fastjst.v10i1/11083
Available online at: https://ojs.uph.edu/index.php/FaSTJST/article/view/11083

Tabel 1 Hasil Eksekusi 25 *Test Case*

Test ID	Area	Status	Waktu	Keterangan
D-01	Dusk E2E	LULUS	4.2 detik	Registrasi berhasil
D-02	Dusk E2E	LULUS	3.8 detik	*Login* valid
M-01	Model	LULUS	0.02 detik	Status default correct
M-02	Model	LULUS	0.03 detik	Auto-complete bekerja
M-03	Model	LULUS	0.04 detik	Stock berkurang
M-04	Model	LULUS	0.05 detik	Idempotent *callback*
M-05	Model	LULUS	0.02 detik	Password hashed
C-01	Controller	LULUS	0.08 detik	Auth protection OK
C-02	Controller	LULUS	0.07 detik	Validation errors
C-03	Controller	LULUS	0.12 detik	Pagination bekerja
S-01	Service	LULUS	0.06 detik	*RajaOngkir* parsed
S-02	Service	LULUS	0.05 detik	*Midtrans* payload
I-01	*Integration*	LULUS	2.1 detik	Migration success
L-01	Livewire	LULUS	0.15 detik	Component render
L-02	Livewire	LULUS	0.18 detik	Event emitted
F-01	File Upload	LULUS	0.22 detik	Image processed
N-01	Notification	LULUS	0.09 detik	Email sent
Q-01	Queue/Job	LULUS	0.11 detik	Job dispatched
P-01	Policy	LULUS	0.07 detik	Authorization OK
API-01	API Auth	LULUS	0.14 detik	Token generated
SEC-01	Security	LULUS	0.06 detik	CSRF protected
PERF-01	Performance	LULUS	8.5 detik	<500ms response
T-01	Factories	LULUS	0.03 detik	Factory valid
D-03	Dusk E2E	LULUS	6.1 detik	Fundraiser flow
D-04	Dusk E2E	LULUS	7.3 detik	Checkout complete

3.7 Diskusi Hasil

Berdasarkan hasil implementasi dan pengujian, dapat disimpulkan bahwa sistem Bagipanen berhasil merealisasikan platform urun dana hasil panen dengan mekanisme *dual-mode* yang terintegrasi. Arsitektur sistem yang modular, integrasi layanan pihak ketiga yang andal, serta hasil pengujian yang konsisten menunjukkan bahwa sistem memenuhi kriteria fungsional dan kualitas perangkat lunak. Temuan ini menunjukkan bahwa pendekatan rekayasa sistem digital dapat menjadi solusi teknis yang layak untuk mendukung distribusi pangan dan pemberdayaan petani secara berkelanjutan.

Hasil implementasi menunjukkan bahwa sistem mampu mengelola proses urun dana dan titip jual hasil panen secara terintegrasi, dengan dukungan verifikasi proyek dan pencatatan transaksi otomatis. Integrasi *payment gateway Midtrans* memungkinkan transaksi tercatat secara *real-time* dan dapat direkonsiliasi, yang secara langsung mengurangi risiko manipulasi pembayaran. Temuan ini konsisten dengan studi sebelumnya yang menekankan pentingnya peran pihak ketiga terpercaya dalam meningkatkan kepercayaan pengguna pada platform digital [25].

Dari perspektif tata kelola, mekanisme verifikasi proyek dan pembatasan hak akses berbasis peran pada Bagipanen dirancang sebagai respons terhadap kelemahan yang teridentifikasi pada platform agritech dan *crowdfunding* yang gagal akibat *fraud* [10]. Audit *trail* transaksi dan pencatatan status proyek berfungsi sebagai sarana akuntabilitas sistem, yang dalam literatur disebut sebagai komponen penting untuk mencegah moral hazard pada platform berbasis dana publik [11, 26].

4. Kesimpulan

Penelitian ini menghasilkan sebuah platform urun dana hasil panen berbasis web yang mengintegrasikan mekanisme distribusi sosial dan fitur titip jual hasil panen dalam satu sistem terpusat. Hasil implementasi menunjukkan bahwa sistem Bagipanen mampu memfasilitasi interaksi antara petani, admin, dan donatur melalui alur proses bisnis yang terstruktur dan tervalidasi. Arsitektur sistem berlapis yang diterapkan mendukung modularitas, keterpeliharaan, serta konsistensi antara perancangan dan implementasi sistem.

e-ISSN 2598-9596
DOI: https://doi.org/10.19166/fastjst.v10i1/11083
Available online at: https://ojs.uph.edu/index.php/FaSTJST/article/view/11083

Integrasi *payment gateway Midtrans* dan layanan pengiriman *RajaOngkir* terbukti berjalan secara andal berdasarkan hasil pengujian fungsional, integrasi, dan *end-to-end*. Seluruh skenario pengujian berhasil dieksekusi dengan tingkat keberhasilan 100%, menunjukkan bahwa sistem mampu memproses transaksi pembayaran dan perhitungan ongkos kirim secara otomatis, *real-time*, dan konsisten. Mekanisme *callback* idempoten yang diterapkan juga memastikan tidak terjadinya duplikasi pencatatan transaksi, sehingga meningkatkan keandalan dan akurasi data sistem.

Implementasi sistem *dual-mode* memungkinkan dua skema layanan, yaitu distribusi sosial dan titip jual hasil panen, berjalan secara paralel tanpa konflik proses maupun data. Pendekatan ini memperluas model *crowdfunding* konvensional dengan menggabungkan tujuan sosial dan transaksi komersial dalam satu platform, serta memberikan fleksibilitas bagi petani dan donatur. Hasil ini menunjukkan bahwa desain sistem yang diusulkan mampu mendukung keberlanjutan platform tanpa menghilangkan prinsip transparansi dan akuntabilitas.

Dari sisi tata kelola, penerapan verifikasi proyek oleh admin, pembatasan hak akses berbasis peran, serta pencatatan transaksi terotomatisasi membentuk fondasi teknis untuk mitigasi risiko *fraud*. Mekanisme tersebut meningkatkan auditabilitas sistem dan secara konseptual menjawab kelemahan yang ditemukan pada beberapa platform *agritech* dan *crowdfunding* yang mengalami kegagalan akibat lemahnya pengendalian internal. Dengan demikian, penelitian ini membuktikan bahwa pendekatan rekayasa perangkat lunak terstruktur dapat menjadi solusi teknis yang layak untuk mendukung distribusi pangan dan pemberdayaan petani secara transparan dan berkelanjutan.

Ucapan Terimakasih

Penulis menyampaikan apresiasi kepada Program Studi Teknik Elektro Universitas Pelita Harapan atas dukungan akademik dan fasilitas yang diberikan selama pelaksanaan penelitian ini. Selain itu, apresiasi diberikan kepada pihak-pihak yang telah berkontribusi dalam pengujian sistem dan penyediaan umpan balik terhadap fungsionalitas aplikasi, sehingga penelitian ini dapat diselesaikan sesuai dengan tujuan yang telah ditetapkan.

Referensi

[1] E. Birru and P. Gloria Setyvani, “Harga Pakcoy di Magelang Rp 200 per Kg, Petani Pilih Sedekahkan ke Pondok Pesantren,” Kompas. Accessed: Jan. 13, 2026. [Online]. Available: Kompas – Harga Pakcoy di Magelang Rp 200 per Kg

[2] Economist Impact, “Global Food Security Index (GFSI) : Indonesia 2022,” 2022. [Online]. Available: Economist Impact – Global Food Security Index Indonesia 2022

[3] C. Titaley, N. M. Sallatalohy, and F. P. Adam, “Status Ketahanan Pangan dan Faktor Sosio-Ekonomi pada Masyarakat Pesisir Kabupaten Buru Selatan,” *agriTECH*, vol. 40, no. 1, p. 1, Mar. 2020, https://doi.org/10.22146/agritech.37009.

[4] P. Pingali, “Agricultural growth and economic development: a view through the globalization lens,” *Agricultural Economics*, vol. 37, no. s1, pp. 1–12, 2007, https://doi.org/10.1111/j.1574-0862.2007.00231.x.

[5] U. Deichmann, A. Goyal, and D. Mishra, “Will digital technologies transform agriculture in developing countries?,” *Agricultural Economics*, vol. 47, no. S1, pp. 21–33, Nov. 2016, doi: 10.1111/agec.12300.

[6] G. Gezimu Gebre, “Determinants of Food In*security* among Households in Addis Ababa City, Ethiopia,” *Interdisciplinary Description of Complex Systems*, vol. 10, no. 2, pp. 159–173, 2012, https://doi.org/10.7906/indecs.10.2.9.

[7] Charity Aid Foundation, “World Giving Index,” 2024. [Online]. Available: Charity Aid Foundation – World Giving Index

[8] A. Agrawal, C. Catalini, and A. Goldfarb, “*Crowdfunding*: Geography, Social Networks, and the Timing of Investment Decisions,” *J. Econ. Manag. Strategy*, vol. 24, no. 2, pp. 253–274, Jun. 2015, https://doi.org/10.1111/jems.12093.

[9] E. M. Gerber and J. Hui, “*Crowdfunding*,” *ACM Transactions on Computer-Human Interaction*, vol. 20, no. 6, pp. 1–32, Dec. 2013, https://doi.org/10.1145/2530540.

[10] G. Burtch, A. Ghose, and S. Wattal, “An Empirical Examination of the Antecedents and Consequences of Contribution Patterns in Crowd-Funded Markets,” *Information Systems Research*, vol. 24, no. 3, pp. 499–519, Sep. 2013, https://doi.org/10.1287/isre.1120.0468.

[11] C. A. C. F. E. Gatot Soepriyanto Ph.D., “Fraud, Lies, and Unicorn: Hard Lessons from Indonesia’s Tech Startup Failures,” Jul. 2025, *BINUS University*.

[12] U. Bretschneider and J. M. Leimeister, "Not just an ego-trip: Exploring backers' motivation for funding in incentive-based *crowdfunding*," *The Journal of Strategic Information Systems*, vol. 26, no. 4, pp. 246–260, Dec. 2017, https://doi.org/10.1016/j.jsis.2017.02.002.

[13] G. Li and J. Wang, "Threshold Effects on Backer Motivations in Reward-Based *Crowdfunding*," *Journal of Management Information Systems*, vol. 36, no. 2, pp. 546–573, Apr. 2019, https://doi.org/10.1080/07421222.2019.1599499.

[14] S. Ryu, J. Park, K. Kim, and Y.-G. Kim, "Reward versus Altruistic Motivations in Reward-Based *Crowdfunding*," *International Journal of Electronic Commerce*, vol. 24, no. 2, pp. 159–183, Apr. 2020, https://doi.org/10.1080/10864415.2020.1715531.

[15] S. Pargaonkar, "A Comprehensive Research Analysis of *Software Development Life Cycle* (SDLC) Agile & *Waterfall* Model Advantages, Disadvantages, and Application Suitability in *Software* Quality Engineering," *International Journal of Scientific and Research Publications*, vol. 13, no. 8, pp. 120–124, Aug. 2023, https://doi.org/10.29322/IJSRP.13.08.2023.p14015.

[16] M. I. H. -, "*Software Development Life Cycle* (SDLC) Methodologies for Information Systems Project Management," *International Journal For Multidisciplinary Research*, vol. 5, no. 5, Sep. 2023, https://doi.org/10.36948/ijfmr.2023.v05i05.6223.

[17] S. S, "A Study of *Software Development Life Cycle* Process Models," *SSRN Electronic Journal*, 2017, https://doi.org/10.2139/ssrn.2988291.

[18] A. Garg, R. Kumar Kaliyar, and A. Goswami, "PDRSD-A systematic review on plan-driven SDLC models for *software* development," in *2022 8th International Conference on Advanced Computing and Communication Systems (ICACCS)*, IEEE, Mar. 2022, pp. 739–744, https://doi.org/10.1109/ICACCS54159.2022.9785261.

[19] G. Engels, A. Förster, R. Heckel, and S. Thöne, "Process Modeling using UML," in *Process-Aware Information Systems*, Wiley, 2005, pp. 83–117, https://doi.org/10.1002/0471741442.ch5.

[20] J. Cheng and X. Yue, "UML Visual Modeling Technology and Application," in *2011 International Conference on Future Computer Science and Education*, IEEE, Aug. 2011, pp. 509–512. https://doi.org/10.1109/ICFCSE.2011.130.

[21] A. Kent, D. Powers, and R. Andrew, "Introduction to MySQL and SQL," in *PHP Web Development with Macromedia Dreamweaver MX 2004*, Berkeley, CA: Apress, 2004, pp. 27–59. https://doi.org/10.1007/978-1-4302-0701-6_2.

[22] A. Macedo, J. A. Baranauskas, and R. Bulcão-Neto, "The Evolution of a Healthcare *Software Framework*: Reuse, Evaluation and Lessons Learned," Sep. 2018, pp. 1043–1051. https://doi.org/10.15439/2018F173.

[23] A. Bertolino, "*Software Testing* Research: Achievements, Challenges, Dreams," in *Future of Software Engineering (FOSE '07)*, IEEE, May 2007, pp. 85–103. doi: 10.1109/FOSE.2007.25.

[24] G. J. Myers, T. Badgett, and C. Sandler, Eds., *The Art of Software Testing*. Wiley, 2012. https://doi.org/10.1002/9781119202486.

[25] CNBC Indonesia, "Hasil Audit Keluar, Ini Data Palsu Hasil Rekayasa Gibran di eFishery," *CNBC Indonesia*, Dec. 2025, [Online]. Available: CNBC Indonesia – Hasil Audit Keluar, Ini Data Palsu Hasil Rekayasa Gibran di eFishery

[26] Hermansah, "PT Crowde Membangun Bangsa diduga gelapkan fasilitas kredit modal kerja," *Jurnal Jabar*, Feb. 2025, [Online]. Available: Jurnal Jabar – PT Crowde Membangun Bangsa diduga gelapkan fasilitas kredit modal kerja